The Role of NSP1 in Rotavirus Pathogenesis

Fan Zhang

Submitted for the degree of Doctor of Philosophy

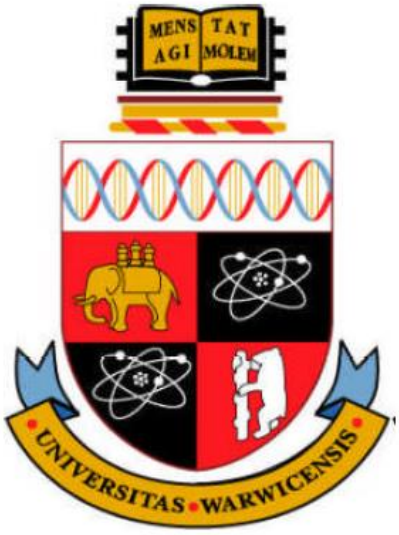

School of Life Sciences

University of Warwick

United Kingdom

September 2012

Table of Contents

List of Figures

List of Tables

Acknowledgements

Firstly, I would like to thank my supervisor Dr Keith Leppard and my previous supervisor Professor Malcolm McCrae for all their invaluable guidance and support in every aspect of my work as well as life. Special thanks must also go to all the present and past members of the rota/adenovirus research group for their assistance and help in the laboratory over the last few years. It is a pleasure to thank all members in Warwick Virology Research Group for asking great questions and giving important feedback throughout the last few years.

I would like to thank all my family, especially my parents for their understanding, support and love during the entire preparation of this project and thesis. I would also like to thank all my friends for their patient and support over the last few years, especially those who have always been supportive under any circumstances. I could not have done this without them.

I would like to dedicate this thesis to my grandmother, who I lost during the course of this project. I miss her every day.

Declaration

I hereby declare that, all the work described in this thesis was undertaken by the author alone under the supervision of Dr Keith Leppard and Professor Malcolm McCrae unless explicitly stated in the text. This thesis has not previously been submitted for any other degree.

Abbreviations

aa	Amino acids
AD	Activating domain
Amp	Ampicillin
APS	Ammonium persulphate
ATP	Adenosine triphosphate
bps	Base pairs
BSA	Bovine serum albumin
C-	Carboxyl-
cDNA	Complementary DNA
cpe	Cytopathic effect
cryoEM	Cryo-electron microscopy
DBD	DNA binding domain
dH_2O	Distilled water
DMEM	Dulbecco's modification of Eagle's minimal essential medium
DMF	Dimethylformamide
DNA	Deoxyribonucleic acid
dNTP	Deoxynucleotide triphosphate
ds	Double-stranded
DTT	Dithiothreitol
E.coli	*Escherichia coli*
EDTA	Ethylenediamine tetracetic acid
ELISA	Enzyme-linked immunosorbent assay
EM	Electron microscopy
ER	Endoplasmic reticulum
FCS	Foetal calf serum
GFP	Green fluorescent protein
GMEM	Glasgow modification of Eagle's minimum essential medium
IEM	Immunoelectron-microscopy
IF	Immunofluorescence
IP	Immunoprecipitation
IPTG	Isopropyl β-D-1-thiogalactopyranoside
Kb	Kilobase

KDa	Kilo Dalton
LB	Luria Bertani
m.o.i.	Multiplicity of infection
MOPS	3-(N-morpholino) propanesulphonic acid
mRNA	Messenger RNA
N-	Amino-
NLS	Nuclear localisation signal
NSP	Non-structural protein
NP40	Nonidet P40
OD	Optical density
ONPG	O-nitrophenyl β-D-galactopyranoside
ORF	Open reading frame
PABP	Poly A binding protein
PAGE	Poly-acrylamide gel electrophoresis
PBS	Phosphate buffered saline
PCR	Polymerase chain reaction
Pfu	Plaque forming unit
RNA	Ribonucleic acid
rpm	Revolutions per minute
SAP	Shrimp alkaline phosphatase
SD	Standard deviation
SDS	Sodium dodecyl sulphate
ss	Single-stranded
SV40	Simian virus 40
TBE	Tris borate EDTA
TBS	Tris-buffered saline
TEMED	N,N,N’N’-tetramethylethylenediamine
Tris	Tris-(hydroxymethyl)-methylamine
UTR	Untranslated region
VP	Viral protein
v/v	Volume to volume
WT	Wild type
w/v	Weight to volume
X-Gal	5-bromo-4-chloro-3-indolyl-β-D-galactopyranoside

Summary

NSP1, a non-structural protein encoded by rotavirus gene segment 5, has been suggested as a virulence determinant for rotavirus and to function as an antagonist of the interferon signalling pathway. Although non-essential for rotavirus replication in cell culture, and is the least conserved in all rotavirus proteins, NSP1 from different rotavirus strains of different species has been demonstrated to interact with several cellular proteins involved in the IFNβ induction pathway. NSP1 from a bovine rotavirus strain (UKtc) has been shown to interact with and to degrade IRF3 in a proteasome dependent manner whereas NSP1 from a porcine rotavirus strain (OSU) fails to target IRF3 but is able to interfere with IFNβ production via similar targeting of β-TrCP.

The research presented in this thesis sought to gain a better understanding of the molecular determinants of NSP1 specificity for targeting the IFNβ pathway by mapping the regions in NSP1 sequences responsible for targeting specific cellular proteins.

NSP1 hybrid constructs with sequences from both UKtcNSP1 and OSUNSP1 were generated and their interactions with both IRF3 and β-TrCP were tested in a series of assays. The initial attempts to map interaction sites using the mammalian two-hybrid assay were not successful. No reporter plasmid signal was generated indicating the expected interaction. The failure of this assay might be due to the insufficient expression of the NSP1 proteins as subsequent modification of the expression vector was shown to improve the expression level of NSP1 proteins in subsequent reporter assay analysis.

Using IFNβ promoter reporter assays to demonstrate the functional consequence of NSP1 action in IRF3, it was found that the constructs containing the entire C-terminal part of UKtcNSP1 were able to reduce IRF3-induced IFNβ promoter activity. Such constructs also caused IRF3 degradation in a proteasome dependent manner in agreement with previous studies. However, the sequence containing the last 135 amino acids from UKtcNSP1 was not sufficient for these activities. Collectively, these data suggested that the sequence between amino acid position 165 and 135 from the C-terminus are required for this interaction and subsequent degradation of IRF3.

Similar experiments focused on determining the interaction site for β-TrCP on NSP1 were more difficult to interpret according the data presented. Unexpectedly in the light of published data, not only OSUNSP1 was able to degrade β-TrCP but UKtcNSP1 appeared to have the similar effect, as well as two reciprocal pairs of NSP1 hybrid constructs.

In summary, it appears that sequences from the C-terminal part of UKtcNSP1 can function in a heterogeneous NSP1 context to target IRF3 from human cells. Further analysis is clearly required to fulfil the understanding of the role of NSP1 in rotavirus pathogenesis, including its interaction with β-TrCP.

Chapter 1

Introduction

1.1 Rotavirus

1.1.1 The discovery of rotavirus

Acute diarrheal diseases have been one of the major causes of death in children, and the young in a wide range of other mammalian and avian species worldwide. Diarrheal disease is one of the most important causes of death in children, particularly in those less than five years old in developing countries; in developed countries, the mortality rate is considerably lower however, it still represents a common infirmity, especially among the youth (Monto *et al*., 1983; Estes and Kapikian, 2007; Martella *et al*., 2010).

Until the early 1970s, no important causative viral factors related to infectious diarrheal diseases had been discovered (Yow *et al*, 1970). The discovery of the Norwalk virus associated with viral gastroenteritis in older children and adults was a big breakthrough, revealing the important role of specific viruses in causing infectious diarrheal diseases (Kapikian *et al*., 1972). In 1973, another viral particle of about 70nm in diameter that was associated with severe diarrhea in infants and young children was directly visualized in duodenal mucosa by thin-section electron microscopy (EM), and due to the wheel-like structure observed it was subsequently designated rotavirus (rota: Latin for wheel) (Bishop *et al*., 1973; Flewett *et al*., 1974; Bishop *et al*., 1974). Human rotaviruses were then linked to previous discoveries of viral particles causing severe diarrhea in infant mice (EDIM), calves (NCDV) and monkeys (SA11) (Adams *et al*., 1963; Mebus *et al*., 1971; Malherbe and Strickland-Chomley, 1967).

Investigators from many countries also reported the detection of rotavirus and it was soon found that rotaviruses were the most important etiologic agents of acute viral gastroenteritis in infants and young children, causing more than half a million deaths annually (Parashar *et al*., 2006). Globally almost every child has experienced rotavirus gastroenteritis by the age of 5, and children in the poorest areas of the world, such as South-East Asia and sub-Saharan Africa account for more than 80% of rotavirus related deaths (Ramig, 2004; Bishop, 2009).

1.1.2 Classification of rotaviruses

Rotavirus is one of the 16 recognized genera of the family *Reoviridae*, together with *Aquareovirus*, *Cardoreovirus*, *Coltivirus*, *Crabreovirus*, *Cypovirus*, *Dinovernavirus*, *Fijivirus*, *Idnoreovirus*, *Mimoreovirus*, *Mycoreovirus*, *Orbivirus*, *Orthoreovirus*, *Oryzavirus*, *Phytoreovirus* and *Seadornavirus* (Attoui *et al*, 2006; Estes and Kapikian, 2007; Deng *et al*, 2012). Members of the family *Reoviridae* are the largest and most diverse group of double-stranded RNA (dsRNA) viruses in terms of host range. All members of the *Reoviridae* family have dsRNA genomes consisting of 10-12 segments and all of them have RNA-dependent RNA polymerase activity associated with the core of the virion, as cells do not have enzymes capable of transcribing dsRNA templates. The transcription process of the *Reoviridae* family is conserved, such that it uses template dsRNA contained within the viral particles rather than free RNA (Patton, 1986; Estes and Kapikian, 2007).

Rotaviruses are divided into seven groups (group A-G) based on the predominant group antigen found on the structural protein VP6 that is detectable by serological

tests such like immunofluorescence (IF), enzyme-linked immunosorbent assay (ELISA) and immunoelectron-microscopy (IEM) (Pedley *et al*., 1986; Mattion *et al*., 1994; Estes and Kapikian, 2007). Rotaviruses group A, B and C are found in humans and other animals; human rotavirus infections are predominantly caused by group A rotaviruses (Parashar *et al*., 2003), group B rotaviruses associated with epidemics of severe diarrhea was primarily reported in adults in China (Chen *et al*,. 1985; Hung *et al*, 1983) and group C rotaviruses have been reported to cause sporadic cases of acute diarrhea in children older than 3 years of age (Von Bonsdorff and Svensson, 1988). Rotaviruses of groups D, E, F, and G have been found only in other animals to date (Saif *et al*,. 1994). The genome of an avian group D rotavirus strain has been reported but much less data has yet been published on rotavirus groups E-G (Trojnar *et al*., 2010; Wakuda *et al*., 2011). The focus of this thesis is the Group A rotaviruses, which have been studied in more details than any other group. The general characteristics of Group A rotaviruses are summarised in Table 1.1.

Table 1.1 General characteristics of Group A rotaviruses (Adapted and summarised from Estes and Kapikian, 2007)

Structure	1. Mature virions are approximately 70nm (100nm including VP4 spikes) in diameter and possess a triple layered icosahedral protein capsid 2. 60 protein spikes extend from the outer layer of the particle 3. Capsid contains all enzymes for mRNA production
Genome	1. 11 segments of double-stranded RNA and capable of genetic reassortment with co-infecting members of the same group 2. Each RNA segment codes for at least one protein
Replication	1. Cytoplasmic replication in infected cells 2. Viral cultivation *in vitro* is facilitated by treatment of mature virus with proteolytic enzymes 3. Exhibit a unique morphogenic pathway

Group A rotaviruses are classified further into two independent serotypes, i.e: G-serotype and P-serotype (Hoshino and Kapikian, 1996). Serotypes are defined by reactivity of viruses in plaque reduction or fluorescent foci reduction neutralization assays in antibody-negative animals (Estes and Kapikian, 2007). These assays measure the reactivity of antibody against the two neutralizing antigens VP7 and VP4 (Hoshino and Kapikian, 1996). At least 16 VP7 (G) serotypes have been identified and strains of animal and human origin may fall within the same serotype. Among these G serotypes, G1-4 and G9 are the most common human strains worldwide (Kobayashi *et al*., 2007; Angel *et al*., 2007). When studies on the protease-sensitive protein VP4 revealed the importance of anti-VP4 neutralization antibody in protection from rotavirus infection *in vivo*, a serotyping system based on VP4, named P-serotype, was proposed (Gorziglia *et al*., 1990). Nevertheless, discrimination of P-serotypes is more difficult to characterize. Although human rotavirus P-serotypes can be determined by ELISA with specific monoclonal antibodies, this method has not become common. So far at least 14 different P-serotypes have been discriminated (Kobayashi *et al*., 2007).

Sequence analysis and hybridization assays based on VP7 and VP4 genes are used to define the genetic typing of rotavirus, i.e: G (VP7)-genotype and P (VP4)-genotype (Kobayashi *et al*., 2007). G-genotype has shown a clear correlation with the serotypes whereas the sero-genotypic correlation has not been clearly defined in P-typing (Estes and Kapikian, 2007). At least 28 different P-genotypes have been reported (Kobayashi *et al*., 2007). To integrate the P-serotype and genotype designation, an open Arabic number following P is used to denote serotype, an

Arabic number in brackets is used to indicate genotype; for instance, the human Wa strain is represented as P1A[8] (Estes and Kapikian, 2007).

1.1.3 Structure of Rotavirus particle

Mature infectious rotavirus particles are approximately 100nm in diameter including the spikes and possess a triple-layered icosahedral protein capsid, hence these are called triple-layered particles (TLPs). The TLP is composed of an outer layer with protein spikes extending from the surface, an intermediate layer and an inner core layer surrounding the dsRNA genome (Flewett *et al*., 1973). The smooth outer layer forming the majority of the outer capsid consists of 780 molecules of the neutralization antigen VP7 arranged as trimers. 60 spikes composed of dimers of haemagglutinin VP4 protrude to a length of around 120Å from this smooth surface (Prasad *et al*., 1990). This outer layer is lost during the uncoating process to leave double-layered particles (DLPs), which are described as rough particles and are transcriptionally active but not infectious (González *et al*., 1995). The intermediate layer is composed of 780 molecules of VP6 arranged as trimers (Bican *et al*., 1982). This VP6 layer may provide structural integrity to the rotavirus capsid by enhancing the morphologic homogeneity and long-term stability of the particle (Zeng *et al*., 1996). Single-layered particles (SLPs or cores) are seen infrequently; they are non-infectious and usually consist of the enzymes VP1 and VP3 together with the dsRNA genome, surrounded by an outer surface layer formed by 120 copies of VP2 (Labbé *et al*., 1991; Lawton *et al*., 1997). A distinctive feature of the viral particle is the 132 aqueous channels that penetrate the virion to link the inner core with the outer surface. These channels are used to import the metabolites required for RNA

transcription and export nascent RNA transcripts during viral replication (Lawton *et al*., 1997; Estes and Kapikian, 2007).

Three-dimensional reconstruction studies of the viral particle using cryo-electron microscopy (cryoEM) and image processing techniques have provided a detailed description of the structures of triple-and double-layered rotavirus particles (Li *et al*., 2009). Current understanding of virions has been enhanced reaching a resolution of about 9.5-Å and all three layers establish an icosahedral organization (**Figure 1.1**).

1.1.4 Rotavirus genome and gene-protein coding assignments

There are 11 segments of dsRNA with sizes ranged from 3302 bps to 667 bps in the rotavirus genome, with around 25% of it forming a dodecahedral structure (Estes and Kapikian, 2007). The nucleotide sequence for all eleven RNA segments has been elucidated for a number of strains and general features have been described.

The open reading frame (ORF) of each segment is surrounded by conserved untranslated regions (UTRs) of varying length dependent upon the gene segment. Although some of the genes possess additional in-phase (such as gene 7, 9, and 10), or out-of-phase (gene 11) ORFs, evidence up to date indicates that all the segments are monocistronic except gene 11, which encodes two non-structural proteins NSP5 and NSP6 (Mattion *et al,*. 1991; Rainsford and McCrae, 2007). In general, the gene sequences of the dsRNA segments are A+U rich (58% to 67%) (Estes and Kapikian, 2007).

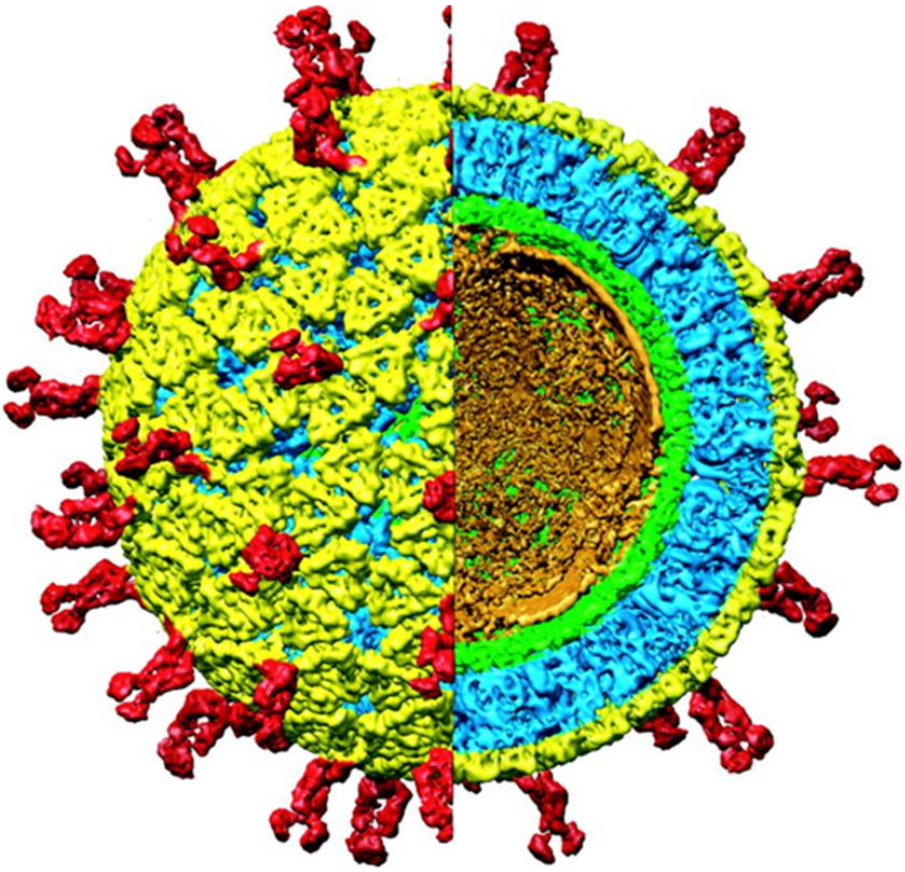

Figure 1.1 Structure of mature rotavirus particle at 9.5-Å resolution.
VP4 spikes are indicated in red, VP7 outer layer in yellow, VP6 intermediate layer in blue, VP2 inner layer in green and the orange colour indicates the internal density consisting of RNA genome and polymerase complex (figure taken from Li *et al*., 2009)

The positive RNA strand has a conserved 5' cap sequence $m^7GpppG^{(m)}Gpy$ but lacks a 3' poly-A tail (Imai *et al*., 1983; McCrae and McCorquodale, 1983); however, the 3' end of the positive sense strand has the conserved sequence 5'-UGUGACC-3' as the minimal essential promoter for the negative RNA strand synthesis (Wentz *et al*., 1996). Similar features of the RNA termini are found in the primary structures of the genomes of other viruses in the family *Reoviridae* such as orbivirus and in other virus families with segmented RNA genomes including *Orthomyxoviridae* and *Arenaviridae* (Estes and Kapikian, 2007). The use of polyacrylamide gel electrophoresis (PAGE) in rotavirus genome analysis is now popular for detecting viruses and monitoring viral outbreaks and transmissions. The electrophoretic pattern of group A rotavirus genomes is made up by four high-molecular-weight segments indicating gene 1-4, two middle-sized segments indicating gene 5 and 6, a distinctive triplet of segments indicating gene 7-9 and the two smallest segments indicating gene 10 and 11(Estes and Kapikian, 2007). However, in viruses with genome rearrangements, these typical RNA segments are decreased in concentration or missing in the electrophoretic profile and are replaced by additional more slowly, or rarely more rapidly, migrating bands of dsRNA (Desselberger, 1996). Virus isolates with rearrangements in segments 5, 6, 8, 10 and 11 have been characterized; of these, segments 5 and 11 appear to be rearranged most frequently (Estes and Kapikian, 2007).

The rotavirus genome segments code for six structural proteins VP1-VP4, VP6 and VP7 that are found in virus particles and six non-structural proteins NSP1-NSP6, found in infected cells. The protein coding assignments for each segment were determined by: (a) *in vitro* translation using mRNA or denatured dsRNA (McCrae

and McCorquodale, 1983); (b) analysis of reassortant viruses (Kantharidis *et al*., 1983; Mason *et al*., 1983; Liu *et al*., 1988); and (c) immunological studies with specific antibodies (Both *et al*., 1983; Greenberg *et al*., 1983). The eleven gene segments and the corresponding viral proteins are summarised in Table 1.2 (Estes and Kapikian, 2007).

Table 1.2 Gene-protein coding assignments of rotavirus. (Adapted from Estes and Kapikian, 2007)

Genome segment	Protein product	Location in virus particles
1	VP1	Core
2	VP2	Core
3	VP3	Core
4	VP4	Outer capsid
5	NSP1	Non-structural
6	VP6	Inner capsid
7	NSP3	Non-structural
8	NSP2	Non-structural
9	VP7	Outer capsid
10	NSP4	Non-structural
11	NSP5 NSP6	Non-structural

1.1.5 Viral protein structure and function

A characteristic feature of rotavirus-infected cells is the presence of highly specialized electron-dense membrane-free cytoplasmic inclusion bodies, termed

viroplasms (Petrie *et al*., 1982; Petrie *et al*., 1984). Viroplasm formation is typical for infections by several members of the *Reoviridae* family and these structures are sites of rotavirus protein accumulation, particle assembly, RNA packaging, and genome replication (Patton *et al*., 2006; Contin *et al*., 2010).

1.1.5.1 Structural proteins

VP1 has been found to be a minor (~2% of the virion mass) but consistent component of rotavirus complexes that has polymerase activity (Gallegos and Patton, 1989; Zeng *et al*., 1996). VP1 is a nucleotide-binding protein that specifically binds the 3' end of viral mRNA in the absence of any other proteins. In addition, VP1 appears to be the RNA-dependent RNA polymerase and functions as both the viral replicase and transcriptase (Patton, 1996).

VP2 forms the inner core layer of the viral particle and constitutes ~12% of the virion protein (Kumar *et al*., 1989). It is known to be essential for replicase activity and is also involved in transcriptase activity (Mansell and Patton, 1990; Estes *et al*., 1983). VP2 has been shown to have sequence-independent RNA binding activity and to associate with both ssRNA and dsRNA, but ssRNA preferentially, which is thought to facilitate its role in viral replication and encapsidation (Boyle and Holmes, 1986; Labbé *et al*., 1994).

VP3 is found in early replication intermediates in the viroplasm and associates with viral mRNA at early stages in virus replication cycle (Gallegos and Patton, 1989). It is known to bind to proteins involved in RNA replication and transcription (Zeng *et*

al., 1998; Sandino *et al*., 1994). VP3 is a guanylyltransferase and has a function in mRNA capping by transferring GMP to the 5' phosphate end of nascent RNAs (Pizarro *et al*., 1991; Liu *et al*., 1992). VP3 has also been demonstrated to have a sequence-independent affinity for ssRNA, but not for dsRNA (Patton and Chen, 1999).

VP4 proteins make up the spikes of the outer layer of the viral particle; it is the viral haemagglutinin and determines the host range and cell tropism (Offit *et al*., 1986; Estes and Kapikian, 2007). Proteolytic cleavage of VP4 to produce VP5* and VP8* potentiates infectivity by greatly enhancing penetration of the virus into cells, but does not affect absorption on to the cell surface (Kalijot *et al*., 1988; Fukuhara *et al*., 1988).

VP6, which forms the intermediate layer of the virion, is the major structural component of the virion, forming ~51% of the total protein content (Estes and Kapikian, 2007). VP6 spontaneously forms trimers which are particularly stable and contains several highly immunogenic epitopes (Estes *et al*., 1987).

VP7 forms the smooth external layer of the outer capsid and constitutes ~30% of the virion protein (Estes and Kapikian, 2007). It is known to be the major neutralisation antigen and is largely responsible for serotype classification of rotaviruses (Sabara *et al*., 1985). VP7 is a glycoprotein with three potential sites for N-linked glycosylation although only two of these sites appear to be used in different rotavirus strains (Kouvelos *et al*., 1984). It is co-translationally glycosylated as it is inserted into the membrane of the endoplasmic reticulum (ER) (Stirzaker *et al*., 1987).

1.1.5.2 Non-structural proteins

NSP1, the least conserved of all rotavirus proteins, is approximately 55kDa in size. Immunofluorescent staining of virus infected cells has shown that NSP1 is localized throughout the cytoplasm and also associated with the cytoskeleton (Hua and Patton, 1994a). By contrast, all other rotavirus proteins are mostly concentrated in the viroplasms. NSP1 does not appear to be essential for rotavirus replication in cell culture since viable virus mutants only able to encode a highly truncated form of the protein can still replicate, although they give smaller virus plaques (Taniguchi *et al*., 1996). NSP1 has been suggested as a virulence determinant for rotavirus. This was initially reported from studies in a mouse model using rotavirus reassortants (Broome *et al*., 1993). Moreover, NSP1 functions as an antagonist of the interferon (IFN) signalling pathway (Arnold and Patton, 2009). Since this thesis is focused on NSP1, a more detailed discussion of this protein will be presented later in this chapter.

NSP2 accumulates predominantly in the viroplasm in rotavirus-infected cells (Petrie *et al*., 1984). It has been shown to interact with NSP5 and to form the viroplasm structure without the presence of other viral proteins (Fabbretti *et al*., 1999). Furthermore, NSP2 is able to interact with the viral polymerase VP1 and it possesses nucleoside triphosphatase (NTPase), RNA triphosphatase (RTPase) and helix-destabilizing activity (Kattoura *et al*., 1994; Taraporewala *et al*., 1999; Aponte *et al*., 1996; Vasquez-Del Carpió *et al*., 2006).

NSP3 is found in the cytoplasm and associates with cytoskeleton in infected cells (Mattion *et al*., 1992). Both monomeric and multimeric forms of NSP3 have

rotavirus mRNA binding activity (Poncet *et al*., 1993). NSP3 has also been shown to interact with the scaffold translation initiation factor eIF4G (Piron *et al*., 1998). eIF4G can bring the initiation factor 4E (eIF4E) and the poly A binding protein (PABP) together to induce circularisation of cellular mRNA for efficient initiation of translation (Preiss and Hentze, 1998). Due to the interaction of NSP3 with eIF4G, the PABP and its associated mRNA are evicted from the cellular translation complex causing in the block of cellular protein synthesis, and suggesting that NSP3 has a role in ensuring efficient translation of viral mRNA (Piron *et al*., 1998).

NSP4 is a transmembrane glycoprotein with three hydrophobic amino-terminal regions maintained in the ER membrane and a hydrophilic carboxy-terminus extended into the cytoplasm (Ericson *et al*., 1982; Chan *et al*., 1988). NSP4 is known to be cytotoxic and functions as a viral enterotoxin in rotavirus-induced diarrhoea by inducing calcium-dependent chloride secretion across the mammalian small intestinal mucosa (Tian *et al*., 1995; Ball *et al*., 1996; Zhang *et al*., 2000). In addition, NSP4 plays a crucial role in viral assembly and facilitates the budding of viral DLPs into the ER lumen to form infectious TLPs (Estes and Kapikian, 2007).

NSP5 is the product of the 5' proximal ORF in gene 11 and is 26 kDa in size. It is a phosphoprotein that exists in several different phosphorylated forms (Afrikanova *et al*., 1996). NSP5 forms homo-dimers and is known to interact with NSP2 to form the viroplasm (Poncet *et al*., 1997). Recent studies demonstrated that the interactions of NSP5-NSP2 and NSP5-VP2 are able to recruit all other viral proteins found in the viroplasms, suggesting that NSP5 plays an important role in the assembly of viroplasms and recruitment of viroplasmic proteins (Contin *et al*., 2010). Moreover,

NSP5 has also been shown to be involved in viral replication (Campagna *et al*., 2005).

NSP6 is encoded by a second out-of-phase ORF in gene 11 with a protein size of 12 kDa. A relatively low level expression of NSP6 is observed in infected cells and the protein co-localizes with NSP5 in viroplasms (Mattion *et al*., 1991; Torres-Vega *et al*., 2000). It has been suggested that NSP6 may play non-essential roles in regulation of the viral replication cycle based on the findings that two viable rotaviruses, the lapine Alabama strain and the porcine OSU strain, encode truncated NSP6 (Gorziglia *et al*., 1989; González and Burrone, 1989).

1.1.6 Rotavirus replication cycle

Rotavirus has a rapid replication cycle in permissive cells with a maximum yield of virus after 10-12 hours (McCrae and Faulkner-Valle, 1981). Although the natural cell tropism for rotavirus is the differentiated enterocyte in the small intestine, suggesting that specific receptors for rotavirus are expressed in these cells, recent investigations have also recognised extraintestinal spread of rotavirus (Azevedo *et al*., 2005; Blutt *et al*., 2006; Kim *et al*., 2011). Studies of the initial stages of rotavirus replication have been primarily conducted in continuous cell cultures derived from MA104 (monkey kidney epithelial cell line) and Caco-2 (polarized human colon carcinoma cell line). Both of the cell lines are highly permissive for most of the mammalian rotavirus infection and Caco-2 cells in particular are thought to reflect the *in vivo* situation of the infection (Estes and Kapikian, 2007; Ciarlet and Estes , 2001).

The general features of rotavirus replication based on studies in cultures of MA104 are summarised as follows (Estes and Kapikian, 2007), and a schematic representation of the virus replication cycle (**Figure 1.2**) demonstrates the process known so far (Trask *et al*., 2012).

(a) Cultivation of most rotavirus strains requires the addition of exogenous proteases to the culture medium to ensure the activation of viral infectivity by cleaving the outer capsid protein VP4.
(b) Replication is entirely cytoplasmic and occurs within cytoplasmic viroplasms.
(c) Host cells do not contain enzymes to replicate dsRNA; thus rotavirus supplies the necessary enzymes.
(d) Viral mRNA transcripts are used both to produce proteins, and as a template for negative stranded RNA synthesis.
(e) Replication occurs in nascent subviral particles and during the replication, both parental dsRNA remain associated with the partially uncoated viral particle, free dsRNA or free negative stranded RNA is never found in infected cells.
(f) Subviral particles are produced in association with viroplasms and the progeny virus particle matures by budding through the membrane of the ER and is then released by cell lysis.
(g) Intracellular calcium levels are important for controlling virus assembly and integrity.

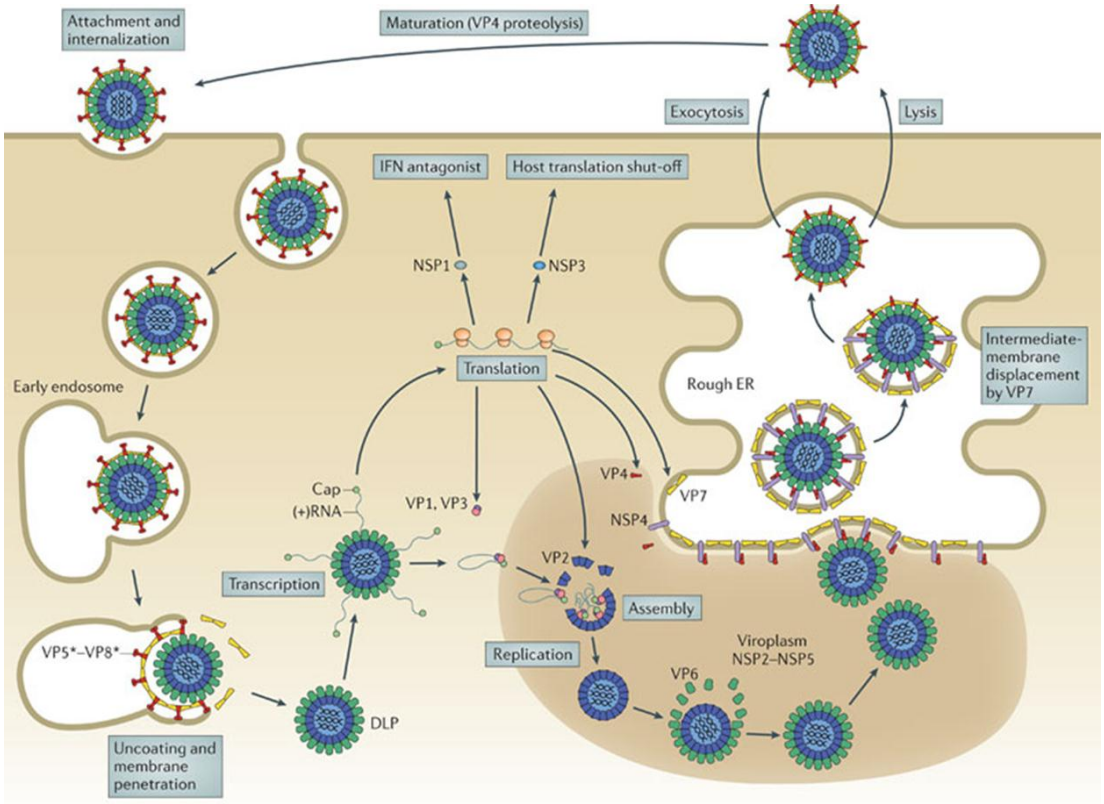

Figure 1.2 The rotavirus replication cycle.

The rotavirus virion first attaches to the target cell followed by virion delivery to the early endosome. The incoming TLP is then uncoated by losing the VP7 outer layer partially and subsequently releases the DLP into the cytosol. This activates the internal polymerase VP1 and VP3 complex to transcribe capped positive-sense RNAs, which then serve either as mRNAs or as templates for synthesis of negative-sense RNAs. When VP1 and VP3 bind the viral positive-sense RNAs, the genome packaging is initiated. Condensation of VP2 triggers dsRNA synthesis. VP6 then assembles onto the nascent core to form the progeny DLP, followed by the assembly of the outer capsid. Through an undefined mechanism, the DLP-VP4-NSP4 complex buds into the ER. Subsequent removal of the ER membrane and NSP4 permits assembly of the ER-resident outer capsid protein VP7, thus the formation of the TLP. Release from the infected cell exposes the virion to trypsin-like proteases, resulting in the specific cleavage of VP4 to produce the fully infectious virion (figure taken from Trask *et al*., 2012).

1.1.6.1 Virus attachment and entry

Viral proteins and host cell surface molecules are essential for rotavirus infections. A broad range of cells can be infected by rotaviruses with different efficiencies (Crawford *et al*., 2006). The current opinion on rotavirus cell entry is that it is a coordinated, multistep process involving sequential interactions with several ligands and a series of conformational changes in the capsid proteins VP4 and VP7 (Estes and Kapikian, 2007). It has been demonstrated that the proteolytic cleave of VP4 and the glycosylation of VP7 are not essential for the initial binding process (Fukuhara *et al*., 1988). A variety of cellular receptors have been reported to be involved in the binding process: N-acetylneuraminic acid (sialic acid), which functions as an attachment receptor for some rotavirus strains; the heat shock cognate protein hsc70, and four integrins namely α2β1, αvβ3, α4β1 and αxβ2 (López and Arias, 2006).

Observations on cells pre-treated with neuraminidase (NA), or pre-incubation of virus with sialic acid-containing compounds, showed reduced infectivity of some viral strains, indicating that sialic acid is able to mediate the initial viral attachment to susceptible cells (López and Arias, 2006). However, most human rotavirus isolates are not affected by prior NA treatment of cells; they can still use sialic acid located in the internal regions of oligosaccharide structure such like ganglioside GM1 for viral recognition (López and Arias, 2006; Haselhorst *et al*., 2009). To date four integrins including α2β1, αvβ3, α4β1 and αxβ2, have been identified to function at the post-attachment level (López and Arias, 2006). Studies have shown that VP4 from a number of rotavirus strains, including those from humans, monkeys and calves, was the viral protein interacting with integrin α2β1 (VLA-2) (Graham *et al*., 2003). The

viral protein responsible for αvβ3 integrin binding was identified to be VP7 (Graham *et al*., 2003; Zárate *et al*., 2004). In addition, integrins α4β1 and αxβ2 have also been reported to promote post-attachment steps in infections by interactions with both VP4 and VP7, and VP7 alone respectively (Graham *et al*., 2005; Fleming *et al*., 2007; Graham *et al*., 2003). Furthermore, studies on Hsc70 have shown that it promotes viral entry at a post-attachment step by interacting with VP4 and VP6 (Gualtero *et al*., 2007).

The entry of the viral particles into host cells is driven by the interaction between the virus and its receptors on the cell surface. Observations made with EM of rotavirus-infected cells suggested that the virus internalization was achieved via endocytosis (Ludert *et al*., 1987). It has been reported that an inhibitor of the vacuolar proton-ATPase pump, bafilomycin A, is able to block rotavirus infectivity, supporting the endocytotic mechanism for virus entry (Chemello *et al*., 2002). However, studies have also revealed that rotavirus infectivity is not inhibited by either preventing the acidification of endosomes or by treatment with drugs that block the intracellular traffic of the endocytic vesicles, these results suggested that the endocytotic pathway might not to be universal for cell entry of all rotaviruses (López and Arias, 2006). Instead, another possible mechanism by direct penetrating of cell membrane was proposed for rotavirus internalization. This was based on the observation that rotavirus infection induced a rapid permeabilization of the cell membrane (Estes and Kapikian, 2007). In summary, it is possible that different viral strains may utilize different mechanisms for their internalization and the precise mechanisms for each pathway still remain unclear (Sánchez-San Martín *et al*., 2004; Gutiérrez *et al*., 2010).

The uncoating process of rotaviruses includes the removal of the outermost layer made from VP4 and VP7. It has been proposed that these proteins are solubilized within an endocytic vesicle because of the low calcium concentration, and this was supported by the inhibition of uncoating of the porcine rotavirus strain OSU in MA104 cells by the calcium ionophore A23187 (Ludert *et al*., 1987). However, different observation have been made by Cuadras *et al,* who showed that the uncoating of rhesus rotavirus strain RRV and monkey rotavirus strain SA11 were not affected by the use of compounds which increased the intracellular calcium level (Cuadras *et al*., 1997). Therefore, the importance of calcium levels for viral entry might also vary between the different viral strains used in different studies.

1.1.6.2 Transcription and translation

The virus-associated transcriptase in TLPs can be activated *in vitro* by treatment with a chelating agent or by heat shock treatment (Cohen and Dobos, 1979; Spencer and Arias, 1981). Such treatments result in the conversion from TLPs to DLPs by losing the outer capsid proteins and subsequently permit transcription to proceed (Estes and Kapikian, 2007).

Synthesis of viral transcripts is initiated by the endogenous viral RNA-dependent RNA polymerase VP1 which utilizes viral dsRNA as template to generate positive sense ssRNA (Lawton *et al*., 1997). The nascent RNA transcripts are capped at their 5' end by the virion-associated guanylyl and methyltransferase activities present in the virion core protein VP3 and possess a methylated structure, m^7GpppGm (Imai *et al*., 1983). As the elongation process proceeds, newly transcribed RNA exits the core

through channels in the VP2 and VP6 layers; multiple mRNA transcripts can be released simultaneously from an actively transcribing particle (Lawton *et al*., 2001). Each genome segment is transcribed by a specific polymerase complex, and the resulting transcripts exit through the channel system at the axis adjacent to their site of synthesis. The positive-stranded RNA transcripts encode the rotavirus proteins and also serve as templates for the negative stranded RNAs synthesis to make progeny dsRNAs (Estes and Kapikian, 2007).

Viral mRNAs released from DLPs are not polyadenylated but capped, and the cellular translation machinery is used to translate viral proteins, with cellular ribosomes being recruited for synthesis of all 12 viral proteins (Patton *et al*., 2006). Viral protein translation is facilitated by the action of NSP3, which has been shown to have an important role in shutting off cellular protein synthesis and enhancing viral protein synthesis by interacting with eIF4G and with RoXaN (rotavirus X protein associated with NSP3). RoXaN is a novel cellular protein containing at least five zinc binding domains, a paxillin leucine-aspartate repeat (LD) motif facilitating protein-protein interactions, and another protein-protein interaction domain called the tetratricopeptide repeat region (TRR) (Vitour *et al*., 2004). Complex consists of NSP3, RoXaN and elF4G can be detected in rotavirus-infected cells, indicating that RoXaN is involved in translation regulation (Patton *et al*., 2006; Harb *et al*., 2008). It has been shown that viral proteins are neither synthesized in equal amounts nor are the amounts in each case similar to those of their corresponding gene transcripts (Johnson and McCrae, 1989). VP6 and NSP4 were found to be synthesized in the largest quantities compared to the other 9 viral proteins, whereas NSP5 and NSP6

were the least actively produced (Johnson and McCrae, 1989; Rainsford and McCrae, 2007).

1.1.6.3 Genome replication

The viroplasm structures provide the sites for synthesis of viral RNAs and formation of DLPs (Petrie *et al*., 1984; Fabbretti *et al*., 1999). The kinetics of RNAs synthesis in infected cells showed that positive- and negative- stranded RNAs were initially detected 3 hours after infection (Stacy-Phipps and Patton, 1987). It is assumed that rotavirus RNA replication takes place in a conservative manner; both strands of parental dsRNA remain within partially uncoated particles, after synthesis, dsRNA remains associated with subviral particles, and free dsRNA is not found in cells (Patton *et al*., 2006). Studies in SA11 infected cells revealed that the replicase complexes consist of the core proteins (VP1 and VP3), small amounts of VP6, large amounts of NSP3, and relatively less amounts of NSP1 and NSP2 (Helmberger-Jonew and Patton, 1986) however, the role of individual proteins in RNA genome replication will be understood better if they are studied *in vivo* with pure species of native rotavirus proteins (Estes and Kapikian, 2007). siRNA knock down experiments demonstrated that NSP4 plays a role in regulating mRNA synthesis and possibly genome encapsidation although the mechanism remains to be determined (Silvestri *et al*., 2005). In addition, a recent study showed that the replication efficiency of rotavirus RRV in MA104 cells is dependent on the ubiquitin-proteasome system (López *et al*., 2011).

1.1.6.4 Virus assembly and release

Rapid assembling of DLPs serves as an intermediate stage in the formation of TLPs (Estes and Kapikian, 2007). Viral cores including VP1, VP2 and VP3, are accumulated in viroplasms (Korolev *et al*., 1981). The assembly of VP1 and VP2 is dependent on both their high affinity for ssRNA and their interaction with NSP2 and NSP5 (Patton *et al*., 2006; Arnoldi *et al*., 2007). VP2 forms the structural basis of the viral core and its simultaneous association with VP1 and VP3 directs the formation of a functional viral core (Zeng *et al*., 1998). During DLP formation in infected mammalian cells, VP6 has been observed in the exterior region of viroplasms, which allows VP6 to associate with newly assembled viral cores to form DLPs as they move toward the periphery of viroplasms (López *et al*., 2005). The glycoproteins VP7 and NSP4 are synthesised on ribosomes associated with the membrane of the ER. NSP4 acts as an intracellular receptor on the ER membrane; it binds newly made DLPs released from viroplasms and mediates the budding of DLPs into the ER lumen. A receptor role for NSP4 is supported by the observation that DLPs bind to ER membranes containing only NSP4 (Meyer *et al*., 1989; Au *et al*., 1989), suggesting that NSP4 alone was sufficient to drive DLPs into the ER lumen.

It has been observed that rotavirus maturation is calcium-dependent. Studies revealed decreased rotavirus production in cells maintained in calcium-depleted medium, and these viruses do not bud into the ER (Shahrabadi and Lee, 1987; Poruchynsky *et al*., 1991). In undifferentiated cells such as MA104, EM studies have shown that the infectious cycle terminates when progeny virus is released by host cell lysis (Musalem and Espejo, 1985; Estes and Kapikian, 2007). However in differentiated

cells like Caco-2, progeny virions are selectively released through the apical membrane involving actin and lipid rafts (Jourdan *et al*., 1997; Chwetzoff and Trugnan, 2006; Gardet *et al*., 2007).

1.1.7 Rotavirus pathogenesis

Rotavirus replicates in non-dividing, mature enterocytes near the tips of the villi. Pathologic changes of infections caused by rotaviruses are mainly limited to the small intestine; nevertheless, the severity of infection varies among animal species across different studies (Burke and Desselberger, 1996). The current understanding of rotavirus pathogenesis is based primarily on working with different animal models, in which rotavirus infection is associated with several of disease including no visible lesions, slight lesions such as enterocyte vacuolization and larger lesions such as crypt hyperplasia and villus blunting (Ramig, 2004).

Pathogenesis of rotavirus infection is multifactorial, both host and viral factors can affect the consequences of infection. There are some major host factors recognised to affect the severity of rotavirus-associated disease: (i) the age of the animals at infection can result in different clinical symptoms including biliary atresia, diarrhea and some extraintestinal replication of virus (Estes and Kapikian, 2007); (ii) increased severity of rotavirus diarrhea can be caused by malnutrition as this delays the recovery of the small intestines (Ramig, 2004); and (iii) the expression of intestinal mucins and the rate of epithelial cell replacement can affect rotavirus infection in the host (Ramig, 2004). Furthermore, the enteric nervous system (ENS) in the intestinal wall has also been shown to be involved in rotavirus-induced watery

diarrhoea (Lundgren *et al*., 2000). A recent study analysed the total gene expression profile of HT29 cells infected with either simian (SA11), bovine (A5-13) or human (Wa) rotavirus strains using microarrays. 131 genes involved in innate immune responses, stress responses, apoptosis and protein metabolism were similarly induced by all three strains (Bagchi *et al*., 2012). In terms of the viral factors, studies on rotavirus-infected intestinal epithelial cells showed that the infection is different depending on whether or not the virus requires sialic acid for initial binding (Estes *et al*., 2001).

1.1.8 Rotavirus vaccines

Three live rotavirus vaccines have been developed, Rotashield (Wyeth), RotaTeq (Merck) and Rotarix (GSK). Both Rotashield and RotaTeq are reassortant viruses based on simian and bovine rotaviruses respectively with gene segments encoding VP4 and VP7 derived from human rotaviruses (Estes and Kapikian, 2007). By contrast, Rotarix is a human rotavirus that was attenuated by passaging in cell culture. RotaShield was the first of these vaccines to be licensed in the United States in 1998 although was withdrawn subsequently because the detection of a temporal association between vaccine administration and gut intussusception (Simonsen *et al*., 2005). The other two rotavirus vaccines were released in 2006 and no similar link with intussusception has been observed (Angel *et al*., 2007). Ongoing vaccination programs in general show great reductions in clinical burden by both of the vaccines. However, despite the success of vaccination programs in the US, Australia and some European countries, only a limited number of other countries have introduced RV vaccination probably due to the cost barrier. Additional live and inactivated vaccines

from emerging manufacturers may be on the market for the next decade, providing competition and potentially reducing the cost of the program (Weycker *et al*., 2009; Lopman *et al*., 2012).

1.2 Innate immune system

1.2.1 Overview

The body is protected from infection by a variety of effector cells and molecules involved in the immune system. An adaptive immune response has its specificity as the production of antibodies is against a definite pathogen or its products; and an adaptation to infection with that pathogen is developed through the lifetime of an individual. On the other hand, the innate immune response can be immediately activated against a wider range of pathogens but has no specificity for any individual pathogen and does not lead to lasting immunity (Biron *et al*., 2002). The studies included in this thesis are mainly focused on innate immunity.

The first line of defence against an invading pathogen is the innate immune response. Synthesis and secretion of type I interferons (IFN) can exhibit antiviral, anti-proliferative and immunomodulatory functions and provide a vital aspect of the antiviral innate immune response (Honda *et al*., 2005). Innate immunity is based on an intricate system of host pattern recognition receptors (PRRs) that specifically recognize pathogen-associated molecular patterns (PAMPs) (Janeway, 1989; Akira *et al*., 2006; Unterholzner and Bowie 2008). PRRs are germline-encoded, non-clonal, and expressed constitutively in the host cells. PRRs can react with specific ligands

leading to different anti-pathogen responses. Four different classes of PRRs found to date include Toll-like receptors (TLRs), retinoic acid-induced gene-1 (RIG-I)-like receptors (RLRs), nucleotide oligomerization domain (NOD)-like receptors (NLRs) and C-type lectin receptors (CLRs). The first three of these PRRs are able to recognise viral nucleic acids (Geijtenbeek *et al*., 2009a; Ting *et al*., 2005; Eisenächer and Krug, 2012) and among them, TLRs and RLRs are important for producing various cytokines and type I interferns (IFNs), while NLRs are able to regulate interleukin-1b (IL-1b) maturation by activating caspase-1 (Pétrilli *et al*., 2007a). Figure 1.3 illustrates these three PRRs for RNA virus recognition (Takeuchi and Akira, 2009).

Toll-like receptors (TLRs) are transmembrane proteins and they are the mammalian homologs of Toll, which was discovered to mediate recognition of pathogens by the innate immune system in *Drosophila* species (Lemaitre *et al*., 1996). There are at least 13 identified mammalian TLRs that share similar extracellular and intracellular domains (Brikos and O'Neil, 2008). The molecular basis of TLR signalling is dependent on the conserved part of their intracellular domain called the Toll/interleukin-1 receptor (TIR) domain, which functions as a linker to connect to the membrane. The glycosylated extracellular domain consists of leucine-rich repeats (LRRs) and they are connected to the cytoplasm by a hydrophobic transmembrane sequence (Gay and Gangloff, 2008). Although historically the role of TLRs in the host immune response to bacteria and fungi was initially more apparent, the more significant role of TLRs to virus infections has been established as several viral structural entities have been identified to be the TLR recognition targets (Brikos and O'Neil, 2008).

Based on the similarities on the sequence, structure and function, a subgroup of TLRs including TLR3, TLR7, TLR8 and TLR9 has been identified to recognize nucleic acids (Hornung *et al*., 2008). ssRNA, anti-viral drugs and short dsRNA containing certain sequence motifs can be sensed by both TLR7 and TLR8 (Heil *et al*., 2004; Hornung *et al*., 2005; Diebold *et al*., 2004; Uematsu and Akira, 2008). dsRNA viruses and synthetic analogues of dsRNA (Poly(I:C)) are recognised by TLR3 (Alexopoulou *et al*., 2001; Beutler *et al*., 2007), and the ligand for TLR9 is the DNA-containing CpG motifs (Hemmi *et al*., 2000). In addition, a number of specific viral structural proteins have been shown to activate signal transduction through other TLRs, for instance, envelope proteins of Measles virus can activate the signal transduction through TLR2 and F protein of respiratory syncytial virus can trigger this pathway via TLR4 (Uematsu and Akira, 2008).

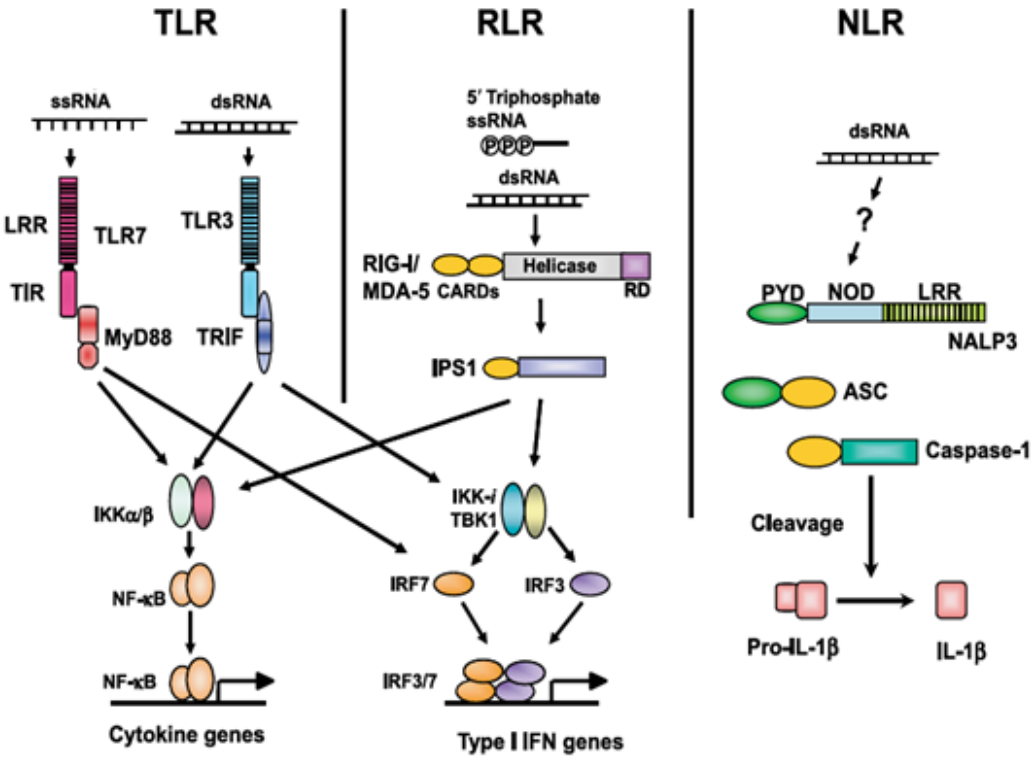

Figure 1.3 Three classes of PRRs for RNA virus recognition.

ssRNA from viruses is recognized by TLR7 in plasmacytoid dendritic cells (pDCs), whereas dsRNA is detected by TLR3 in conventional dendritic cells (cDCs). TLR7 and TLR3 trigger signaling cascades via the myeloid differentiation factor 88 (MyD88) and Toll/IL-1 receptor (IL-1R) homology domain-containing adapter inducing IFN- β (TRIF), respectively. RIG-I and MDA5 recruit another adapter protein, IFN-β promoter stimulator-1 (IPS-1). TRIF and IPS-1 share signaling molecules for phosphorylation of IRF3 and IRF-7 by TBK1/IKK-i. MyD88-dependent signaling directly activates IRF-7 in pDCs. Phosphorylated IRF-3 and IRF-7 activate the expression of type I IFN genes. Simultaneously, TLRs and RLRs induce the translocation of NF-κB to induce the expression of cytokine genes. NALP3, one of the NLR proteins, detects the presence of dsRNA and induces the catalytic activity of caspase-1 via an adapter, apoptosis-associated speck-like protein containing a CARD (ASC) (figure taken from Takeuchi and Akira, 2009).

In 2005, a new pathway was identified when the retinoic acid-induced gene-1 (RIG-I)-like receptors (RLRs) was discovered. This pathway recognizes viral nucleic acids exclusively in the cytoplasm of infected cells and it has been shown to be independent of the TLR system (Rothenfusser *et al*., 2005). The RLRs consist of three cytosolic RNA helicases namely RIG-I, MDA5 (melanoma differentiation-associated gene 5) and LGP2 (laboratory of genetics and physiology-2), which are all capable of unwinding dsRNA molecules (Andrejeva *et al*., 2004; Tanner and Linder, 2001). RIG-I can bind both Poly (I:C) and viral dsRNA and is activated only in the presence of dsRNA although over-expression of the N-terminal region of RIG-I containing two tandem caspase recruitment domains (CARDs) is sufficient to activate IRF3 and NF-κB without viral infection (Seth *et al*., 2006). In contrast, the nature of RNAs for MDA5 activation is less understood although it shares the N-terminal CARDs structure with RIG-I and can also activate the IFNβ promoter (Meylan *et al*., 2005). LGP2 doesn't contain the N-terminal CARDs, but has a repressor domain at the C-terminus. This domain is able to not only facilitate the binding of dsRNA but also to inhibit multimerization and the signalling of RIG-I, but not MDA5, thus to act as a negative regulator of the RIG-I pathway (Yoneyama *et al*., 2005; Saito *et al*., 2007; Pippig *et al*., 2009).

The transcriptional activation of type I interferon (IFN) genes is a key step in the mammalian antiviral response. IFN genes include multiple IFNα isoforms, IFNβ and other members of the type I interferon family such like IFN-ω, ε, and κ (Der *et al*., 1998). In humans there are at least 13 subtypes of IFNα (Randall and Goodbourn, 2008), though only a single gene exists for IFNβ. Both IFNα and IFNβ are produced by many types of cells, including macrophages, fibroblasts, lymphocytes, endothelial

cells and epithelial cells. The activation of IFN regulatory factors (IRFs) and/or NFκB is triggered by the engagement of PRRs by PAMPs, which subsequently induce the production and secretion of type I IFN proteins. The binding of these type I IFN proteins to their receptors on the surface of both infected and uninfected cells prompts a cascade of signalling events involving signal transducers and activators of transcription (STAT) and Janus kinases (JAK) molecules, which can translocate to the nucleus after phosphorylation. They then induce the expression of many IFN-stimulated genes (ISG) that encode proteins with antiviral properties to establish an antiviral state. Importantly, this occurs in both infected and uninfected cells and so is responsible for helping to control the spread of infection (Takeuchi and Akira, 2007; Randall and Goodbourn, 2008).

1.2.2 Interferon regulatory factors regulated pathway

Nine interferon regulatory factors (IRF1-9) have been established and are characterized by a conserved DNA-binding domain near the N-terminus of the protein (Taniguchi *et al*., 2001). IRF3-9 have an IRF-associated domain (IAD) within the carboxy terminus which is important for protein-protein interactions upon phosphorylation-mediated activation (Taniguchi *et al*., 2001). The IAD typically promotes either homodimer or heterodimer formation among IRF family members, but they can also interact with other protein families such as members of the STAT family (Taniguchi *et al*., 2001). Several IRFs have been implicated in type I IFN induction including IRF1, IRF3, IRF5, and IRF7. Nevertheless, studies in $IRF1^{-/-}$ and $IRF5^{-/-}$ mice indicate that these transcription factors are dispensable for type I IFN induction (Takaoka and Yanai, 2005).

Early studies identified that the main steps in the activation of IRF3 and IRF7 are similar (Servant *et al*., 2002a). IRF3 is localized to the cytoplasm in a monomeric and inactivated form in uninfected cells (Mercurio *et al.*, 1997). Subsequent to viral infection, IRF3 becomes phosphorylated and dimerized (Honda *et al.*, 2006). The dimers accumulate in the nucleus, bind consensus DNA sequences, recruit histone acetyltransferases (HATs) to promote gene induction, and then are degraded in a proteasome-dependent manner (Sato *et al*., 1998; Yoneyama *et al*., 1998). Hyperphosphorylation of serine and threonine residues near the C-terminus of IRF3 by TBK1 and IKKi is necessary for IRF3 activation (Hemmi *et al*., 2004). Hyperphosphorylated IRF3 dimers form a complex with histone acetyltransferases such as CREB-binding protein (CBP) or p300 (Yoneyama *et al*., 1998; Lin *et al*., 1998). Binding both DNA and CBP or p300 results in nuclear retention of IRF3 dimers (Kumar *et al*., 2000); while in the nucleus, IRF3 is targeted for proteasome-mediated degradation dependented on a peptidyl-prolylisomerase, PIN1 (Saitoh *et al*., 2006). The E3 ubiquitin ligase that directs IRF3 polyubiquitination to signal its degradation is likely to be a Skp1-Cull1-F-box multiprotein complex, based on the requirement of cullin 1 for IRF3 degradation (Bibeau-Poirier *et al*., 2006).

IRF7 has a short half-life, and is only present in high concentrations when a viral infection is in progress (Taniguchi and Takaoka, 2002). Sequence alignments show that IRF7 has serine and threonine residue spacing near its C-terminus similar to that found in IRF3 (Servant *et al*., 2002b). IRF7 is also activated by hyperphosphorylation mediated by TBK1 and IKKi similar to IRF3 (Sharma *et al*., 2003). The expression of IRF7 in most cells is low and the expression is upregulated by IFN signalling (Sato *et al*., 1998). It was originally thought that IRF3, but not

IRF7, was essential for the early phase of type I IFN induction since IRF3$^{-/-}$ mice have an impaired type I IFN response (Sato *et al*., 1998). However, it has also been demonstrated that IRF7$^{-/-}$ mice completely lost the ability to express type I IFN (Honda *et al*., 2005). Therefore, a revised model suggests that IRF3/IRF7 heterodimers or IRF7 homodimers are important for the initial induction of type I IFN (Honda *et al*., 2005). Following induced expression of IRF7 by IFN signalling, IRF7 is the major driver of a positive feedback mechanism that upregulates the expression of a wide range of type I IFN genes and it is considered the 'master regulator' of the IFN response, as it also induces the expression of IFNα (Honda *et al*., 2005).

1.2.3 NFκB regulated pathway

NFκB is a dimeric transcription factor made up with members of the Rel family including NFκB1 (p105/p50), NFκB2 (p100/p52), Rel (c-Rel), RelA (p65) and RelB. NFκB is required for the optimal expression of IFN-β (Takeuchi and Akira, 2009). The activity of NFκB is tightly regulated by the inhibitor IκB. Phosphorylation of IκB by IκB kinases (IKK) leads to its rapid ubiquitination by the E3 ligase Skp1/Cull/F-box complex named SCF$^{\beta\text{-TrCP}}$ and subsequent degradation by the 26S proteasome. This in turn leads to the translocation of NFκB subunits to the nucleus and promotes binding and transcription of NFκB target genes (Holloway *et al*., 2009; Kroll *et al*, 1999).

IKK activation is initiated with the phosphorylation of key serine residues in the kinase domains of the IKKα and IKKβ subunits in the IKK complex (Häcker and

Karin, 2006). As a negative feedback loop, activated IKK also phosphorylates the IKKγ regulatory subunit; this leads to dissociation of IKKγ and conformational changes in IKKα and IKKβ, which allows for the recognition and dephosphorylation of the kinase domain serine residues to inactivate the IKK complex (Kray *et al*., 2005; Palkowitsch *et al*., 2008). Once activated, the IKK complex can phosphorylate three NFκB inhibitor (IκB) proteins, IκBα, IκBβ, and IκBε (Didonato *et al*., 1997). Phosphorylated IκB is recognized by the $SCF^{\beta\text{-}TrCP}$ E3 ubiquitin ligase complex leading to polyubiquitination of IκB, which is subsequently degraded by the proteasome (Kroll *et al*., 1999).

The most common NFκB dimer is composed of the p65 and p50 subunits and is usually inhibited by association with IκBα (Hayden *et al*., 2008). IκBα in complex with p65:p50 normally shuttles between the cytoplasm and the nucleus, but is predominantly found in the cytoplasm (Baeuerle and Baltimore, 1988). The inhibitory activity of IκBα was initially recognised as a function of maintaining the cytoplasmic localization of p65:p50, however it was then found that the p65:p50 still remains mostly cytoplasmic in cells deficient in all three IκB proteins (Tergaonkar, 2006). Robust nuclear accumulation of p65:p50 free from IκB inhibition occurs when the DNA binding of this dimer is enhanced by phosphorylation of the p65 subunit on serine 276 (Vermeulen *et al*., 2003). This phosphorylation has been shown to be essential for p65:p50 interaction with the histone acetyltransferases, CBP and p300 (Chen *et al*., 2005). CBP/p300 then acetylates p65 to maximize transcriptional activity of this complex (Chen *et al*., 2005). Figure 1.4 summarises the signalling pathways triggered by viral infection (Kawai and Akira, 2006).

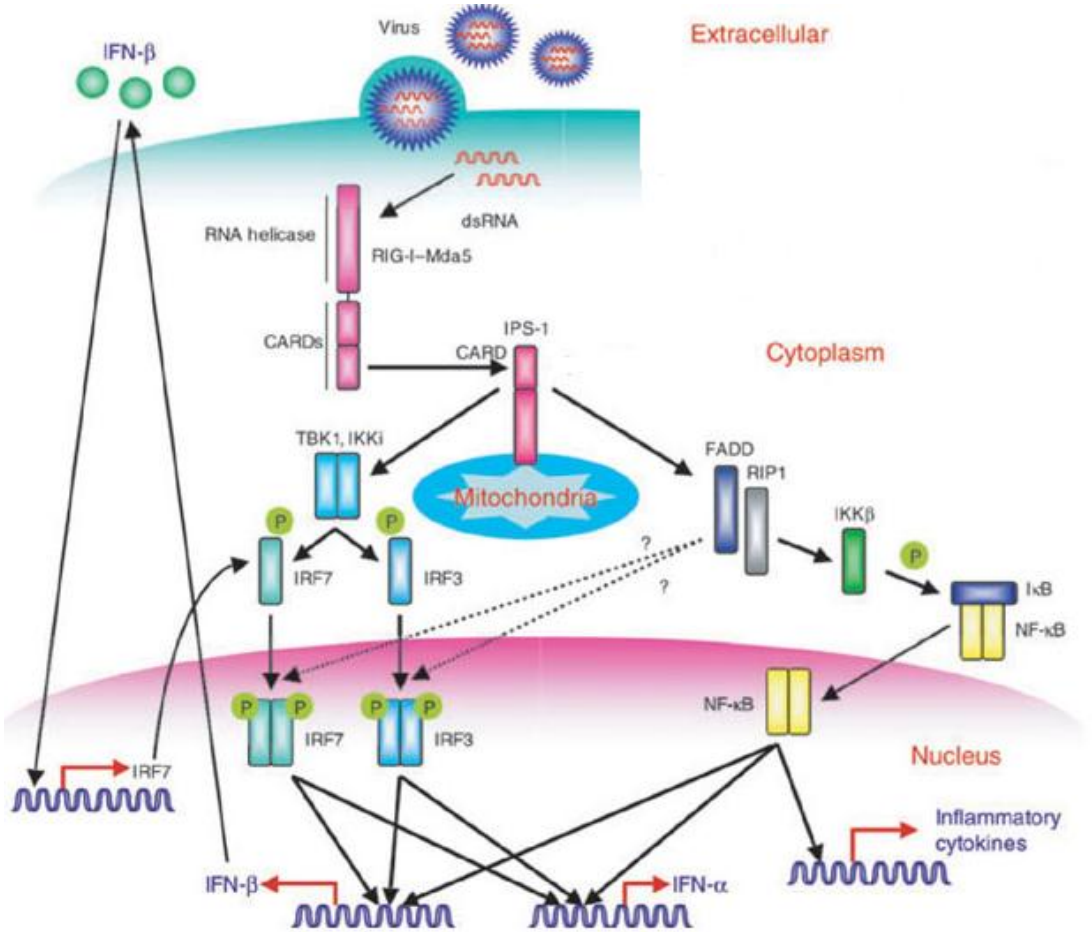

Figure1.4 Signalling pathways triggered by viral infection.

Antiviral signalling is initiated by the recognition of dsRNA in the cytoplasm, followed by the activation of IRF3 and IRF7 via TBK1-and IKKi-dependent phosphorylation, and the activation of NFκB via stimulation of phosphorylated IκB. After translocation of these proteins to the nucleus, the type I interferon promoters are activated (adapted from Kawai and Akira, 2006).

The IFN response also leads to general antiviral responses other than those described above. Treatment of cells with type I IFNs sensitizes them to apoptosis upon viral infection (Stetson and Medzhitov, 2006). p53, a tumour suppressor which promotes apoptosis, is directly induced by interferon and is thought to confer antiviral activity through this function (Stetson and Medzhitov, 2006). This hypothesis is supported by the observation that a number of viruses, including poliovirus and adenovirus, actively degrade p53 during the course of infection (Pampin *et al.*, 2006, Weitzman and Ornelles, 2005).

1.3 Non-structural protein NSP1

1.3.1 NSP1 shows high levels of primary sequence variability

It is common for some viral proteins, such as neutralization antigens, to exhibit a high level of sequence divergence among different virus isolates as a result of the selective pressure supplied by the host adaptive immune system. This selection facilitates viral spread by providing the opportunity for the virus to escape from previously established immunity. By contrast, non-structural proteins tend to be relatively more conserved as they are not part of the virus particle and therefore not subjected to selection pressure from antibody-based immunity. However, NSP1 shows very high levels of divergence in its primary sequence between different virus isolates (Mitchell and Both, 1990; Xu *et al*., 1994).

The sequence of a bovine rotavirus (RF) NSP1 was the first gene 5 sequence to be published (Bremont *et al*., 1987). When the corresponding gene sequence from the

UKtc strain of bovine rotavirus was determined, it showed a high level of sequence conservation with the RF sequence (Tian and McCrae unpublished observation). By contrast the simian rotavirus SA11 strain showed a high level of sequence divergence in its gene 5, revealing 50% conservation at the nucleotide level and only 39% at the amino acid level with the bovine isolates (Mitchell & Both, 1990). It was thought that this diversity might be linked to the species of origin of the virus until the gene 5 sequence from a second simian virus isolate (RRV) was found to show very high sequence divergence from that of the SA11 isolate (Xu *et al*., 1994). Therefore sequence variability in NSP1 is not entirely related to species of origin as was initially postulated (**Table 1.3** Xu *et al*., 1994).

Table 1.3. Levels of nucleotide and amino acid conservation across gene 5 and NSP1 sequences (table taken from Xu *et al*., 1994)

		Nucleotide conservation (%)															
		RF	UKtc	B223	69M	DS1	4F	4S	Hochi	Wa	IGV803	OSU	St 3	EHP	EW	SA11	SA11P	RRV
Amino acid conservation (%)	RF	**100**	88·7	74	65·8	65·9	66·8	66·9	65·7	64·8	64·6	65·6	66	52·3	52·3	51·7	52·4	52·8
	UKtc	95·5	**100**	75·1	66·5	66·3	67·3	67·2	66·7	66·2	66·5	66	65·6	52·6	53·9	53·8	53·7	53·6
	B223	71·5	71·3	**100**	66·9	65·8	67·1	67	67·8	66·8	67	65·6	67·4	50·9	50·9	54·7	53·9	54·4
	69M	57·9	57·9	56·5	**100**	93	75·5	75·4	75·3	75·3	75·8	74·4	75·5	51·6	52	55·9	56·2	53·6
	DS1	58·1	58·1	58·3	91·8	**100**	75·8	75·7	75·3	74·6	76·1	74·3	75·9	51·1	51·1	56·4	55·7	54·2
	4F	59·3	59·1	58·5	68·8	69·4	**100**	99·9	81·3	81·1	82	81·7	82·3	51·9	52·7	54·8	54·9	53·4
	4S	59·3	59·1	58·5	68·8	69·4	100	**100**	81·4	81·1	82·1	81·8	82·4	51·9	52·8	54·9	54·9	53·4
	Hochi	55·9	56·1	56·5	66·5	64·9	78·2	78·2	**100**	98	91·9	84·5	84·9	53	52·8	54·4	54·4	53·2
	Wa	57·7	57·7	58·3	68·4	66·7	80·9	80·9	95·9	**100**	91·9	84·1	84·7	52·6	52·3	55·4	55·2	53·4
	IGV803	57·3	56·9	58·7	67·4	68·8	79·7	79·7	88·1	90·6	**100**	84·7	84·9	52·3	51·1	55·7	54·4	53·6
	OSU	59·3	59·1	59·8	66·5	67·4	82·1	82·1	82·8	85	84·8	**100**	84·9	51·3	52	54·7	54·4	53
	St 3	58·9	58·7	58·9	68	68·8	82·3	82·3	81·3	84	84·2	85·4	**100**	52·5	51·4	54·6	54·4	52·7
	EHP	38·2	39	38·1	37·3	37·4	39·8	39·8	40·1	41	40·2	40·5	38·5	**100**	91·3	55·2	54·8	58·3
	EW	39·1	40·1	31·1	37·4	39·5	40·7	40·7	40·7	42·6	40·7	41	37·7	91·9	**100**	55·6	55·5	59
	SA11	38·9	38·7	37·9	36·2	38	36·4	36·4	34·9	36·2	36·8	36·9	38·5	44·4	44·8	**100**	98·9	64·5
	SA11P	38·1	37·1	37·3	37	37·6	36·2	36·2	34·3	35·3	36	36·1	37·8	43·4	43·8	97·8	**100**	64·2
	RRV	38	37·8	37·1	37·3	37·7	38·6	38·6	38·7	39·8	37·9	38	40·1	49·6	50·6	57·4	56·8	**100**

Although the C-terminal half of NSP1 is highly diverse between strains, the N-terminal region is much more conserved. As an example, analysis of the first three NSP1 sequences including two bovine strains and one simian strain showed that the first 150 amino acids have a higher sequence similarity than the carboxy terminus, and from these sequences, a cysteine-rich region within the amino terminus was identified, which is not only conserved in group A rotaviruses but also in a group C rotavirus (Mitchell & Both, 1990; Bremont *et al*., 1993). The consensus sequence for this domain is C-X_2-C-X_8-C-X_2-C-X_3-H-X-C-X_2-C-X_5-C and subsequently these structures were proposed to be a C_4HC_3 two finger sequence based on comparisons to known zinc binding motifs (Hua *et al*., 1993; Freemont *et al*., 1991; Arnold and Patton, 2009).

The first 81 amino acids of NSP1 were demonstrated to be essential for dsRNA-binding activity, and the binding to the 5' ends of rotavirus mRNAs was also shown to be specific as the interaction could be competitively inhibited by unlabelled rotavirus mRNA but not by control yeast RNA however, the specific target of the binding activity and the role of RNA binding remains undefined (Brottier *et al*., 1992; Hua *et al*., 1994b). Mapping studies using deletion mutants suggested that a region of around 100 amino acids immediately downstream of the cysteine-rich region was responsible for the localization of NSP1, which is demonstrated in the cytoplasm, using immunofluorescence staining and cellular fractionation studies (Hua *et al*., 1994a). The more detailed sequence comparison between different rotavirus strains used in this project will be illustrated in Chapter 3 (Figure 3.1).

Despite the high levels of primary sequence divergence seen in NSP1, conservation was observed when predicted secondary structures of 17 strains of NSP1 from different species were aligned as shown in figure 1.5 (Hua *et al*., 1993; Xu *et al*., 1994). This strongly suggests that the higher-ordered structure of NSP1 may be maintained despite sequence divergence, consistent with a unified, conserved role for this protein in the virus life cycle.

1.3.2 NSP1 can interact with Interferon Regulatory Factors (IRFs)

When MA104 cell cDNA library was screened in a yeast two hybrid system using the NSP1 of B641 (bovine rotavirus strain) as bait, IRF3 was identified as a primary cellular interaction partner of NSP1 (Graff *et al*., 2002). A gluthathione S-transferase (GST) pull-down assay provided further evidence that NSP1 synthesized in rotavirus-infected cells (MA104) was also able to bind IRF3 (Graff *et al*., 2002). In the same study, NSP1 of the murine EW strain, which only shares 37% amino acid identity with B641 NSP1, was also shown to interact with murine IRF3 (Graff *et al*., 2002).

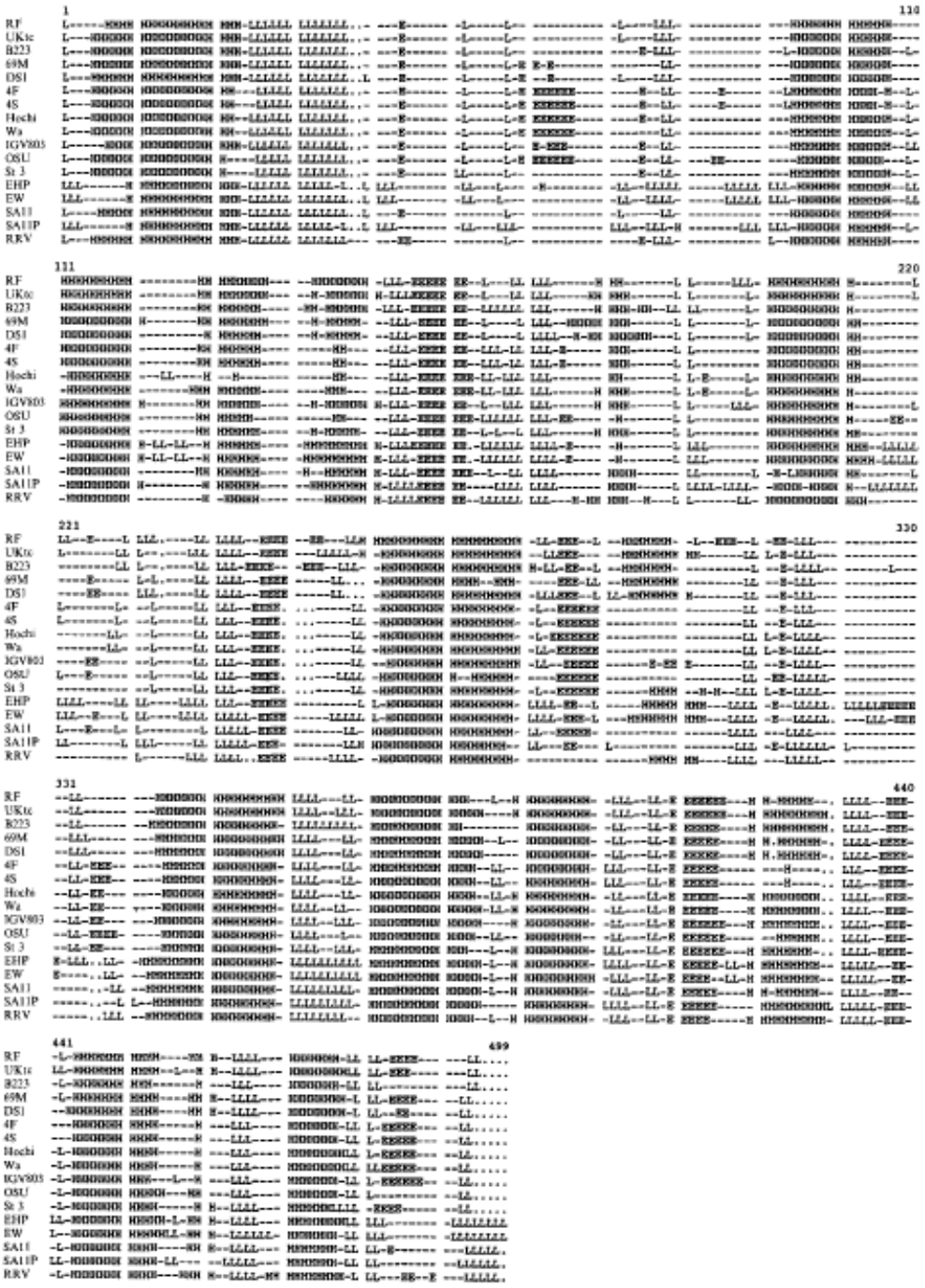

Figure 1.5 Conservation of predicted secondary structure across rotavirus NSP1.

E indicates positions predicted to have β-sheet structure, H denotes positions predicted as being α-helix and L denotes positions predicted to be in loops. Positions at which no prediction with an acceptable level of confidence could be made are indicated by '-' and gaps introduced to optimize the alignment by a '.' (figure taken from Xu *et al*., 1994).

The interaction between NSP1 and IRF3 has also been tested in virus-infected cells using the simian rotavirus SA11-4F strain. Immunoprecipitates made from SA11-4F infected MA104 cells showed co-precipitation of IRF3 with NSP1 indicating that an NSP1-IRF3 complex is formed during the viral replication cycle (Barro and Patton, 2005). By contrast, in a yeast two-hybrid screen, no interaction was seen between the NSP1 of the porcine strain OSU and MA104 cellular IRF3; furthermore in a GST pull-down assay, binding between these two proteins was less than 10% of that seen with the bovine B641 NSP1 (Graff *et al*., 2007). This specific interaction between NSP1 and IRF3 has also been studied in some other cell lines with other rotavirus strains: NSP1 from simian strain RRV and murine strain ETD have been shown to interact and degrade IRF3 in both COS7 (simian kidney fibroblast-like cells) and MEF (mouse embryonic fibroblast) cells (Feng *et al*., 2009; Sen *et al*., 2009). Bovine strain UKtc NSP1 has been demonstrated to have the same effect in Cos7 but not in MEF (Sen *et al*., 2009) while porcine strain OSU NSP1 has no such ability in either MA104 nor HEK293 (human embryonic kidney) cells (Graff *et al*., 2009). All these investigations indicated that the interaction between NSP1 and IRF3 is dependent on the virus strain type and cell line being used.

A series of mutations in NSP1 have been made to try to identify the IRF3 binding domain in the protein. It has been found that there is at least one point of contact with IRF3 in the C-terminal domain of NSP1 (Graff *et al*., 2002). Meaningful site directed mutagenesis within the C-terminal of NSP1 is problematic due to the high variability of the primary sequence. Consequently point mutations have to-date only been made within the zinc finger motif, and the mutants abolished the NSP1-IRF3 interaction,

suggesting that the zinc finger motif is important for NSP1-IRF3 interaction. However, because of the earlier mutagenesis results from the same group, at present the only conclusion that has been possible is that this region of NSP1 is involved in, but is not sufficient for, the interaction between the two proteins (Graff *et al*., 2002, 2007).

When NSP1 was found to interact with a key transcription factor (IRF3) required for activation of the innate immune system (Barro and Patton, 2005; Graff *et al*., 2002), it was suggested that the selection force driving NSP1 divergence could be the ability to interrupt the host's innate immune response. Further work has supported this idea, and suggested that the interaction between NSP1 and IRF3 functions to subvert the innate immune response by inducing degradation of IRF3. Immunoprecipitation studies with SA11-4F infected cells showed that the amount of IRF3 in infected cells was several-fold less than that in uninfected cells, indicating that IRF3 was being actively degraded during viral infection (Barro and Patton, 2005). Two naturally occurring viable C-terminal truncation mutants of NSP1 were also examined in this series of experiments. It was clear that less IRF3 degradation occurred in mutant infected cells than in those infected with wild type virus, providing further evidence that the region of NSP1 responsible for promoting degradation of IRF3 is near to the C-terminus of the protein (Barro and Patton, 2005). Studies using the proteasome inhibitor MG132 showed the level of IRF3 was maintained in cells cotransfected with wtNSP1 in the presence of the drug. By contrast a 50% reduction in the level of IRF3 was observed in the absence of MG132, indicating that the interaction of NSP1 with IRF3 triggers the latter's degradation through a proteasome-dependent pathway (Barro and Patton, 2005).

The current position is therefore that there appears to be two different areas of NSP1 involved in its interaction with IRF3, the highly variable C-terminal region responsible for the possible binding of IRF3, and the conserved zinc finger motif near the N-terminus of the protein. However, it is likely that mutation of the zinc-binding motif caused significant misfolding of NSP1 that inactivates the ability of NSP1 to degrade IRF3. This indicates that a better understanding of the overall structure of NSP1 is required to clearly define the molecular details of its interaction with IRF proteins.

1.3.3 NSP1 can induce proteasome-dependent degradation of β-TrCP

β-transducin repeat containing protein (β-TrCP), a component of the cellular E3 ubiquitin ligase complex $SCF^{\beta\text{-TrCP}}$, has been shown to be a target of NSP1 from a porcine rotavirus strain OSU for proteasome-dependent degradation (Graff *et al*, 2009). Cells transfected with plasmids encoding either OSU NSP1 or NCDV NSP1 (which was shown to degrade IRF3 in early studies, Graff *et al*, 2002), together with a reporter plasmid encoding firefly luciferase under control of the IFNβ promoter were analysed. When the cells were stimulated with a PAMP, it was found that the reporter expression in cells transfected with OSU NSP1 was inhibited ~20 fold compared to cells transfected with an empty vector, similar to that caused by NCDV NSP1, which could be attributed to IRF3 degradation (Graff *et al*., 2002). Therefore OSU NSP1 might utilize a different mechanism to inhibit IFNβ promoter-driven gene expression without a viral infection since it had previously been shown not to interact with IRF3 to cause its degradation (Graff *et al*., 2007).

Like IRF3, NFκB can also stimulate the expression of IFNβ and consequently Graff *et al* examined NFκB activation. Using an NFκB-responsive reporter, they showed that OSU NSP1 caused a 20-fold inhibition of NFκB driven reporter gene expression relative to cells transfected with the empty vector, which NCDV NSP1 only caused a 5-fold inhibition (Graff *et al*., 2009). These results suggest that the interference with activation of NFκB seem to be the predominant mechanism of IFN antagonism in OSU-infected cells. Additionally, the group tested the functionality of the $SCF^{\beta\text{-TrCP}}$ E3 ligase complex in the presence of NSP1, as it mediates proteasome-dependent degradation of IκBα and NFκB subunits which subsequently has an effect on NFκB activation. The results showed that, in contrast to uninfected cells, β-TrCP was detected only in cells infected with rotavirus strain A5-16, which encodes a truncated NSP1 (Taniguchi *et al*, 1996), not in those infected with OSU or NCDV. This result suggested that both OSU and NCDV NSP1s can target β-TrCP for degradation, even though the latter has a significantly reduced effect on NFκB signalling. When cells were transfected with Flag-β-TrCP then infected in the presence of MG132 with OSU and NCDV, β-TrCP levels remained stable, indicating that, as for IRF3, this degradation is also proteasome-dependent. The interaction between NSP1 and β-TrCP was eventually confirmed in OSU infected cells by co-immunoprecipitation of NSP1 with β-TrCP from cells expressing Flag-β-TrCP proteins (Graff *et al*, 2009). Studies on interactions between NSP1 and β-TrCP have been done in human cell lines with some other virus strains including murine strain ETD, simian strain SA11, canine strain K9, lapine strain 30-96, bovine UKtc and human Wi61. The results suggested that only the NSP1 from Wi61 has a similar effect on β-TrCP as that previously demonstrated for porcine strain OSU (Arnold and Patton, 2011).

1.3.4 Other NSP1 targets

Because the fact that there are shared multiple structural features in the IRF family, it is possible that by interacting with one of the common domains, the cellular targets for rotavirus NSP1 may not be limited to IRF3 and β-TrCP. Apart from the conserved DNA-binding domain near the N-terminal of all the IRF family members, some members have a serine-rich activation domain at the C-terminal region for phosphorylation, and others have a protein-protein interaction domain for mediating IRF dimerization (Barnes *et al*., 2002). It has been shown that NSP1 of SA11 can degrade IRF5 and IRF7 in addition to IRF3 (Barro and Patton, 2007), furthermore, murine strain ETD, rhesus strain RRV and lapine strain 30-96 also have the ability to induced degradation of IRF3, IRF5 and IRF7 (Arnold and Patton, 2011). Although the biological significance of this additional activity remains unclear, the degradation of IRF7 suggests that some rotaviruses may be particularly efficient in infecting specialized cells such like pDCs (plasmacytoid dendritic cells) which constitutively express IRF7 (Izaguirre *et al*., 2003). IRF5 is primarily detected in certain specialized cells such as DCs and B cells (Barnes *et al*., 2001); the ability of NSP1 to degrade IRF5 provided further evidence that NSP1 may support the virus in infecting specialised cells, which allows infections beyond the gut (Barro and Patton, 2007). Furthermore, it has also been reported that NSP1 from strains SA11 and OSU is able to inhibit RIG-I mediated activation of IFN-β in a dose-dependent way by interacting with RIG-I and causing subsequent RIG-I down regulation in a proteasome-independent manner (Qin *et al*., 2011), suggesting that RIG-I might be another target for NSP1 in antagonizing the innate immune system.

1.4 Aims of the study

Whilst there is considerable amount of evidence that NSP1 has evolved a number of ways to target components involved in the host innate immunity pathway, the complete nature of its IFN antagonist activity has yet to be revealed. Therefore the identification of the determinant of NSP1 sequence variations which influence its target specificity and activation efficiency may help to complete the mechanisms of NSP1 in rotavirus pathogenesis. The aim of this thesis is to gain a better understanding of the molecular determinant of NSP1 specificity for targeting the interferon production pathway by mapping the regions in NSP1 sequences responsible for specific host cellular targets.

Chapter 2

Materials and Methods

2.1 Materials

This section includes the complete collection of suppliers, cell lines, virus strains, bacterial strains, antibodies, primers and plasmids that were used in this study.

Table 2.1.1 List of suppliers used in this study

Supplier	Address
BD Biosciences	Edmund Halley Road, Oxford Science Park, Oxford, UK
Biorad	Bio-Rad Laboratories Ltd. Bio-Rad House, Maxted Road, Hempstead, UK
Cell Signaling Technology	Cell Signaling Technology, Inc, 3 Trask Lane, Danvers, MA 01923, USA
Clontech	Clontech Laboratories, Inc. A Takara Bio Company 1290 Terra Bella Ave. Mountain View, CA 94043, USA
Eppendorf	Eppendorf UK Ltd. Endurance House, Chivers Way, Histon, Cambridge, UK
Fermentas	Opelstrasse 9, St. Leon-Rot 68789, Germany
Fisher Scientific	Fisher Scientific UK Ltd. Bishop Meadow Road, Loughborough, UK
FUJIFILM	FUJIFILM UK Ltd. Unit 10A, St Martins Business Centre, St Martins Way, Bedfordshire, UK
GE Healthcare	GE Healthcare Life Sciences, Amersham Place, Little Chalfont, UK
Invitrogen	Life Technologies Ltd. 3 Fountain Drive, Inchinnan Business Park, Paisley, UK
Melford Laboratories Ltd	Melford Laboratories Ltd. Bildeston Road, Chelsworth, Ipswich, Suffolk, UK
New England Biolabs Inc	New England Biolabs (UK) Ltd. 75/77 Knowl Piece, Wilbury Way, Hitchin, Herts, UK

PEQLAB Ltd.	Building 34, Universal Marina, Sarisbury Green, UK
Promega	Promega UK, Delta House, Southampton Science Park, Southampton, UK
Qiagen	QIAGEN HOUSE, Fleming Way, Crawley, UK
Santa-Cruz Biotechnology	Santa Cruz Biotechnology, Inc. Bergheimer Str. 89-2 69115 Heidelberg, Germany
Sigma-Aldrich	Sigma-Aldrich Company Ltd. Dorset, UK
Stratect Scientific Ltd	Acorn Business Centre, Oaks Drive, Suffolk, UK
Thermo Scientific	Building 2B, 28 Schenck Parkway, Suite 400 Asheville, NC 28803, USA
Vector Laboratories Ltd	Vector Laboratories Ltd, 3 Accent Park, Bakewell Road, Orton Southgate, Peterborough, UK

Table 2.1.2 List of cell lines used in this study

Cell Line	Origin/Description	Culture medium
BSC-1	African green monkey kidney cells (Supplied by Prof. M. A. McCrae, University of Warwick)	GMEM NEAA + 5% (v/v) Fetal Bovin Serum (FBS)
HEK293	Human embryonic kidney cells (Supplied by Dr. K. N. Leppard, University of Warwick)	DMEM + 10% (v/v) Newborn Calf Serum (NBCS)
MA104	African green monkey kidney cells (Supplied by Prof. M. A. McCrae, University of Warwick)	GMEM NEAA + 5% (v/v) FBS

Table 2.1.3 List of Rotavirus strains used in this study

Strain	Phenotype
UKtc	Wild type tissue culture adapted Group A bovine RV
OSU	Wild type tissue culture adapted Group A porcine RV
P9Δ5	NSP1 Frame-shift deletion tissue culture adapted Group A feline RV

Table 2.1.4 List of bacterial strain used in this study

***Escherichia coli* strain**	**Genotype**
DH5α	F^- endA1 glnV44 thi-1 recA1 relA1 gyrA96 deoR nupG Φ80d*lacZ*ΔM15 Δ(*lacZYA-argF*)U169, hsdR17(r_K^- m_K^+), λ–

Table 2.1.5 List of primary antibodies used in this study

Antibody	Detail/Supplier	Dilution for Western Blotting
Rabbit anti-IRF3	Polyclonal FL-425 Santa Cruz Biotechnology	1:1000
Rabbit anti-β-TrCP	Polyclonal H-300 Santa Cruz Biotechnology	1:1000
Rabbit anti-HA epitope	Polyclonal Y-11 Santa Cruz Biotechnology	1:5000
Mouse anti-FLAG epitope	Monoclonal F3165 Sigma-Aldrich	1:100000

Rabbit anti-β-actin	Rabbit monoclonal #4970 Cell Signaling Technology	1:2000
Rabbit anti-p53	Polyclonal FL-393 Santa Cruz Biotechnology	1:10000
Rabbit anti-Gal4	Polyclonal SC-577 Santa Cruz Biotechnology	1:1000
Mouse anti-VP16	Monoclonal SC-7546 Santa Cruz Biotechnology	1:1000

Table 2.1.6 List of secondary antibodies used in this study

Antibody	**Detail/Supplier**	**Dilution for Western Blotting**
Goat anti-Mouse	Horseradish peroxidase conjugate Sigma-Aldrich	1:100000
Goat anti-Rabbit	Horseradish peroxidase conjugate Santa Cruz Biotechnology	1: 100000

Table 2.1.7 List of primers used in this study

Primer name	Sequence 5'-3'	Application
mpCR2.1_PstI 5'	GTCCGGTGCCCTGAATGAACTCCAGGACGAGGCAGCGCGGCTA	Mutation of *Pst* I site in mpCR2.1vector
mpCR2.1_PstI 3'	CGATAGCCGCGCTGCCTCGTCCTGGAGTTCATTCAGGGCACCG	Mutation of *Pst* I site in mpCR2.1vector
UKtc-EcoI 5'	GCGCGAATTCATGGCTACGTTCAAAGACGC	PCR primer for cloning UKtcNSP1 into mpCR2.1 vector
UKtc-XhoI 3'	GCGCCTCGAGTTATTCAACATCTGAAAGTTCTAAGTCG	PCR primer for cloning UKtcNSP1 into mpCR2.1 vector
OSU-BamHI 5'	GCGCGGATCCATGGCTACTTTTAAGGATGC	PCR primer for cloning OSUNSP1 into mpCR2.1 vector
OSU-XhoI 3'	GCGCCTCGAGTTATTCAACATCAGATATACCG	PCR primer for cloning OSUNSP1 into mpCR2.1 vector
UKtc-StuI 5'	GCAAATGATGAATGGAGGCCTGCACCAGTGACAAAATACAAAGGG	Mutagenesis PCR primer for UKtcNSP1 to create *Stu* I site
UKtc-StuI 3'	CCCTTTGTATTTTGTCACTGGTGCAGGCCTCCATTCATCATTTGC	Mutagenesis PCR primer for UKtcNSP1to create *Stu* I site
UKtc-PmlI 5'	GGATGTGCTTTGTACCACGTGTGTCAGTGG	Mutagenesis PCR primer for UKtcNSP1to create *Pml* I site
UKtc-PmlI 3'	CCACTGACACACGTGGTACAAAGCACATCC	Mutagenesis PCR primer for UKtcNSP1to create *Pml* I site
UKtc-AclI 5'	CGGAAACGTTGGGCAGTGTTCG	Mutagenesis PCR primer for UKtcNSP1to create *Acl* I site

UKtc-AclI 3’	CGAACACTGCCCAACGTTTCCG	Mutagenesis PCR primer for UKtcNSP1to create *Acl* I site
UKtc-HpaI 5’	GGACTATGAAGTTAACTGGGAAGTGAGAGG	Mutagenesis PCR primer for UKtcNSP1to create *Hpa* I site
UKtc-HpaI 3’	CCTCTCACTTCCCAGTTAACTTCATAGTCC	Mutagenesis PCR primer for UKtcNSP1to create *Hpa* I site
UKtc-PstI 5’	GCCAATAACACTGCAGGCATTAACTATAAAACTTGAAGATAGC	Mutagenesis PCR primer for UKtcNSP1to create *Pst* I site
UKtc-PstI 3’	GCTATCTTCAAGTTTTATAGTTAATGCCTGCAGTGTTATTGGC	Mutagenesis PCR primer for UKtcNSP1to create *Pst* I site
UKtc-HindIII 5’	GGGATTATATCAAAGCTTGTAAAGCC	Mutagenesis PCR primer for UKtcNSP1to create *Hind* III site
UKtc-HindIII 3’	GGCTTTACAAGCTTTGATATAATCCC	Mutagenesis PCR primer for UKtcNSP1to create *Hind* III site
OSU-StuI 5’	GGAGTTAATGATACATGGAGGCCTTCACCTCCAACTAAATACAAAG	Mutagenesis PCR primer for OSU to create *Stu* I site
OSU-StuI 3’	CCTTTGTATTTAGTTGGAGGTGAAGGCCTCCATGTATCATTAACTCC	Mutagenesis PCR primer for OSU to create *Stu* I site
OSU-PmlI 5’	GGCTGTACCATGTATCACGTGTGTCAATGGTGTAGTCAATATGG	Mutagenesis PCR primer for OSU to create *Pml* I site
OSU-PmlI 3’	CCATATTGACTACACCATTGACACACGTGATACATGGTACAGCC	Mutagenesis PCR primer for OSU to create *Pml* I site
OSU-AclI 5’	CGAGCTTTAGTTAAATCAAACGTTAATGTTGG	Mutagenesis PCR primer for OSU to create *Acl* I site

OSU-AclI 3’	CCAACATTAACGTTTGATTTAACTAAAGCTCG	Mutagenesis PCR primer for OSU to create *Acl* I site
OSU-PstI 5’	GCCAATAACACTGCAGTCTCTGTCAATTGAATTGG	Mutagenesis PCR primer for OSUNSP1to create *Pst* I site
OSU-PstI 3’	CCAATTCAATTGACAGAGACTGCAGTGTTATTGGC	Mutagenesis PCR primer for OSUNSP1to create *Pst* I site
OSU-HindIII 5’	GCGCAAACTCAAAATAGCATCTAAGCTTATAAAACC	Mutagenesis PCR primer for OSUNSP1to create *Hind* III site
OSU-HindIII 3’	GGTTTTATAAGCTTAGATGCTATTTTGAGTTTGCGC	Mutagenesis PCR primer for OSUNSP1to create *Hind* III site
UKtc-Flag 5’	AATTCACCATGGATTACAAGGATGACGACGATAAGC	PCR primer for addition of Flag tag at UKtcNSP1 N-terminal
UKtc-Flag 3’	GTGGTACCTAATGTTCCTACTGCTGCTATTCGTTAA	PCR primer for addition of Flag tag at UKtcNSP1 N-terminal
OSU-Flag 5’	GATCCACCATGGATTACAAGGATGACGACGATAAGCC	PCR primer for addition of Flag tag at OSUNSP1 N-terminal
OSU-Flag 3’	GTGGTACCTAATGTTCCTACTGCTGCTATTCGGCTAG	PCR primer for addition of Flag tag at OSUNSP1 N-terminal
IRF3-EcoRI 5’	GCGCGAATTCATGGGAACCCCAAAGCCACGGATCC	PCR primer for cloning IRF3 into PM/PVP16 vector
IRF3-EcoRI 3’	GCGCGGATTCTCAGCTCTCCCCAGGGCCCTGGAAATCC	PCR primer for cloning IRF3 into PM/PVP16 vector
β -TrCP-BamHI 5’	GCGCGGATCCAAATGGACCCGGCAGAGGCGGTGC	PCR primer for cloning β -TrCP into PM/PVP16 vector

β -TrCP-BamHI 3’	GCGCGGATCCTTATCTGGAGATGTAGGTGTATGTTCG	PCR primer for cloning β -TrCP into PM/PVP16 vector
PM seq F primer	GCGGCTTCAGTGGAGACTGATATGCC	Sequencing primer for PM vector associated genes
PM seq R primer	GCGCGGTTCAGGGGGAGGTGTGG	Sequencing primer for PM vector associated genes
PVP16 seq F primer	GCCGGGATTTACCCCCACGACTCCG	Sequencing primer for PVP16 vector associated genes
PVP16 seq R primer	GCATTCATTTTATGTTTCAGGTTCAGGG	Sequencing primer for PVP16 vector associated genes
M13 F primer	GTAAAACGACGGCCAG	Sequencing primer for pCR2.1 vector associated genes
M13 R primer	CGAGAAACAGCTATGAC	Sequencing primer for pCR2.1 vector associated genes
UKtc CMV seq primer	GCTCCTAGTTTAAGTACTAAGC	Sequencing primer for CMV promoter
OSU CMV seq primer	GGT CTC CAT GTA TCA TTA ACT CC	Sequencing primer for CMV promoter
RT_common F primer	GCGCTAACGCAGTCAGTGCTTCTGAC	Common forward PCR primer for UKtc and OSUNSP1 to detect RT reaction
RT_UKtc R primer	GCCCATTCATCATTTGCTCC	PCR reverse primer for UKtcNSP1 to detect RT reaction
RT_OSU R primer	GCCCATGTATCATTAACTCC	PCR reverse primer for OSUNSP1 to detect RT reaction

Table 2.1.8 List of plasmids used in this study

Plasmid	Description
mpCR2.1 vector	Modified pCR2.1 vector with altered *Acl* I (p2315 and 2688), *Pst* I (p1499) and *Hind* III (p235) sites
mpCR2.1-UKtcNSP1	UKtcNSP1 cloned into mpCR2.1 vector between restriction enzyme sites *EcoR* I and *Xho* I
mpCR2.1-OSUNSP1	OSUNSP1 cloned into mpCR2.1 vector between restriction enzyme sites *BamH* I and *Xho* I
mpCR2.1-UKtc-StuI	UKtcNSP1expressing plasmid with *Stu* I site generated
mpCR2.1-UKtc-PmlI	As mpCR2.1-UKtc-StuI with *Pml* I site generated
mpCR2.1-UKtc-HpaI	UKtcNSP1expressing plasmid with *Hpa* I site generated
mpCR2.1-UKtc-AclI	As mpCR2.1-UKtc-HpaI with *Acl* I site generated
mpCR2.1-OSU-StuI	OSUNSP1expressing plasmid with *Stu* I site generated
mpCR2.1-OSU-PmlI	As mpCR2.1-OSU-StuI with *Pml* I site generated
mpCR2.1-OSU-AclI	OSUNSP1expressing plasmid with *Acl* I site generated
mpCR2.1-UKtcNSP1-4RE	UKtcNSP1expressing plasmid with *Stu* I, *Pml* I, *Acl* I and *Hpa* I sites generated
mpCR2.1-OSUNSP1-4RE	OSUNSP1expressing plasmid with *Stu* I, *Pml* I and *Acl* I sites generated
pM-53	4.6 kb positive control plasmid expressing a fusion of the GAL4 DNA-BD to the mouse p53 protein(Clonetech)
pVP16-T	5.3 kb positive control plasmid expressing a fusion of the VP16 AD to the SV40 large T-antigen which is known to interact with p53(Clonetech)
pVP16-CP	4.5 kb negative control plasmid expressing a fusion of the VP16 AD to a viral coat protein which does not interact with p53(Clonetech)
pM-OSUNSP1	OSUNSP1 expression plasmid fused to the GAL4 DNA-BD
pM-UKtcNSP1	UKtcNSP1 expression plasmid fused to the GAL4 DNA-BD (Provided by Dr K.T.Chung, University of Warwick)

pVP16-UKtcNSP1	UKtcNSP1 expression plasmid fused to the VP16 AD (Provided by Dr K.T.Chung, University of Warwick)
pVP16-OSUNSP1	OSUNSP1 expression plasmid fused to the VP16 AD
pEFplink2-IRF3	IRF3 expression plasmid (Provided by Dr S Goodbourn, University of London)
pcDNA3.1-HA-IRF3	IRF3 expression plasmid with 3 HA epitope sequence tagged at C-terminal of IRF3
pM-IRF3	IRF3 expression plasmid fused to the GAL4-DNA-BD
pVP16-IRF3	IRF3 expression plasmid fused to the VP16 AD
pcDNA3.1-HA- β-TrCP1a	β-TrCP expression plasmid with HA tagged (Provided by Dr A Stephanou, University of London)
pM-β-TrCP	β-TrCP expression plasmid fused to the GAL4-DNA-BD
pVP16-β-TrCP	β-TrCP expression plasmid fused to the VP16 AD
pcDNA3.1- UKtcNSP1-4RE	Expression plasmid for UKtcNSP1 with 4 selected RE sites generated
pcDNA3.1- OSUNSP1-4RE	Expression plasmid for OSUNSP1 with 4 selected RE sites generated
pcDNA3.1- Flag_UKtcNSP1-4RE	As pcDNA3.1- UKtcNSP1-4RE with a FLAG epitope sequence (MDYKDDDDK) tagged upstream of the NSP1 translation initiation codon
pcDNA3.1- Flag_OSUNSP1-4RE	As pcDNA3.1- OSUNSP1-4RE with a FLAG epitope sequence (MDYKDDDDK) tagged upstream of the NSP1 translation initiation codon
pCIneo- Flag_UKtc NSP1-4RE	Expression plasmid for UKtc NSP1-4RE
pCIneo- Flag_OSU NSP1-4RE	Expression plasmid for OSU NSP1-4RE
pA	Expression plasmid for NSP1 with the sequences between RE sites *Stu* I and *Acl* I came from OSUNSP1 and the rest from UKtcNSP1
pB	Expression plasmid for NSP1 with the sequences between RE sites *Stu* I and *Acl* I came from UKtcNSP1 and the rest from OSUNSP1
pC	Expression plasmid for NSP1 with the sequences between RE sites *EcoR* I and *Pml* I came from UKtcNSP1 and the rest from OSUNSP1
pD	Expression plasmid for NSP1 with the sequences between RE sites *EcoR* I and *Pml* I came from OSUNSP1 and the rest from UKtcNSP1

pE	Expression plasmid for NSP1 with the sequences between RE sites *Hpa* I and *Xho* I came from OSUNSP1 and the rest from UKtcNSP1
pF	Expression plasmid for NSP1 with the sequences between RE sites *Hpa* I and *Xho* I came from UKtcNSP1 and the rest from OSUNSP1
pG	Expression plasmid for NSP1 with the sequences between RE sites *Eco* I and *Stu* I came from UKtcNSP1 and the rest from OSUNSP1
pH	Expression plasmid for NSP1 with the sequences between RE sites *Eco* I and *Stu* I came from OSUNSP1 and the rest from UKtcNSP1
pI	Expression plasmid for NSP1 with the sequences between RE sites *Acl* I and *Hpa* I came from OSUNSP1 and the rest from UKtcNSP1
pJ	Expression plasmid for NSP1 with the sequences between RE sites *Acl* I and *Hpa* I came from UKtcNSP1 and the rest from OSUNSP1
pK	Expression plasmid for NSP1 with the sequences between RE sites *Acl* I and *Xho* I came from OSUNSP1 and the rest from UKtcNSP1
pL	Expression plasmid for NSP1 with the sequences between RE sites *Acl* I and *Xho* I came from UKtcNSP1 and the rest from OSUNSP1
pIFNβ-Luc	A firefly luciferase reporter plasmid of the *Homo sapiens* interferon β promoter. The promoter lies upstream of the firefly luciferase gene. (King & Goodbourn, 1994)
pPRDI/III-Luc	ptk-Luciferase reporter plasmid (Promega) containing the PRDI/III element of the IFN β promoter (Provided by Dr Y Ke, Peking University College of Oncology)
pConA-Luc	A firefly luciferase reporter driven by the NFkB sites in the Concanavalin A promoter (Mankouri et al. 2010 PLoS Pathogens)
pcDNA3.1-HisB::*lac*Z	β-galactosidase expression plasmid driven by the CMV IE promoter region (Invitrogen)
pUAST-hrGFP-neo	GFP expression plasmid under the control of a Gal4-responsive promoter (Provided by Dr K.T.Chung, University of Warwick)

2.2 Methods

2.2.1 Bacteriological techniques

2.2.1.1 Growth of bacteria

The bacteria were grown in liquid LB medium containing appropriate antibiotics (100μg/ml of ampicillin or 25 μg/ml of kanamycin) in a sterile vessel with approximately four times the volume of the liquid culture at 37°C and shaken vigorously.

2.2.1.2 Preparation of competent cells

DH5α was used as competent cells throughout the entire study. 2ml of fresh overnight bacterial culture was inoculated into 200ml of pre-warmed liquid LB medium and shaken vigorously at 37°C until OD_{600} of the culture reached 0.39. The culture was then put on ice for 5 minutes followed by centrifugation (Beckman Coulter Allegra^{TM} X-12R Centrifuge) at 6,000rpm for 10 minutes at 4°C. The pellet was resuspended in 80ml of ice-cold transformation buffer I (10Mm $RbCl_2$, 30mM potassium acetate, 10mM $CaCl_2$, 50Mm $MnCl_2$ and 15% (v/v) glycerol, pH 5.8) and then left on ice for 5 minutes. Centrifugation was repeated at 6,000rpm for another 10 minutes at 4°C; the pellet was subsequently resuspended in 8ml of ice-cold transformation buffer II (75mM $CaCl_2$, 10mM $RbCl_2$, 10mM MOPS and 15% (v/v) glycerol, pH 6.5) and left on ice for 2 hours. The competent cells were transferred

into 100µl aliquots for use or frozen with dry ice before storage at -70°C (up to three months).

2.2.1.3 Transformation of competent bacterial cells by heat shock

Ligation product or plasmid DNA (typically 50ng) was added into 100µl of thawed competent cells and left on ice for 30 minutes. Cells were heat shocked for 45 seconds in a 42°C water bath followed by immediate incubation on ice for another 2 minutes. 400µl of pre-warmed liquid LB medium was added to the competent cell mixture and incubated at 37°C in a shaking incubator for 1 hour; the cells were then plated onto LB plates containing appropriate selection of antibiotics and incubated at 37°C overnight.

2.2.1.4 Transformation of competent bacterial cells by electroporation

Competent bacterial cells for electroporation were prepared as described previously until the OD_{600} reached around 0.39. Cells were then pelleted and washed in equal, half and a quarter volumes of ice-cold H_2O containing 10% glycerol, cells were finally resuspended in 3ml of ice-cold H_2O containing 10% glycerol. The resuspended cells were aliquoted into 100µl and used immediately or stored at -70°C until used. The entire electroporation procedures were carried out on ice. Pre-cooled 0.2cm cuvettes containing competent cells and DNA (typically total volume of 50µl) were inserted into the cuvette slides of Bio-Rad Gene Pulser system which was previously set with voltage at 2.5 kV, capacitance at 25µFD, capacitance extender at 150 µFD and pulse controller at 200 Ohms resistance. The time constant value was

used to monitor electroporation with a reading above 4.6 being considered as a successful electroporation. Cells were then incubated in liquid LB medium for 1 hour at 37°C and then plated on LB agar plates containing appropriate antibiotics.

2.2.1.5 Extraction of plasmid DNA (Mini Prep, Midi Prep and Maxi Prep)

Plasmids were extracted using Qiagen MiniprepKit™, Promega Pureyield™ Plasmid Midiprep System or Sigma GenEluteTM Plasmid Maxiprep Kit according to specific requirements for the utility of the plasmids; all the protocols were obtained from the manufacturers' instructions.

2.2.1.6 Quantification of nucleic acid

The concentration of DNA and RNA samples was quantified using Nanodrop-ND1000 spectrophotometer (Thermo Scientific) by measuring OD_{260}. The purity of DNA and RNA was indicated by the absorbance ratio of OD_{260} to OD_{280}, where a ratio of 1.8 indicates pure DNA and a ratio of 2 indicates pure RNA.

2.2.1.7 Blue/white selection of bacterial colonies

LB plates containing appropriate antibiotics were aseptically covered with 40µl of 20mg/ml X-Gal (Melford Laboratories Ltd.) in DMF and 4µl of IPTG (Melford Laboratories Ltd.). The plates were then left to dry at 37°C for 1 hour and ready for inoculation overnight. On the next day, plates were examined for white colonies as these indicate the ones containing the plasmid carrying the inset of interest. Selected

white colonies were transferred to 5ml of pre-warmed liquid LB medium containing appropriate antibiotics and incubated overnight in a 37°C shaking incubator for plasmid DNA extraction.

2.2.2 Manipulation of DNA

2.2.2.1 Standard Polymerase Chain Reaction (PCR)

Standard PCR amplifications were carried out in a final volume of 50µl in 0.5ml microcentrifuge tubes using a Primus 96 advanced Gradient Innovative PCR Technology (PeQLab). The reaction mixture usually included 50ng of template DNA, 100ng of each primer, 0.25µM of each dNTP, 5µl of 10X PCR Buffer, 1.5mM of $MgCl_2$ and 2 units of *Taq* polymerase (Invitrogen). The mixture was incubated at 94°C for 1 min and subjected to 40 PCR cycles as follows: denaturing at 94°C for 1 min, annealing at 55-60°C for 1 min and extending at 72°C for 1 min/kb of amplicon. The annealing temperature was adjusted depending on the GC content of the specific primers used in order to reduce non-specific amplification in some individual PCR reactions.

2.2.2.2 Site-Direct Mutagenesis PCR

All mutagenesis PCR was performed with Platinum *Pfx* DNA polymerase (Invitrogen) to ensure higher fidelity. According to the manufacture's instruction, $MgSO_4$ was used as a source of magnesium. The reaction mixture (typically 50µl) containing 100ng of template DNA, 100ng of each primer, 0.25µM of each dNTP,

5µl of 10X PCR Buffer, 1.5-3mM of $MgSO_4$ and 2 units of Platinum *Pfx* DNA polymerase was incubated at 94°C for 1 min followed by 30 cycles of 94°C for 1 min, 55-58°C for 1 min and 68°C for 1 min/kb of amplicon. The annealing temperature was adjusted depending on the GC content of the specific primers used and the final concentration of magnesium was adjusted in some individual PCR reactions for optimization. The mutagenesis PCR product was digested with *Dpn* I to remove methylated template before ligating into the appropriate vectors.

2.2.2.3 Restriction Enzyme Digest

Typically up to 1µg of plasmid DNA or PCR product was digested in a total reaction volume of 50µl. Restriction enzymes were used with recommended reaction buffers according to the manufacturer's instructions. In reactions requiring multiple restriction enzyme digests, reaction buffer selected was the most optimal for all enzymes; in which this was not possible, sequential digestions were carried out, with DNA being purified after each reaction with a GFX PCR DNA and gel band purification kit (GE Healthcare) according to the manufacturer's instructions.

2.2.2.4 De-phosphorylation of vector DNA

Removal of 5' phosphate groups from DNA was achieved by adding 1 unit of shrimp alkaline phosphatise (SAP) (Fermentas) to per µg of DNA treated according to the manufacturer's instructions. SAP was inactivated by incubating the reaction mixture at 65°C for 15 minutes.

2.2.2.5 Conversion of 5' overhangs restriction enzyme ends to blunt ends

5' overhangs generated in a restriction enzyme digestion were filled in using large fragment of DNA polymerase I (1unit/µg DNA treated) (Invitrogen) in the supplied buffer together with 0.5mM of each dNTP at room temperature for 15 minutes. The fill-in reaction was subsequently terminated by phenol extraction.

2.2.2.6 Phenol/Chloroform extraction

An equal volume of Phenol/Chloroform/iso-amyl alcohol solution was added to the DNA sample followed by vortexing for 1 minute, the mixture was centrifuged at 16,000 x g in a micro-centrifuge for 2 minutes. The upper layer was then transferred to a clean tube and an equal volume of chloroform/iso-amyl alcohol was added. The mixture was vortexed and centrifuged again as before. The upper layer was transferred to a clean tube containing distilled H_2O making the final volume of 250µl and stored at -20°C until needed.

2.2.2.7 Ethanol precipitation of DNA

DNA in aqueous solution was precipitated by adding 1/10 volume of 3M sodium acetate pH 5.2 and 2.5 X volume of 100% ice-cold ethanol. After incubation at -70°C for 1 hour, precipitated DNA was collected by centrifuging at 13,200rpm at 4°C for 10 minutes using a tabletop microcentrifuge. Pellets were washed in 80% ice-cold ethanol followed by drying in a vacuum dessicator for 20 minutes. Pellets were then resuspended in 50µl of sterile distilled water.

2.2.2.8 Agarose gel electrophoresis of DNA

DNA molecules were typically separated by elecreophoresis on 1% (w/v) agarose in 1X TBE buffer (89mM Tris base, 89mM Boric acid and 2mM EDTA) containing 0.5µg/ml ethidium bromide. DNA samples were loaded onto the gel in 1X loading buffer (5% (w/v) glycerol, 0.04% (w/v) bromophenol blue and 0.04% (w/v) xylene cyanol). Electrophoresis was carried out in 1X TBE buffer at 70V for 1 hour. DNA fragments were visualised under UV light and imaged using a BioRad Gel/Chemi Doc system with associated software.

2.2.2.9 Agarose Gel Extraction of DNA

DNA bands of interest were excised from the agarose gel using a clean scalpel under UV light. The DNA was recovered using a Qiagen Gel Extraction Kit or a GFX PCR DNA and gel band extraction kit under the instructions recommended by the manufacturers.

2.2.2.10 DNA Ligation

Ligation of DNA molecules was performed in a final reaction volume of 20-50µl. A 3:1 molar ratio of insert DNA to vector DNA was typically used. This ratio was changed to 5:1 in some particular reactions to increase ligation efficiency. T4 DNA ligase was used according to the manufacturer's instructions with supplied buffers under recommended conditions.

2.2.2.11 DNA Sequencing

All DNA sequencing was done in-house by the Molecular Biology Service at University of Warwick using an automated ABI PRISM 3130xl Genetic Analyse. Sequencing data were viewed using Chromas Lite 2.0 and analysed using Clone Manager, SciEd Central, v7.04 software.

2.2.2.12 Transfection of plasmid DNA

Lipofectamine 2000 (Invitrogen) was used for liposome-mediated transfection of plasmid DNA throughout the entire study. A ratio of 2µl of reagent per µg of plasmid DNA transfected was used, and this ratio was applied to all transfections in all cell lines used during this study.

All transfections were performed in 12 or 24-well plates. Cells were seeded about 24 hours before the procedure to allow approximately 60-70% of cell confluence by the time of transfection. Transfection reagent and DNA mixture was prepared in pre-warmed OptiMEM medium to make a total volume of 100µl (24-well plate) or 200µl (12-well plate) per well. After incubation for 20 minutes at room temperature the complex mixtures were gently pipetted onto the cells containing serum medium. Cells were then incubated at 37°C in a 5% CO_2 incubator for 24 or 40 hours depending on different requirements for individual experiment.

2.2.3 Manipulation of RNA

2.2.3.1 Extraction of RNA from cultured 293 cells

RNA sample was extracted from one well of confluent cells in 12-well plates. Cells were washed twice with 500µl of ice-cold sterile TBS and harvested by centrifuging at 3,000rpm for 3 minutes at 4°C. The pellets were resuspended in 40µl of ice-cold isotonic buffer (150mM NaCl, 10mM Tris/HCl and 1.5mM $MgCl_2$, pH 7.6) containing 10% NP40 (200µl of 10%NP40 per 3ml of isotonic buffer). 250µl of TRI reagent (Sigma-Aldrich) was added to the cell suspension and left at room temperature for 2 minutes. 50µl of chloroform was then added and left at room temperature for another 10 minutes. The mixture was subsequently centrifuged at 13,000rpm for 10 minutes at 4°C. The upper aqueous layer of the mixture was carefully removed into a fresh tube containing 200µl of ice-cold isopropanol, and the mixture was left at -20°C overnight or longer for storage until required.

When RNA was needed, the mixture was centrifuged at 13,000rpm for 10 minutes at 4°C. The pellet was washed with 75% ice-cold ethanol and centrifuged again at 13,000rpm for 10 minutes at 4°C. The pellet was then air-dried for 15 minutes and if required, it can be left to dry for another 20 minutes in a vacuum dessicator. Finally the pellet was resuspended in 50µl of RNAse-free water and used for analysis immediately or stored at -20°C until required.

2.2.3.2 Reverse-Transcription (RT) PCR

1µg of RNA was used per reaction for reverse transcription. Reactions were performed in a total volume of 50µl using SS-Reverse Transcriptase (Fermentas) according to the manufacturer's instructions. Reactions were left to proceed for 1 hour at 42°C before incubation at 70°C for 15 minutes to terminate reverse transcriptase activity. 0.5µl of RNase H was added to the reaction followed by incubation at 37°C for 20 minutes. 2.5µl of the final reaction volume was used for subsequent PCR analysis.

2.2.3.3 Transfection of cells by poly (I:C)

Lipofectamine 2000 (Invitrogen) was used for transfecting cells with poly (I:C) with a ratio of 2µl of transfecting reagent per µg of poly(I:C) throughout the entire study. The mixtures were prepared in pre-warmed OptiMEM medium to make a total volume equivalent to 100µl (24-well plate) or 200µl (12-well plate) per well. The mixture was left for incubation at room temperature for 20 minutes and gently pipetted into the cells containing serum medium. Cells were incubated for 16 hours before being harvested for further analysis.

2.2.4 Mammalian cell culture techniques

2.2.4.1 Maintenance of tissue culture cells

Mammalian cell lines were maintained at 37°C in a 5% CO_2 incubator in a humidified atmosphere using appropriate medium (Table 2.1.2). Cells were passaged every 3 to 4 days based on different demands. When confluent, the cells were detached by rinsing the cell monolayer with versene (0.02% EDTA in PBS) followed by incubation with trypsin/versene (1:5 v/v) for cell disaggregation; cell suspensions were then centrifuged at 13,000rpm for 3 minutes to form pellet; cell pellets were resuspended and reseeded at appropriate ratios (1:4 for 293, BSC-1 and MA104 cells). All manipulations were carried out under sterile conditions in a Class II Laminar Flow Cabinet using standard aseptic techniques.

2.2.4.2 Growth of rotavirus

Cell monolayers were washed twice with serum-free medium and inoculated with pre-treated rotavirus (10μg of trypsin per μl of virus inoculum) diluted in serum-free medium with an m.o.i of 0.5 for 40 minutes at 37°C. The inoculum was then removed by aspiration and serum-free medium was replaced, the cells were incubated at 37°C until the cytopathic effect (CPE) reached about 80% after typically 5-6 days. A sterile rubber policeman was used to harvest the infected cell. The infected cells were treated with three freeze-thaw cycles, aliquoted and stored at -70°C until required.

2.2.4.3 Titration of virus stocks

Serial ten-fold dilutions of pre-trypsin treated virus stock were prepared in serum-free GMEM, and 0.2ml of each virus dilution was added to confluent BSC-1 cell monolayers in 12-well plates. After incubation at 37°C for 40 minutes, the inoculum was removed by aspiration and 2ml of serum-free GMEM overlay containing 1μg/μl trypsin was added to each well and incubated at 37°C for 4-5 days for development of virus plaques. The cells were then fixed with formal-saline (30% (v/v) formaldehyde in PBS) overnight. The virus plaques were visualised by staining the remaining cells with 0.1% (w/v) crystal violet.

2.2.4.4 MG132 treatment

293 cells were transfected with plasmid DNA as described previously. 40 hours post transfection, the medium was replaced with 1ml of 10% FBS DMEM containing 50μM MG132 (Sigma-Aldrich or Stratect Scientific Ltd). Cells were left to incubate at 37°C for a further 8 hours before harvest.

2.2.4.5 Mammalian two-hybrid assay

Mammalian two-hybrid assay was performed using Matchmaker^{TM} Mammalian Assay Kit according to the manufacturer's instructions and recommended protocol. pUAST-hrGFP-neo expressing green fluorescent protein (provided by Dr K.T.Chung, University of Warwick) was used as the reporter plasmids and cells were visualised under UV microscopy.

2.2.5 Protein expression and analysis

2.2.5.1 Coupled Transcription/Translation system

Coupled transcription/translation was performed using TNT T7 Quick Coupled Transcription/Translation system (Promega) according to the manufacture's recommended protocol with ^{35}S methionine incorporated for visualization.

2.2.5.2 Determination of protein concentration

The Bio-Rad protein assay™ was used according to the manufacture's instructions using bovine serum albumin (BSA) generating a standard curve for comparison of protein concentrations.

2.2.5.3 Harvesting of total cellular protein

Cell monolayers were washed once with PBS before incubation with 100µl of 1X sample buffer with DTT (50µl of 2X sample buffer (2ml 10% SDS stock solution, 1ml glycerol, 250µl of 1M Tris-HCl pH6.8, 1.75ml of dH_2O and grains bromophenol blue), 10µl of DTT and 40µl of dH_2O) per well in a 24-well plate at room temperature for 5 minutes. The cell lysates were collected and boiled for 10 minutes to denature the proteins and used immediately or stored at -70°C for future analysis.

2.2.5.4 SDS-Polyacrylamide Gel Electrophoresis (SDS-PAGE)

Denatured protein samples were separated by SDS-PAGE. Gels were made of a 5% acrylamide stacking gel and a 10% acrylamide resolving gel. Typically, electrophoresis was performed for 1.5 hours at 120V in 1X running buffer (25mM Tris, 192mM glycine and 0.1%SDS, pH8.3) at room temperature. All SDS-PAGE performed in this study utilised the Bio-Rad mini-PROTEIN III systems according to the manufacturer's instructions.

2.2.5.5 Transfer of proteins onto nitrocellulose membranes

Prior to transfer the stacking gel was removed, and the separated proteins from the resolving gel were transferred onto nitrocellulose membranes. Transfers were performed in 1X transfer buffer (25mM Tris base, 192mM glycine and 20% methanol) at 4°C at 350mA for 1.5 hours or 80mA overnight using the Bio-Rad Mini Trans-Blot Electrophoretic Transfer Cell system according to the manufacturer's instructions. All transfers utilised Hybond^{TM} ECL^{TM} nitrocellulose membranes throughout this study.

2.2.5.6 Western Blotting

Nitrocellulose membranes were incubated for 1.5 hours in 20ml of blocking solution (2% milk in PBS containing 0.05% (v/v) Tween-20 or 5% BSA in TBS containing 0.1% (v/v) Tween-20) at room temperature on an orbital shaker. Membranes were then probed with 3ml of selected primary antibody against the protein of interest

diluted in appropriate blocking solution for 1 hour at room temperature on the shaker. The dilution of the primary antibody was dependent upon the protein of interest (Table 2.1.5). Membranes were then washed for 1 hour on the shaker with PBS containing 0.05% (v/v) Tween-20 or TBS containing 0.1% (v/v) Tween-20 with the washing buffer replaced every 8-10 minutes. The membranes were then probed with 3ml of the appropriate secondary antibody (Table 2.1.6) diluted in blocking solution for 1 hour. Membranes were then washed for 1 hour again with the washing buffer replaced every 8-10 minutes. The blots were developed using ECL^{TM} Advance according to the manufacturer's instructions and exposed to FUJI superRX X-Ray Film and developed using an AGFA Curix60 developer.

2.2.5.7 Co-Immunoprecipitation

Co-Immunoprecipitation was performed using ANTI-FLAG M2 Affinity Gel (Sigma) according to the manufactures' instruction. All transfection were performed in duplicates on sub-confluent (70%-80%) 293 cell monolayers in 6 well plates. Each well of cells was transfected with 2.5µg of total DNA including 1.25µg of each of the two plasmids transfected. 40 hours post transfection; the samples were mock-treated or treated with MG132 for another 8 hours. The cell harvesting procedure was performed on ice. Cells were washed twice with 2ml of ice-cold PBS-pic1(Protease Inhibitor Cocktail) before harvested in 500µl of Guccionne buffer (25mM HEPES pH7, 0.1% NP40, 0.5M NaCl, 1mM Nabutyrate) in combination with 1% pic1 per well. Cell lysates were left on ice for 20 minutes, sonication treatment was performed for 10 seconds and cells were centrifuged at 12,000 x g for 20 minutes in a pre-cooled tabletop centrifuge at 4°C. Supernatant was transferred

into a new chilled tube and diluted with an equal volume of 50mM salt buffer to get a final solution of 275mM salt. 10% of the input at this stage was removed and added into equal volume of 1 x SB for direct western blotting analysis. 100µl of 1 x SB was added to the pellet. The supernatant samples were stored on ice until the binding step.

ANTI-FLAG M2 Affinity Gel was resuspended thoroughly before use, suspended gel was transferred in bulk and 20µl of resin was used per reaction. The resin was centrifuged for 5 seconds at 10,000 x g and settled on ice for 2 minutes. 23G needles and syringe on aspirator were used to remove the supernatant. The resin was washed twice with 0.2ml of TBS-pic1 per 20µl of resin, and the resin was washed again with 0.2ml of 1.1M Gly-HCl pH2.8, supernatant was discarded and the resin was then washed twice with TBS-pic1. The third TBS-pic1 wash was applied and the resin was thoroughly suspended. 220µl of suspension of each sample was aliquoted into pre-cooled tubes, centrifuged and aspirated. Cell lysate supernatant was added to the washed affinity gel-containing tubes. Samples were agitated by strapping to rotary mixer in cold room for 3 hours or overnight. The resin was centrifuged again for 5 seconds at 10.000 x g and the supernatant was removed. The resin was then washed 6 times with 500µl of TBS-pic1. Elution of the FLAG fusion protein was performed at room temperature. 40µl of 2 X SB was added to each sample, the samples were then boiled for 5 minutes followed by centrifuging at 10,000 x g for 5 seconds to pellet any undissolved gel. The supernatants were transferred to fresh tubes using needles and syringes and 10µl of DTT was added to each sample. Samples were stored at -70°C until required in SDS-PAGE and immunoblotting.

2.2.6 Luciferase reporter assay

2.2.6.1 Preparation of cell lysates

All transfections were performed in triplicate on sub-confluent (50%-60%) 293 cell monolayers in 24 well plates. Each well of cells was transfected with 500ng of total DNA, in which 250ng of the expression plasmid of interest and 250ng of a combination of reporter plasmids of inducible reporter (pIFNβ-Luc, pPRDI/III-Luc or pConA-Luc) to autonomous reporter (pcDNA3.1-hisB::*lac*Z) with a ratio of 9:1. 24 hours later cells were mock-transfected or transfected with 1μg of poly (I:C) per well. Cells transfected with poly (I:C) were then incubated for a further 16 hours before harvest. Cells were washed with 200μl of PBS and subsequently harvested in 100μl of 1X passive lysis buffer (Promega) per well, after shaking the plates for 1 hour at room temperature, cells lysates were collected and used immediately or stored at -20°C for short-term storage until used.

2.2.6.2 β-Galactosidase Assay

All β-Galactosidase assays were performed in clear 96-well plates (BD Falcon). 20μl of cell lysate was mixed with 130μl of Z-buffer (60mM $Na_2HPO_4.7H_2O$, 40mM $NaH_2PO_4.H_2O$, 1mM KCl and 1mM $MgSO_4.7H_2O$), 32μl of ONPG and 0.382μl of β-mercaptoethanol in each well. The plates were then incubated at 37°C until the reaction mixture became visibly yellow in colour, at which point reactions were stopped by adding 80μl of 1M Na_2CO_3. The OD_{405nm} was measured using a colorimeter (Labsystems Multiskan RC) and associated software.

2.2.6.3 Bright-Glo Luciferase Assay

All assays were performed in opaque, half-volume 96-well plates (Greiner). 20µl of cell lysates were mixed with 25µl of Bright-Glo Luciferase Assay Substrate (Promega) in each well. Luciferase activities were measured using a Luminoskan Ascent microplate luminometer and associated software.

2.2.6.4 Luciferase Assay Data Analysis

Relative Luciferase Activity (RLA) for each sample was calculated in order to normalise luciferase activity to the general transfection efficiency of the cells. This was achieved by dividing the value of luciferase activity by the value of the activity of β-Galactosidase reporter for each sample. All RLA values were calculated independently for each sample either treated or untreated with Poly (I:C). Finally all the RLA values were normalised to the respective control with the control sample having the value of 1. Within each experiment the standard deviation from the mean of the ratios obtained from each set of triplicates was calculated. As the experiment was repeated three to four times under the same condition, a two-tailed Student's t-test analysis was performed to all the values to investigate whether or not the datasets were significantly different from the subjected control values.

Chapter 3

Generation of chimeric rotavirus NSP1 hybrids

3.1 Introduction

In a yeast two-hybrid interaction screen of an MA104 cDNA library, that employed NSP1 of a bovine rotavirus (strain B641) as bait, the interferon regulatory factor 3 (IRF3) was identified as the primary cellular interaction partner of NSP1 (Graff *et al*., 2002). The same research group also found that NSP1 synthesized in infected MA104 cells interacted with host cellular IRF3 in a GST pull-down assay suggesting that the interaction was not unique to the yeast two-hybrid system (Graff *et al*., 2002). Similarly, NSP1 of another bovine rotavirus (strain UKtc) has also been shown to interact with IRF3 in a yeast two-hybrid assay (Goodbourn *et al*., unpublished results) and in addition, this interaction caused IRF3 degradation in a proteasome dependent manner (Barro and Patton, 2005). Despite these results with bovine rotavirus strains, in MA104 cells infected with a porcine rotavirus (strain OSU), the cellular IRF3 levels remained stable, little interaction between OSU NSP1 and IRF3 was observed in a GST pull-down assay. From these results it was concluded that the binding between OSU NSP1 and IRF3 was less than 10% of that seen with the bovine B641 NSP1 (Graff *et al*., 2007).

The porcine NSP1 was however shown to interact and promote degradation of a second component involved in the innate immune response, namely the β-transducin repeat containing protein (β-TrCP), which functions as part of an E3 ligase Skp1/Cull/F-box complex ($SCF^{\beta\text{-}TrCP}$) involved in the ubiquitination of inhibitor kappa B (IκBα) (Graff *et al*., 2009). By contrast UKtcNSP1 has been shown to have little effect on β-TrCP (Arnold and Patton, 2011). Therefore, based on the fact that UKtcNSP1 and OSUNSP1 were able to interact and degrade different cellular

proteins and they share only 59.3% and 66% conservation at the amino acid and the nucleotide sequence levels respectively (Xu *et al*., 1994), it was decided to use these two NSP1s for generating chimeric NSP1 hybrid constructs to map the important regions in NSP1 responsible for their specific interactions with the different cellular proteins. Figure 3.1 illustrated the amino acid sequence comparison between a few NSP1 proteins from different rotavirus strains including the selected bovine UKtc, porcine OSU strains used in this study and some other strains analysed in others' studies (Figure 3.1).

The strategy employed was to select or create by site directed mutagenesis restriction enzyme (RE) sites spread at intervals across both UKtc and OSU NSP1 sequences to facilitate the swapping of cDNA fragments between the two parental molecules to generate a series of reciprocal hybrid gene constructs. A total of seven possible restriction enzyme sites spread across the two sequences were initially identified although a *Nru* I site (at UKtcNSP1 nucleotide position 669) was eliminated as it is the only RE site of those identified that was sensitive to *dam* methylation. Six RE sites finally chosen to be generated in the two parental NSP1 sequences are shown (**Figure 3.2A**). These positions were selected on the basis that the generation of the RE sites should not cause any change in the amino acid sequence in order to eliminate the possibility that their introduction would change the structure of the NSP1 proteins. The predicted secondary structures of both proteins were also taken in consideration when selecting these potential RE sites (**Figure 3.2B**) to ensure that the higher order structure of the protein was maintained as much as possible in the hybrids being generated.

```
Consensus       MATFKDACYHYKRLNKLNSLVLKLGANDEWRPAPVTKYKGWCLDCCQYTDLTYCRGCALYHVCQWCSQYNRCFLDEEPHLLRMRTFKDVVTKDDLEGLLTM
6 Sequences              10        20        30        40        50        60        70        80        90       100
Bovine B641     MATFKDACYHYKKLNKLNSLVLKLGANDEWRPAPVTKYKGWCLDCCQYTNLTYCRGCALYHVCQWCSQYNRCFLDEEPHLLRMRTFKDVVTKEDIEGLLTM
Bovine NCDV     MATFKDACYHYKRLNKLNSLVLKLGANDEWRPAPVTKYKGWCLDCCQYTNLTYCRGCALYHVCQWCSQYNRCFLDEEPHLLRMRTFKDVVTKEDIEGLLTM
Bovine UKtc     MATFKDACYHYKKLNKLNSLVLKLGANDEWRPAPVTKYKGWCLDCCQYTNLTYCRGCALYHVCQWCSQYNRCFLDEEPHLLRMRTFKDVITKEDIEGLLTM
Human WA       MATFKDACYYYKRINKLNHAVLKLGVNDTWRPSPPTKYKGWCLDCCQHTDLTYCRGCTMYHVCQWCSQYGRCFLDDEPHLLRMRTFKNEITKDDLKNLIDM
Porcine OSU    MATFKDACYYYKRINKLNHAVLKLGVNDTWRPSPPTKYKGWCLDCCQHTDLTYCRGCTMYHVCQWCSQYGRCFLDNEPHLLRMRTFKNEVTKDDLMNLVDM
Simian SA11    MATFKDACFHYRRLTALNRRLCNIGANSICMPVPDAKIKGWCLECCQIADLTHCYGCSLPHVCKWCVQNRRCFLDNEPHLLKLRTVKHPITKDKLQCIIDL

Consensus       YETLFPINEKLVNKFINSVKQRKCRNEYLLEWYNHLLMPITLQALTIELDDNVYYIFGYYDCMEHENQTPFQFINLLEKYDKLLLDDRNFHRMSHLPVIL
6 Sequences            110       120       130       140       150       160       170       180       190       200
Bovine B641     YETLFPINEKLVNKFINSVKQRKCRNEYLLEWYNHLLMPITLQALTINLEDNVYYMFGYYDCMEHENQTPFQFVNLLEKYDKLLLDDRNFHRMSHLPVIL
Bovine NCDV     YETLFPINEKLVNKFINSVKQRKCRNEYLLEWYNHLLMPITLQALTINLEDNVYYIFGYYDCMEHENQTPFQFINLLEKYDKLLLDDRNFHRMSHLPVIL
Bovine UKtc     YEILFPINEKLVNKFINSVKQRKCRTEYLLEWYNHLLMPITLQALTIKLEDSTYYIFGYYDCMEHENQTPFQFINLLEKYDKLLLDDRNFNRMLHLPTIL
Human WA       YSTLFPMNQKIVCKFINNTKQHKCRNECMTQWYNHLLMPITLQSLSIELDGDVYYVFGYYDNMNSVNQTPFSFTNLIDMYDKLLLDDVNFVRMSFLPTSL
Porcine OSU    YDTLFPMNQKIVDKFINNTRQHKCRNECVNQWYNHLLMPITLQSLSIELDGDVYYIFGYYDDMNNVNQTPFSFVNLVDIYDKLLLDDVNFTRMSFLPVTL
Simian SA11    YNIIFPINDKVIRKFERMIKQRKCRNQYKIEWYNHLLLPITLNAAAFKFDENNLYYVFGLYEKSVSDIYAPYRIVNFINEFDKLLLDDINFTRMSNLPIE

Consensus       QQEYALRYFSKSRFLSKGKKRLSRSDFSDNLLEDRHSPTSLMQVVRNCISLHINDNEWNKACTLVVDARNYLSIMNSSYTEHYSVSQRCKLFTLKKFGIV
6 Sequences            210       220       230       240       250       260       270       280       290       300
Bovine B641     QQEYALRYFSKSRFLSKGKKRLSRSDFSDNLMEDRHSPTSLMQVVRNCISIHIDDCEWNKACTLIVDARNYISIMNSSYTEHYSVSQRCKLFTKYKFGIV
Bovine NCDV     QQEYALRYFSKSRFLSKGKKRLSRSDFSDNLMEDRHSPTSLMQVVRNCISIHINDCEWNKACTLIVDARNYISIMNSSYTEHYSVSQRCKLFTKYKFGIV
Bovine UKtc     QQEYALRYFSKSRFLSKGKKRLNRNDFSDNLVEDRHSPTSLIQVVRNCISTHPNDYEWNKACTFVVDARNYININMNSSYTEHYSVSQRCKLFTKYKFGII
Human WA       QQEYAIRYFSKSRFISEQRKCVNDSHFSINVLENLHNPSFKVQITRNCSELLLGWNEACKLVKNVSAYFDMLKTSRIEFYSVSTRCRIFTQHKLKMASKL
Porcine OSU    QQEYALRYFSKSRFISEQRKCVSDSHFSINVLENLHNPSFKMQITRNCSELSSDWNGACKLVKDTSAYFNILKTSHVEFYSISTRCRVFTQRKLKIASKL
Simian SA11    LRNHYAKKYFQLSRLPSSKLKQIYFSDFTKETVIFNTYTKTPGRSIYRNVTEFNWRDELELYSDLKNDKNKLIAAMMTSKYTRFYAHDNNFGRLKMTIFE

Consensus       SKLVKPNYIFSSHESCALNVHNCSWCQINTHYKVWEDFRLRDIYNNVMDFIRALVKSNGNVGHCSSQESVYKYIPDLFLICKTEKWNEAVENLFNYLEPV
6 Sequences            310       320       330       340       350       360       370       380       390       400
Bovine B641     SKLVKPNYIFSSHESCALNVHNCKWCQINNHYKVWEDFRLRKIYNNVMDFIRALVKSNVNVGHCSSQESVYKYVPDLFLICKTEKWSEAVEMLFNYLEPV
Bovine NCDV     SRLVKPNYIFSSHESCALNVHNCKWCQINNHYKVWEDFRLRKIYNNVMDFIRALVKSNGNVGHCSSQESVYKYIPDLFLICKTEKWNEAVEMLFNYLEPV
Bovine UKtc     SKLVKPNYIFSSHESCALNVHNCRWCQINSHYKVWEDFRLKKIYNNVMDFIRALVKSNGNVGQCSSQESVYKCIPDIFLICKMEKWNEAVEVLFNYLEPV
Human WA       IKPNYITSNHRTSATEVHNCKWCSVNNSYTVWNDFRVKKIYDNIFSFLRALVKSNVNIGHRSSQEKIYEYVEDVLNVCDNEKWKTSIMKVFNCLEPVELD
Porcine OSU    IKPNYITSNHRTSATEVHNCKWCSINSSYTVWNDFRVKKIYDNIFNFLRALVKSNVNVGHCSSQEKIYECVENILDVCDNEKWKTSVTKIFNYLEPVELN
Simian SA11    LGHHCQPNYVASNHPGNASDIQYCKWCNIKYFLSKIDWRIRDMYNLLMEFIKDCYKSNVNVGHCSSVENIYPLIKRLIWSLFTNHMDQTIEEVFNHMSPV

Consensus       DVNGTEYVLLDYEVNIEVRGLVMQNMDGKVPRILNINDTKSILSAWIFDWFDTRYMRETPMTTSTTNQLRTLNKRNELIDEYDLELSDVE
6 Sequences            410       420       430       440       450       460       470       480       490
Bovine B641     NVNGTEYVLLDYEVNWEVRGLVMQNMDGKVPRILNMNDTKKILSAMIFDWFDTRYMRETPMTTSTTNQLRTLNKRNELIDEYDLELSDVE
Bovine NCDV     DINGTEYVLLDYEVNWEVRGLVMQNMDGKVPRILNMNDTKKILSAMIFDWFDTRYMRETPMTTSTTNQLRTLNKRNELIDEYDLELSDVE
Bovine UKtc     DINGTEYVLLDYEVNWEVRGLVMQSMDGKVPRILNINDTKKILSTIIFDWFDVRYMRETPMTTSTTNQLRTLNKRNELIDEYDLELSDVE
Human WA       NVKYVLFNHEINWDVINVLVQSIGKVPQILTLKNVITIIQSIIYEWFDIRYMRNTPMVTFTIDKLRRLHTELKTAEYDSGISDVE
Porcine OSU    AVNYVLFNHEVNWDVINVLVQSIGKVPQILTLNDVTTIMQSIIYEWFDTKYMRNTPMTTFTVDKLRRLCTGSKTVDYDSGISDVE
Simian SA11    SVEGTNVIMLILGLNISLYNEIKRTLNVDSIPMVLNLNEFSSIVKSISSKWYNVDELDKLPMSIKSTEELIEMKNSGI
```

Figure 3.1 Sequence comparision between NSP1s of different rotavirus strains. Sequence alignment was generated using DNASTAR's Lasegene Core Suite software. The three NSP1s from the bovine strains (B641, NCDV and UKtc) showed over 90% of sequence identity among themselves. However the NSP1 of the porcine strain OSU showed only around 60% of sequence identity with bovine NSP1, but around 85% with the NSP1 from the human strain Wa. The NSP1 from the simian stratin SA11 showed less than 40% sequence identity with the porcine OSU NSP1, the human Wa NSP1 and all the bovine NSP1s.

A

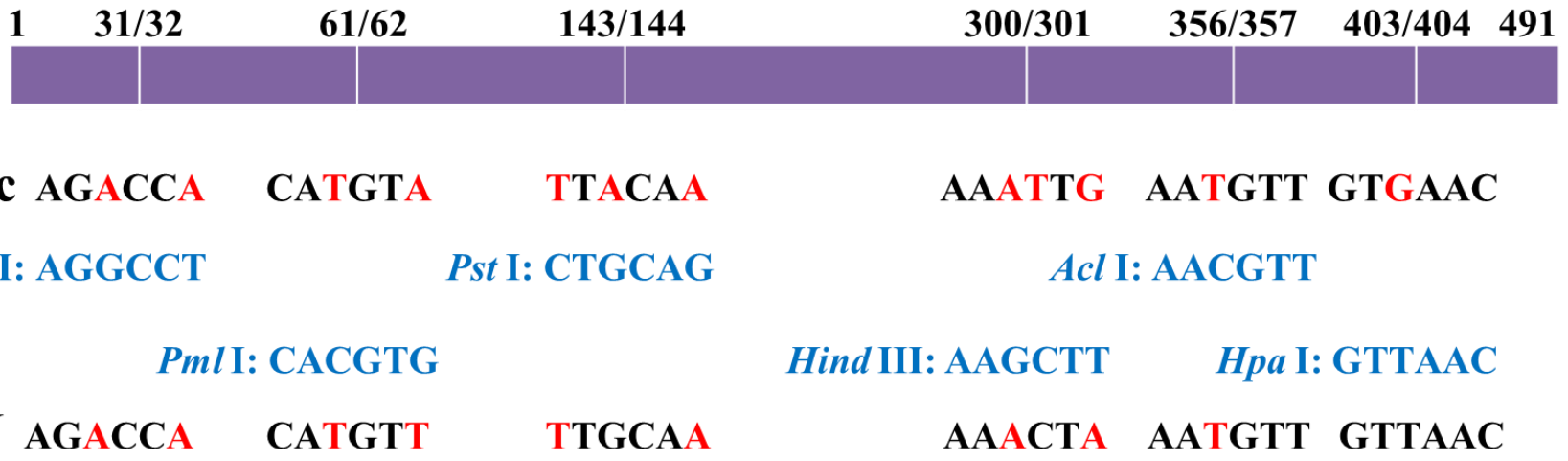
1
31/32
61/62
143/144
300/301
356/357
403/404
491
UKtc AGACCA CATGTA TTACAA AAATTG AATGTT GTGAAC
Stu I: AGGCCT
Pst I: CTGCAG
Acl I: AACGTT
Pml I: CACGTG
Hind III: AAGCTT
Hpa I: GTTAAC
OSU AGACCA CATGTT TTGCAA AAACTA AATGTT GTTAAC

B

Figure 3.2 Schematic diagrams illustrating the selected restriction enzyme (RE) sites to be generated in both UKtc and OSU NSP1 sequences.

(A). Schematic diagram of six selected RE sites including *Stu* I, *Pml* I, *Pst* I, *Hind* III, *Acl* I and *Hpa* I to be generated in both UKtc and OSU NSP1 sequences (*Hpa* I already exists in OSUNSP1). The amino acid positions of the corresponding sites in UKtcNSP1 are indicated. The nucleotides highlighted in red indicate those in both NSP1 sequences mutated to generate the RE site without changing the amino acid sequence of the protein.

(B). Predicted secondary structures of the two NSP1 proteins (adapted from Xu *et al*., 1994) with the selected RE sites highlighted indicating that the overall structure of the NSP1 proteins was maintained mostly in the hybrids constructed while introducing the six RE sites. E indicates positions predicted to have β-sheet structure, H represents positions predicted as being α-helix and L denotes positions predicted to be in loops. Positions at which no prediction with an acceptable level of confidence could be made are indicated by '-' and gaps introduced to optimize the alignment by a '.'.

3.2 Cloning vector preparation for generating chimeric NSP1 hybrid cDNAs

The experimental plan was that the NSP1 hybrids should be analysed for their interaction first in a mammalian two-hybrid assay. However, because the mammalian two-hybrid vectors pM and pVP16 contain several of the RE sites chosen for use in generating hybrid constructs, including *Stu* I, *Pst* I, *Hind* III, *Acl* I and *Hpa* I; the cloning vector pCR2.1 was used as the vehicle for introducing RE sites into the two NSP1 genes. However as indicated in Figure 3.3 two *Pst* I sites (position 309 and 1499), two *Acl* I sites (position 2315 and 2688) and one *Hind* III site (position 235) are also present in the pCR2.1 vector sequence and consequently the vector was modified prior to its use in these experiments to remove these RE sites.

The preparation of the pCR2.1 cloning vector is illustrated in Figure 3.4. It was first digested with each of the six restriction enzymes selected for use in NSP1 hybrid construction and the digestion outcomes were those expected from the vector sequence (**Figure 3.4A**). These two *Acl* I sites in pCR2.1 were destroyed by filling-in the 5' overhangs generated by digestion and ligating the blunt ends to re-circularise the plasmid. The deletion of the nucleotides between the two *Acl* I sites within the ampicillin persistence gene of the vector destroyed the ampicillin selectivity marker. This was confirmed by transforming re-circularised plasmid into DH5α competent cells and plating onto LB plates containing either Ampicillin or Kanamycin, and as expected colonies were only seen from the Kan^+ plates, DNA extracted from colonies obtained on Kan^+ plates were then transformed again and re-plated on plates containing ampicillin, and no colonies were observed, confirming that the ampicillin selectivity has been destroyed. 12 colonies were picked from Kan^+ plates, DNA was

extracted with Qiagen mini-prep kit and digested with *Acl* I again, no cutting of the plasmid occurred (**Figure 3.4B**), indicating that the *Acl* I sites in the starting pCR2.1 vector plasmid had been destroyed. One of the 12 clones was selected to use for subsequent manipulations.

A similar procedure was repeated to remove the *Hind* III site present in the starting vector plasmid (**Figure 3.3**). Although the situation of the two *Pst* I sites in pCR2.1 differed, the site at position 1499 was within the Kanamycin ORF, therefore in order to maintain kanamycin resistance marker for colony selection, mutagenesis PCR was applied to alter this restriction enzyme site without changing the amino acids encoded (from CTGCAG to CTCCAG). The second *Pst* I site at position 309 did not require alteration as *EcoR* I/*Bam* HI (position 283, 252) and *Xho* I (position 332) digestion was going to be used for insertion of UKtcNSP1 and OSUNSP1 respectively. This being the case, the sequences between these sites, including the second *Pst* I site, were going to be replaced by NSP1 gene. Following mutagenesis PCR, digestion with *Pst* I confirmed that only one *Pst* I site remained in the vector, named mpCR2.1, and it was ready for use.

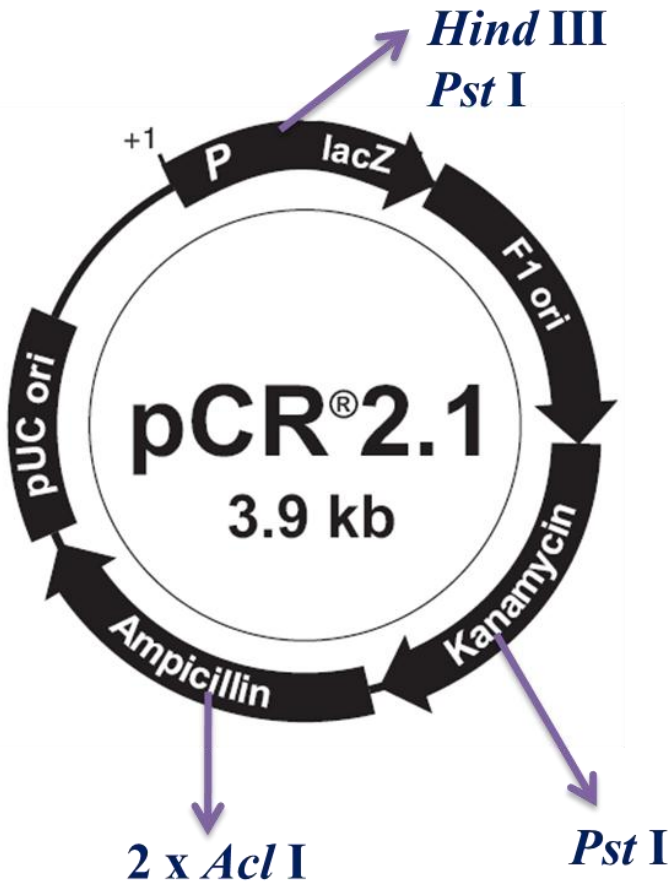

Figure 3.3 Illustration of the cloning vector pCR2.1 indicating the selected RE sites already exist in the vector sequence.

The selected RE sites already exist in the cloning vector are labelled.

3.3 Cloning of the UKtcNSP1 and OSUNSP1 genes into mpCR2.1 vector

The UKtcNSP1 gene was amplified from plasmid pVP16-NSP1 (provided by Dr K.T.Chung, University of Warwick) by PCR using primers UKtc-*EcoR*I 5' and UKtc -*Xho*I 3' (**Table 2.1.7**). The modified vector mpCR2.1 was digested with *EcoR* I and *Xho* I and dephosphorylated with shrimp alkaline phosphatase (SAP). The amplified

UKtcNSP1 was also digested with the same restriction enzymes and ligated into the prepared vector to generate the mpCR2.1-UKtcNSP1 construct. Recombinant clones carrying the inserted UKtcNSP1 gene were selected using blue/white colony screening and six of them confirmed to be correct by double digestion with *EcoR* I and *Xho* I. Two of the clones (S2 and S5) (**Figure 3.5A**) were sequenced across the inserted gene and S5 was confirmed to have been inserted accurately and to have the correct orientation (**Figure 3.5B**).

In a similar fashion, OSUNSP1 gene (provided by Prof M.A.McCrae, University of Warwick) was amplified by PCR using primers OSU *BamH*I 5' and OSU *Xho*I 3' (**Table 2.1.7**). The modified vector mpCR2.1 was digested with *BamH* I and *Xho* I followed by dephosphorylation with SAP. The PCR amplicon was digested with the same restriction enzymes and ligated into the prepared vector to generate the mpCR2.1-OSUNSP1 construct. 12 recombinant clones were selected using blue/white colony screening and confirmed by double digestion with *BamH* I and *Xho* I. Four clones containing NSP1 inserts, S1, S2, S4 and S5 were identified (**Figure 3.6A**). S1 was sequenced across the NSP1 insert which confirmed that the gene had been inserted accurately in the correct orientation with respect to the promoter in mpCR2.1 (**Figure 3.6B**).

A

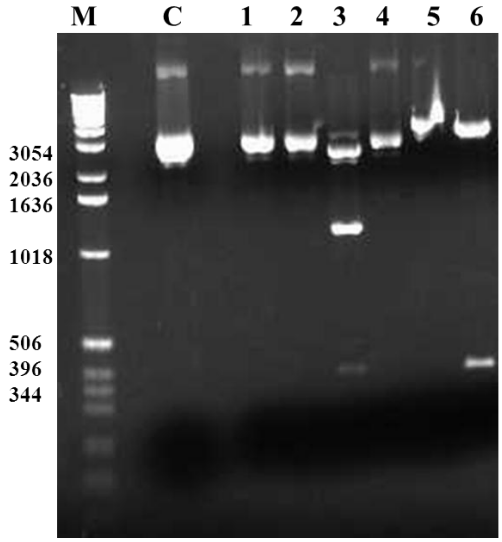

M: 1Kb DNA ladder
C: undigested pCR2.1
1: pCR2.1 digested with *Stu* I
2: pCR2.1 digested with *Pml* I
3: pCR2.1 digested with *Pst* I
4: pCR2.1 digested with *Hpa* I
5: pCR2.1 digested with *Hind* III
6: pCR2.1 digested with *Acl* I

B

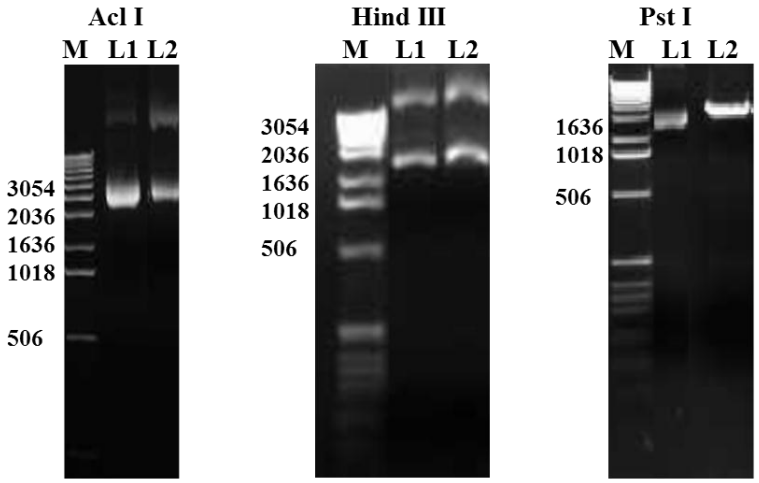

M: 1Kb DNA ladder
L1: Undigested pCR2.1
L2: Modified pCR2.1 digested with indicated REs

Figure 3.4 Modification of the pCR2.1 cloning vector for use in generating NSP1 hybrids.

(A). pCR2.1 was digested with the 6 restriction enzymes indicated; and the products were analysed by electrophoresis on a 1% TBE agarose gel as described in Materials and Methods. *Stu* I, *Pml* I and *Hpa* I (indicated lane 1, 2 and 4) were unable to digest the vector and showed the same pattern as the undigested vector control (indicated as lane C) whereas the other enzymes were able to digest this vector. The sizes of the markers used are given down the left hand side of each gel in base pairs.

(B). Through filling-in and site directed mutagenesis, selected RE sites were destroyed and the modified vector was subjected to corresponding enzyme digestion again. The products were analysed by electrophoresis on a 1% TBE agarose gel as described in Materials and Methods. It indicates that the vector could no longer be digested by the selected restriction enzymes. The sizes of the markers used are given down the left hand side of each gel in base pairs.

A

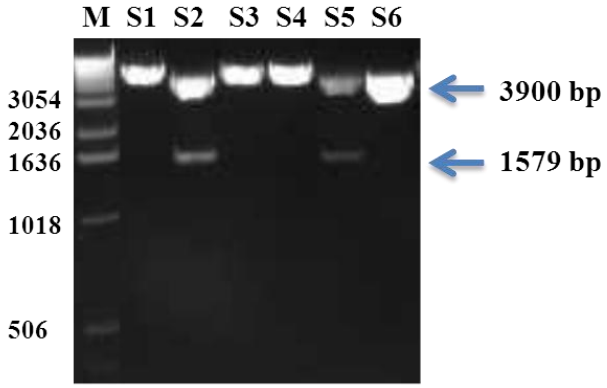
M S1 S2 S3 S4 S5 S6
3054
2036
1636
1018
506
3900 bp
1579 bp

B

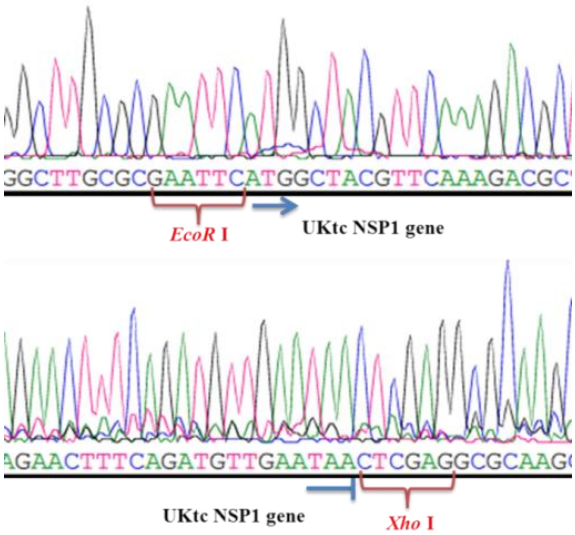
GGCTTGCGCGAATTCATGGCTACGTTCAAAGACGC
EcoR I
UKtc NSP1 gene
AGAACTTTCAGATGTTGAATAACTCGAGGCGCAAG
UKtc NSP1 gene
Xho I

Figure 3.5 Cloning of UKtcNSP1 into mpCR2.1 vector.

(A). Plasmid DNA from 6 independent clones, generated following the ligation reactions between mpCR2.1 and PCR amplified UKtcNSP1, was prepared and double-digested with *EcoR* I and *Xho* I. The products were analysed by electrophoresis on a 1% TBE agarose gel as described in Materials and Methods. The inserted UKtcNSP1 was released by this double digestion resulting in a band of 1579 bps with a 3900 bps vector band also being generated, as indicated by arrows on the right side of the gel. Lane M was loaded with 1Kb DNA ladder and the sizes of the markers are given in base pairs down the left hand side of the gel.

(B). Clone S5 was sequenced using M13 reverse and forward primers (Table 2.1.7) and the sequence of the vector-insert junction regions are illustrated. The sequencing confirmed that the UKtcNSP1 gene was inserted without any additional nucleotide changes having been introduced and in the correct orientation in the mpCR2.1 vector.

A

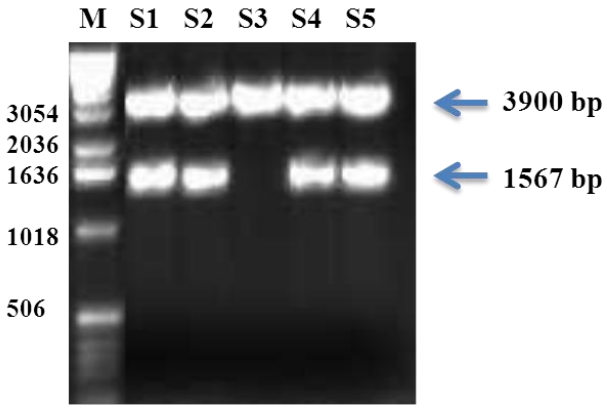
M S1 S2 S3 S4 S5
3054
2036
1636
1018
506
3900 bp
1567 bp

B

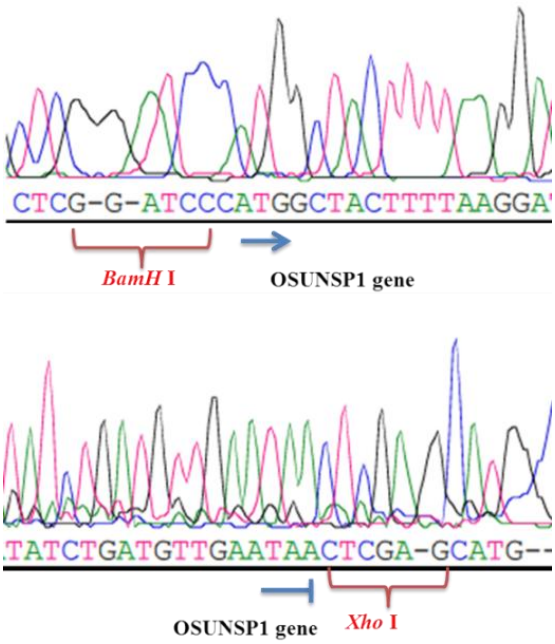
CTCG-G-ATCCCATGGCTACTTTTAAGGA
BamH I
OSUNSP1 gene
TATCTGATGTTGAATAACTCGA-GCATG--
OSUNSP1 gene
Xho I

Figure 3.6 Cloning of OSUNSP1 into mpCR2.1 vector.

(A). Plasmid DNA from 5 independent clones, generated following the ligation reactions between mpCR2.1 and PCR amplified OSUNSP1, was prepared and double-digested with *BamH* I and *Xho* I. The products were analysed by electrophoresis on a 1% TBE agarose gel as described in Materials and Methods. The inserted OSUNSP1 was released by the double digestion resulting in a band of 1567 bps with 3900 bps vector band also being generated, as indicated by arrows on the right side of the gel. Lane M was loaded with 1Kb DNA ladder and the sizes of the markers are given in base pairs down the left hand side of the gel.

(B). Clone S1 was sequenced using M13 reverse and forward primers and the sequence of the vector-insert junction regions are illustrated. The sequencing confirmed that the OSUNSP1 gene was inserted without any additional nucleotide changes having been introduced and in the correct orientation in the mpCR2.1 vector.

3.4 Sequential mutagenesis PCR of mpCR2.1-UKtcNSP1 and mpCR2.1-OSUNSP1

Site direct mutagenesis PCR was performed to create the desired restriction enzyme sites in both mpCR2.1-UKtcNSP1 and mpCR2.1-OSUNSP1. The RE sites were generated sequentially starting from both 5' and 3' ends of the genes to minimise the possibility of creating unwanted mutations through the PCR process. Consequently *Stu* I, *Pml* I and *Pst* I were generated sequentially from the 5' end of both genes and *Hind* III, *Acl* I and *Hpa* I from the 3' end of the genes (as the *Hpa* I site already existed in OSUNSP1, it would only need to be created in UKtcNSP1). Subsequently, modified UKtcNSP1 constructs, one containing the 3 RE sites near the 5' end and the other one containing the 3 RE sites near the 3' end, were digested with *SanB* I to generate the final mutated version of the gene carrying all six inserted RE sites (**Figure 3.7**). The same strategy was followed to generate the equivalent OSUNSP1 construct.

Stu I was the first RE site to be generated in each case via mutagenesis PCR using primers UKtc-*Stu*I 5' and UKtc-*Stu*I 3' for mpCR2.1-UKtcNSP1 or OSU-*Stu*I 5' and OSU-*Stu*I 3' for mpCR2.1-OSUNSP1 (**Table 2.1.7**). Ten colonies for each NSP1 gene were selected and DNA was extracted via mini-prep, these constructs were then subjected to *Stu* I digest and one clone from each NSP1 was selected and sequencing analysis was performed to confirm the correct restriction enzyme site had been generated and that no other change had been made during the PCR process (**Figure 3.8**).

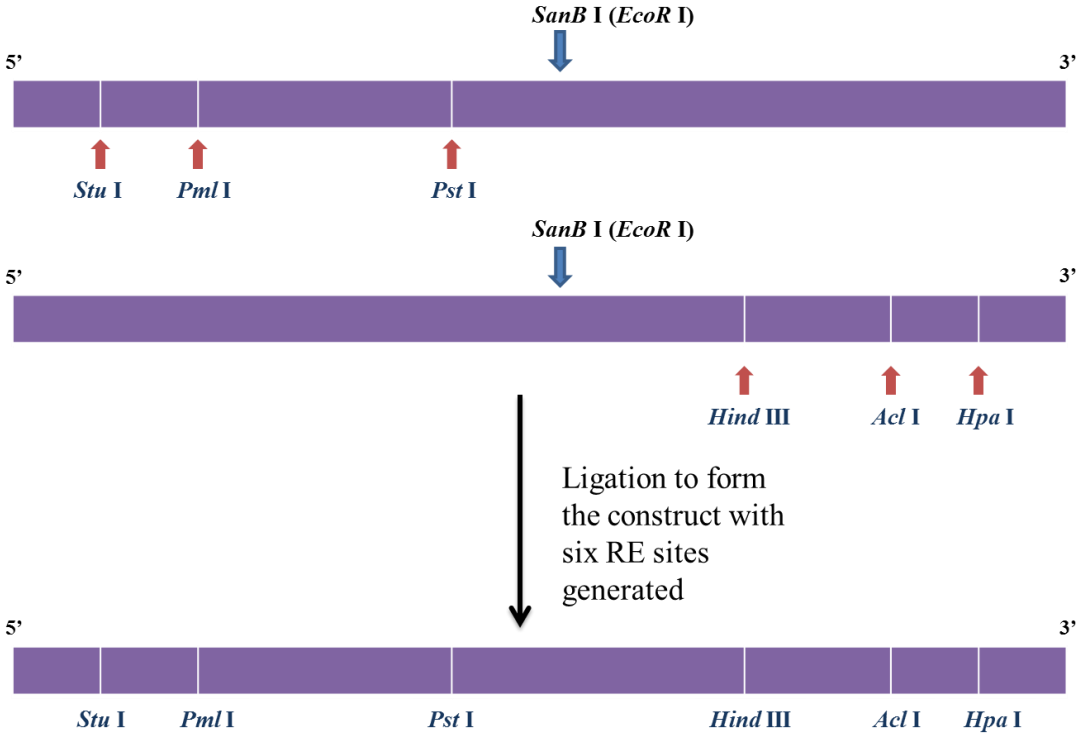

Figure 3.7 The cloning strategy employed for constructing NSP1 genes containing six selected RE sites.

The aim was to create three selected RE sites in both the 5' end and 3' end portions of the NSP1 gene via site directed PCR based mutagenesis. The two constructs should then be digested with *SnaB* I (for UKtcNSP1) and *EcoR* I (for OSUNSP1) and ligated to form the final constructs containing all six RE sites.

The newly generated constructs were then used as the template in the next step to generate *Pml* I sites using the appropriate primers (**Table 2.1.7**). The selected clones were subjected to *Pml* I digestion and sequencing analysis to ensure the correct creation of the desire restriction enzyme sites and that the rest of the sequences were intact (**Figure 3.8**).

Using the same strategy starting from the 3' end of the gene, the *Hpa* I site for mpCR2.1-UKtcNSP1 and the *Acl* I site for mpCR2.1-OSUNSP1 were generated via mutagenesis PCR using appropriate primers (**Table 2.1.7**). The selected clones were subjected to digestion and sequencing analysis to ensure the correct creation of the desire restriction enzyme sites and that the rest of the sequences were intact (**Figure 3.8**). Subsequently, this UKtcNSP1 construct containing the *Hpa* I site was used as the template to generate the *Acl* I site in UKtcNSP1 employing the same protocol.

In the cases of the *Pst* I and *Hind* III sites several unsuccessful attempts were made to generate these RE sites into the relevant cDNA clones. It was therefore decided that creation of these last two domain swap proteins should be abandoned. This left four RE sites to be utilised for further manipulations in plasmids designated OSUNSP1-4RE and UKtcNSP1-4RE.

A mpCR2.1-UKtcNSP1

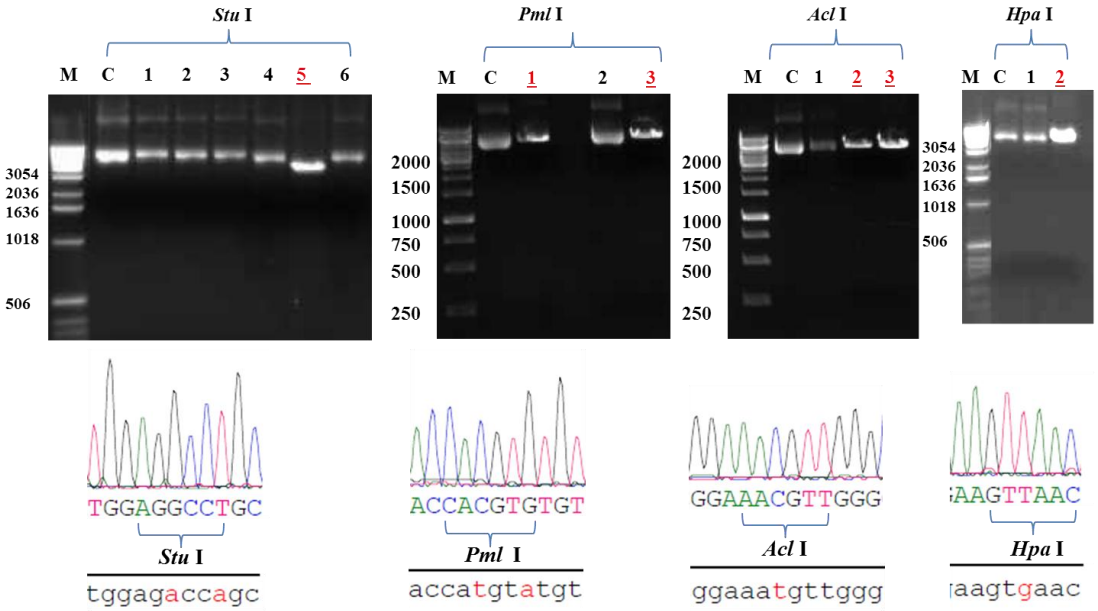

B mpCR2.1-OSUNSP1

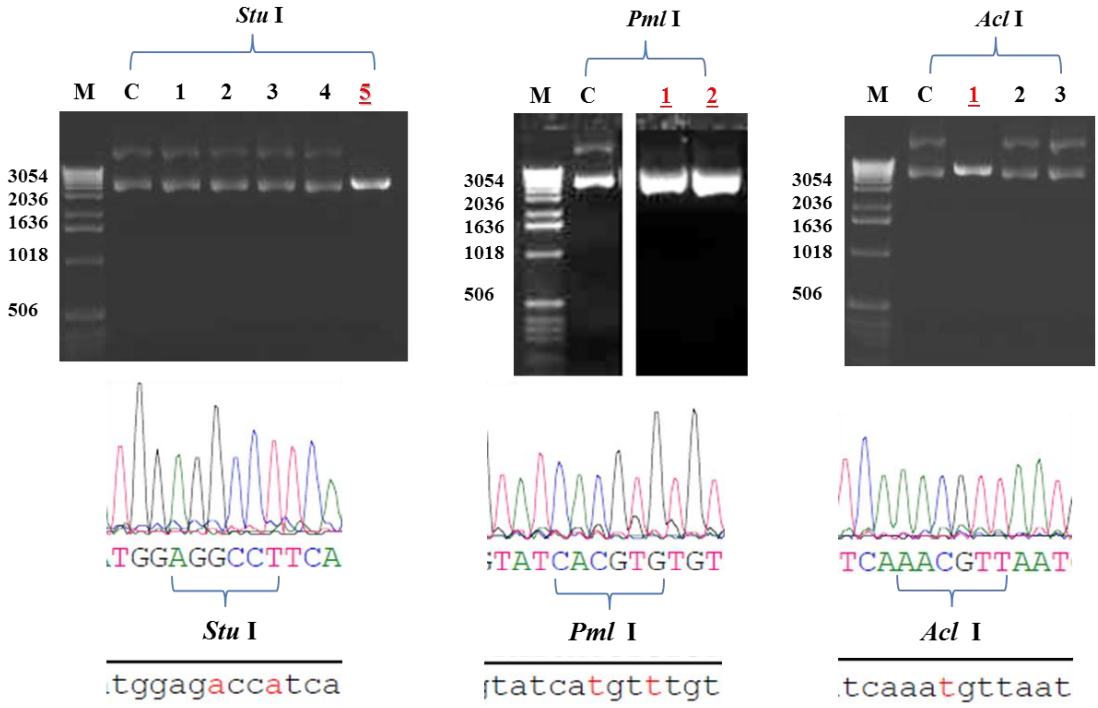

Figure 3.8 Analysis of RE sites generated in UKtcNSP1 and OSUNSP1 cDNA clones.

(A). Confirmation of four RE sites generated in mpCR2.1-UKtcNSP1.
Four RE sites generated in mpCR2.1-UKtcNSP1 were confirmed by restriction enzyme digestions and subsequent sequencing. Following each mutagenesis PCR, plasmid DNA from a selection of clones prepared by mini-prep was digested with the appropriate restriction enzyme and the products of the digest were analysed by electrophoresis on a 1% TBE agarose gel as described in Materials and Methods. Lanes C contain the wild type mpCR2.1-UKtcNSP1 which does not contain the RE sites. The numbered lanes contain the digestions of DNA made from different clones; those highlighted in red indicate the correct clone selected for subsequent sequencing. The results of sequence analysis carried out to confirm the introduced mutational change are shown below each gel.

(B). Confirmation of three RE sites generated in mpCR2.1-OSUNSP1.
Three RE sites generated in mpCR2.1-OSUNSP1 were confirmed by restriction enzyme digestions and subsequent sequencing. Following each mutagenesis PCR, plasmid DNA from a selection of clones prepared by mini-prep was digested with appropriate restriction enzymes and the products of the digest were analysed by electrophoresis on a 1% TBE agarose gel as described in Materials and Methods. Lanes C contain the wild type mpCR2.1-OSUNSP1 which does not contain the RE sites. The numbered lanes contain the digestions of DNA made from different clones; those highlighted in red indicate the correct clone selected for subsequent sequencing. The results of sequence analysis carried out to confirm the introduced mutational change are shown below each gel.

3.5 Generating chimeric NSP1 hybrid constructs using mutated UKtcNSP1 and OSUNSP1 cDNAs

NSP1 hybrid genes were generated by ligating together different sections of the NSP1 sequences from both UKtcNSP1-4RE and OSUNSP1-4RE produced by digestion at combinations of newly generated RE sites. Constructs pA and pB (**Figure 3.10**) were obtained by digesting both UKtcNSP1-4RE and OSUNSP1-4RE with *Stu* I and *Acl* I. The products of the digests were then fractionated on a 1% TBE agarose gel and the relevant DNA bands were extracted using Qiagen Gel Extraction Kit. The larger DNA bands containing the mpCR2.1 vector and part of the UKtc or OSU NSP1 gene were dephosphorylated and then ligated to the smaller DNA bands containing the remainder of the NSP1 gene sequence from the other strain of virus. Colonies were selected, DNA extracted was then sequenced to confirm the correct domain swap had occurred (**Figure 3.9**). In a similar fashion other pairs of restriction enzymes were selected and used to generate other chimeric NSP1 hybrids. Due to continuous unsuccessful swaps using other RE combinations and time limitation, 12 NSP1 hybrids in total were generated, as shown in Figure 3.10.

A.

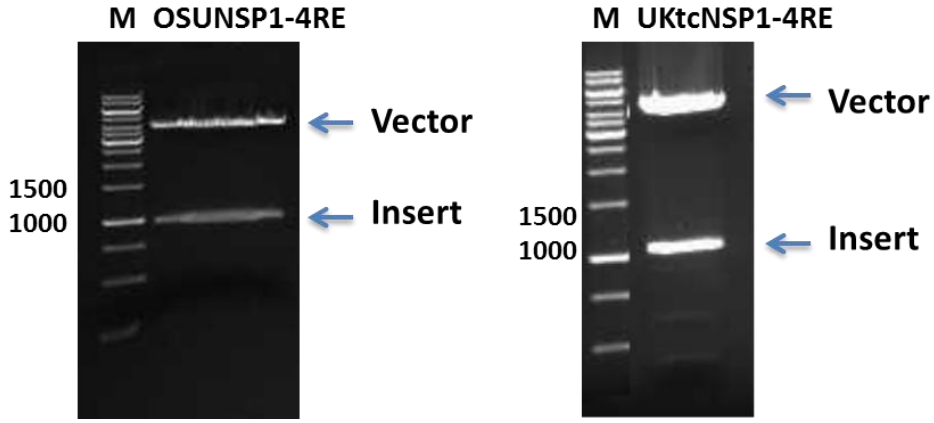

B. Construct A: pA

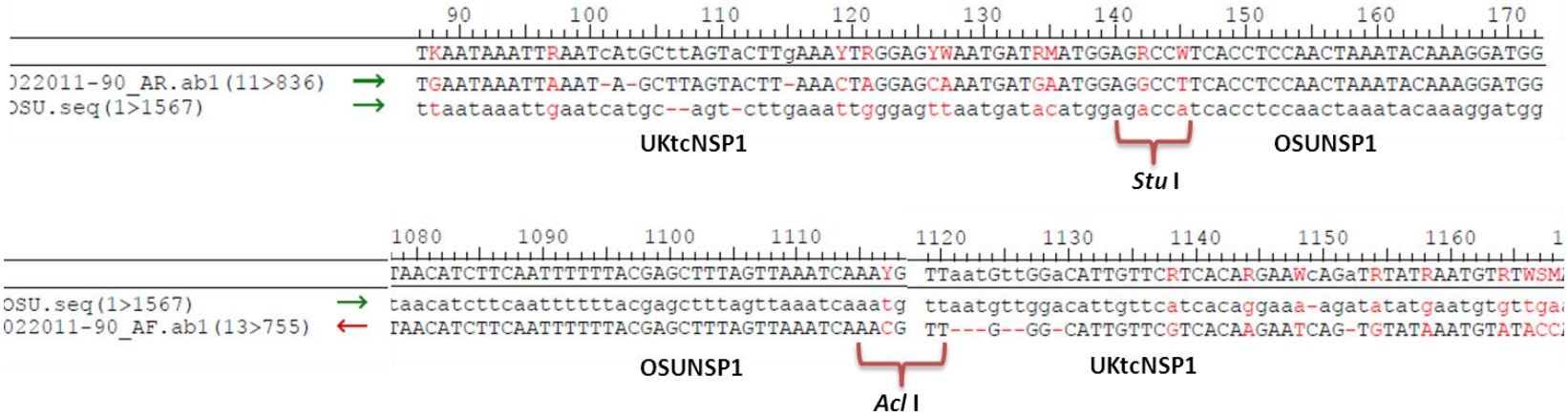

Figure 3.9 Analysis of the chimeric NSP1 hybrid pA.

(A). OSUNSP1-4RE and UKtcNSP1-4RE were digested with both *Stu* I and *Acl* I and the digests were analysed on 1% TBE agarose gel as described in Materials and Methods. The positions of the vector DNA and released cDNA fragment in each case are indicated by arrows on the right hand side of each gel. Vector and insert bands were separately eluted from the gel using the procedure described in Materials and Methods. DNA from the insert band from OSUNSP1 was then ligated into the DNA extracted from the vector band from UKtcNSP1 and vice versa to generate constructs pA and pB respectively.

(B). The complete cDNA insert of hybrid pA was sequenced and this revealed that the sequences between restriction enzyme sites *Stu* I and *Acl* I was identical with the original OSUNSP1 sequence whereas the rest of the sequence matched the UKtcNSP1 sequence as shown in this partial sequence alignment.

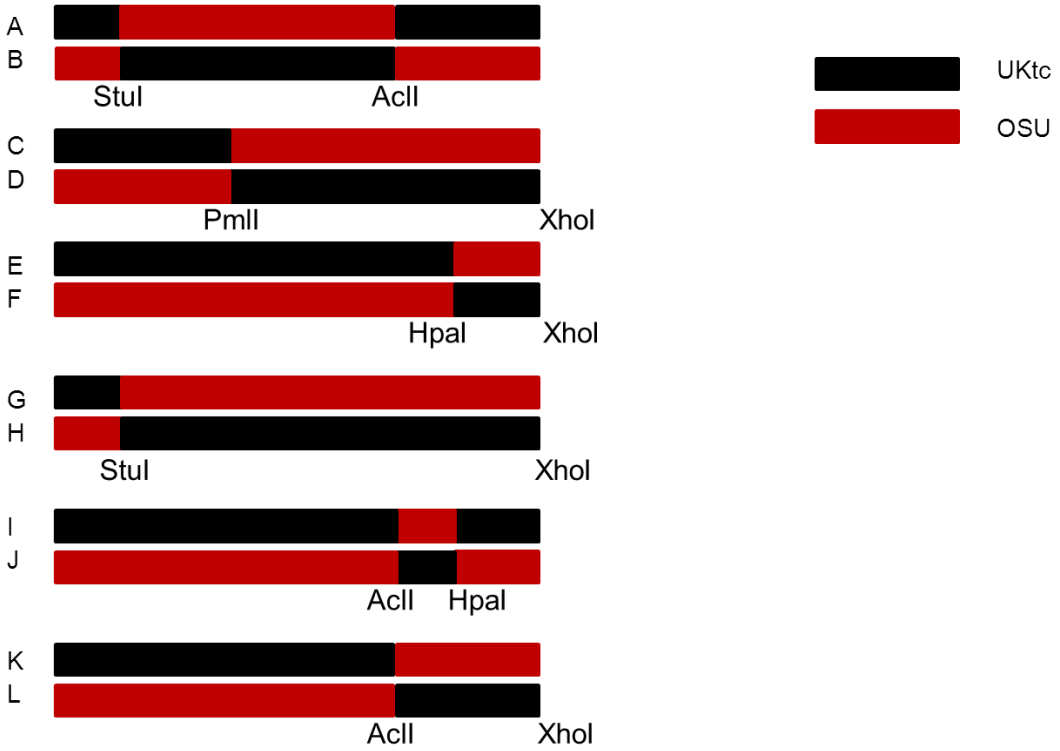

Figure 3.10 Schematic illustrations of the chimeric NSP1 hybrid protein sequences generated with UKtcNSP1 and OSUNSP1.

Six pairs of chimeric NSP1 hybrids were generated in the mpCR2.1 vector and designated A-L. Black bars indicate the sequences derived from UKtcNSP1 and red bars indicate the sequences derived from OSUNSP1. In all cases the constructs were sequenced to confirm the correct swaps at these restriction enzyme junctions (Appendix).

3.6 Discussion

The DNA constructs described in this chapter were intended for use in a range of key assays to map the interaction sites on viral NSP1 proteins responsible for interacting with and promoting the degradation of cellular proteins involved in the host innate immune system. The hybrid constructs were originally designed primarily for a mammalian two-hybrid assay, the vector was therefore modified to avoid multiple desire restriction enzyme sites present in both pCR2.1 and the mammalian two-hybrid vectors.

Difficulties were encountered with selecting the correct clones from the PCR cloning products initially. White and blue screening technique was applied to increase the possibility of selecting the correct clones as the plasmid containing bacteria *lac*Z gene can produce β-gal if its ORF is not interrupted by any foreign DNA, the functional β-gal can be produced by transforming this *lac*Z containing plasmid into *E.coli* which expresses the α peptide, the β-gal is able to turn the X-gal into a blue coloured product. If a foreign DNA is inserted within the *lac*Z gene, the ORF of *lacZ* is therefore changed and no β-gal can be produced which makes the recombinant colony to be in white colour (Messing *et al*., 1977). However, there were still white colonies appearing that were subsequently identified as incorrect clones. The reason for this might be that only part of the desired DNA was inserted. As a result, a number of colonies (typically 20-50) were picked each time and DNA was extracted for analysis separately. Mutagenesis PCR conditions were also optimised for this reason, the magnesium concentration used was higher than standard PCR as the standard 1.5mM of

$MgSO_4$ could not give any detectable PCR product at the end of the reaction. However, increased magnesium concentration might bring reduction of the fidelity and unwanted product and this might be the reason why selected colonies sometimes contain undesired clones.

Several attempts were made to generate *Hind* III and *Pst* I sites within the NSP1 genes but no mutated clones were isolated. On average, approximately 50 colonies have been analysed in each attempt, various adjustments including changing the annealing temperature, the Mg^{2+} concentration, the elongation time, still revealed no correct mutation clones. PCR control was carried out alongside each time and transformation control was also included at the same time to ensure the PCR and transformation process was working. It remained unclear that the reason for the unsuccessful mutagenesis. Therefore due to time limitation these two sites were left in this study.

Chapter 4

Analysis of protein-protein interactions between rotavirus NSP1 and host cellular proteins

4.1 Introduction

The rotavirus NSP1 protein is expressed at relatively low levels from early in the virus replication cycle and may well function at an early stage in the viral replication process (Johnson and McCrae, 1989). It has been shown that NSP1 from the bovine UKtc strain of rotavirus is able to interact with and promote the degradation of IRF3 in a proteasome-dependent manner whereas the protein from the porcine OSU strain of rotavirus interacts with and promotes the degradation of a different component of the innate immune response namely β-TrCP (Goodbourn *et al*., unpublished observation, Graff *et al*., 2009; Arnold and Patton, 2011). In a follow-up study from the Graff lab an initial attempt was made to localise the IRF3 interaction site(s) in NSP1 of the bovine B641 strain, which shares ~88% sequence identity with the UKtc protein (Graff *et al*., 2002; Xu *et al*., 1994). Three deletion mutants of B641NSP1 were constructed and examined for interaction with human IRF3 in a yeast two-hybrid assay. The results of these deletion studies suggested that there is at least one point of contact with IRF3 in the C-terminal half of NSP1 (Graff *et al*., 2002). The C-terminal half of NSP1 is the most highly variable region of the protein (Xu *et al*., 1994) and so subsequent point mutations were made within the conserved N-terminal zinc finger motif at positions 29, 54 and 57 (H29L, C54A and C57A in B641NSP1), all of these point mutants abolished the NSP1-IRF3 interaction, suggesting that is the second region of the protein also important for this particular interaction (Graff *et al*., 2007).

By contrast no data have been published as yet on the interaction site(s) of the OSU NSP1 with β-TrCP. Against this background the strategy pursued in this study was to

use chimeric UKtc/OSU NSP1 hybrid genes in different assays to determine the site(s) responsible for interactions between NSP1 and these two cellular proteins. The two assay systems chosen initially to study these interactions were mammalian two-hybrid assays and co-immunoprecipitation analysis.

The mammalian two-hybrid system is a development of the original yeast two hybrid system which is a sensitive assay for detecting protein-protein interactions in *vivo* (Luo *et al*., 1997). To set up the assay, one of the two potentially interacting proteins is fused to the Gal4 DNA-binding domain and its potential partner protein is fused to a transcriptional activation domain, in this case from herpes simplex virus VP16 protein. Plasmids encoding these two fusion proteins are then transfected into mammalian cells together with a suitable reporter gene plasmid. If there is an interaction between the two proteins under analysis, it will bring the DNA binding and activation domain together and result in the activation of reporter gene expression. In this study the reporter chosen was a green fluorescent protein which can be easily visualised under a UV microscope. If the two proteins under analysis do not interact with each other, the reporter gene will not be switched on and no fluorescent signal will be detected (**Figure 4.1**).

The second assay system chosen to complement the mammalian two hybrid assay for studying the physical protein-protein interaction between NSP1 and IRF3/ β-TrCP was co-immunoprecipitation. This technique relies on the fact that a specific antibody against NSP1 can precipitate the protein from a complex mixture. Any proteins that are complexed to the target protein should also be precipitated and can then be identified in subsequent analysis of the precipitate. For the purposes of this

study, a FLAG epitope was added to the N-terminal of the parental and hybrid NSP1 proteins to ensure constant efficiency of precipitation of the different variants, and FLAG-Sepharose was used to isolate the antibody-antigen complexes. It is important to bear in mind that one shortcoming of co-immunoprecipitation studies is that on their own they do not necessarily show the existence of a direct protein-protein interaction with the protein targeted by the precipitating antibody as they may be one component of a large complex that is held together by a complex set of protein-protein interactions.

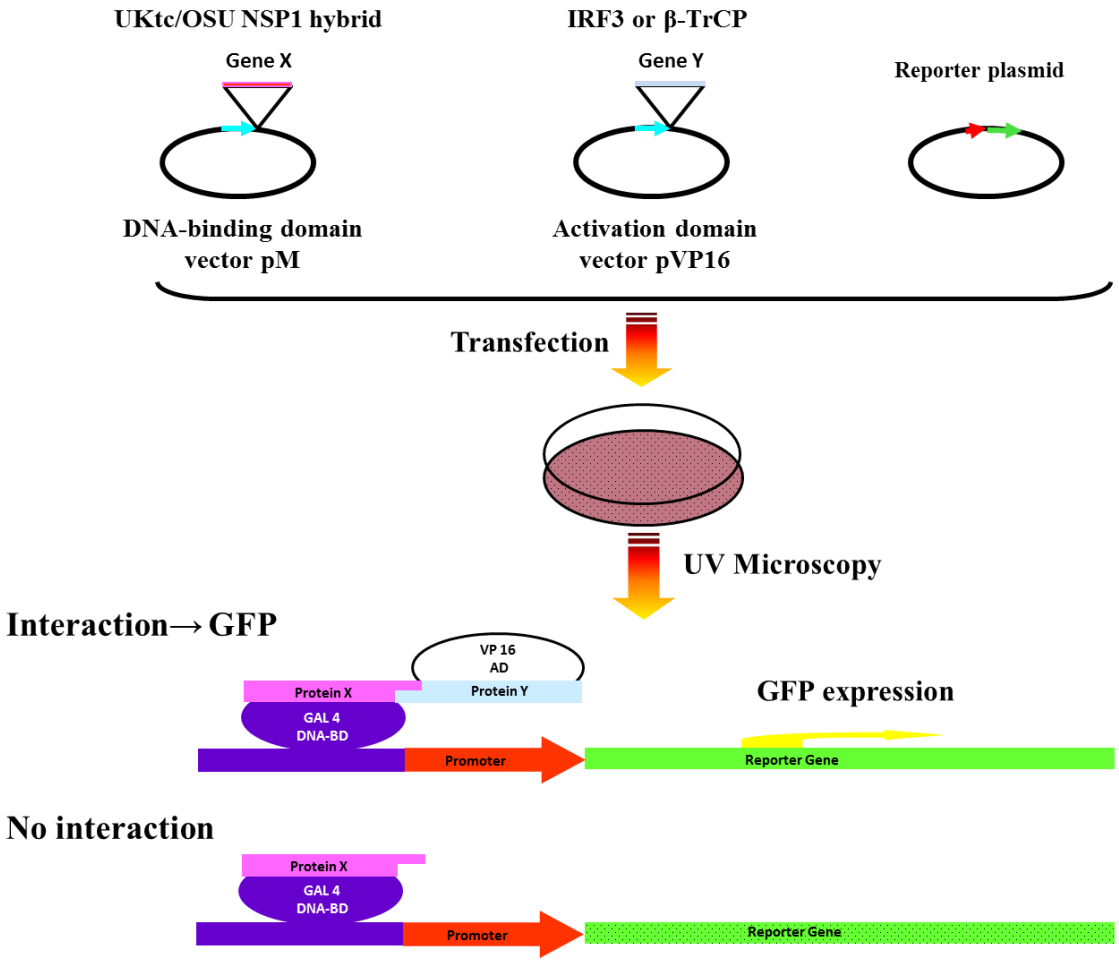

Figure 4.1 Schematic representation of the mammalian two-hybrid assay. Regular transcription of the reporter gene under the control of a GAL4 responsive promoter is triggered when the Activation domain (AD) and the DNA-binding (BD) domain are intact. In the two-hybrid system, these two domains are physically separated and fused to the two genes of interest (here, UKtc/OSU NSP1 hybrid and IRF3/β-TrCP), then transfected into cells with the reporter plasmid (here, GFP expression plasmid). When the two genes of interest interact with each other, the two domains come into proximity to each other initiating reporter gene transcription, as GFP expression plasmid is used, the cells can be visualised under UV microscopy. In the case of two non-interacting proteins, the two domains remain separated and there is no reporter gene transcription.

4.2 Molecular cloning of protein coding sequences for interaction studies in the mammalian two-hybrid assay system

The human IRF3 coding sequence was obtained from the pEFplink2-IRF3 (kindly provided by Prof S Goodbourn) via restriction enzyme digestion with *Nco* I and *Xba* I (**Figure 4.2**). As one of the host cellular proteins previously shown to interact with rotavirus NSP1, the IRF3 coding sequence had to be cloned into the mammalian two-hybrid vectors pM and pVP16 for subsequent analysis and RE sites *EcoR* I and *Hind* III have been selected for this cloning (**Figure 4.3**). These two RE sites were generated in IRF3 plasmid via PCR using primers listed in table 2.1.7. The *EcoR* I site was generated just before the start codon of IRF3 ORF, whereas the *Hind* III site was created at the end of the coding sequence before the stop codon, in which case the gene will be using the stop codon from the vector (**Figure 4.4**). Positive colonies were selected via Blue/White screening and the DNA extracted was subjected in restriction enzyme double digestion followed by sequencing (**Figure 4.5A**). However this analysis revealed that the original design of the primer used for IRF3 cDNA amplification had made IRF3 protein to be out of frame with the upstream DNA binding and transcription activation domains of the fusion protein. To overcome this oversight the fusion construct plasmid was digested with *EcoR* I, the staggered ends of the *EcoR* I site were filled in using Klenow DNA polymerase I and the plasmid was re-circularised to give a construct in which the two halves of the fusion protein were joined to each other in frame (**Figure 4.5B**).

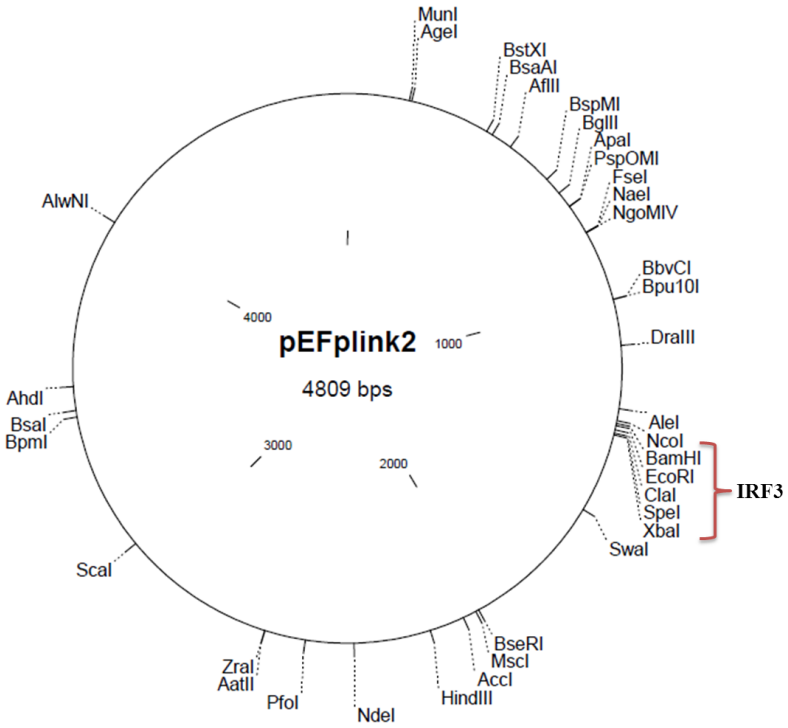

Figure 4.2 IRF3 obtained from vector pEFplink2.

IRF3 expression plasmid was obtained by double digestion with restriction enzymes *Nco* I and *Xba* I from the pEFplink2-IRF3 plasmid, which is ready for the subsequence re-amplification with PCR to add other restriction enzyme sites for cloning into the mammalian two-hybrid vectors.

Figure 4.3 Experimental strategies for re-amplifying IRF3 coding sequence into the mammalian two-hybrid vectors.

EcoR I and *Hind* III sites are generated using PCR with appropriate primers at both the 5' and 3' end of the IRF3 coding sequence for re-amplifying IRF3 coding sequence into the mammalian two-hybrid vectors.

A.

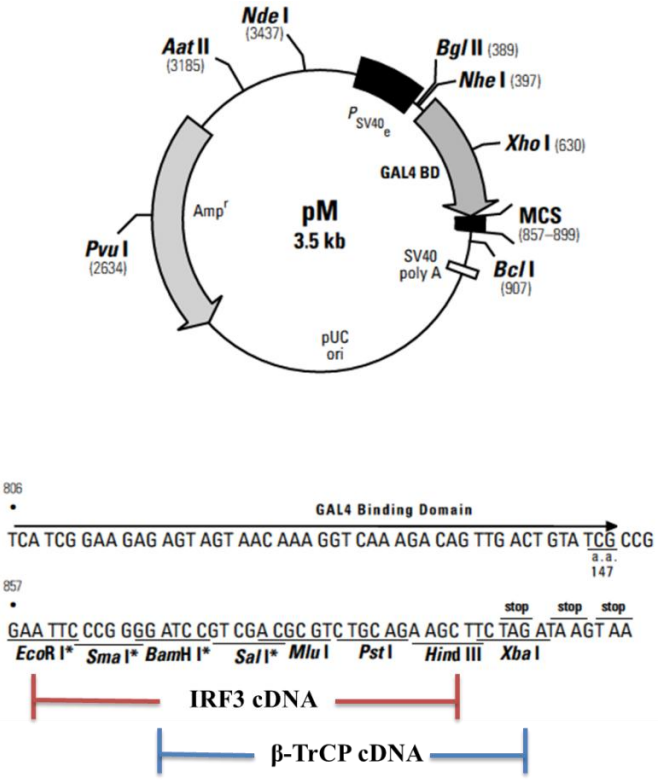
Nde I
(3437)
Aat II
(3185)
Bgl II (389)
Nhe I (397)
P SV40 e
Xho I (630)
GAL4 BD
MCS
(857–899)
Bcl I
(907)
SV40
poly A
pM
3.5 kb
Amp r
Pvu I
(2634)
pUC
ori
806
GAL4 Binding Domain
TCA TCG GAA GAG AGT AGT AAC AAA GGT CAA AGA CAG TTG ACT GTA TCG CCG
a.a.
147
857
stop stop stop
GAA TTC CCG GGG ATC CGT CGA CGC GTC TGC AGA AGC TTC TAG ATA AGT AA
EcoR I* Sma I* BamH I* Sal I* Mlu I Pst I Hind III Xba I
IRF3 cDNA
β-TrCP cDNA

B.

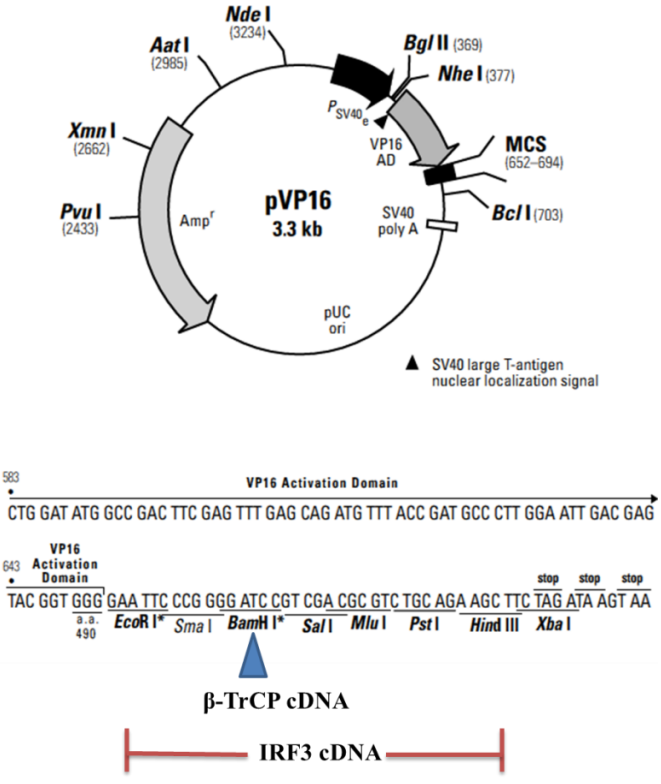
Nde I
(3234)
Aat I
(2985)
Bgl II (369)
Nhe I (377)
P SV40 e
Xmn I
(2662)
VP16
AD
MCS
(652–694)
Bcl I (703)
SV40
poly A
pVP16
3.3 kb
Amp r
Pvu I
(2433)
pUC
ori
SV40 large T-antigen
nuclear localization signal
583
VP16 Activation Domain
CTG GAT ATG GCC GAC TTC GAG TTT GAG CAG ATG TTT ACC GAT GCC CTT GGA ATT GAC GAG
643
VP16
Activation
Domain
stop stop stop
TAC GGT GGG GAA TTC CCG GGG ATC CGT CGA CGC GTC TGC AGA AGC TTC TAG ATA AGT AA
a.a.
490
EcoR I* Sma I BamH I* Sal I Mlu I Pst I Hind III Xba I
β-TrCP cDNA
IRF3 cDNA

Figure 4.4 Schematic diagrams of the mammalian two-hybrid system cloning vectors pM and pVP16, showing the multi-cloning site sequence and unique restriction enzyme sites.

Schematic diagrams of the main features of vectors pM **(panel A)** and pVP16 **(panel B)** are shown. pM expresses the DNA binding domain (amino acids 1-147) of the GAL4 protein. pVP16 generates the transcriptional activation domain (amino acids 446-490) of the HSV VP16 protein. These plasmids have unique RE sites located in the multi-cloning site (MCS) region at the 3' end of the open reading frame for either the GAL4 DNA binding domain or the VP16 activation domain. The gene encoding the protein of interest is ligated into the MCS in the correct orientation and reading frame, such that fusion proteins with the GAL4 or VP16 domains are expressed. The unique restriction sites that chosen to be used for cloning both IRF3 (*EcoR* I and *Hind* III) and β-TrCP (*BamH* I and *Xba* I) in the MCS of these vectors are indicated below each plasmid diagram (This figure is adapted from the Clontech Matchmaker Mammalian Assay Kit User Manual).

A

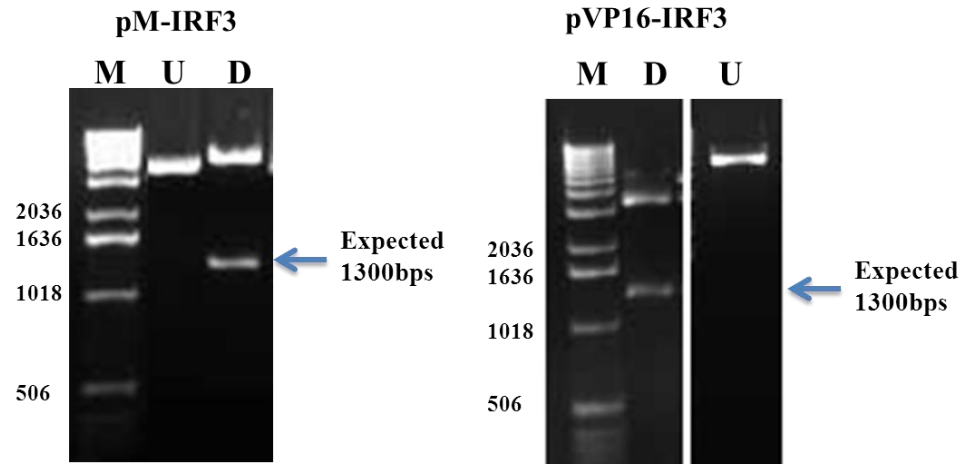
pM-IRF3
M U D
2036
1636
1018
506
Expected
1300bps
pVP16-IRF3
M D U
2036
1636
1018
506
Expected
1300bps

B

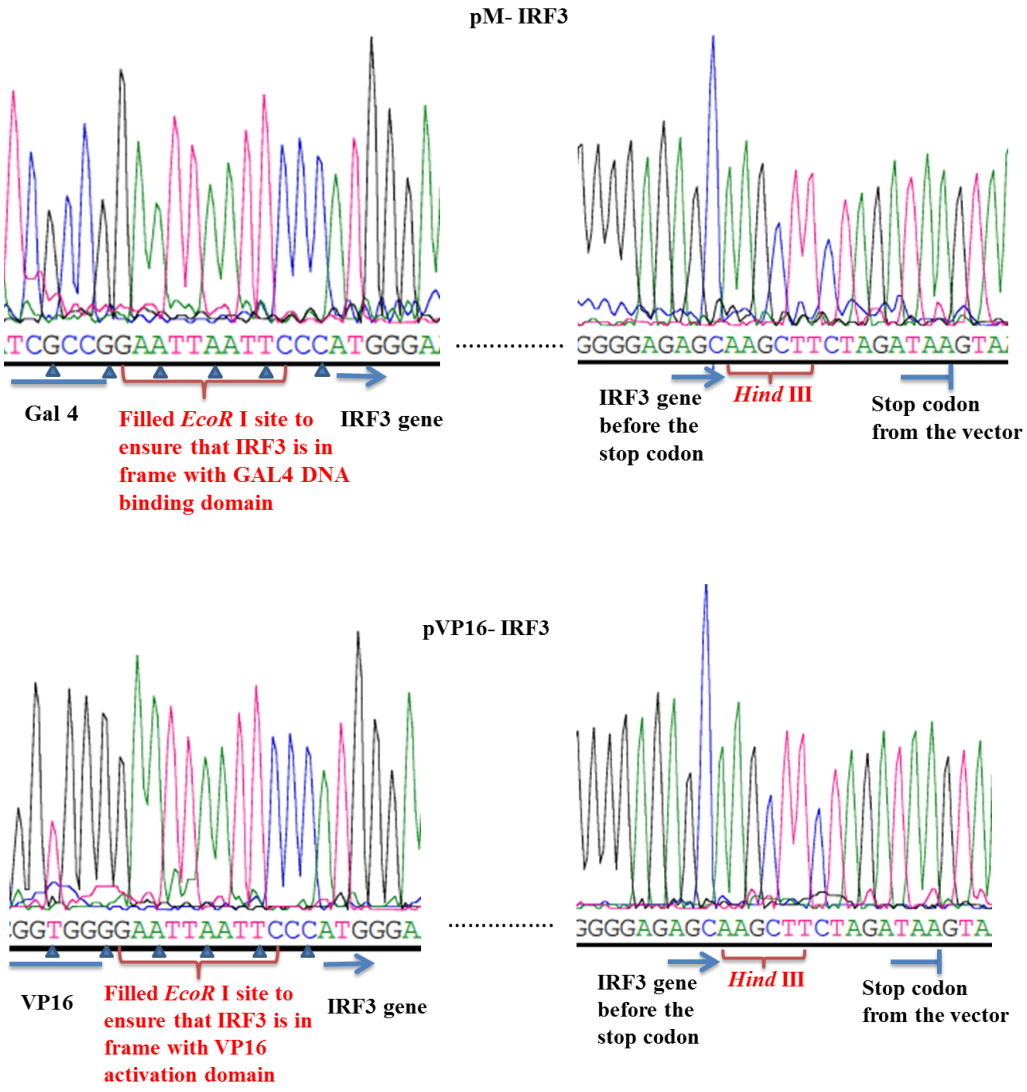
pM- IRF3
TCGCCGGGAATTAATTCCCATGGGA
GGGGAGAGCAAGCTTCTAGATAAGTA
Gal 4
Filled EcoR I site to ensure that IRF3 is in frame with GAL4 DNA binding domain
IRF3 gene
IRF3 gene before the stop codon
Hind III
Stop codon from the vector
pVP16- IRF3
GGTGGGGAATTAATTCCCATGGGA
GGGGAGAGCAAGCTTCTAGATAAGTA
VP16
Filled EcoR I site to ensure that IRF3 is in frame with VP16 activation domain
IRF3 gene
IRF3 gene before the stop codon
Hind III
Stop codon from the vector

Figure 4.5 Confirmation of the constructs pM-IRF3 and pVP16-IRF3.

(A) DNAs of the pM-IRF3 and pVP16-IRF3 constructs were amplified in *E.coli* and purified by maxi-prep as described in Materials and Methods. Plasmid DNA was then double digested with *EcoR* I and *Hind* III and fractionated on a 1% agarose gel as described in Materials and Methods. The position of the expected 1300bp IRF3 insert band is indicated down the right hand side of each gel. Lanes labelled D indicate the samples after double digestion and lanes labelled U indicate the undigested samples, lanes labelled M indicate the 1kb DNA marker and the sizes of the markers are given in base pairs.

(B) Sequencing analysis was performed to confirm the correct orientation and open reading frame of IRF3 at the junction with the Gal4 domain in the pM vector, or the VP16 domain in the pVP16 vector.

Similarly, β-TrCP, the other possible interaction partner for rotavirus NSP1, was also cloned into pM and pVP16 vectors. The β-TrCP coding region from a plasmid carrying HA-tagged human β-TrCP (TRcP 1a/Fbw 1a) (Kindly provided by Dr A Stephanou) was amplified with primers listed in table 2.1.7 and cloned into the mammalian two-hybrid vectors between RE sites *BamH* I and *Xba* I for pM or only *BamH* I in the case of pVP16 (**Figure 4.3**). *BamH* I and *Xba* I sites were created at respectively the 5' end of the β-TrCP coding sequence upstream of the start codon and the 3' end of the ORF following the stop codon for cloning into the pM vector. For cloning into pVP16 activation domain vector, *BamH* I sites were generated at both ends of the β-TrCP ORF. Positive colonies were selected via Blue/White screening, and plasmid DNA extracted was subjected to restriction enzyme double digestion (**Figure 4.6A**). Selected clones were then sequenced to confirm the correct joining points in both vectors (**Figure 4.6B**).

A

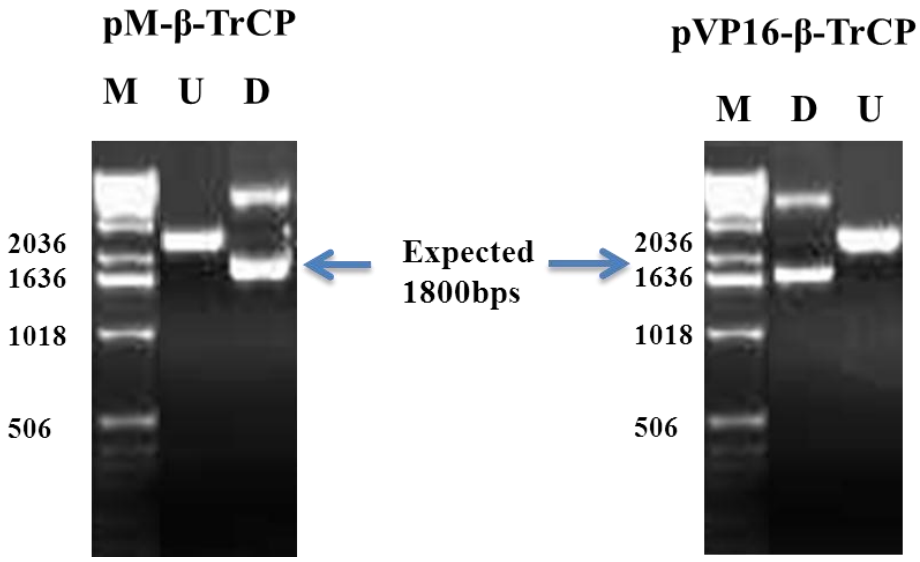
pM-β-TrCP
M U D
pVP16-β-TrCP
M D U
2036
1636
1018
506
Expected
1800bps
2036
1636
1018
506

B

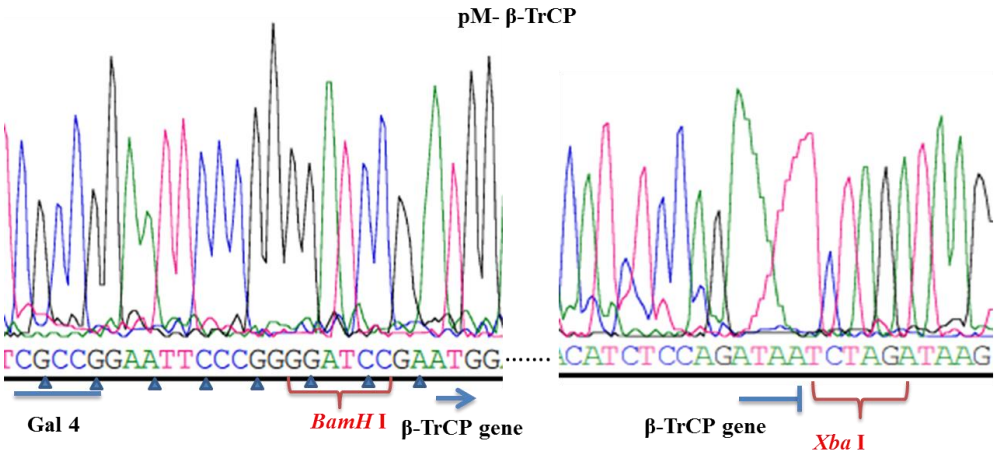
pM- β-TrCP
TCGCCGGAATTCCCGGGGATCCGAATGG
CATCTCCAGATAATCTAGATAAG
Gal 4
BamH I
β-TrCP gene
β-TrCP gene
Xba I

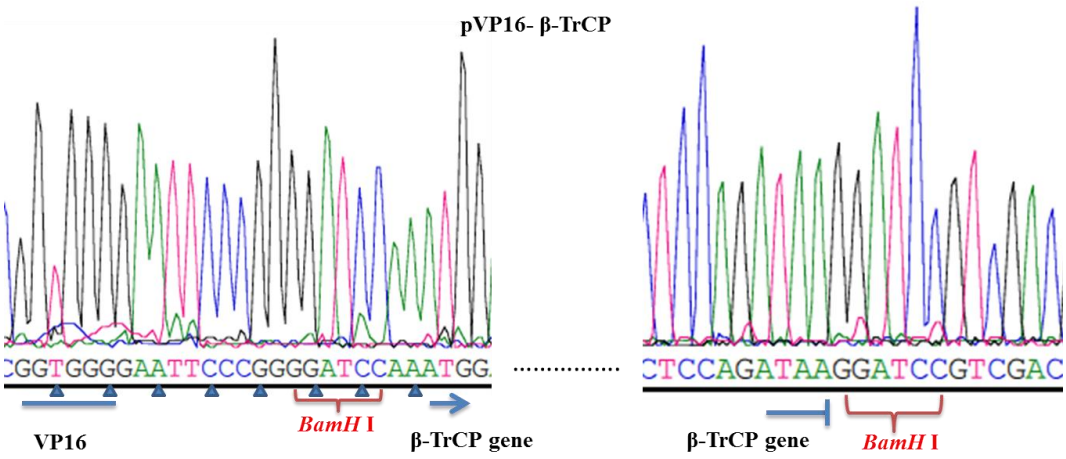
pVP16- β-TrCP
CGGTGGGGAATTCCCGGGGATCCAAATGG
CTCCAGATAAGGATCCGTCGAC
VP16
BamH I
β-TrCP gene
β-TrCP gene
BamH I

Figure 4.6 Confirmation of the constructs pM-β-TrCP and pVP16-β-TrCP.

(A) DNAs of the pM- β-TrCP and pVP16- β-TrCP constructs were amplified in *E.coli* and purified by maxi-prep as described in Materials and Methods. Plasmid DNA was then double digested with *BamH* I and *Xba* I or digested with *BamH* I alone, and fractionated on a 1% agarose gel as described in Materials and Methods. The position of the expected 1800bp β-TrCP insert band is indicated down the right hand side of each gel. Lanes labelled D indicate the samples after digestion and lanes labelled U indicate the undigested samples, lanes labelled M indicate the 1kb DNA marker and the sizes of the markers are given in base pairs.

(B) Sequencing analysis was performed to confirm the correct orientation and open reading frame of β-TrCP at the junction with the Gal4 domain in the pM vector, or the VP16 domain in the pVP16 vector.

The parental UKtcNSP1 and OSUNSP1 cDNAs were also cloned into the two mammalian two-hybrid vectors. The UKtcNSP1 coding sequence was cloned in between *EcoR* I and *Hind* III restriction enzyme sites using the same strategy as that employed for IRF3. The OSUNSP1 coding sequence was cloned in between *BamH* I and *Hind* III restriction enzyme sites again using the strategy described earlier for their putative interaction partners, i.e: IRF3 and β-TrCP. The expected insert bands were detected as indicated (**Figure 4.7A**, **Figure 4.8A**) and the sequencing results of the corresponding junctions in all constructs confirmed the correct construction of these plasmids (**Figure 4.7B**, **Figure 4.8B**).

A

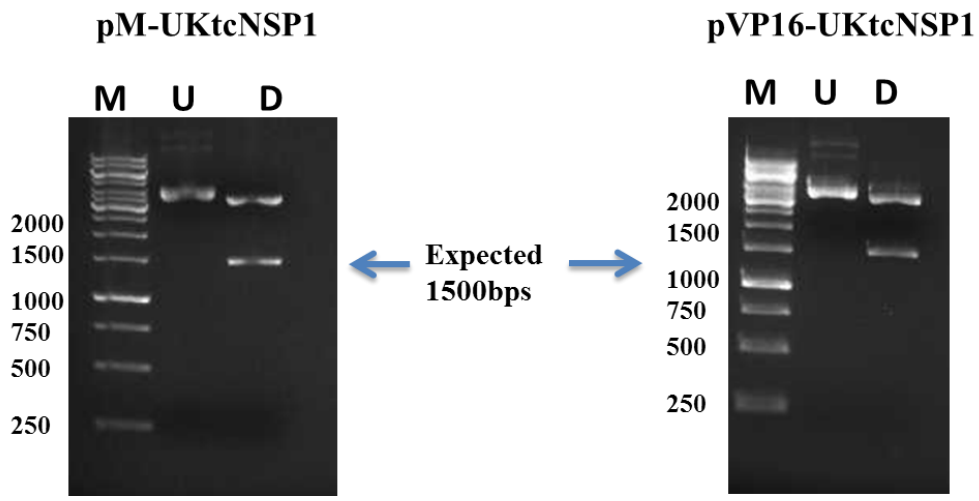
pM-UKtcNSP1
M U D
2000
1500
1000
750
500
250
Expected
1500bps
pVP16-UKtcNSP1
M U D
2000
1500
1000
750
500
250

B

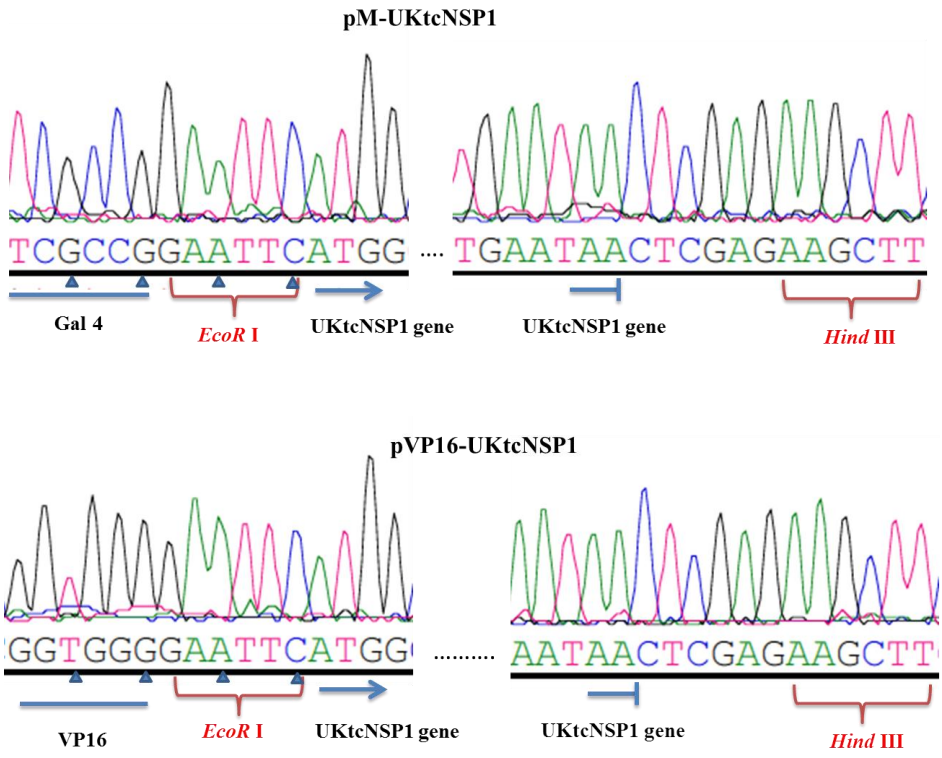
pM-UKtcNSP1
TCGCCGGAATTCATGG
....
TGAATAACTCGAGAAGCTT
Gal 4
EcoR I
UKtcNSP1 gene
UKtcNSP1 gene
Hind III
pVP16-UKtcNSP1
GGTGGGGAATTCATGG
.....
AATAACTCGAGAAGCTT
VP16
EcoR I
UKtcNSP1 gene
UKtcNSP1 gene
Hind III

Figure 4.7 Cloning of UKtcNSP1 into mammalian two-hybrid vectors pM and pVP16.

(A) Around 500ng of DNA sample were digested with *EcoR* I and *Hind* III and correct sized bands were released indicating the correct insert of the UKtcNSP1. U indicates the undigested product and D indicates the products after digestion, 1kb DNA marker on the left hand side indicates the sizes of the bands.

(B) Selected clones were sequenced using pM and pVP16 sequencing primers (Table 2.1.7) and the junction regions are illustrated. Sequencing analysis confirmed that the UKtcNSP1 gene was inserted correctly with correct orientation in both pM and pVP16 vectors.

A

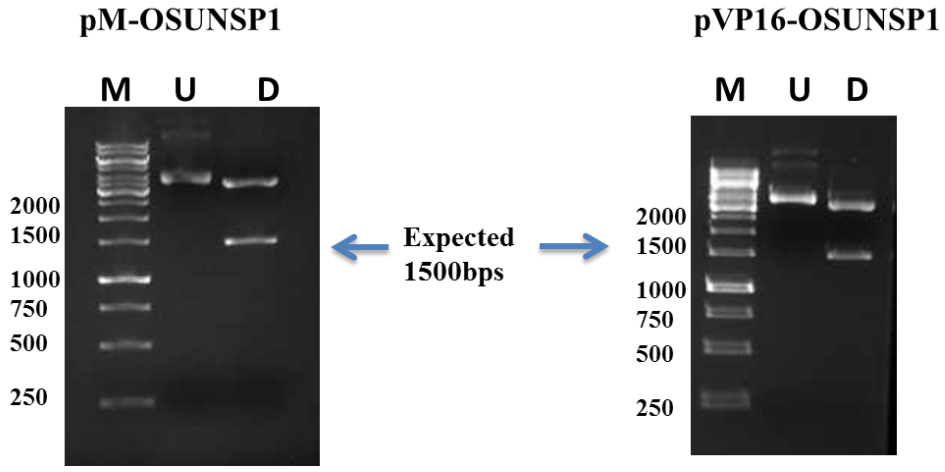
pM-OSUNSP1
M U D
2000
1500
1000
750
500
250
Expected
1500bps
pVP16-OSUNSP1
M U D
2000
1500
1000
750
500
250

B

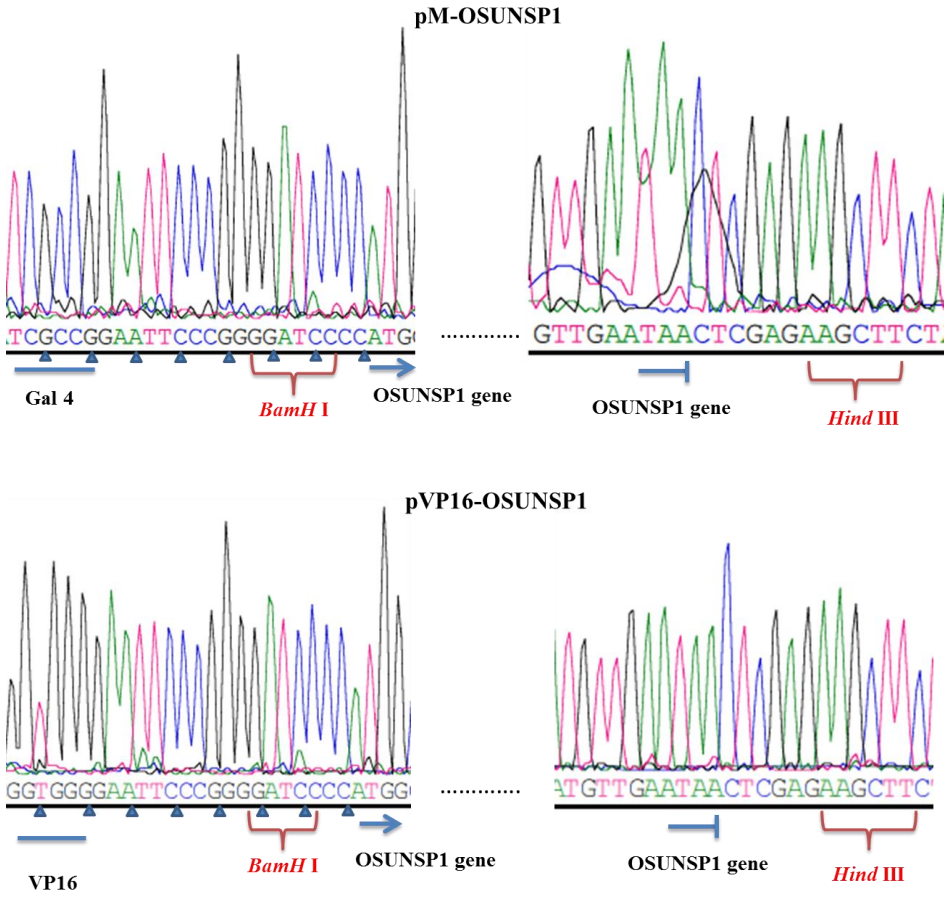
pM-OSUNSP1
TCGCCGGAATTCCCGGGGATCCCCATG
GTTGAATAACTCGAGAAGCTTCT
Gal 4
BamH I
OSUNSP1 gene
OSUNSP1 gene
Hind III
pVP16-OSUNSP1
GGTGGGGAATTCCCGGGGATCCCCATGG
ATGTTGAATAACTCGAGAAGCTTC
VP16
BamH I
OSUNSP1 gene
OSUNSP1 gene
Hind III

Figure 4.8 Cloning of OSUNSP1 into mammalian two-hybrid vectors pM and pVP16.

(A). Around 500ng of DNA sample were digested with *BamH* I and *Hind* III, and correct sized bands were released indicating the correct insert of the NSP1. U indicates the undigested product and D indicates the products after digestion, 1kb DNA marker on the left hand side indicates the sizes of the bands.

(B). Selected clones were sequenced using pM and pVP16 sequencing primers (Table 2.1.7) and the junction regions are illustrated. Sequencing analysis confirmed that the OSUNSP1 gene was inserted correctly with correct orientation in both pM and pVP16 vectors.

4.3 Protein-Protein interaction studies using the mammalian two-hybrid assay system

Positive and negative control reactions were included in each mammalian two-hybrid assay. The positive control plasmids used for the assay were pM-p53, which expresses a fusion of the GAL4DNA-BD to the mouse p53 protein, and pVP16-LT, which expresses a fusion of the VP16 AD to the SV40 large T-antigen. Mouse p53 and SV40 large T-antigen have been shown to interact (Lane and Crowford, 1979) and the purpose of this positive control was to verify that the system was detecting an expected protein-protein interaction between the two known interacting proteins. pVP16-CP plasmid encodes and expresses a fusion of the VP16 AD to a viral coat protein, which does not interact with p53. The transfection with pM-p53 and pVP16-CP was therefore used as a negative control indicating no interaction is detected. The reporter gene chosen for these studies was GFP, because its expression could be

easily and rapidly screened for living cells by UV microscopy. The plasmid pUAST-hrGFP-neo (kindly provided by Dr K.T.Chung, University of Warwick) which contains a GFP gene under the control of a Gal4-responsive promoter (**Figure 4.9**) was the reporter plasmid actually used in the series of experiments.

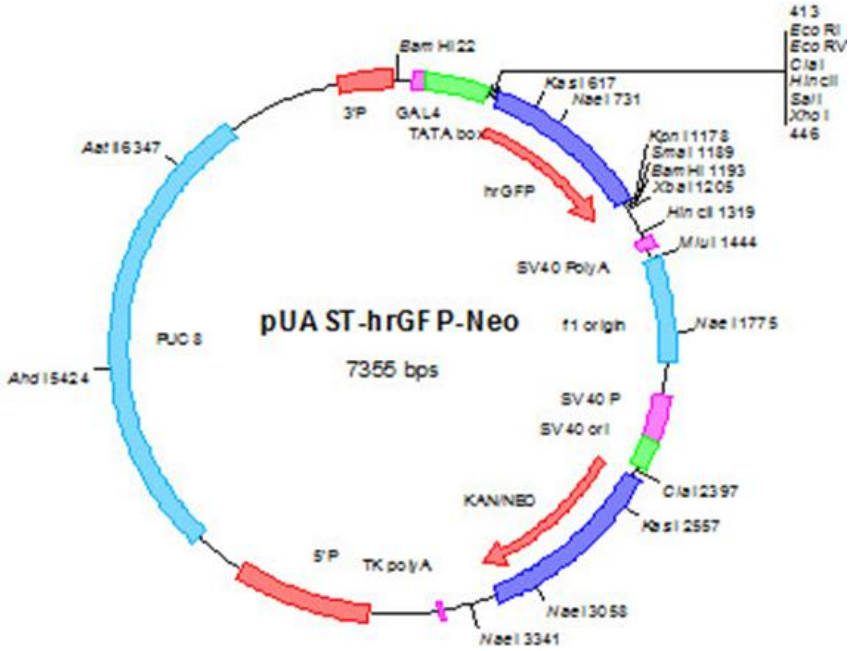

Figure 4.9 Reporter gene plasmid used in the mammalian two-hybrid system. pUAST-hrGFP-neo contains the green fluorescent protein (GFP) gene positioned downstream of the Gal4 responsive element and a minimal promoter from the Adenovirus E1b gene. It is used as a qualitative reporter in this mammalian two-hybrid assay as the GFP expression can be easily visualised under the UV microscope in live cells.

To establish the utility of the mammalian two hybrid assay in attempts to map protein-protein interaction sites, the two parental NSP1 plasmids, i.e: those from UKtc and OSU were analysed first. Highly transfectable human embryonic kidney cells (293) were mock transfected or co-transfected with a combination of a Gal4-BD fusion protein plasmid, a VP16-AD fusion protein plasmid and the reporter GFP plasmid, 48 hours later, the cells were visualised under UV microscopy to monitor reporter gene expression. In initial tranfections, not even samples co-transfected with the positive control plasmids showed any evidence of reporter gene expression. Therefore a variety of changes were made to the transfection protocol, including changing of the ratio of the total amount of DNA to the transfection reagent, changing cells and making new batches of plasmid DNA. These changes proved successful with ~ 50% of the 293 cells showing positive GFP expression with the control plasmids (**Figure 4.10B**). Despite the positive control giving good reporter gene expression in the experimental samples, few fluorescent cells were observed (**Figure 4.10 D-G**). A positive signal was observed in one of the experimental samples in Figure 4.10D. However control transfections with individual plasmids and reporter plasmid revealed that the positive signal was due to self-activation by pM-IRF3 (**Figure 4.11**). The failure to demonstrate protein-protein interaction between the parental NSP1 proteins used in this study and IRF3 or β-TrCP in the mammalian two-hybrid assay was particularly surprising as UKtc and IRF3 have been shown to interact in a yeast two-hybrid assay (Goodbourn *et al*., unpublished observations).

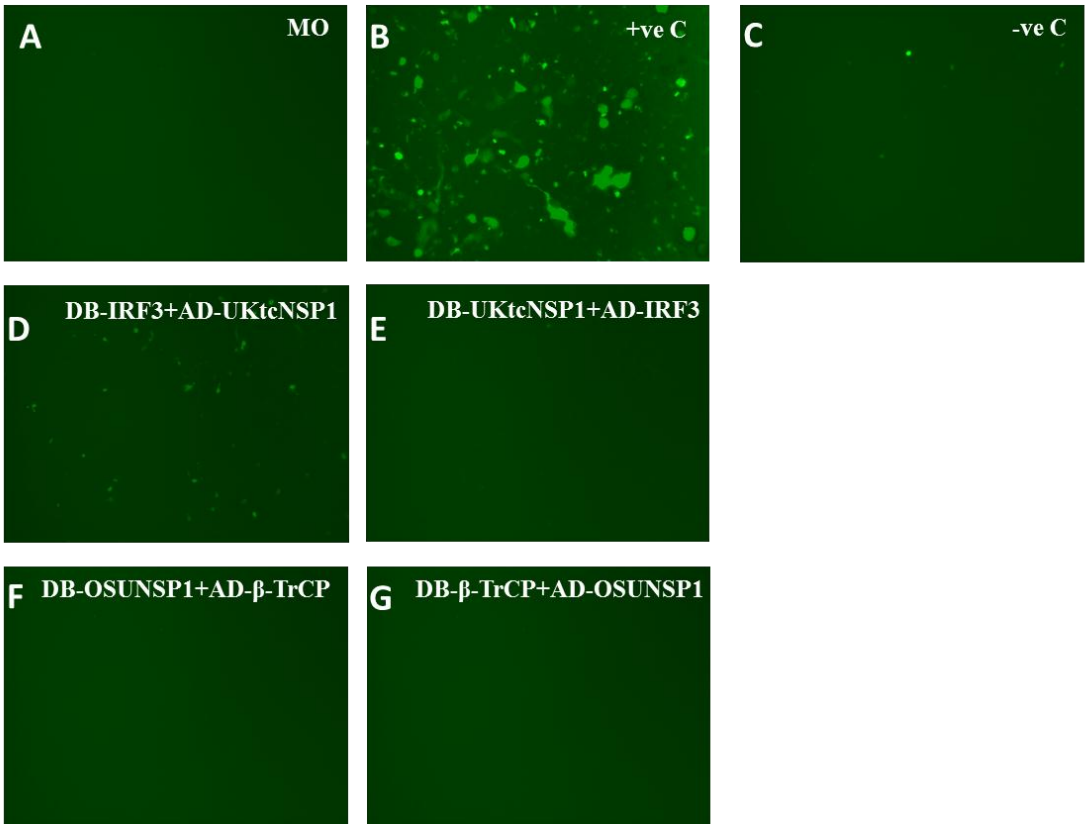

Figure 4.10 NSP1-host protein interaction analysed in mammalian two-hybrid assay.

3.6 x10^5 293 cells were mock transfected or co-transfected with a combination of Gal4-BD fusion protein plasmid, VP16-AD fusion protein plasmid and reporter GFP plasmid. 48 hrs post transfection, cells were visualised under UV microscope as described in Materials and Methods. **(A).** Cells mock transfected, showing no fluorescent cells as expected. **(B).** Cells co-transfected with positive control plasmids, around 50% of the cells exhibit fluorescent cells indicating the expected interaction between p53 and large T-antigen. **(C).** Cells co-transfected with negative control plasmids, little GFP expression is observed indicating no interaction between p53 and CP. **(D).** Cells co-transfected with pVP16-UKtcNSP1 and pM-IRF3, a few fluorescent cells were observed although they only account around 10% of the total cell number. **(E).** Cells co-transfected with pM-UKtcNSP1 and pVP16-IRF3, no obvious GFP expression is observed. **(F+G).** Cells co-transfected with pM-OSUNSP1 and pVP16-β-TrCP; pM-β-TrCP and pVP16-OSUNSP1 respectively, no obvious GFP expression is observed.

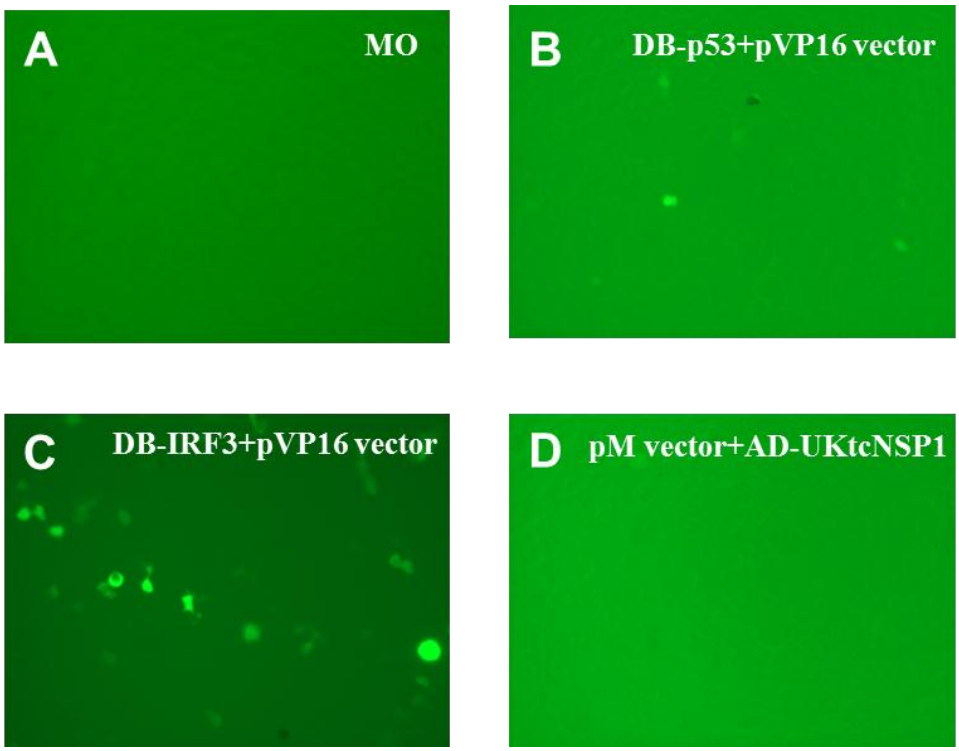

Figure 4.11 selected individual transfection analysing self-activated GFP expression.

3.6 x10^5 293 cells were mock transfected or co-transfected with individual Gal4-BD or VP16-AD fusion protein plasmid, accompanied with the empty pVP16 or pM vector, and reporter GFP plasmid. 48 hrs post transfection, cells were visualised under UV microscope as described in Materials and Methods. **(A).** Cells mock transfected, showing no fluorescent cells as expected. **(B).** Cells co-transfected with one of the positive control plasmid, pM-p53, and empty pVP16 vector, less than 1% of the cells exhibit fluorescent cells. **(C).** Cells co-transfected with pM-IRF3 and pVP16 empty vector, less than 10% of cells showed GFP expression indicating the ability of self-activation of this pM-IRF3 plasmid. **(D).** Cells co-transfected with pVP16-UKtcNSP1 and pM empty vector, no obvious GFP expression is observed.

4.4 NSP1 expression in transfected cells

Given the previously demonstrated interaction between UKtcNSP1 and IRF3, one possible explanation for the failure to detect it in the mammalian two-hybrid assay system was that the proteins might not be expressed correctly in the transfected 293 cells. To investigate this possibility 293 cells were transfected with a number of plasmids including pM vector, pM-p53, pM-UKtcNSP1, pM-OSUNSP1, pVP16 vector, pVP16-LT, pVP16-UKtcNSP1 and pVP16-OSUNSP1 individually. Cell extracts at 48 hours post transfection were examined via SDS-PAGE followed by western blot using anti-Gal4 and anti-VP16 antibodies respectively to detect the fusion proteins (**Figure 4.12**). No obvious protein expression was detected using these two antibodies; the experimental samples exhibited the similar appearance as the mock-transfected samples. No obvious difference in band pattern between the one transfected with vector only and the ones transfected with the fusion protein plasmids. The size of Gal 4 is around 40kDa and therefore the expected bands in the lanes should appear around 95-105kDa region, since the NSP1 is around 55kDa in size, therefore it is similar to p53, suggesting similar bands should appear in all transfected samples (**Figure 4.12A**), however, these bands are absent in this blot. Blot probed by anti-VP16 antibody shows no obvious difference between the cells transfected with pVP16 vector only and cells transfected with VP16 fusion proteins, the size of VP16 is around 30kDa and therefore the expected band in each lane transfected with NSP1 fusion protein plasmid should be around 85-95kDa, whereas the lane transfected with the control plasmid pVP16-LT should have a band around 120kDa as the SV40 large T antigen has a molecular weight around 90kDa (**Figure 4.12B**), none of the band was observed.

A

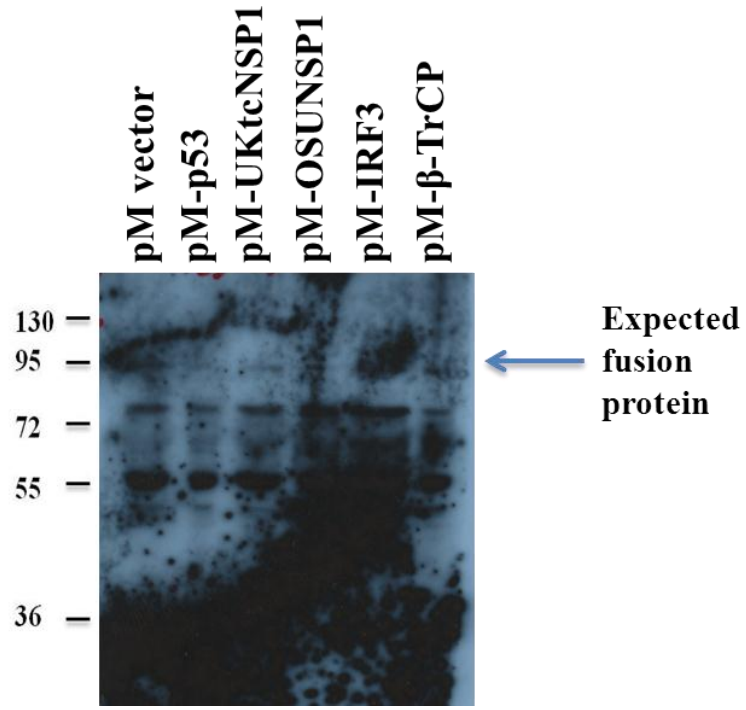
pM vector
pM-p53
pM-UKtcNSP1
pM-OSUNSP1
pM-IRF3
pM-β-TrCP
130
95
72
55
36
Expected fusion protein

B

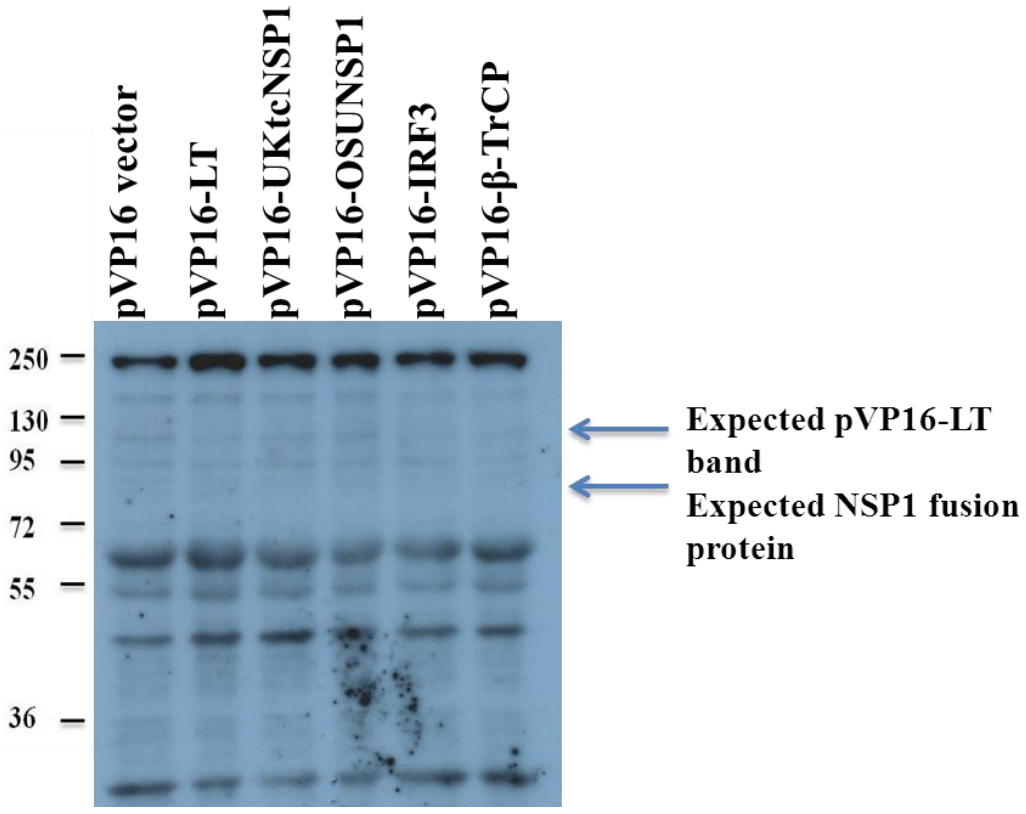
pVP16 vector
pVP16-LT
pVP16-UKtcNSP1
pVP16-OSUNSP1
pVP16-IRF3
pVP16-β-TrCP
250
130
95
72
55
36
Expected pVP16-LT band
Expected NSP1 fusion protein

Figure 4.12 Protein expression analysis from mammalian two-hybrid vectors. 2×10^5 293 cells were transfected with individual Gal4 and VP16 fused protein plasmids. 48 hrs later, cell lysate were collected and proteins were separated on SDS-PAGE and probed with anti-Gal4 (A) or anti-VP16 (B) respectively as described in Materials and Methods. Protein molecular weight markers are indicated on the left hand side in both figures.

The fact that levels of positive control protein that were undetectable could nevertheless give a positive result in the two-hybrid assay suggested that even low level of the protein expression are still able to give a result. Therefore, we considered whether or not the constructs were actually able to expression the intended proteins.

4.5 Expression of NSP1 proteins in pCDNA3.1 vector

In order to confirm the unsuccessful results of the reporter assay was due to the poorly expressed NSP1 proteins in 293 cells, further analysis was carried out. Rotavirus NSP1 is normally expressed in the cytoplasm of its permissive cells; therefore it is possible the NSP1 cDNA expression was limited as it took place in the nucleus. Subsequently, both parental NSP1 cDNAs were cloned into another mammalian vector pCDNA3.1, which contains a powerful CMV promoter to enhance expression (**Figure 4.13**). Proteins encoded by open reading frames cloned downstream of this promoter are routinely expressed to high levels in transient translation experiments.

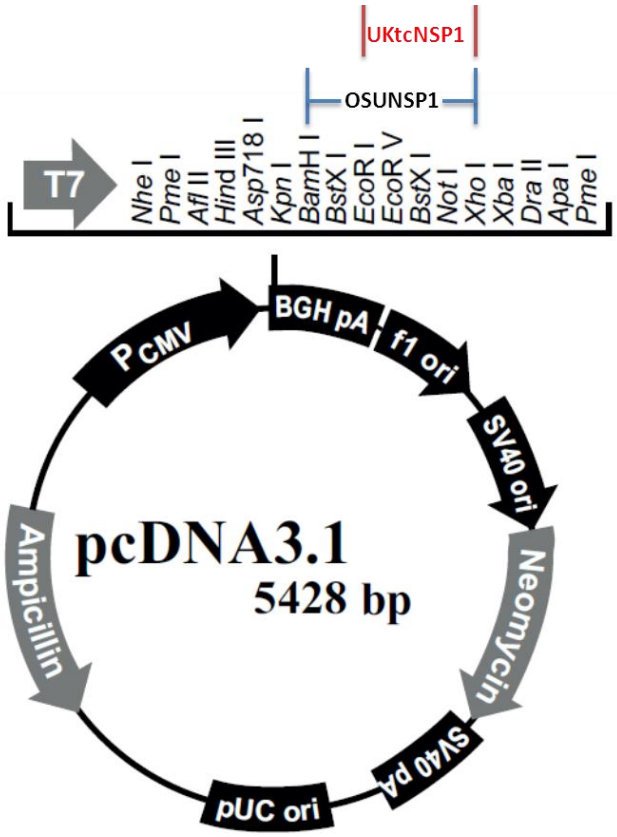

Figure 4.13 Cloning of NSP1 genes into vector pcDNA3.1.
Parental UKtcNSP1 cDNA was cloned into the vector between sites *Eco*R I and *Xho* I while OSUNSP1 cDNA was cloned into the vector between sites *Bam*H I and *Xho* I via PCR.

A FLAG epitope was added at the N-terminus of both UKtc and OSU NSP1 cDNAs via PCR with appropriate primers (**Table 2.1.7**) for conventional detection using anti-FLAG antibody. Constructs pCDNA3.1-FLAG-UKtcNSP1 and pCDNA3.1-FLAG-OSUNSP1 were therefore generated. The aim of this was to make the protein

product reading detectable via an antibody that was fully validated in our hands. The expression of NSP1 proteins from these plasmids was determined using anti-FLAG antibody in western blot (**Figure 4.14**). Despite the background of the blot, it is evident that only the positive control FLAG-PML plasmid (Beech *et al*,. 2005) expressed a detectable product; a strong band at around 100kDa in lane C was clearly observed overlaying a weaker background band present in all samples. Both pCDNA3.1-FLAG-UKtcNSP1 and pCDNA3.1-FLAG-OSUNSP1 showed very similar patterns to the mock-transfected negative control, suggesting that neither of the NSP1 plasmids expressed detectable products.

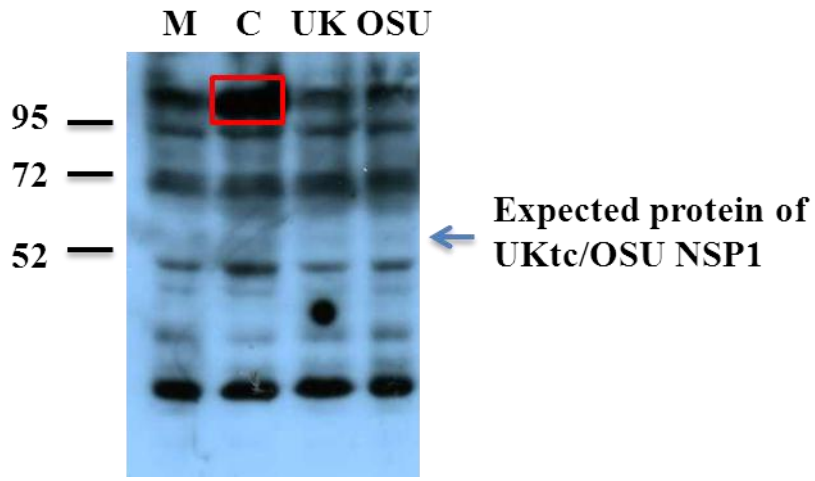

Figure 4.14 pCDNA3.1-FLAG-NSP1s cannot be detected in 293 cells.
2 x 10^5 293 cells were mock-transfected or transfected with a positive control FLAG-PML plasmid, pCDNA3.1-FLAG-UKtcNSP1 or pCDNA3.1-FLAG-OSUNSP1 individually. 48 hours later, cells were harvested and the total lysates were subjected to 10% SDS-PAGE and western blotting as described in Materials and Methods. The blot was probed by a polyclonal anti-FLAG antibody. Protein sizes of marker proteins are indicated in kDa on the left hand side of the blot.

4.6 Protein interaction studies via co-immunoprecipitation

With the intention of optimising the expression of NSP1 cDNAs, FLAG-tagged parental NSP1 genes were cloned into a pCI-neo vector between sites *Nhe* I and *Sal* I (**Figure 4.15**). pCI-neo vector contains a chimeric intron, upstream the inserted cDNA sequence, to facilitate RNA splicing. Early studies with SV40 virus demonstrated that splicing is a prerequisite for stable cytoplasmic 16S mRNA production (Hamer and Leder, 1979). It was subsequently shown that the addition of a splice to the 5' –untranslated leader can dramatically increase protein expression from a vector that contains no introns (Callis *et al*., 1987). Furthermore, splicing has been confirmed to lead to an increased level of both nuclear and cytoplasmic poly (A)-containing RNA (Buchman and Berg, 1988). Huang and Gorman using two expression vectors which differ only in the presence of absence of an intron reported that transient transfection into four mammalian cell lines resulted in up to 50 fold increased levels of the indicator protein from the vector carrying an intron, and that cytoplasmic RNA concentration corresponded directly to the resultant protein levels (Huang and Gorman, 1990). Therefore, the problem with the undetectable NSP1 proteins in transfected cells might be resolved by cloning it to the pCI-neo vector, and this was subsequently tested in the co-immunoprecipitation assay.

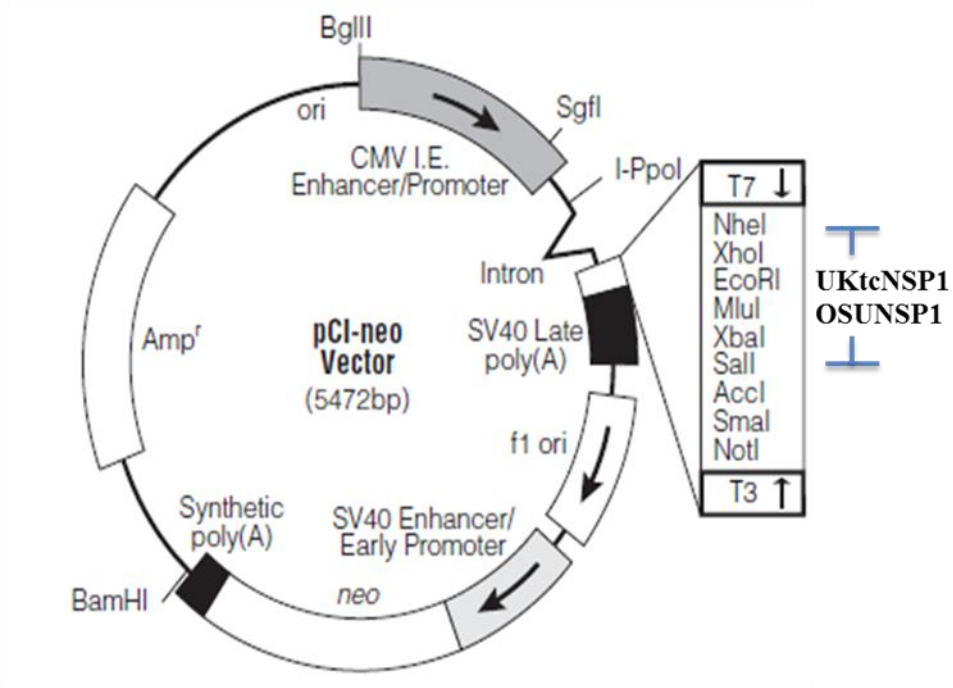

Figure 4.15 Map of cloning vector pCI-neo.
Both UKtcNSP1 and OSUNSP cDNAs were cloned into the vector between restriction enzyme sites *Nhe* I and *Sal* I.

Co-immunoprecipitation is a frequently used method of studying protein-protein interactions. An initial study was performed to determine if transfected pCI-neo-FLAG-UKtcNSP1 and pCI-neo-FLAG-OSUNSP1 were co-immunoprecipitated with IRF3 protein from transfected pCDNA-IRF3 in the presence or absence of proteasome inhibitor MG132, as it has been shown that UKtcNSP1 degrade IRF3 in a proteasome dependent manner. Cells mock-transfected or co-transfected with IRF3 and an empty vector or corresponding NSP1 plasmids were processed and precipitated using FLAG-Sepharose to isolate the antibody bound complex; samples before and after passing the resin were probed with anti-IRF3 and anti-FLAG antibodies. However, this experiment showed little co-precipitation of IRF3 with

either UKtcNSP1 or OSUNSP1. Figure 4.16 panel A and B showed the detection before the precipitation. Anti-IRF3 antibody detected a similar amount of the endogenous IRF3 in the mock transfected and FLAG control adenovirus 33kDa (Ad33) transfected samples, and much stronger bands were observed when additional IRF3 was transfected into the cells (**Figure 4.16A**); anti-FLAG antibody only detected the positive control Ad 33 at around 33kDa position before binding, none of the UKtcNSP1 or OSUNSP1 were probed (**Figure 4.16B**); however after binding to the FLAG-Sepharose, the elution detected by anti-IRF3 or anti-FLAG respectively showed no clear distinguish band across the blot, the expected band should appear on the samples transfected with UKtcNSP1 at least as it has been shown previously in other groups to be interacting with IRF3, and the addition of MG132 should restore the level of IRF3. However, bands all appeared to be the same with no expected binding in the UKtcNSP1 and OSUNSP1 transfected samples and no indication of precipitation (**Figure 4.16C+D**) and this observation suggested that the interaction between NSP1 and host cellular proteins were still very difficult to be detected so did the protein expression.

A

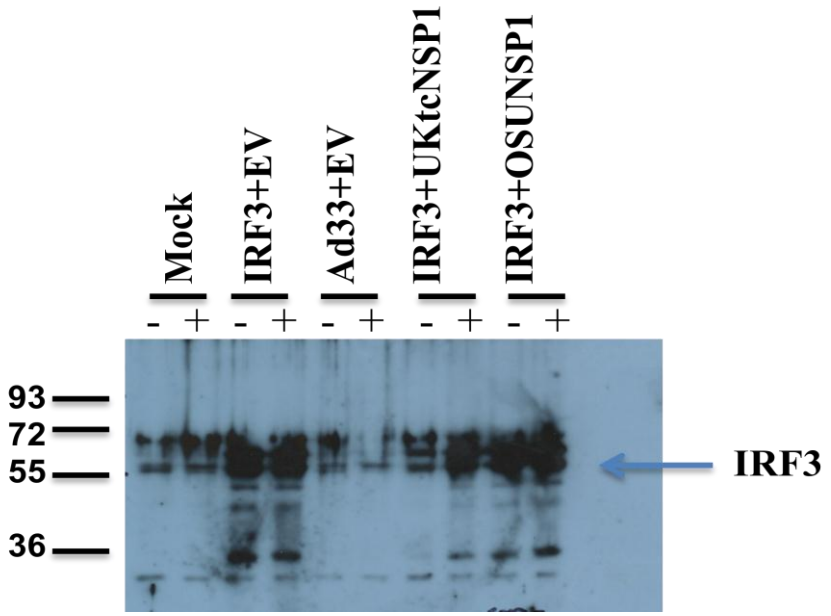
Mock
IRF3+EV
Ad33+EV
IRF3+UKtcNSP1
IRF3+OSUNSP1
- + - + - + - + - +
93
72
55
36
IRF3

B

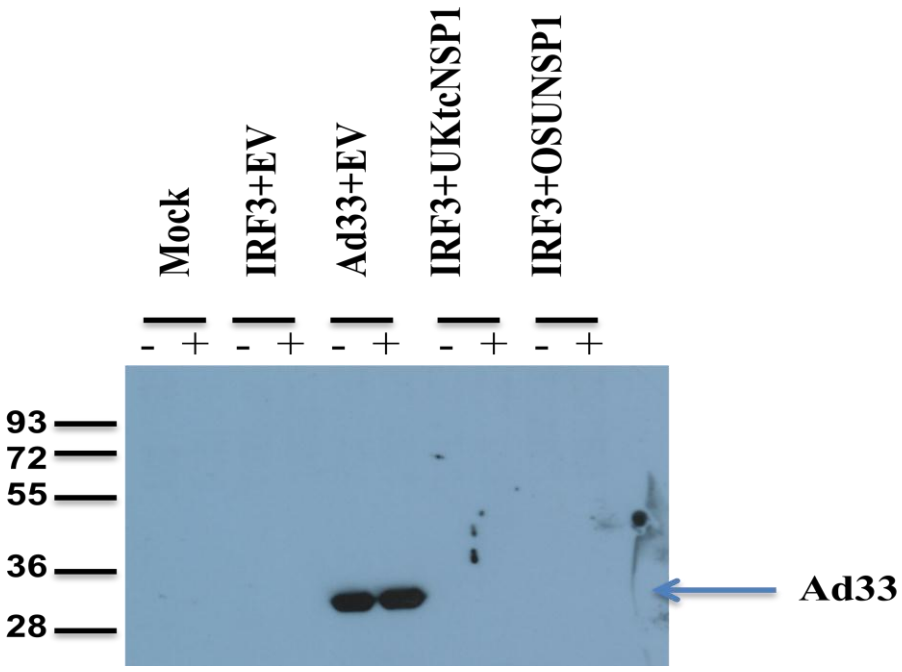
Mock
IRF3+EV
Ad33+EV
IRF3+UKtcNSP1
IRF3+OSUNSP1
- + - + - + - + - +
93
72
55
36
28
Ad33

C

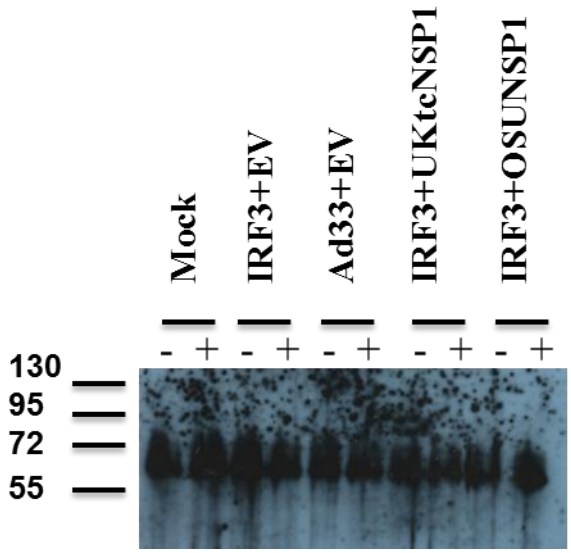
Mock
IRF3+EV
Ad33+EV
IRF3+UKtcNSP1
IRF3+OSUNSP1
- + - + - + - + - +
130
95
72
55

D

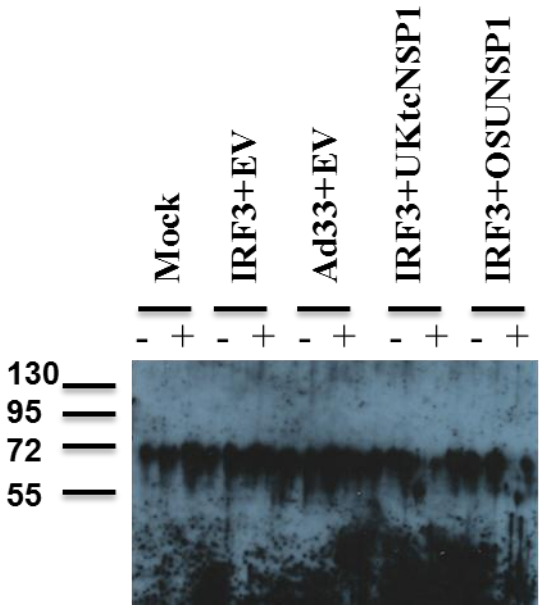
Mock
IRF3+EV
Ad33+EV
IRF3+UKtcNSP1
IRF3+OSUNSP1
- + - + - + - + - +
130
95
72
55

Figure 4.16 Analysis of protein interaction between NSP1 and IRF3 via co-immunoprecipitation.

(A) 293 Cell monolayer in 6-well plates were mock transfected or transfected with a combination of indicated plasmids in duplicates, 40 hrs later, medium was replaced by either fresh serum-containing medium or serum-containing medium with 50 µM of MG132, and the cells were incubated for a further 8 hrs ('+'and '-' indicate the presence and absence of MG132) as described in Materials and Methods. Cells were collected and samples were prepared and 10µl of the sample were kept whereas the rest were subjected in the next step, the kept samples were analysed in SDS-PAGE and detected using anti-IRF3 antibody. The protein marker on the left hand side indicates the corresponding protein sizes and the endogenous and transfected IRF3 bands are illustrated.

(B) Samples before passing through the Sepharose were analysed on SDS-PAGE followed by western blot as described in Materials and Methods. The blot was probed with anti-FLAG antibody and the protein marker on the left hand side indicates the corresponding protein sizes and the endogenous and transfected IRF3 bands are illustrated.

(C) Samples were eluted after the binding to the Sepharose and analysed on SDS-PAGE followed by western blot as described in Materials and Methods. The blot was probed with anti-IRF3 antibody, and the protein marker on the left hand side indicates the corresponding protein sizes and the endogenous and transfected IRF3 bands are illustrated.

(D) Samples were eluted after the binding to the Sepharose and analysed on SDS-PAGE followed by western blot as described in Materials and Methods. The blot was probed with anti-FLAG antibody, and the protein marker on the left hand side indicates the corresponding protein sizes and the endogenous and transfected IRF3 bands are illustrated.

4.7 Discussion

The mammalian two-hybrid assay system utilized in this study to determine protein-protein interactions is not a quantitative assay, if two proteins of interest interact, the reporter gene activation occurred, if not, no reporter protein expressed. A complement experiment with flow cytometry was considered to analyse the data quantitatively. However, as the mammalian two-hybrid assay failed to illustrate convincible results of the protein-protein interaction, the flow cytometry experiment was not carried out. The two-hybrid assays investigating potential interactions between UKtcNSP1-IRF3 and OSUNSP1-β-TrCP in this study all yielded negative results, even though direct protein interaction of IRF3 and UKtcNSP1 have been observed in a yeast two-hybrid assay system (Goodbourn *et al*., unpublished results).

Several possible explanations could be put forward for these failures of detecting the interaction in the two-hybrid system: some proteins might not be expressed correctly from the plasmids, there might be weak interactions that were not able to activate the reporter gene above a threshold level, the lack of nuclear localisation of the proteins lead to insufficient expression of the NSP1 proteins, and a low transfection efficiency may also inhibit the detection of protein-protein interaction. The two-hybrid assays were carefully repeated a number of times with fresh cells, fresh batch of plasmid preparations, altered transfection conditions and altered incubation time. However the outcome remained the same that no convincible interactions between the parental NSP1 proteins and the targeted cellular proteins were detected.

As one possibility was that the proteins might not be expressed correctly from some or all of plasmids, anti-Gal4 and anti-VP16 antibodies were used to detect the expression of proteins fused to the mammalian two-hybrid vectors, however, it has been unsuccessful to detect any fusion proteins expressed from the mammalian two-hybrid vectors. Nevertheless, the expression studies also revealed negative results in the positive control plasmids, which showed clear GFP expression in the two-hybrid system. Therefore the lack of detectable protein bands on the blot might due to the possibility that the proteins were only expressed to very limited amounts, such that the antibodies were not able to detect the expression.

In order to enhance the expression of both NSP1 proteins, pcDNA3.1 vector was firstly put in use instead of the mammalian two-hybrid vectors and eventually changed to a pCI-neo vector containing a chimeric intron upstream of the inserted cDNA. A FLAG-tag was introduced to both NSP1 proteins for consistent detection with the anti-FLAG antibody. Similarly as the previous expression results, the change of vectors did not show any better detection of the NSP1 expression compared with the observation from the mammalian two-hybrid vectors. However in the functional assays employing the pCI-neo-NSP1 plasmid (Chapter 5), evidences had been obtained to illustrate the expression of the NSP1 in this particular vector. Therefore the main reason of the failure of this assay might be that the proteins have not been expressed to a sufficient level either to be detected or to be able to initiate the activation of the reporter gene.

Chapter 5

Functional analysis of NSP1 hybrid proteins

5.1 Introduction

There are several lines of evidence that one of the functions of rotavirus NSP1 is to antagonise the host innate immune system via inhibiting the production of IFNβ (Barro and Patton, 2005; Arnold and Patton, 2009), and that this is achieved by interactions between NSP1 and the host cellular proteins IRF3 and β-TrCP promoting their subsequent proteasome-dependent degradation (Graff *et al*., 2002; Barro and Patton, 2005; Graff *et al*., 2009). In this study, hybrid NSP1 genes consisting of different sequence domains from both UKtcNSP1 and OSUNSP1 (Chapter 3) were first tested in functional assays in an attempt to localise the interaction sites responsible for the degradation of these two cellular proteins.

Despite the unsuccessful outcome of these studies reported in Chapter 4, the biological phenotype of these NSP1 hybrid proteins could still be examined through the use of reporter gene assays. Three firefly luciferase reporter plasmids were used in this study (i) reporter expression driven by the full-length IFNβ promoter, (ii) reporter expression driven by a sub-element of that promoter: PRD I/III, which is activated specifically by IRF3-induced IFNβ production, (iii) reporter expression driven by a ConA promoter element that detects NFκB activity. The promoters in each case are activated by a signalling cascade that is induced by the detection of double-stranded RNA (in this case transfected PolyI:C) within the cell. This chapter describes the details of setting up of these reporter assays, and their use to determine the functionality of the various NSP1 hybrid proteins constructed in this study.

5.2 pcDNA3.1-NSP1 constructs do not stimulate the activation of the IFNβ promoter

A reporter plasmid carrying the firefly luciferase gene driven by a full-length interferon β promoter was used initially to determine the effect of co-transfected NSP1 hybrid genes on the stimulation of IFNβ production by poly (I:C). Although the parental NSP1 proteins showed little physical interaction and undetectable expression in the mammalian two-hybrid vector system (Chapter 4), and expression of these proteins were undetectable when cloned into the CMV promoter containing vector pcDNA3.1 (Chapter 4), it is possible that even though the amount of protein expressed is undetectable, the protein can still be examined functionally. Therefore parental constructs pcDNA3.1-UKtcNSP1 and pcDNA3.1-OSUNSP1 were subjected to this reporter assay to test if a detectable signal generated by the reporter plasmid can be observed.

293HEK cells were co-transfected with a combination of the IFNβ promoter reporter plasmid and parental NSP1 plasmids or an empty vector plasmid. A control plasmid carrying *E.coli* LacZ (β-galactosidase) under the control of the constitutive immediate early promoter of cytomegalovirus (CMV) was included in all the transfections as a basal control for measuring the general transfection efficiency. 24 hrs after transfection the cells were mock transfected or transfected with poly (I:C), an analogue of dsRNA known to be a powerful stimulant of IFNβ production. The Poly (I:C) was transfected into the 293 cells as they do not have a Toll-like receptor expressed on their cell surface under normal culture conditions so do not respond to Poly (I:C) unless it's transfected into the cells. 16 hrs after this second transfection

the cells were harvested, and cell lysates were analysed for firefly luciferase activity (**Figure 5.1B**).

Overall, transfections with NSP1 parental gene plasmids did not cause significant changes in the reporter activity over the empty vector transfected control. However, cells transfected with a combination of the reporter gene plasmid and the empty vector did cause an ~70-fold stimulation of the IFNβ reporter activity when transfected with poly (I:C) (**Figure 5.1A**), indicating the reporter activity can be stimulated by the transfected poly (I:C); typically, in the experiments repeated in this chapter, stimulation of reporter activity varied from 50-fold to 80-fold. This result suggested that 293 cells were able to respond to poly (I:C) stimulation and subsequently activate the IFNβ promoter but the NSP1 genes were unable affect the signalling pathways to cause any reduction in IFNβ promoter activity as expected. The reason for this observation might be either the NSP1 genes were not expressed sufficiently in cells to cause any changes on the promoter activity or the expressed proteins were unable to cause any detectable changes in the IFNβ promoter activity. A new batch of 293 cells and new stocks of NSP1 plasmids were prepared and the assay was repeated for several times. Similar results were obtained and there was little effect on the level of IFNβ promoter activity caused by the pcDNA3.1-parental NSP1 constructs.

A

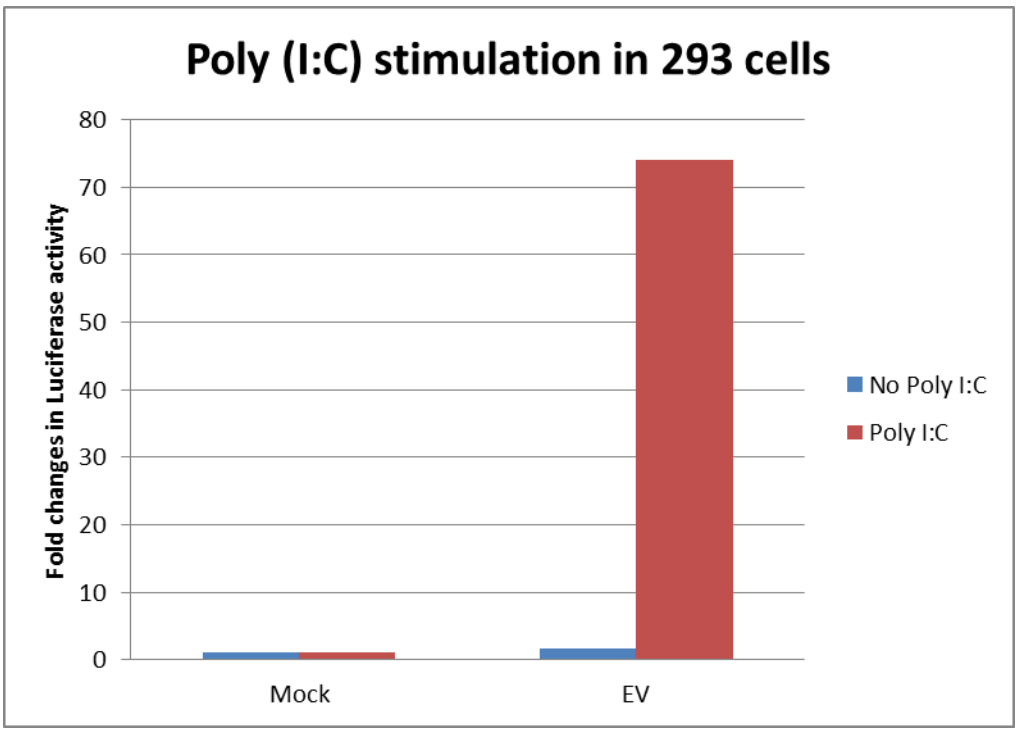
Poly (I:C) stimulation in 293 cells
Fold changes in Luciferase activity
80
70
60
50
40
30
20
10
0
Mock
EV
No Poly I:C
Poly I:C

B

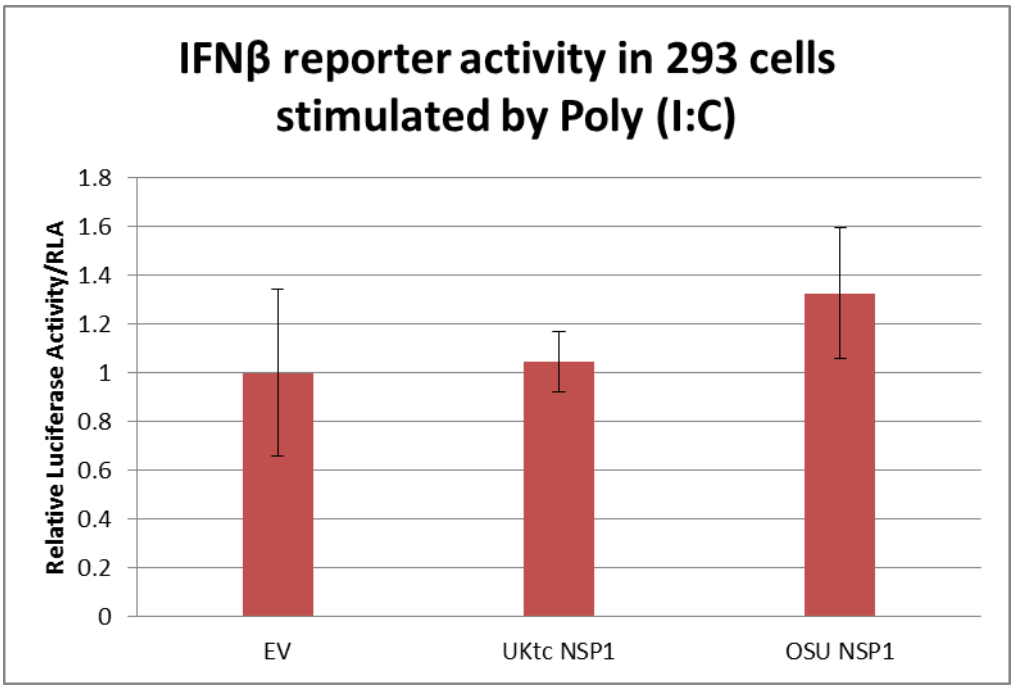
IFNβ reporter activity in 293 cells stimulated by Poly (I:C)
Relative Luciferase Activity/RLA
1.8
1.6
1.4
1.2
1
0.8
0.6
0.4
0.2
0
EV
UKtc NSP1
OSU NSP1

Figure 5.1 Studies on IFNβ promoter activities in 293HEK cells.

2 x 10^5 293 cells were co-transfected with 225ng pLuc-IFNβ, 25ng pcDNA3.1-HisB::*lacZ* and 250ng pcDNA3.1 vector, pcDNA3.1-UKtcNSP1 or pcDNA3.1-OSUNSP1 as described in Materials and Methods. 24 hrs after transfection cells were mock transfected or transfected with 1μg of poly (I:C). Cells were incubated for a further 16 hrs before harvested and assayed for β-galactosidase and luciferase activities as described in Materials and Methods. Luciferase activity was normalised to β-galactosidase activity generating a relative luciferase activity (RLA) value for each sample as described in Materials and Methods.

(A) Histogram of the fold changes in RLA of mock transfected cells and cells co-transfected with pLuc-IFNβ, pcDNA3.1-HisB::*lacZ* and the empty vector pcDNA3.1 in the presence and absence of the stimulation of Poly (I:C).

(B) Histogram of IFNβ promoter activity of cells co-transfected with pLuc-IFNβ, pcDNA3.1-HisB::*lacZ* and an empty vector or the pcDNA3.1-parental NSP1 plasmids. The RLA values were expressed as a ratio of the values obtained from the cells transfected with the NSP1 plasmids to those from cells transfected with the empty pcDNA3.1 vector as described in Materials and Methods. Error bars indicate the approximate upper and lower 95% of confidence limits (upper and lower 95% limit = mean value $\pm$ standard error x 1.96) from the mean value.

One possible explanation for the failure of the transfected parental NSP1 genes to affect reporter gene expression from the IFNβ reporter was that insufficient NSP1 protein was being expressed in the assay. To investigate this possibility, these reporter assays were carried out in which NSP1 was being expressed under ideal conditions i.e: following virus infection. The control employed in these experiments was p9Δ5 virus which had been shown in previous studies (Xu *et al*., 1994) to carry a deletion in gene 5 (NSP1) that precludes expression of anything beyond the amino-terminal third of NSP1 which is not stable in infected cells and therefore would not be expected to influence IFNβ expression.

293HEK cells were mock infected or infected with rotaviruses p9Δ5, UKtc or OSU at an m.o.i of 3. 40 mins later, virus inoculum was removed, replaced by fresh serum-free medium. After 8 hrs of incubation, cells were mock transfected or transfected with poly (I:C), and cells were harvested after 16 hrs of incubation. The lysates were analysed for firefly luciferase activity.

Cells infected with p9Δ5 showed a similar promoter activity compared with the mock-infected cells. On the other hand, cells infected with UKtc showed around 40% reduction in the IFNβ promoter activity compared with the mock-infected cells, nevertheless, cells infected with OSU showed no significant effect on the promoter activity compared with the control as the error bar was very significant (**Figure 5.2**). This result indicated that viral NSP1 proteins expressed from UKtc was able to induce a decreased IFNβ promoter activity in infected 293 cells, suggesting the failure of the pcDNA3.1-NSP1 plasmids to achieve the same effect might due to insufficient expression of NSP1 proteins.

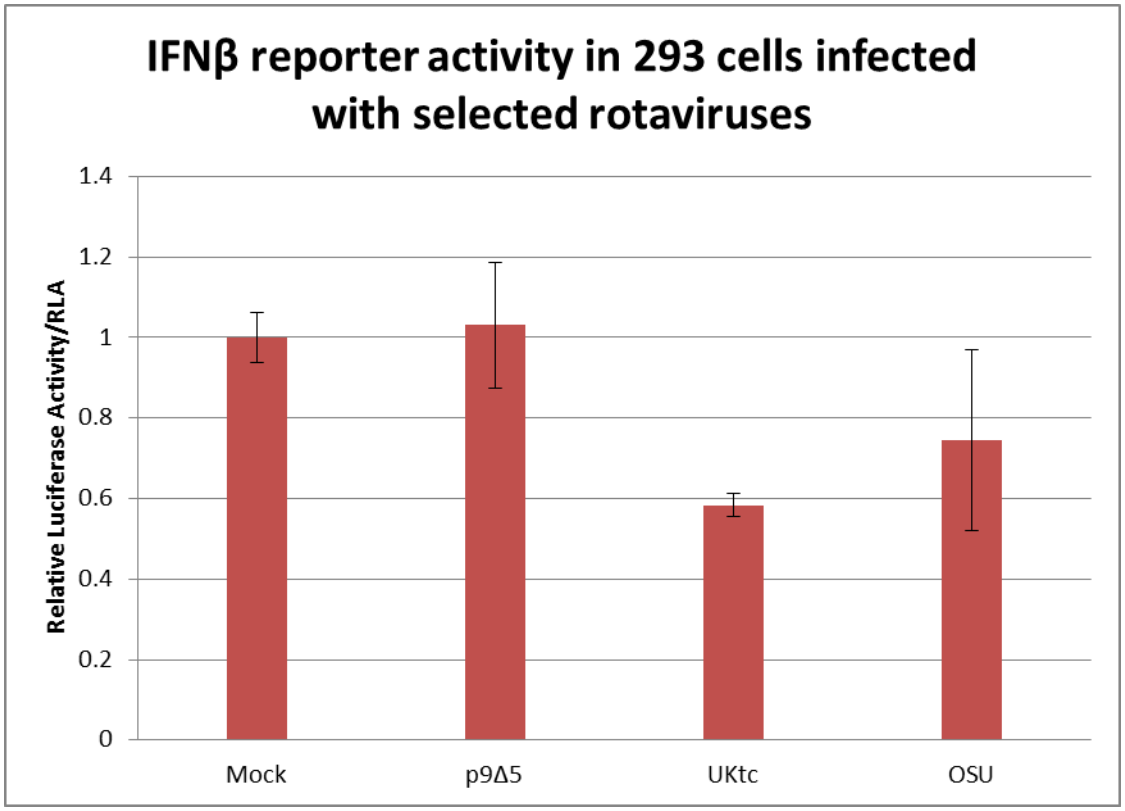

Figure 5.2 Studies of IFNβ reporter activity in 293 cells infected with selected rotaviruses.

2 x 10^5 293 cells were co-transfected with 225ng pLuc-IFNβ, 25ng pcDNA3.1-HisB::*lacZ*. 24 hrs later cells were mock-infected or infected with p9Δ5, UKtc and OSU at an m.o.i of 3. 40 mins later virus inoculum were removed and free medium was replaced. 8 hrs after the incubation, cells were transfected with 1µg of poly (I:C) and were harvested and assayed after a further 16 hrs of incubation as described in Materials and Methods. The luciferase activity which was normalised to β-galactosidase activity generating a RLA value for each sample whereas RLAs were expressed as a ratio of the values from the experimental samples to the values from mock infected cells. Error bars indicate the approximate upper and lower 95% of confidence limits (upper and lower 95% limit = mean value ± standard error x 1.96) from the mean value.

5.3 pCI-neo-NSP1 constructs can cause reduction of IFNβ promoter activity

Despite the fact that the co-immunoprecipitation employing parental NSP1 genes cloned in a pCI-neo vector failed to show any convincible precipitation (Chapter 4), the biological function of these two parental NSP1 constructs were tested in the reporter assay to examine if the proteins expressed in this particular vector could achieve a sufficient amount so as to affect the IFNβ promoter activity. Similar transfection procedures were carried out. 293HEK cells were co-transfected with a combination of an IFNβ promoter reporter plasmid and the two parental pCI-neo-NSP1 genes or an empty vector plasmid together with the CMV-β-Gal control plasmid. 24 hrs after transfection the cells were mock transfected or transfected with poly (I:C), 16 hrs later cells were harvested and the lysates were analysed for firefly luciferase activity (**Figure 5.3**).

Cells transfected with pCI-neo-UKtcNSP1 showed a ~60% reduction of IFNβ promoter activity compared with the ones transfected with the empty pCI-neo vector, whereas cells transfected with pCI-neo-OSUNSP1 showed more or less similar effect on the IFNβ promoter activity as the ones transfected with the empty vector. This result was expected as the reduction of IFNβ promoter activity might be caused by the reduced expression of IRF3 protein which can be degraded by UKtcNSP1 but not OSUNSP1 based on previously published literature (Graff *et al*., 2002, 2007).

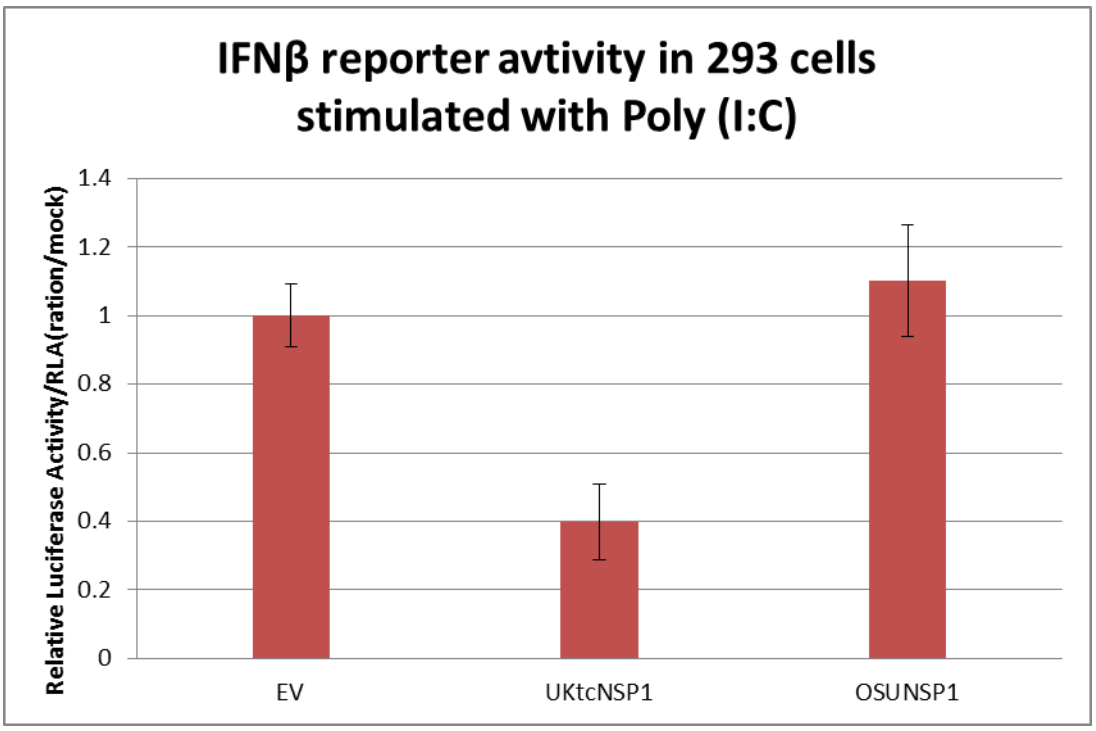

Figure 5.3 Studies of IFNβ reporter activities in 293 cells transfected with parental pCI-neo-NSP1 plasmids.

2 x 10^5 293 cells were co-transfected with 225ng pLuc-IFNβ, 25ng pcDNA3.1-HisB::*lacZ* and 250ng pCI-neo vector, pCI-neo-UKtcNSP1 or pCI-neo-OSUNSOP1 individually. 24 hrs later cells were transfected with 1μg of poly (I:C). All cells were harvested after 16 hrs and β-glactosidase and luciferase activity of cell lysates were measured as described in Materials and Methods. Luciferase activity was normalised to β-galactosidase activity generating an RLA value for each sample as described in Materials and Methods. These values were then expressed as a ratio to those from cells transfected with pCI-neo vector. Error bars indicate the approximate upper and lower 95% of confidence limits (upper and lower 95% limit = mean value $\pm$ standard error x 1.96) from the mean value.

5.4 Analysis of protein expression of all NSP1 hybrid genes in pCI-neo vector

As one of the parental pCI-neo-NSP1 genes plasmids showed some functional effect in the reporter assay, suggesting that NSP1 in this particular vector can be expressed to a sufficient level for exhibiting biological functions in this assay. Therefore, the collection of all NSP1 hybrid genes constructed (Chapter 3) was subsequently cloned into this pCI-neo vector, producing constructs pCI-neo-pA to pCI-neo-pL (**Figure 5.7A**). In order to confirm the expression of all NSP1 hybrid cDNAs, two independent experiments were conducted.

An *in-vitro* coupled transcription translation system with labelled ^{35}S methionine was used to demonstrate the expression of all NSP1 hybrid cDNAs in pCI-neo (**Figure 5.4**). The positive control plasmid encoding the T7 luciferase showed a strong band at the expected position around 61kDa and the empty vector (EV) showed no obvious band as expected. Among all the NSP1 cDNA constructs, apart from the parental OSUNSP1 plasmid, all the rest showed a band at around 55kDa indicating that they were able to express NSP1 proteins. The pCI-neo-OSUNSP1 plasmid was tested twice and the same observation was revealed confirming the absence of the band was not due to experimental errors.

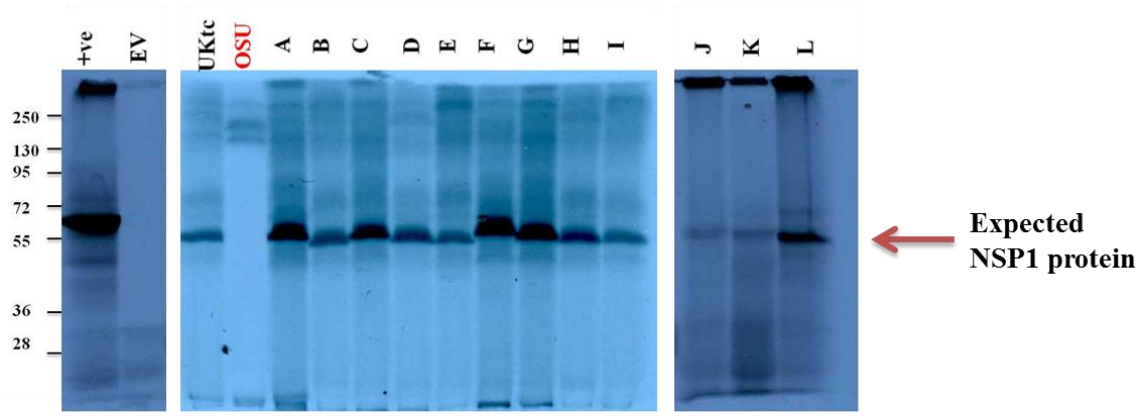

Figure 5.4 Expression of NSP1 hybrid gene constructs labelled with ^{35}S methionine analysed in *in-vitro* transcription translation system.

A total volume of 15µl reaction mixture including 10µl of Quick Master Mix, 3µl of ^{35}S (3µCi) and 2µl of DNA plasmid was used for each sample. The reaction mixture was incubated at 30ºC for 90 minutes followed by analysis on SDS-PAGE. The gel was fixed in 25% of methanol and 7% of acidic acid overnight before drying in a gel dryer. The gel containing the radiolabelled ^{35}S was then exposed and developed as described in Materials and Methods. EV indicates the pCI-neo vector and the positive control indicates the T7 Luciferase Control DNA included in the assay kit, the expected protein position is also indicated. The marker on the left hand side of the figure is shown in kDa.

The pCI-neo-OSUNSP1 was therefore re-constructed by re-generating the RE sites for cloning OSUNSP1 into pCI-neo vector followed by subsequent digestion and ligation. Another independent method: reverse-transcription (RT) PCR was used subsequently to test the ability of mRNA production for this newly constructed pCI-neo-OSUNSP1 plasmid and all the rest NSP1 hybrid constructs tested in the coupled transcription translation system previously. 293HEK cells were transfected with an empty vector or the NSP1 gene plasmids individually, 24 hrs post transfection, cytoplasmic RNA was harvested and reverse-transcribed into cDNA. The reaction involved the use of a common forward primer just upstream the chimeric intron in the vector pCI-neo and individual reverse primers for either UKtcNSP1 or OSUNSP1 depending on the hybrid constructs (**Figure 5.5A**). The expected PCR product from the plasmid was around 420bps; as the size of the intron is 132bps, therefore a 300bp sequence was expected for amplification from cDNA after the intron has been cleaved (**Figure 5.5B**). As a positive control for RNA quality, actin primers were utilized in this reaction and showed similar amount of actin expression across all transfected cells. In addition, PCR samples with no reverse transcriptase added were also included as the negative control. The results revealed that all the NSP1 constructs were able to produce mRNA and these constructs including the newly constructed parental OSUNSP1 plasmid were used in all the subsequent assays presented in this chapter.

A

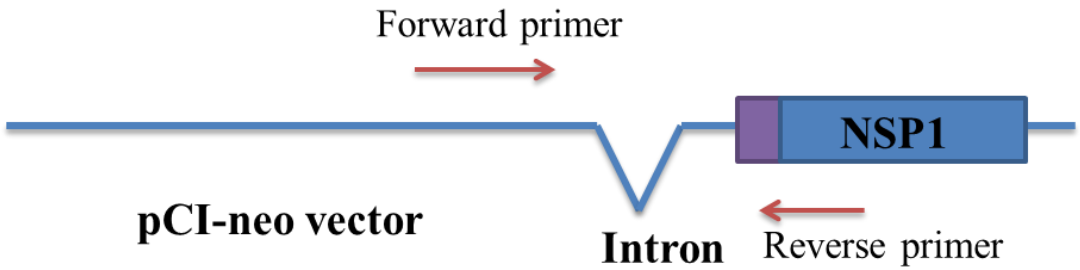
Forward primer
NSP1
pCI-neo vector
Intron
Reverse primer

B

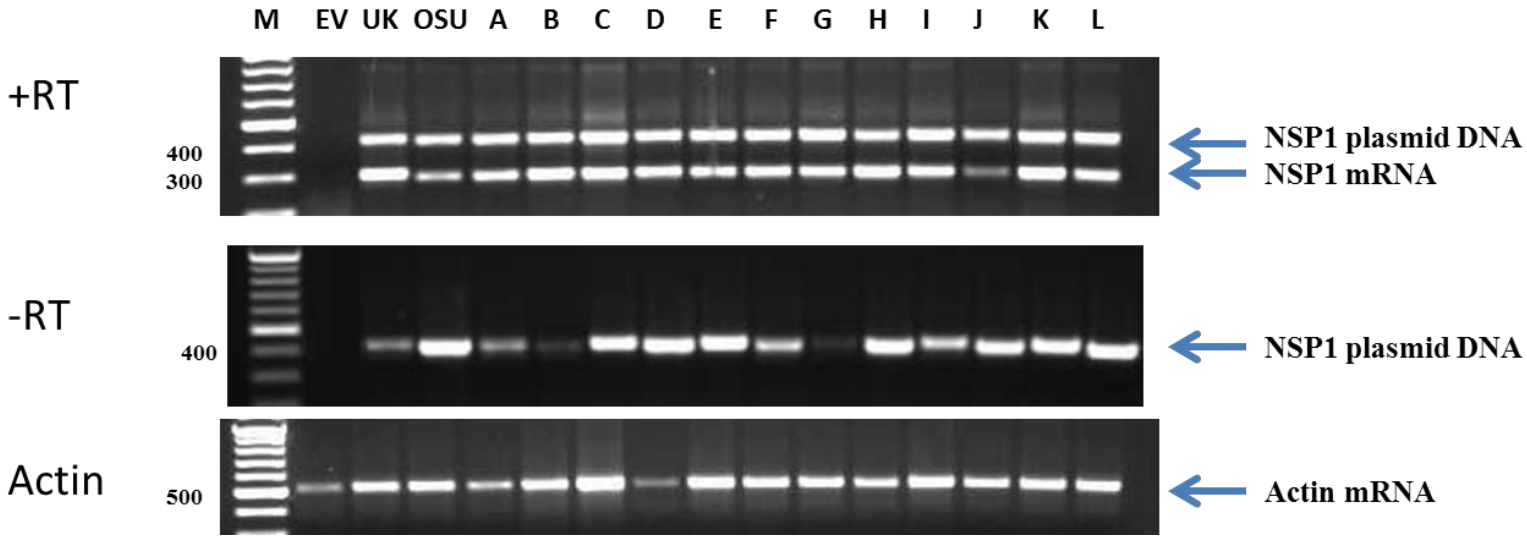
M EV UK OSU A B C D E F G H I J K L
+RT
400
300
NSP1 plasmid DNA
NSP1 mRNA
-RT
400
NSP1 plasmid DNA
Actin
500
Actin mRNA

Figure 5.5 mRNA expressions analysis of all NSP1 constructs by RT-PCR.

3.6×10^5 293 cells were transfected with an empty vector or an NSP1 gene plasmid, 24 hrs later cytoplasmic RNA was extracted and analysed by RT-PCR as described in Materials and Methods.

(A) Schematic illustration of the respective primers used in this RT-PCR analysis.

(B) 1µg of total cytoplasmic RNA was used as template for reverse transcriptation using 5' common forward primer and 3' reverse primers specific for UKtcNSP1 and OSUNSP1 in the presence (+RT) or absence (-RT) of reverse transcriptase. 2.5µl of the resulting cDNA was used as template in a PCR using either actin 5' and 3' primers as a control, or the combination of the primers for NSP1. PCR products were separated by electrophoresis through a 1% agarose gel as described in Materials and Methods. The arrow indicates the expected cDNA amplification from the plasmid (NSP1 plasmid DNA), mRNA lacking the intron (NSP1 mRNA) or the control (actin mRNA). DNA sizes are indicated in bps on the left hand side of the panels.

5.5 Mapping of the interaction sites with different pCI-neo-NSP1 hybrids analysed in the reporter assay

As the NSP1 hybrid genes had all been shown to be able to express proteins, the biological function of these hybrid genes was subsequently examined in the IFNβ reporter assays. There are four positive regulatory domains (PRDs I-IV) responsible for transcriptional activation of the IFNβ gene in its promoter sequence (**Figure 5.6**). The four PRDs can induce IFNβ promoter activity independently, PRD I and PRD III require the binding of IRF3 or IRF1 for function, PRD II appears to require NFκB whereas PRD IV requires ATF-2/c-Jun (King and Goodbourn, 1994; Qing *et al*., 2004).

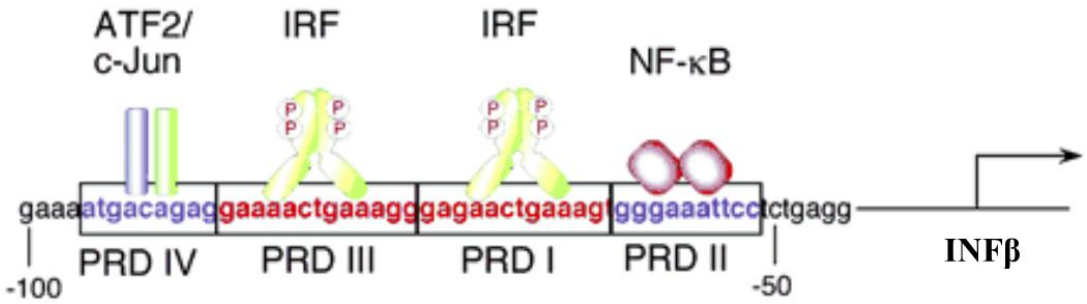

Figure 5.6 Schematic illustration of INFβ promoter sequence including four PRDs.

Four positive regulatory domains in the INFβ promoter sequence are indicated. PRD IV requires the binding of ATF2/c-Jun, PRD I and PRD III function via binding of IRFs whereas NF-κB can bind PRD II (Honda *et al*., 2005).

As IRF3 has been shown to be the target for UKtcNSP1 but not OSUNSP1 for degradation causing reduced level of IFNβ production, a ptk-Luciferase reporter plasmid containing the PRDI/III element of the IFNβ promoter responsible for IRF3 induced IFNβ activity (kindly provided by Dr Y Ke, Peking University College of Oncology) was used instead of the full promoter of IFNβ to ensure higher specificity of the subsequent results.

The 12 NSP1 hybrid constructs shown in Figure 5.7A were tested in the transfection based reporter assay using the PRDI/III promoter. The assay was repeated four times under the same conditions and the results presented in Figure 5.7B are the averaged values from these experiments. Consistent with the results obtained previously with the full-length IFNβ promoter, parental UKtcNSP1 caused a >75% significant reduction in PRDI/III activity whereas promoter activity was not changed significantly in OSUNSP1 transfected cells (~10% reduction observed). Turning next to the NSP1 hybrid genes, constructs D and H reduced PRDI/III promoter activity by around 70% and 80% compared to that seen in control transfections (**Figure 5.7B**). However, the remaining hybrids all showed less than a 50% reduction in PRDI/III activity. Student's T-test analysis was performed on these data to compare them against both the parental UKtcNSP1 and OSUNSP1 controls (**Table 5.1**). Table 5.1 shows that constructs D and H had a statistically significant difference from OSUNSP1, whereas constructs F and L exhibited a significant difference from both UKtcNSP1 and OSUNSP1. This suggests that the C-terminal region of UKtcNSP1 is responsible for repressing IRF3 induced increase in IFNβ activity but that the last 135 amino acids in the C-terminal region of UKtcNSP1 are not sufficient to fully repress activation of the PRDI/III promoter triggered by Poly (I:C). The other hybrid

gene constructs all showed more significant difference from UKtcNSP1 suggesting that similar to the OSUNSP1, the rest of the NSP1 hybrid proteins were unable to repress the PRDI/III promoter activity.

A

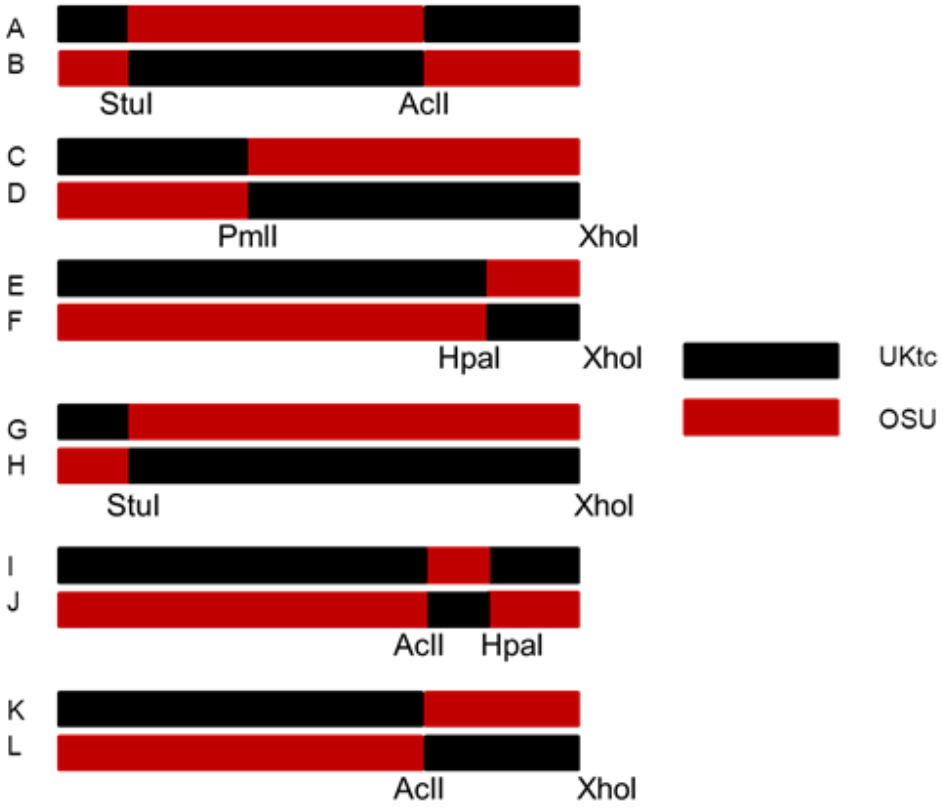
A
B
StuI
AclI
C
D
PmlI
XhoI
E
F
HpaI
XhoI
G
H
StuI
XhoI
I
J
AclI
HpaI
K
L
AclI
XhoI
UKtc
OSU

B

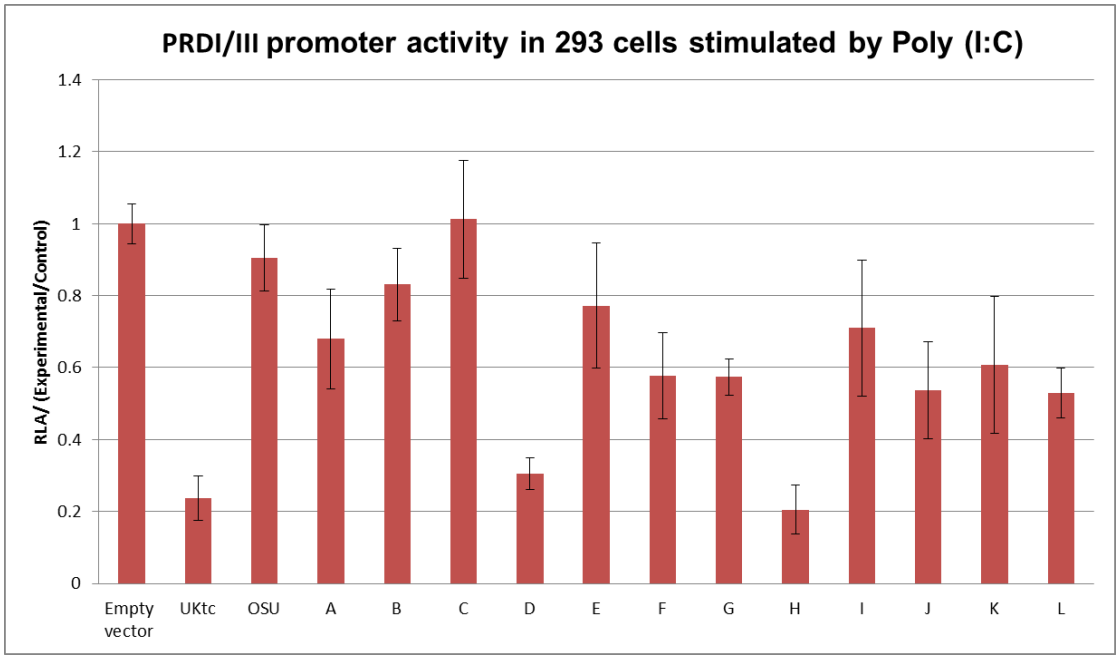
PRDI/III promoter activity in 293 cells stimulated by Poly (I:C)
RLA/ (Experimental/Control)
1.4
1.2
1
0.8
0.6
0.4
0.2
0
Empty vector
UKtc
OSU
A
B
C
D
E
F
G
H
I
J
K
L

Figure 5.7 Studies of PRDI/III promoter activities in 293 cells transfected with NSP1 hybrid gene constructs.

(A) Schematic diagram of the NSP1 hybrid constructs tested in the experiments.
Six pairs of NSP1 hybrid constructs are shown with the restriction enzymes sites used to create the hybrids being indicated for each pair.

(B) Histogram of effect of NSP1 hybrid genes on Poly (I:C) induced PRDI/III IFNβ promoter activity.
2 x 10^5 293 cells were co-transfected with 225ng pPRDI/III-Luc, 25ng pcDNA3.1-HisB::*lacZ* and 250ng of either control empty vector, or individual NSP1 hybrid plasmids. 24 hours later cells were transfected with 1μg of poly (I:C). After a further 16 hrs of incubation, cells were harvested and β-glactosidase and luciferase activity of cell lysates were measured as described in Materials and Methods. Luciferase activity was normalised to β-galactosidase activity generating an RLA value for each sample. Error bars indicate the approximate upper and lower 95% of confidence limits (upper and lower 95% limit = mean value $\pm$ standard error x 1.96) from the mean value.

Construct	P against UKtcNSP1	P against OSUNSP1
A	0.000139636	0.019389431
B	1.97663E-07	0.306269522
C	4.8261E-06	0.279225009
D	0.098884985	1.08875E-07
E	0.000205899	0.211828681
F	0.000325347	0.000689642
G	4.4076E-07	3.81715E-05
H	0.511396336	4.94575E-09
I	0.000950966	0.094249425
J	0.00224831	0.000606755
K	0.004056097	0.017896454
L	1.3848E-05	1.21841E-05

Table 5.1 The P value of each NSP1 hybrid construct against parental UKtc and OSU NSP1 constructs.

By applying student's T-test to the data shown in Figure 5.7B, the P value of each NSP1 hybrid construct against both parental NSP1 constructs is generated. The Bonferroni corrected p value (0.05/sample size = 0.004167) is used to adjust the data. The ones indicated in red are the two constructs showing significant difference from OSUNSP1, i.e: constructs D and H. The ones indicated in blue are the constructs showing significant difference from UKtcNSP1, i.e: constructs A, B, C, E, I and K. The ones indicated in purple are the constructs showing significant difference from both UKtc and OSU NSP1s, i.e: constructs F, G, J and L.

5.6 The effect of NSP1 hybrid genes on NFκB activity

The NSP1 of the porcine OSU strain has previously been shown to target and degrade β-TrCP, a component of the E3 ligase SCF $^{\beta\text{-TrCP}}$, responsible for degrading inhibitor κB which in turn releases NFκB to travel into the nucleus and activate the IFN response. The effect of this increased degradation of β-TrCP should therefore be able to reduce activation of the IFNβ promoter. In order to test if this is also the case for some of the NSP1 hybrids. A Luciferase reporter plasmid in which the reporter expression was under the control of the NFκB regulated Concanavalin A promoter (Kindly provided Dr A Macdonald) (Mankouri *et al*., 2010) was used. As the parental OSUNSP1 should promote the degradation of β-TrCP, co-transfection of the parental OSUNSP1 plasmid should reduce reporter gene expression.

In this particular reporter assay, Poly (I:C) was not introduced due to the results obtained by others in our lab (Chen's unpublished observations) that this reporter plasmid did not respond to stimulation caused by Poly(I:C) in 293HEK cells. There was little effect on ConA promoter activity in cells co-transfected with OSUNSP1 (**Figure 5.8**). The whole of the C-terminal region and part of the zing finger motif from the UKtcNSP1 (construct D) showed some reduction in reporter gene expression i.e: ConA promoter activity. Given the sizes of the error bar indicated in Figure 5.8, no other construct has demonstrated a significant difference in the promoter activity compared with the control.

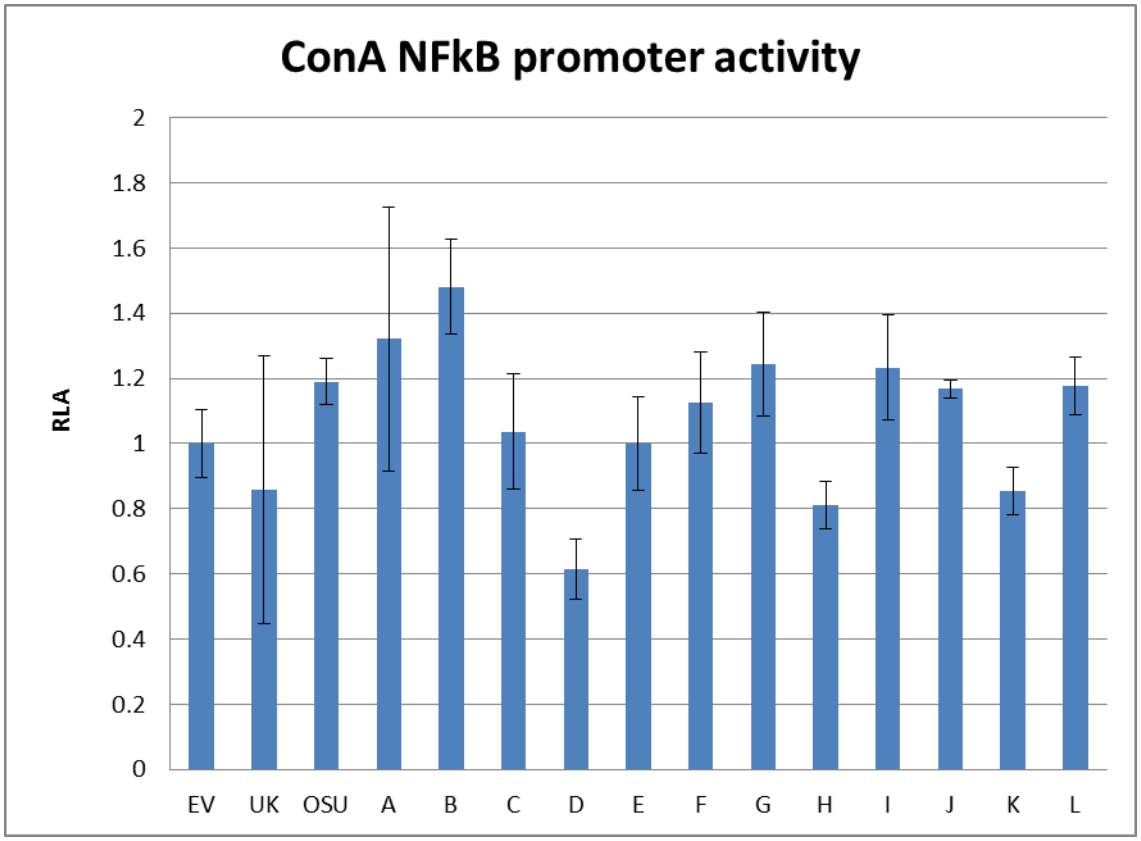

Figure 5.8 NFκB ConA promoter activities of NSP1 hybrid constructs.
2 x 10^5 293 cells were co-transfected with 225ng pConA-Luc, 25ng pcDNA3.1-HisB::*lacZ* and 250ng of either control empty vector, or individual NSP1 hybrid plasmids. 24 hours later cells were harvested and β-glactosidase and luciferase activity of cell lysates were measured as described in Materials and Methods. RLA was calculated as previously described. Error bars indicate the approximate upper and lower 95% of confidence limits (upper and lower 95% limit = mean value ± standard error x 1.96) from the mean value.

5.7 NSP1 induced degradation of IRF3 and/or β-TrCP

IRF3 is a constitutively expressed cellular protein and this has meant that demonstrating that NSP1 affects its level in cells, whilst straightforward in virus infected cells where all cells can be infected synchronously, has met with problems of consistency in transfected cells where NSP1 will only be expressed by a fraction of the cell population. To overcome this problem with transfected cells a plasmid construct was generated which expresses a tagged version of IRF3. To do this the IRF3 gene was inserted into a pcDNA3 vector containing 3 HA tags (**Figure 5.9A**). This construct allows the NSP1 induced degradation of IRF3 to be assayed using anti-HA antibodies. The final pcDNA3-IRF3 construct was sequenced with appropriate forward and reverse primers (**Table 2.1.7**) to confirm that the HA tags were in frame downsteam of IRF3 (**Figure 5.9B**). The β-TrCP plasmid available for this study was already tagged with HA and consequently anti-HA antibody could be used for detecting both of the cellular proteins being analysed.

Western blot analysis of 293HEK cells transfected with NSP1 hybrid plasmids and IRF3 or β-TrCP in the presence or absence of the proteasome inhibitor MG132 revealed the different abilities of these hybrid NSP1s to degrade the corresponding cellular proteins (**Figure 5.10**). For this analysis 293HEK cells were transfected in duplicates with either empty vector or individual NSP1 hybrid plasmids, 40 hrs later, one set of the cells were treated with 50μM of MG132 for a further 8 hrs, cell lysates were harvested and analysed in SDS-PAGE followed by probing for IRF3 or β-TrCP using anti-HA antibody.

A.

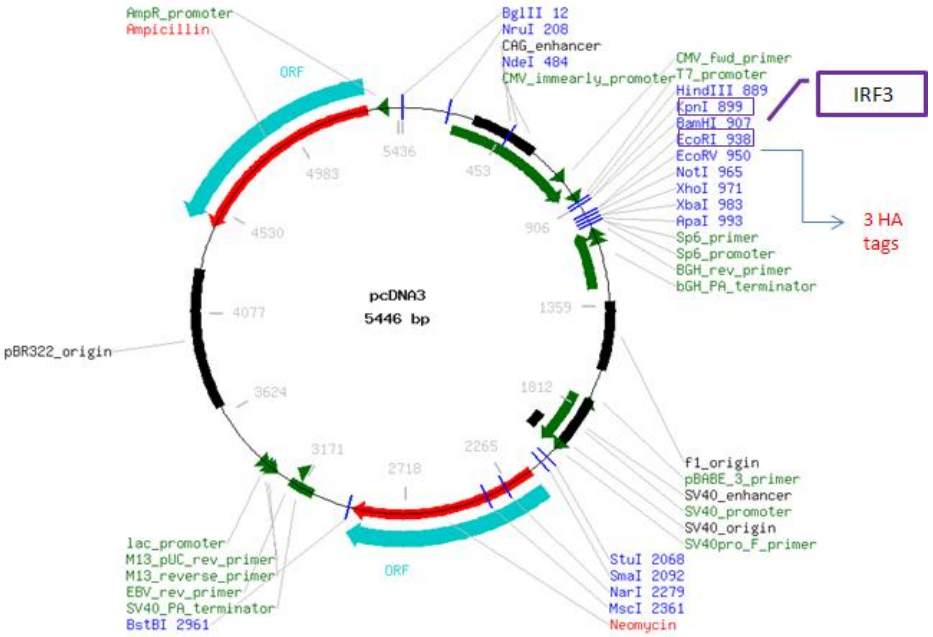
AmpR_promoter
Ampicillin
ORF
BglII 12
NruI 208
CAG_enhancer
NdeI 484
CMV_immearly_promoter
CMV_fwd_primer
T7_promoter
HindIII 889
KpnI 899
BamHI 907
EcoRI 938
EcoRV 950
NotI 965
XhoI 971
XbaI 983
ApaI 993
Sp6_primer
Sp6_promoter
BGH_rev_primer
bGH_PA_terminator
IRF3
3 HA tags
pcDNA3
5446 bp
pBR322_origin
f1_origin
pBABE_3_primer
SV40_enhancer
SV40_promoter
SV40_origin
SV40pro_F_primer
lac_promoter
M13_pUC_rev_primer
M13_reverse_primer
EBV_rev_primer
SV40_PA_terminator
BstBI 2961
ORF
StuI 2068
SmaI 2092
NarI 2279
MscI 2361
Neomycin

B.

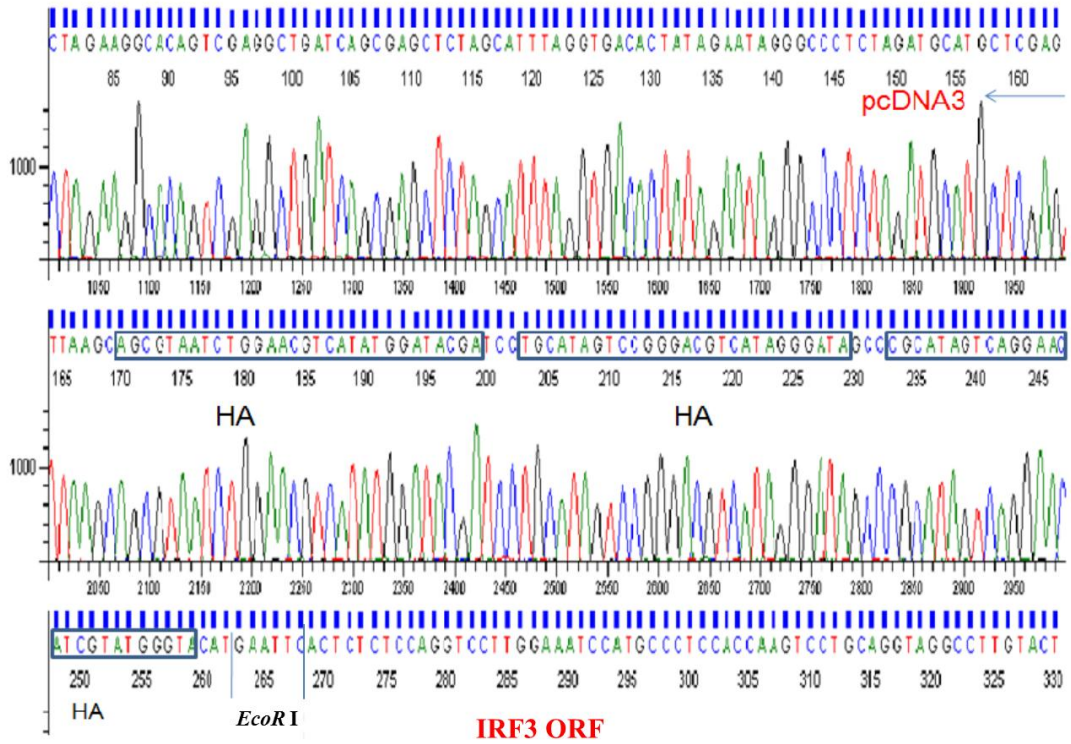
pcDNA3
HA
HA
HA
EcoR I
IRF3 ORF

Figure 5.9 Construction of HA-tagged pcDNA3-IRF3 plasmid.

(A). Schematic illustration of the pcDNA3 vector with the *Kpn* I and *EcoR* I restriction enzyme sites used for insertion of the IRF3 gene sequence highlighted. The position of the three HA tags is also indicated on the vector map.

(B). Sequencing trace confirming the correct insertion of the IRF3 gene sequence, and that the HA tags are in frame with the IRF3 coding sequence.

Figure 5.10A shows that in the absence of MG132, the level of IRF3 in UKtcNSP1 transfected cells was reduced significantly compared to vector only control whereas in the presence of MG132, the level of IRF3 was similar to that in the control transfection. This contrasted with the result seen for cells transfected with parental OSUNSP1 where the level of IRF3 showed little change in the presence or absence of MG132. In agreement with the results obtained in transfections with the luciferase reporter plasmid, the hybrid constructs D and H showed similar effect to the UKtcNSP1 parental gene, with IRF3 being degraded significantly in the absence of MG132 compared to when proteasomal based degradation was blocked with MG132. Also consistent with the luciferase reporter assay, the remaining hybrid genes had little effect on IRF3 expression. These results showed that the ability of NSP1 to promote IRF3 degradation co-incided with its effects on activation of the PRDI/III promoter in reporter gene assays. Furthermore the fact that only the D and H hybrids had a similar effect to the parental UKtcNSP1 in these IRF3 degradation assays suggests that the C-terminal half of the NSP1 protein is important for this function, although it is important to note that neither hybrid F or hybrid L which carried

respectively the C-terminal 88 and 135 amino acids of the UKtcNSP1 gene were able to mediate proteasome dependent IRF3 degradation.

The results for similar degradation assays carried out on HA tagged β-TrCP are shown in Figure 5.10B. The parental OSUNSP1 was, as expected from previously published results (Graff *et al*., 2009; Arnold and Patton, 2011), able to stimulate proteasomally based degradation of β-TrCP. However in contrast to what has been seen previously the UKtc NSP1 was also able to promote β-TrCP degradation. In addition the C, D, G and H hybrid gene constructs also stimulated β-TrCP degradation in the absence of the MG132 proteasome inhibitor.

A

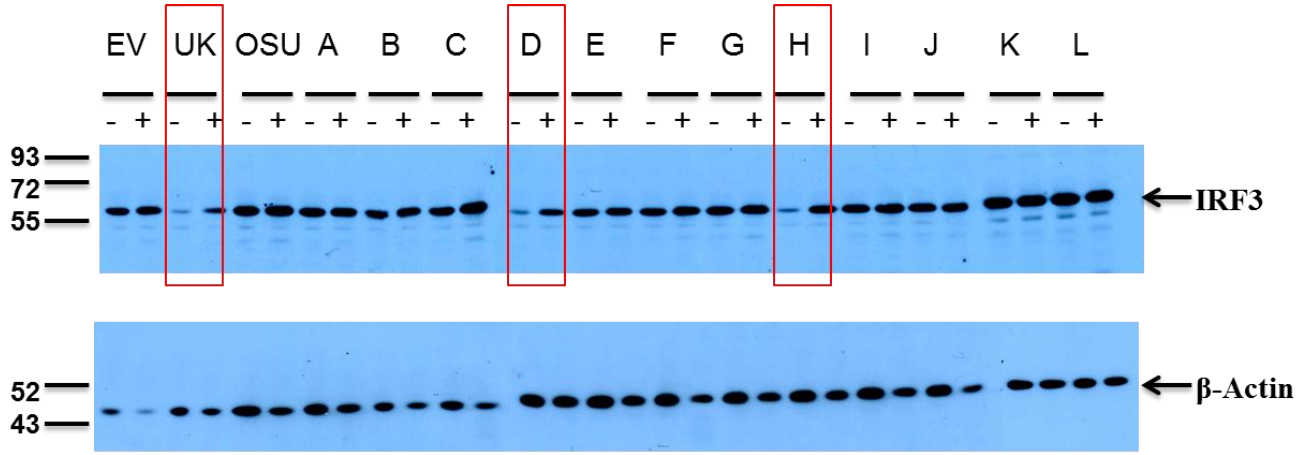
EV UK OSU A B C D E F G H I J K L
- + - + - + - + - + - + - + - + - + - + - + - + - + - + - +
93
72
55
IRF3
52
43
β-Actin

B

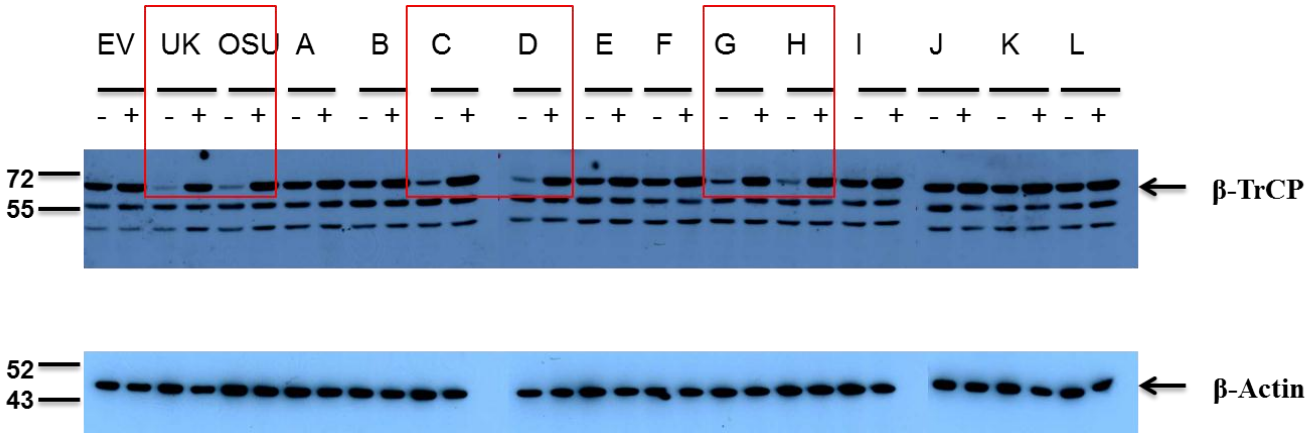
EV UK OSU A B C D E F G H I J K L
- + - + - + - + - + - + - + - + - + - + - + - + - + - + - +
72
55
β-TrCP
52
43
β-Actin

Figure 5.10 Testing of parental UKtc and OSU NSP1 genes and hybrid constructs between these two genes in proteasomal based degradation assays of IRF3 and β-TrCP.

(A) Degradation studies of IRF3 employing parental UKtc and OSU NSP1 genes and the hybrid constructs.

293HEK cells were co-transfected with HA-IRF3 together with either an empty vector control or a NSP1 gene plasmid. 40 hrs after transfection, the medium was replaced by either fresh serum-containing medium or the serum-containing medium with 50μM of MG132, cells were incubated for a further 8 hrs at 37ºC and harvested as described in Materials and Methods. Cell lysates were analysed on SDS-PAGE followed by western blot as described in Materials and Methods. The blots were probed using anti-HA antibody for IRF3 and anti- β-actin was used for detection of β-actin as a positive control. The presence or absence of proteasome inhibitor MG132 is indicated as (+) or (-) respectively. Protein molecular weights in kDa are indicated on the right hand side of the blots.

(B) Degradation studies of β-TrCP employing parental UKtc and OSU NSP1 genes and the hybrid constructs.

293HEK cells were co-transfected with HA- β-TrCP together with either an empty vector control or a NSP1 gene plasmid. 40 hrs after transfection, the medium was replaced by either fresh serum-containing medium or the serum-containing medium with 50μM of MG132, cells were incubated for a further 8 hrs at 37ºC and harvested as described in Materials and Methods. Cell lysates were analysed on SDS-PAGE followed by western blot as described in Materials and Methods. The blots were probed using anti-HA antibody for β-TrCP and anti- β-actin was used for detection of β-actin as a positive control. The presence or absence of proteasome inhibitor MG132 is indicated as (+) or (-) respectively. Protein molecular weights in kDa are indicated on the right hand side of the blots.

5.8 Discussion

The aim of the analysis described in this chapter was to investigate the biological function of the hybrid NSP1 genes generated in this study. The two parental genes were cloned initially into pcDNA3.1 vector, however when co-transfected with reporter gene under the control of the IFNβ promoter, they had little effect on reporter gene expression. When analysed using virus infected cells, the promoter activity was reduced significantly with UKtc infected cells, whereas in cells infected with OSU or p9Δ5, the promoter activity showed similar pattern with the mock infected cells. However, the origins of these virus strains used are all different. p9Δ5 encoding the truncated form of NSP1 is from the feline origin, whereas UKtc and OSU are originated from bovine and porcine respectively. Therefore, ideally, based on the ability of rotaviruses to undergo reassortment, reassortant viruses containing either the UKtc or the OSU genome background with truncated NSP1 genes should be used for this analysis for increased comparability.

The two parental genes were then cloned into the pCI-neo expression vector and the UKtcNSP1 gene cloned in this vector was able to produce a significant reduction in IFNβ promoter activity, in agreement with the previously published literature (Arnold and Patton, 2011). Consequently all of the NSP1 hybrid genes were sub-cloned into the pCI-neo vector for functional analysis.

A cell-free transcription/translation system was used for studying protein expression for the pCI-neo-NSP1 hybrid constructs and the expressed protein was detected using

incorporated ^{35}S methionine labelling. This system is a convenient single-tube reaction for a coupled eukaryotic transcription-translation system and the reaction mixture is designed to give the highest expression for most expression constructs. With the exception of the parental OSUNSP1, all the remaining constructs tested including the positive control construct showed the expected protein band indicating the expression of proteins from these constructs. This confirmed that these hybrid proteins can be expressed to a detectable level and the reporter assay employing the pCI-neo-UKtcNSP1 has given a true reduction of promoter activity caused by UKtcNSP1 protein. Unfortunately, the expression of the parental pCI-neo-OSUNSP1 construct could not be detected in this system; therefore this particular plasmid was re-constructed by re-generating the corresponding restriction enzyme sites on OSU NSP1 sequence and followed by subsequent digestion and ligation into the vector. Due to time limitation, this newly constructed plasmid was not tested in this transcription translation system. Instead, this newly constructed pCI-neo-OSUNSP1 together with all the rest of the NSP1 gene constructs were tested in another assay to complement the transcription translation system assay. All of the NSP1 hybrid constructs including the newly-reconstructed pCI-neo-OSUNSP1 were tested in RT-PCR and all of them showed the expected mRNA products indicating that all these constructs were able to make mRNA. The subsequent degradation studies also showed that at least some of the constructs were expressed at certain levels to induce the degradation of the target proteins.

The functions of these NSP1 hybrids were tested in a reporter assay and the correlation between interaction and degradation was studied in the degradation investigations. The reporter plasmid initially used contains the full-length IFNβ

enhancer including four overlapping positive regulatory domains (PRDs) which contribute to the magnitude of the induction, and when multimerized, each PRD can induce the transcription upon a synthetic promoter independently of other IFNβ promoter sequences (King and Goodbourn, 1994; Sato *et al*., 1998; Du *et al*., 1992). Several members of the IRF family including IRF3 have been shown to bind PRD I/III elements (Escalanete *et al*., 1998; Fujii *et al*., 1999), NFκB p50/p65 binds PRD II and ATF-2/c-Jun binds to PRD IV (Berkowitz *et al*., 2002; Panne *et al*., 2004). Therefore, in order to increase the specificity of the reporter assay, the reporter plasmid employed in the assay was changed to a PRD I/III element containing promoter plasmid, ensuring the inducible promoter activity was caused by IRF3, which was expected to be degraded in cells transfected with some NSP1 constructs. Similarly, the ConA plasmid driven by NFκB was chosen to be used as OSUNSP1 was expected to affect NFκB induced INFβ production.

The results from the reporter assay employing PRD I/III promoter plasmid revealed that apart from the parental UKtcNSP1 construct, only two other constructs (D and H) containing the entire C-terminal region of UKtcNSP1 showed similar level of reduction on the promoter activity. However, in the assay employing ConA plasmid, no significant activity reduction was observed in any of the construct. It has to be noted that in the particular assay employing ConA reporter plasmid, Poly (I:C) was not included as it has been shown to have no significant effect on the reporter activity. This might be one of the reasons that most of the NSP1 constructs had shown no significant effect on the reporter activity. Another possible reason for this might be the E1A protein constitutively expressed in 293 cells has inhibited the NFκB pathway therefore the induction could not be detected (Cook *et al*., 2002). The

IRF3 degradation studies carried out subsequently were in agreement with the reporter assay results. The constructs showing most of the degradation in the absence of a proteasome inhibitor were the ones containing the entire C-terminal region of the UKtcNSP1 protein. Although it has been demonstrated by others that the IRF3 binding domain located in the last 165 amino acids of NSP1, the results from this study indicated that constructs containing the last 135 or 88 amino acids of the UKtcNSP1 failed to show significant reduction of promoter activity in the reporter assay or degradation of IRF3, indicating that the sequence between 165 and 135 from the C-terminal of UKtcNSP1 are essential for IRF3 binding activity.

Interestingly, the results observed from the β-TrCP degradation were different from the published literature. The OSUNSP1 transfected cells showed significant degradation of β-TrCP in the absence of proteasome inhibitor as expected, UKtcNSP1 also showed a substantial degradation of β-TrCP, among the hybrid constructs, two reciprocal pairs of constructs showed similar observation supporting the ability of UKtcNSP1 to degrade β-TrCP. One possible reason might be that the interaction site responsible for β-TrCP is close to the IRF3 binding site although the degradation studies were not analysed quantitatively therefore the exact amount of protein degraded was not able to be analysed.

Chapter 6

Final Discussion

Viral infection of most cells can induce the secretion of type I interferon which subsequently establishes an antiviral state in surrounding cells that can limit the spread of infection. Therefore viruses have evolved diverse mechanisms to interfere with this process and variation in the efficiency of this interference is a major factor in determining the differences in viral pathogenicity. Rotaviruses, which are of interest because they account for up to 50% of diarrheal illnesses worldwide in infants and young children and are responsible for more than half million deaths in this age group annually (Estes and Kapikian, 2007). Rotaviruses are able to evade this host antiviral response via interactions between their non-structural protein NSP1 and certain host cellular proteins. A better understanding of the mechanism of the interactions may provide insights that lead to novel strategies for antiviral research and live-attenuated vaccine development.

At the start of this project, published data had shown that some rotavirus NSP1 proteins target IRF3, a key transcription factor for IFN expression. Subsequently, one was found to target β-TrCP, which indirectly regulates a second important factor in this process- NFκB. In both cases, this limits subsequent IFNβ expression (Chapter 1). Given this information, 12 NSP1 hybrid genes were constructed for analysis in this project, each containing sequences from UKtc (bovine rotavirus strain) and OSU (porcine rotavirus strain) NSP1, by swapping sequence equivalent gene segments in plasmid expression constructs (Chapter 3). These were intended for use in a range of key assays to map the sites on viral NSP1 proteins responsible for interacting with and promoting the degradation of cellular proteins involved in the host's innate immune system. However, the cloning process took much longer than planned. There were problems with generating the restriction enzyme sites within both NSP1

sequences, and with expressing the proteins at a detectable amount in cell culture. Different approaches were attempted to address these problems including adding a FLAG tag for better antibody detection and changing the expression vector; the mammalian two-hybrid vectors containing the SV40 promoter was changed to pCDNA3.1 vector containing a more powerful CMV promoter and then the expression cassette was changed to use pCI-neo vector, the one containing an intron upstream of the inserted cDNA (Chapter 4 and Chapter 5).

In retrospect, other strategies for obtaining these hybrid NSP1 genes may have been more efficient. For example, domain swaps for the two parental NSP1 genes could be achieved via a two-step PCR approach with separated primer sets. However, a significant time commitment had been made to the restriction enzyme site approach and so it was decided to carry on with it.

A mammalian two-hybrid system was utilized to determine if direct protein-protein interactions occurred between NSP1 and cellular proteins IRF3 and β-TrCP in cells transfected with parental NSP1 plasmid constructs (Chapter 4). The assays investigating potential interactions between UKtcNSP1, IRF3 and OSUNSP1, β-TrCP all yielded negative results. These results seemed to suggest that there might not be direct interactions between NSP1 and the specific cellular proteins. However, it had been shown in a yeast two-hybrid assay system that direct interactions of UKtcNSP1 with IRF3 could be observed (Goodbourn *et al* unpublished results). One obvious possibility was that the proteins might not be expressed correctly from some or all of the plasmids employed in Chapter 4. Anti-Gal4 and anti-VP16 antibodies, which should detect the fusion protein domains expressed from these constructs both

failed to detect any protein expression from these constructs in those mammalian hybrid assay vectors. Nevertheless, these expression studies also revealed negative results for the positive control plasmids of the mammalian two-hybrid assay, which had shown clear evidence of protein-protein interaction in the assay system. Therefore the proteins might only be expressed in very limited amounts from the experimental constructs, such that the antibodies were not able to pick up the expression, or there may indeed have been a failure to express functional levels of proteins from one or more of the constructs.

NSP1 is normally expressed in the cytoplasm in rotavirus-infected host cells by using the viral polymerase. A possible reason why NSP1 cDNA did not give detectable expression in tissue culture cells following transfection of the plasmid might be the different transcription mechanisms employed by the viral genome RNA and cDNA. Since the rotavirus gene sequence is not normally expressed in the nucleus, it is never exposed to the RNA splicing machinery. RNA splicing at cryptic, unintended splice signals in the cDNA, might therefore cause disturbance to expression from the NSP1 cDNA during transcription and therefore inhibit the expression of NSP1 protein. Alternatively, it has been shown that RNA splicing from an artificial intron can increase protein expression from cDNA in mammalian cells significantly (Huang and Gorman, 1990). In their studies, two vectors which differ only in the presence or absence of an intron upstream to the 5'-untranslated sequence of the fusion proteins were compared. The results revealed that under transient transfection conditions, expression with the intron-containing vector in four mammalian cell lines: 293 (human embryonic kidney cells), Hela (cervical cancer cells), CV-1 (African green monkey kidney cells) and CHO (Chinese hamster ovary cells) all showed different

degrees of increase in protein synthesis and cytoplasmic RNA production compared with the expression in the intron-lacking vector (Huang and Gorman, 1990). In another study, it has also been shown that some sequences including β-globin cDNA exhibit a 400-fold increase in expression from the addition of an intron for splicing (Buchman and Berg, 1988), indicating that the introduction of an intron is able to maximize the gene expression in mammalian cells. This is thought to be due to the splicing event tagging the mRNA with proteins that promote mRNA export from the nucleus and/or its stability in the cytoplasm.

Consequently, the parental and hybrid NSP1 gene sequences were cloned into pCI-neo, a vector containing a chimeric intron upstream of the inserted cDNA sequences to prevent utilization of possible cryptic 5' –donor splice sites within the NSP1 cDNA sequence and to improve expression of full length mRNA (Chapter 4 and Chapter 5). In order to test for expression of NSP1 proteins from pCI-neo vector, a FLAG-tag was inserted at the N-terminal of the parental NSP1 gene sequences. However, this addition did not allow detection of expression of the parental NSP1 proteins any better than from the other vectors used. Therefore the proteins might still be expressed only at a very limited level so that they were not detectable. To avoid any issues with splicing and to give the most sensitive detection of protein, a coupled transcription and translation system with labelled ^{35}S methionine was used to analyse the expression of all the NSP1 hybrid proteins *in vitro*; and positive results were obtained with clear expression from all the hybrid NSP1 proteins and the UKtc parental NSP1 protein. After the re-construction of the OSU parental NSP1 plasmid, another assay was carried out to complement the couple transcription and translation system. By applying reverse transcriptase PCR using a common forward primer

starting upstream of the chimeric intron in the pCI-neo vector and a reverse primer for UKtc and OSU NSP1 respectively, all the constructs tested including the newly constructed OSU parental NSP1 showed the production of mRNA (Chapter 5). This RNA expression and processing was occurring as expected. Thus all these NSP1 constructs in pCI-neo vector were likely able to produce proteins.

Having obtained the evidence that the NSP1 proteins could be expressed, the function of these NSP1 hybrid constructs was then determined. The IFNβ promoter reporter assay applying these pCI-neo-NSP1 hybrid constructs showed evidence that these proteins were expressed in sufficient levels such that to have an impact on the promoter activity, i.e: functionally significant amount of protein were present. The results included analysis of these NSP1 hybrids utilizing either a full-length IFNβ promoter, a sub-element of that promoter: PRD I/III, which is activated specifically by IRF3-induced IFNβ production or a ConA promoter element that detects NFκB activity, in each case to test whether the NSP1 hybrid construct could inhibit induction of the promoter by a synthetic inducer of IFN that activates signalling via IRF3 and NFκB. Out of the 12 different NSP1 hybrids, constructs D and H (Figure 3.9/5.6A) containing the last 430 and 460 amino acids of the UKtc NSP1 respectively, showed similar level of reduction of PRDI/III promoter activity compared with the parental UKtcNSP1 construct. This result agreed with the previous finding that the binding site for IRF3 in NSP1 is located at the C-terminal part of the NSP1. However, results from other NSP1 constructs containing smaller parts of the C-terminal region from UKtc NSP1 sequence, such as constructs A, L and F which contain the last 135 amino acids or last 88 amino acids from UKtcNSP1 gene sequence, indicated that these amino acid sequences from UKtc NSP1 were not

sufficient to impact on the level of IRF3 activity induced. Interestingly, when using the ConA plasmid as the reporter, OSU NSP1 did not show an obvious reduction of the ConA promoter activity although, based on previous findings, OSU NSP1 should be able to reduce NFκB activity due to its interaction with β-TrCP. None of the constructs showed significant reduction of the ConA promoter activity. This might suggest that the reporter assay using this specific promoter was not sensitive enough to test the impact caused by the different NSP1 hybrid constructs. This might be due to the reason that the NFκB response could be inhibited by Adenoviral E1A protein expressed in 293 cells (Janaswami *et al*., 1992; Shao *et al*., 2001; Cook *et al*., 2002).

One of the expected reasons for the reduced levels of induction of IFNβ promoter in the presence of NSP1 was the degradation of IRF3 or/and β-TrCP caused by NSP1 proteins (Graff *et al*., 2002; Barro and Patton, 2005; Graff *et al*., 2009). To investigate whether the observed reduced induction of IFNβ by certain NSP1s correlated with the degradation of the corresponding cellular proteins, studies for cellular protein degradation were carried out in the presence or absence of the proteasome inhibitor MG132. The IRF3 degradation results were in agreement with the PRDI/III promoter assay results, such that the parental UKtcNSP1 together with the constructs D and H showed significant reduction of IRF3 in the absence of MG132 and the level of IRF3 was restored when MG132 was added. However, in the case of the β-TrCP degradation study, both UKtcNSP1 and OSUNSP1 caused significant decreases of the level of β-TrCP which were restored in the presence of MG132. Although this result was different from the published observation that UKtc NSP1 does not cause considerable β-TrCP degradation in transfected cells (Arnold and Patton, 2011), it was supported by the fact that two pairs of reciprocal constructs

C and D (containing the last 430 aa from OSUNSP1 and UKtcNSP1 respectively), G and H (containing the last 460 aa from OSUNSP1 and UKtcNSP1 respectively) also showed reduction of transfected β-TrCP protein levels in my observation. This result is difficult to explain, one possible reason might be that the regions responsible for IRF3 and β-TrCP degradation are close and there might be a conserved region in both UKtc and OSU NSP1s that is important for the interactions.

Take together the previous results have showed that rotavirus NSP1 has evolved numerous ways to antagonize the IFN-β signalling pathway by targeting IRF family members, β-TrCP or RIG-I depending on different virus strains (Arnold and Patton, 2011; Qin *et al*., 2011). However, relevant mapping studies on the interaction sites for NSP1 with cellular proteins were limited to using deletion mutants of bovine rotavirus (B641) (Graff *et al*., 2002). These results identified that a binding domain for IRF3 was located somewhere in the C-terminal region within the last 163 amino acids in the tested B641 NSP1 sequence. Subsequent studies using point mutations in the conserved zinc domain showed that these also abolished the NSP1-IRF3 interaction indicated the importance of this structural domain in this interaction in addition to the C-terminal region (Graff *et al*., 2002).

These published data taken together with the results reported in the thesis do not give a clear picture of which region in NSP1 is responsible for interactions with β-TrCP. However the regions in NSP1 responsible for IRF3 degradation-induced reduction of IFNβ activity can be summarised as shown in figure 6.1.

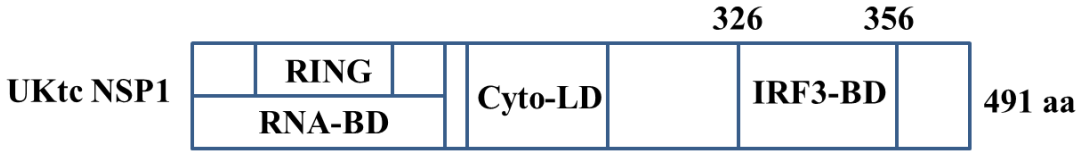

Figure 6.1. Schematic of proposed structural and functional domains in UKtcNSP1.

NSP1 protein consists of a RNA-binding domain (RNA-BD), a zinc binding RING domain (RING) and a cytoplasm localization domain (Cyto-LD) near the N-terminal of the protein (Hua *et al*., 1994b, Arnold and Patton, 2009). The IRF3-binding requires sequences located between amino acids 326 and 356 at the C-terminal of the UKtcNSP1 protein (IRF3-BD).

NSP1 has been postulated to have E3 ubiquitin ligase activity based on several observations. Like other known E3 ubiquitin ligases, NSP1 targets its binding partners for degradation (Pickart *et al*., 2001), a RING domain structure can be found in both NSP1 and other E3 ligases that is important for activity (Jackson *et al*., 2000, Graff *et al*., 2007), and both E3 proteins and NSP1 are subjected to proteasomal degradation and can accumulate in cells when treated with a proteasome inhibitor (Piña-Vázquez *et al*., 2007, Graff *et al*., 2007). The typical RING finger has been defined by the consensus sequence C_3HC_4 in which the Cys (C) and His (H) represent the zinc binding residues (Joazeiro *et al*., 2000), whereas the RING domain in NSP1 proteins has been predicted to be in a C_4HC_3 arrangement. However, this variant arrangement is typical of other viral RING-containing proteins such as p28 protein from Poxvirus and K3 protein from Kaposi sarcoma herpesvirus (Aravind *et al*., 2003; Dodd *et al*., 2004; Nerenberg *et al*., 2005). Protein polyubiquitination

occurs through a series of events. It starts with the transfer of the Ub moiety to an E2 Ub-conjugating enzyme by an E1 Ub-activating enzyme, the loaded E2 then interacts with E3 Ub ligases which can direct the transfer of ubiquitin from the E2 onto target proteins. The RING domain of the E3 ligase serves as an adaptor between the E2 ligase and the target protein. However, in the case of rotavirus NSP1, direct evidence supporting its function as an E3 ligase has yet to be discovered as the putative E2 conjugase for NSP1 remains to be identified although the targeted IRF3 or/and β-TrCP can be degraded via proteasome dependent pathway. One of the reasons for using hybrid NSP1 proteins in this study rather than deletion mutants (as described previously by others) was to maintain the important functional domains in the protein and to try to avoid major structural changes of the protein.

There are other viral proteins that act as an E3 ubiquitin ligase which have been studied in more detail. For instance, herpes simplex virus type I ICP0, which has been reported to act as E3 ubiquitin ligases during viral infection and to target several cellular proteins including DNA-dependent protein kinase, components of the PML nuclear bodies, and centromeric proteins for proteasome-mediated degradation (Boutell *et al*., 2002; Gu and Roizman, 2003; Lilley *et al*., 2010). Another classic example of viral proteins exhibiting E3 ligase activity is the adenovirus E1b55K/ E4orf6 complex. It assembles with subunits of the cellular cullin 5 class of E3 ubiquitin ligases including elongins B and C, Rbx1 and cullin 5, substitutes for their substrate-binding subunits in order to redirect the ubiquitin ligase activity which causes p53 polyubiquitination, its recognition and degradation by proteasomes (Pennella *et al*., 2010). In addition, Poxvirus p28 protein and Kaposi sarcoma herpesvirus K3 protein haven also been shown to exhibit E3 ligase activity (Dodd *et*

al., 2004; Nerenberg *et al*., 2005). Thus there is considerable precedent for NSP1 to be a viral ligase enzyme.

All the results described in the previous chapters have set a foundation for some interesting avenues for rotavirus research which would have been pursued had time permitted. Further studies and analyse are clearly required to investigate the role of NSP1 in rotavirus pathogenesis in more detail. The interaction site responsible for β-TrCP degradation remains to be understood as the results, that UKtc NSP1 can degrade β-TrCP, have revealed some conflicts with other published data. Specifically, Arnold and Patton found that the NSP1 of NCDV and UKtc were unable to cause degradation in cells co-transfected with β-TrCP (Arnold and Patton, 2011). However, in direct contrast, another group demonstrated that the NSP1 from the bovine strain NCDV was able to cause β-TrCP degradation in cells co-transfected with β-TrCP (Graff *et al*., 2009). NCDV and UKtc show great sequence similarity in terms of nucleotide and amino acid, 90% and 95% respectively (Figure 3.1). Therefore it is not entirely surprising when the results presented in this thesis were observed; UKtc NSP1 showed the ability to degrade transfected β-TrCP in the absence of MG132 which is similar to NCDV. However, a more intense sequencing study comparing NSP1 sequences from rotaviruses that target a broader range of host species might provide more information on this matter. Regarding to the E3 ubiquitin ligase activity, an obvious question to be determined is the identification of the E2 partner protein involved in this process. In addition, although the plasmid-based reverse genetics for rotavirus has not yet been developed, the reverse genetics using a recombinant vaccinia virus expressing T7 RNA polymerase has been proved to be

successful (Taniguchi and Komoto, 2012) which might be applied to analyse the function of these NSP1 hybrid proteins *in vivo*.

Appendix

Construct B

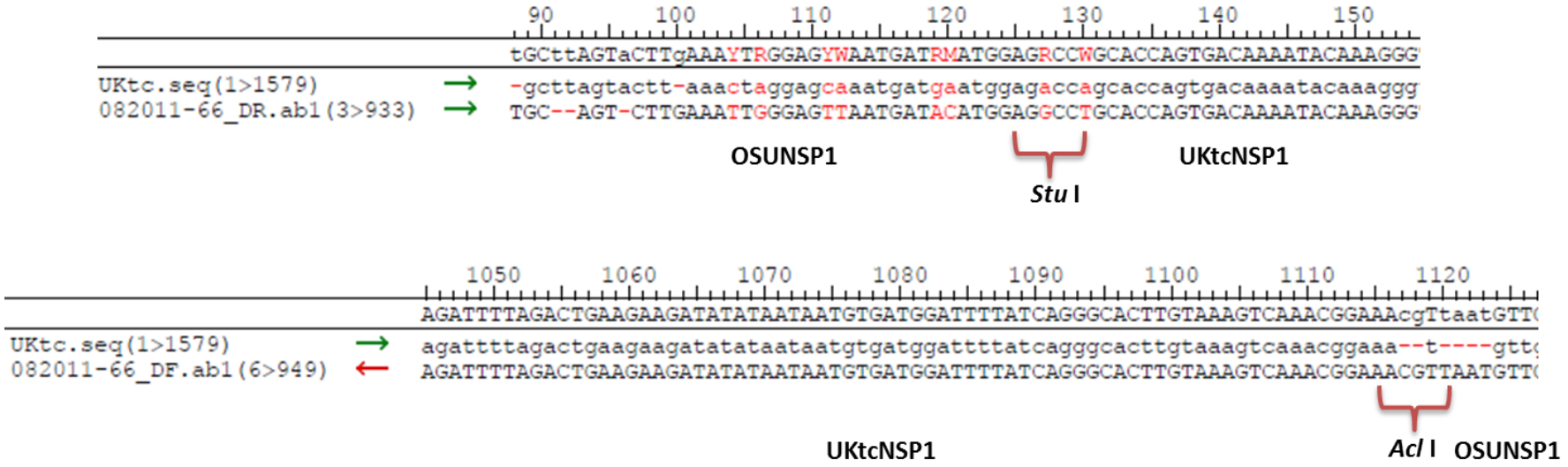
90 100 110 120 130 140 150
tGCttAGTaCTTgAAAYTRGGAGYWAATGATRMATGGAGRCCWGCACCAGTGACAAAATACAAAGGG
UKtc.seq(1>1579)
082011-66_DR.ab1(3>933)
-gcttagtactt-aaactaggagcaaatgatgaatggagaccagcaccagtgacaaaatacaaaggg
TGC--AGT-CTTGAAATTGGGAGTTAATGATACATGGAGGCCTGCACCAGTGACAAAATACAAAGGG
OSUNSP1
UKtcNSP1
Stu I
1050 1060 1070 1080 1090 1100 1110 1120
AGATTTTAGACTGAAGAAGATATATAATAATGTGATGGATTTTATCAGGGCACTTGTAAAGTCAAACGGAAAcgTtaatGTT
UKtc.seq(1>1579)
082011-66_DF.ab1(6>949)
agattttagactgaagaagatatataataatgtgatggattttatcagggcacttgtaaagtcaaacggaaa--t----gtt
AGATTTTAGACTGAAGAAGATATATAATAATGTGATGGATTTTATCAGGGCACTTGTAAAGTCAAACGGAAACGTTAATGTT
UKtcNSP1
Acl I
OSUNSP1

Construct C

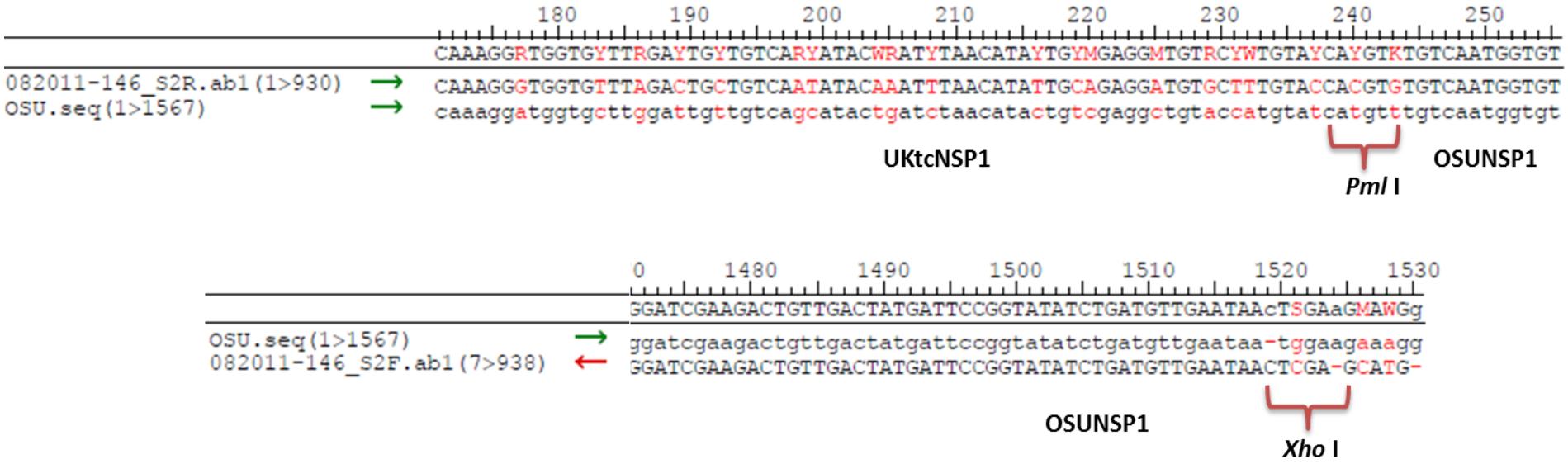
180 190 200 210 220 230 240 250
CAAAGGRTGGTGYTTRGAYTGYTGTCARYATACWRATYTAACATAYTGYMGAGGMTGTRCYWTGTAYCAYGTKTGTCAATGGTGT
082011-146_S2R.ab1(1>930)
OSU.seq(1>1567)
CAAAGGGTGGTGTTTAGACTGCTGTCAATATACAAATTTAACATATTGCAGAGGATGTGCTTTGTACCACGTGTGTCAATGGTGT
caaaggatggtgcttggattgttgtcagcatactgatctaacatactgtcgaggctgtaccatgtatcatgtttgtcaatggtgt
UKtcNSP1
OSUNSP1
PmlI
0 1480 1490 1500 1510 1520 1530
GGATCGAAGACTGTTGACTATGATTCCGGTATATCTGATGTTGAATAAcTSGAaGMAWGg
OSU.seq(1>1567)
082011-146_S2F.ab1(7>938)
ggatcgaagactgttgactatgattccggtatatctgatgttgaataa-tggaagaaagg
GGATCGAAGACTGTTGACTATGATTCCGGTATATCTGATGTTGAATAACTCGA-GCATG-
OSUNSP1
XhoI

Construct D

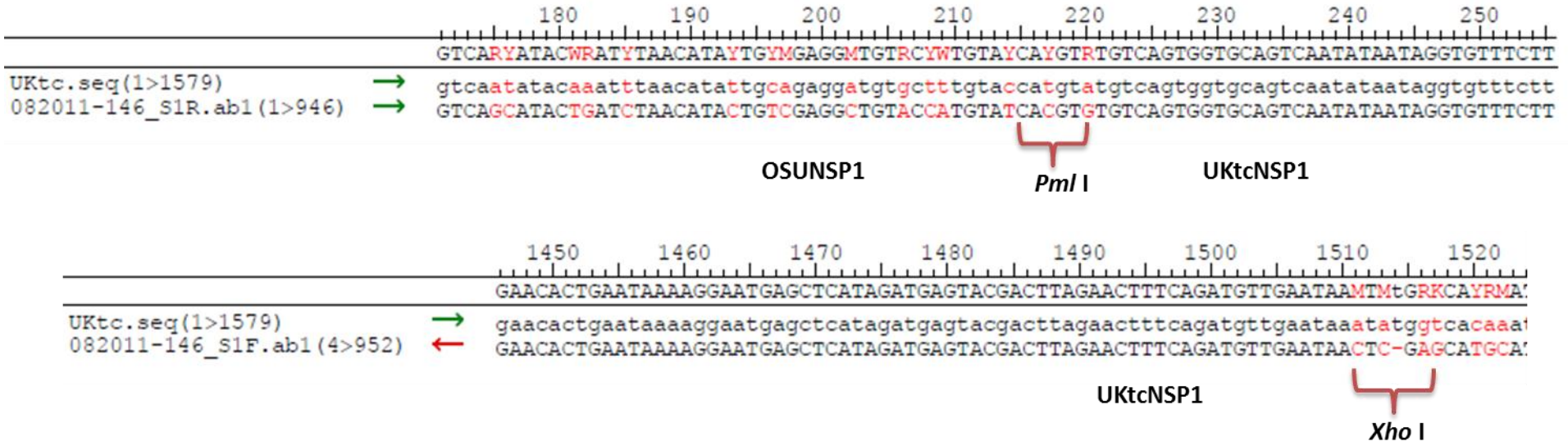
180 190 200 210 220 230 240 250
GTCARYATACWRATYTAACATAYTGYMGAGGMTGTRCYWTGTAYCAYGTRTGTCAGTGGTGCAGTCAATATAATAGGTGTTTCTT
UKtc.seq(1>1579)
082011-146_S1R.ab1(1>946)
gtcaatatacaaatttaacatattgcagaggatgtgctttgtaccatgtatgtcagtggtgcagtcaatataataggtgtttctt
GTCAGCATACTGATCTAACATACTGTCGAGGCTGTACCATGTATCACGTGTGTCAGTGGTGCAGTCAATATAATAGGTGTTTCTT
OSUNSP1
Pml I
UKtcNSP1
1450 1460 1470 1480 1490 1500 1510 1520
GAACACTGAATAAAAGGAATGAGCTCATAGATGAGTACGACTTAGAACTTTCAGATGTTGAATAAMTMtGRKCAYRMA
UKtc.seq(1>1579)
082011-146_S1F.ab1(4>952)
gaacactgaataaaaggaatgagctcatagatgagtacgacttagaactttcagatgttgaataaatatggtcacaaat
GAACACTGAATAAAAGGAATGAGCTCATAGATGAGTACGACTTAGAACTTTCAGATGTTGAATAACTC-GAGCATGCA
UKtcNSP1
Xho I

Construct E

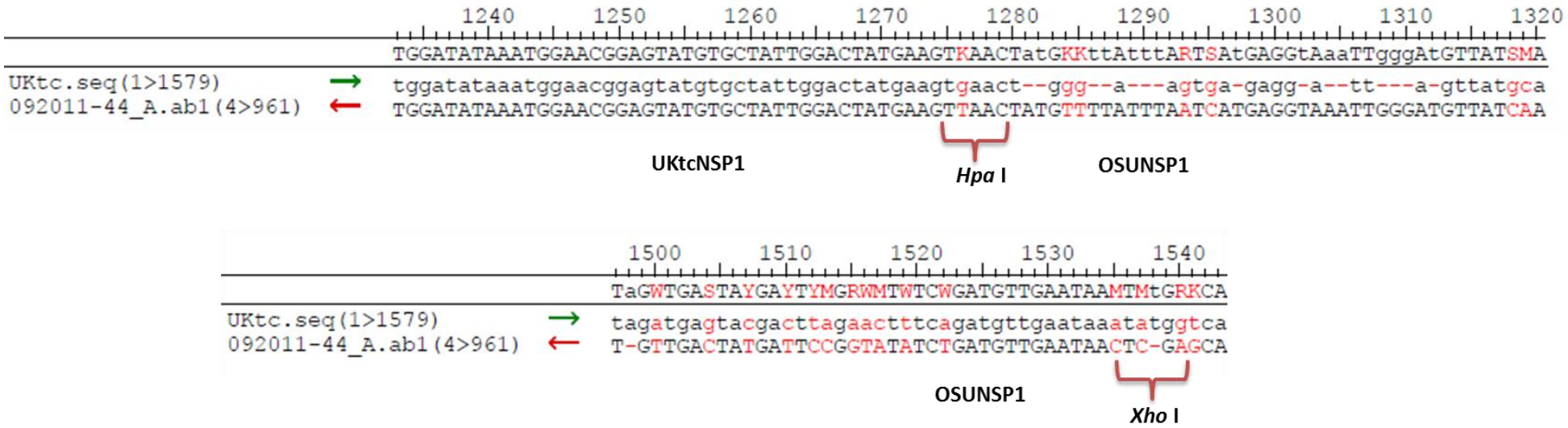
1240 1250 1260 1270 1280 1290 1300 1310 1320
TGGATATAAATGGAACGGAGTATGTGCTATTGGACTATGAAGTKAACTatGKKttAtttARTSAtGAGGtAaaTTgggAtGTTATSMA
UKtc.seq(1>1579)
092011-44_A.ab1(4>961)
tggatataaatggaacggagtatgtgctattggactatgaagtgaact--ggg--a---agtga-gagg-a--tt---a-gttatgca
TGGATATAAATGGAACGGAGTATGTGCTATTGGACTATGAAGTTAACTATGTTTTATTTAATCATGAGGTAAATTGGGATGTTATCAA
UKtcNSP1
Hpa I
OSUNSP1
1500 1510 1520 1530 1540
TaGWTGASTAYGAYTYMGRWMTWTCWGATGTTGAATAAMTMtGRKCA
UKtc.seq(1>1579)
092011-44_A.ab1(4>961)
tagatgagtacgacttagaactttcagatgttgaataaatatggtca
T-GTTGACTATGATTCCGGTATATCTGATGTTGAATAACTC-GAGCA
OSUNSP1
Xho I

Construct F

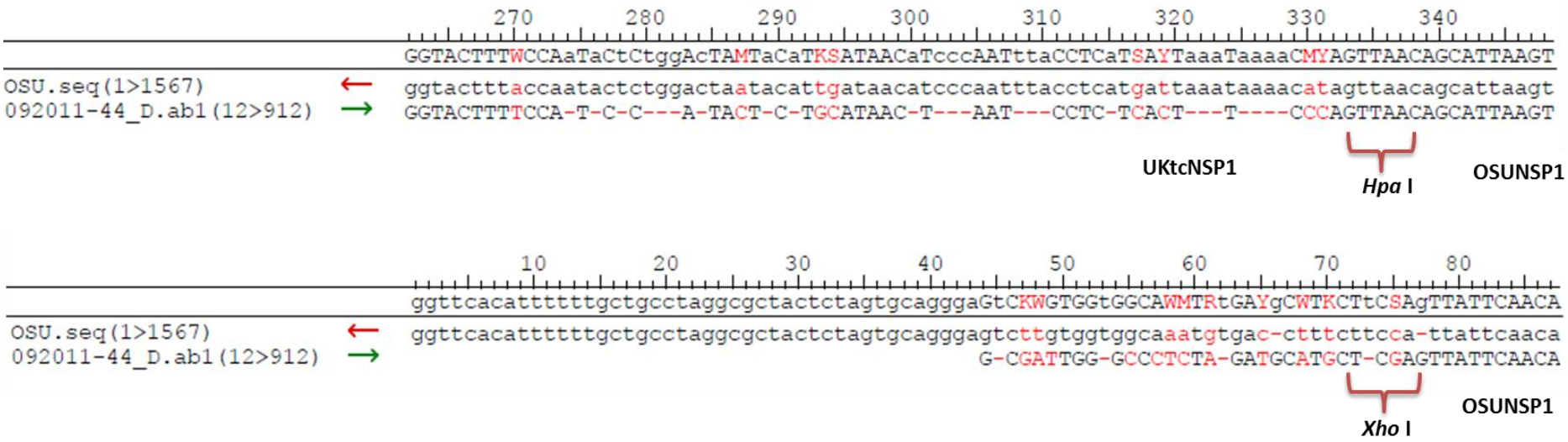
270 280 290 300 310 320 330 340
GGTACTTTWCCAaTaCtCtggAcTAMTaCaTKSATAACaTcccAATttaCCTCaTSAYTaaaTaaaaCMYAGTTAACAGCATTAAGT
OSU.seq(1>1567)
092011-44_D.ab1(12>912)
ggtactttaccaatactctggactaatacattgataacatcccaatttacctcatgattaaataaaacatagttaacagcattaagt
GGTACTTTTCCA-T-C-C---A-TACT-C-TGCATAAC-T---AAT---CCTC-TCACT---T----CCCAGTTAACAGCATTAAGT
UKtcNSP1
Hpa I
OSUNSP1
10 20 30 40 50 60 70 80
ggttcacatttttttgctgcctaggcgctactctagtgcagggaGtCKWGTGGtGGCAWMTRtGAYgCWTKCTtCSAgTTATTCAACA
OSU.seq(1>1567)
092011-44_D.ab1(12>912)
ggttcacatttttttgctgcctaggcgctactctagtgcagggagtcttgtggtggcaaatgtgac-ctttcttcca-ttattcaaca
G-CGATTGG-GCCCTCTA-GATGCATGCT-CGAGTTATTCAACA
OSUNSP1
Xho I

Construct G

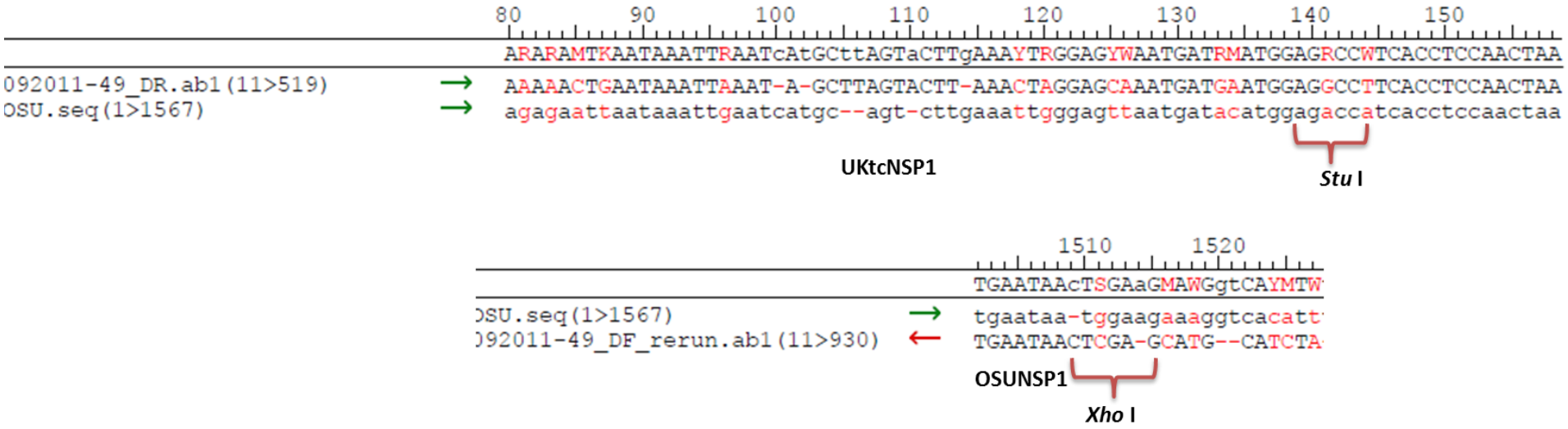
80
90
100
110
120
130
140
150
ARARAMTKAATAAATTRAATcAtGCttAGTaCTTgAAAYTRGGAGYWAATGATRMATGGAGRCCWTCACCTCCAACTAA
092011-49_DR.ab1(11>519)
AAAAACTGAATAAATTAAAT-A-GCTTAGTACTT-AAACTAGGAGCAAATGATGAATGGAGGCCTTCACCTCCAACTAA
OSU.seq(1>1567)
agagaattaataaattgaatcatgc--agt-cttgaaattgggagttaatgatacatggagaccatcacctccaactaa
UKtcNSP1
Stu I
1510
1520
TGAATAAcTSGAaGMAWGgtCAYMTW
OSU.seq(1>1567)
tgaataa-tggaagaaaggtcacatt
092011-49_DF_rerun.ab1(11>930)
TGAATAACTCGA-GCATG--CATCTA
OSUNSP1
Xho I

Construct H

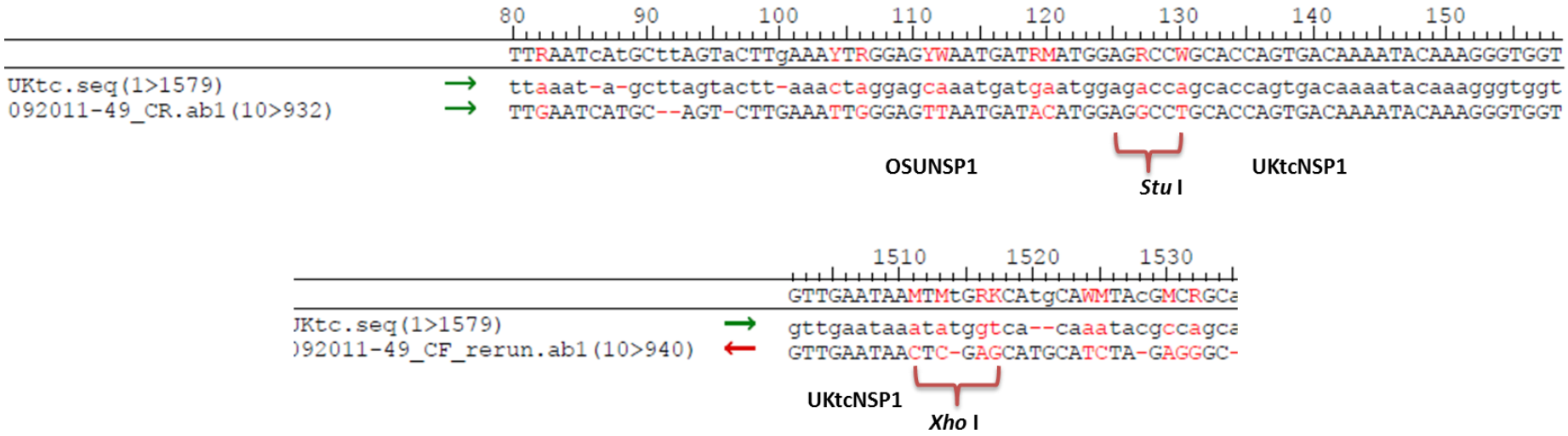
80 90 100 110 120 130 140 150
TTRAATcAtGCttAGTaCTTgAAAYTRGGAGYWAATGATRMATGGAGRCCWGCACCAGTGACAAAATACAAAGGGTGGT
UKtc.seq(1>1579)
092011-49_CR.ab1(10>932)
ttaaat-a-gcttagtactt-aaactaggagcaaatgatgaatggagaccagcaccagtgacaaaatacaaagggtggt
TTGAATCATGC--AGT-CTTGAAATTGGGAGTTAATGATACATGGAGGCCTGCACCAGTGACAAAATACAAAGGGTGGT
OSUNSP1
UKtcNSP1
Stu I
1510 1520 1530
GTTGAATAAMTMtGRKCAtgCAWMTAcGMCRGCa
JKtc.seq(1>1579)
)92011-49_CF_rerun.ab1(10>940)
gttgaataaatatggtca--caaatacgccagca
GTTGAATAACTC-GAGCATGCATCTA-GAGGGC-
UKtcNSP1
Xho I

Construct I

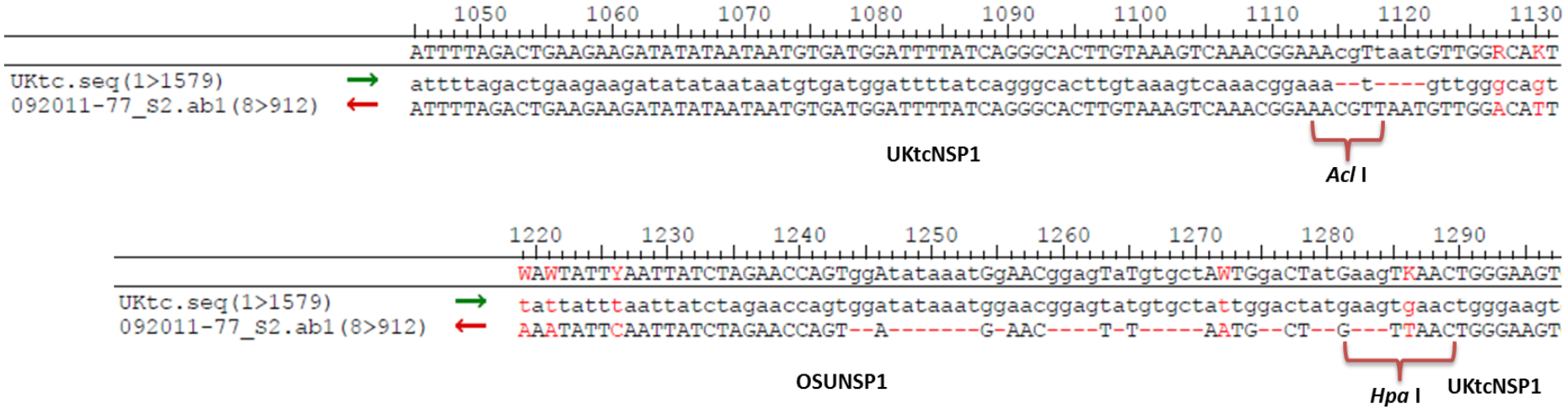
1050 1060 1070 1080 1090 1100 1110 1120 1130
ATTTTAGACTGAAGAAGATATATAATAATGTGATGGATTTTATCAGGGCACTTGTAAAGTCAAACGGAAAcgTtaatGTTGGRCAKT
UKtc.seq(1>1579)
092011-77_S2.ab1(8>912)
attttagactgaagaagatatataataatgtgatggattttatcagggcacttgtaaagtcaaacggaaa--t----gttgggcagt
ATTTTAGACTGAAGAAGATATATAATAATGTGATGGATTTTATCAGGGCACTTGTAAAGTCAAACGGAAACGTTAATGTTGGACATT
UKtcNSP1
AclI
1220 1230 1240 1250 1260 1270 1280 1290
WAWTATTYAATTATCTAGAACCAGTggAtataaatGgAACggagTaTgtgctAWTGgaCTatGaagTKAACTGGGAAGT
UKtc.seq(1>1579)
092011-77_S2.ab1(8>912)
tattatttaattatctagaaccagtggatataaatggaacggagtatgtgctattggactatgaagtgaactgggaagt
AAATATTCAATTATCTAGAACCAGT--A-------G-AAC----T-T-----AATG--CT--G---TTAACTGGGAAGT
OSUNSP1
HpaI
UKtcNSP1

Construct J

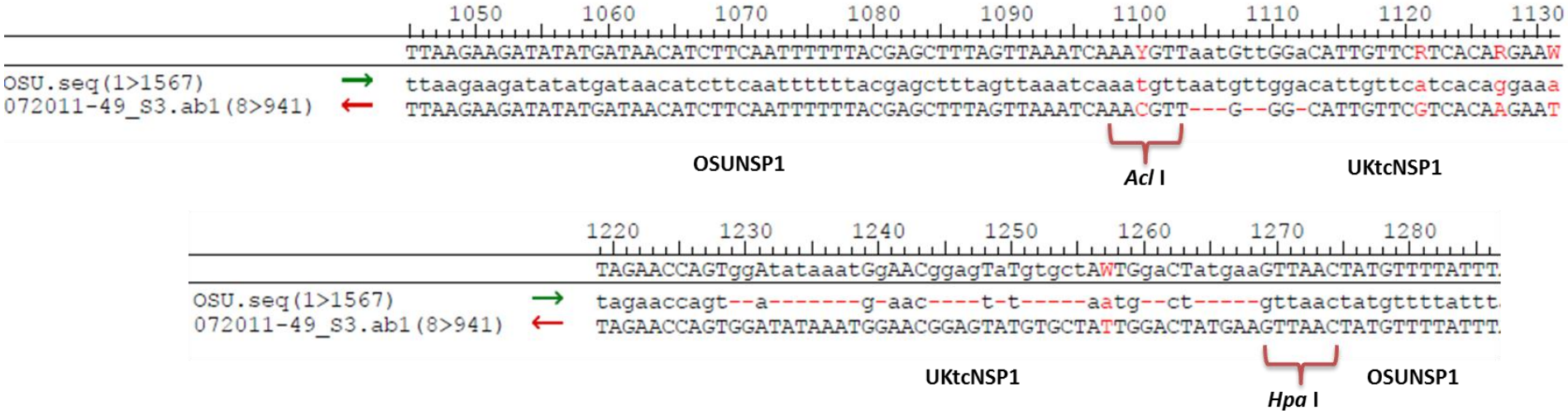
1050 1060 1070 1080 1090 1100 1110 1120 1130
TTAAGAAGATATATGATAACATCTTCAATTTTTTACGAGCTTTAGTTAAATCAAAYGTTaatGttGGaCATTGTTCRTCACARGAAW
OSU.seq(1>1567)
072011-49_S3.ab1(8>941)
ttaagaagatatatgataacatcttcaatttttacgagctttagttaaatcaaatgttaatgttggacattgttcatcacaggaaa
TTAAGAAGATATATGATAACATCTTCAATTTTTTACGAGCTTTAGTTAAATCAAACGTT---G--GG-CATTGTTCGTCACAAGAAT
OSUNSP1
AclI
UKtcNSP1
1220 1230 1240 1250 1260 1270 1280
TAGAACCAGTggAtataaatGgAACggagTaTgtgctAWTGgaCTatgaaGTTAACTATGTTTTATTT
OSU.seq(1>1567)
072011-49_S3.ab1(8>941)
tagaaccagt--a-------g-aac----t-t-----aatg--ct-----gttaactatgttttattt
TAGAACCAGTGGATATAAATGGAACGGAGTATGTGCTATTGGACTATGAAGTTAACTATGTTTTATTT
UKtcNSP1
HpaI
OSUNSP1

Construct K

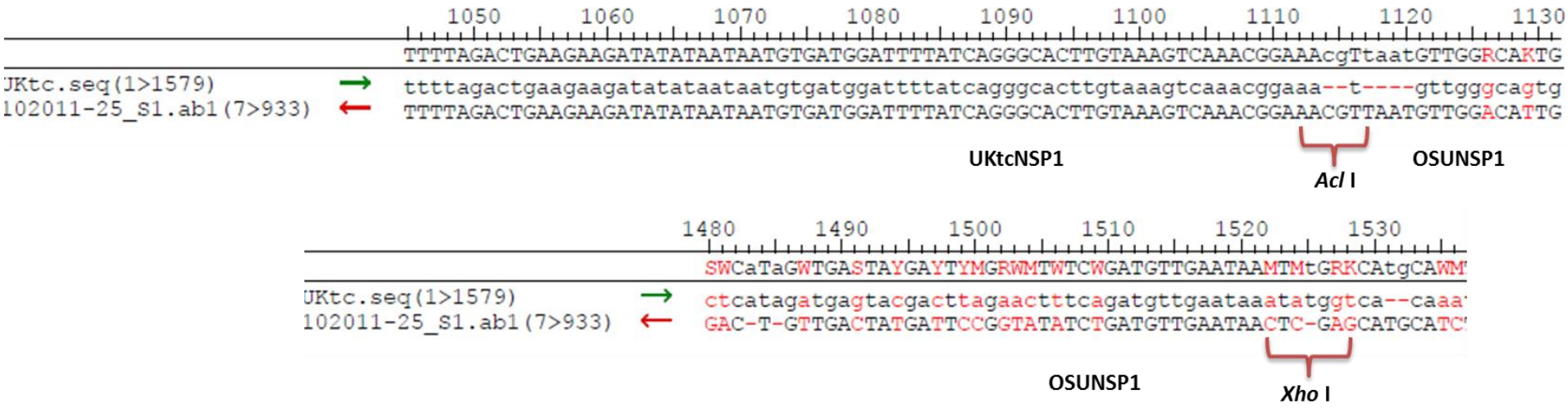
1050 1060 1070 1080 1090 1100 1110 1120 1130
TTTTAGACTGAAGAAGATATATAATAATGTGATGGATTTTATCAGGGCACTTGTAAAGTCAAACGGAAAcgTtaatGTTGGRCAKTG
JKtc.seq(1>1579)
102011-25_S1.ab1(7>933)
ttttagactgaagaagatatataataatgtgatggattttatcagggcacttgtaaagtcaaacggaaa--t----gttgggcagtg
TTTTAGACTGAAGAAGATATATAATAATGTGATGGATTTTATCAGGGCACTTGTAAAGTCAAACGGAAACGTTAATGTTGGACATTG
UKtcNSP1
OSUNSP1
AclI
1480 1490 1500 1510 1520 1530
SWCaTaGWTGASTAYGAYTYMGRWMTWTCWGATGTTGAATAAMTMtGRKCAtgCAWM
UKtc.seq(1>1579)
102011-25_S1.ab1(7>933)
ctcatagatgagtacgacttagaactttcagatgttgaataaatatggtca--caaa
GAC-T-GTTGACTATGATTCCGGTATATCTGATGTTGAATAACTC-GAGCATGCATC
OSUNSP1
XhoI

Construct L

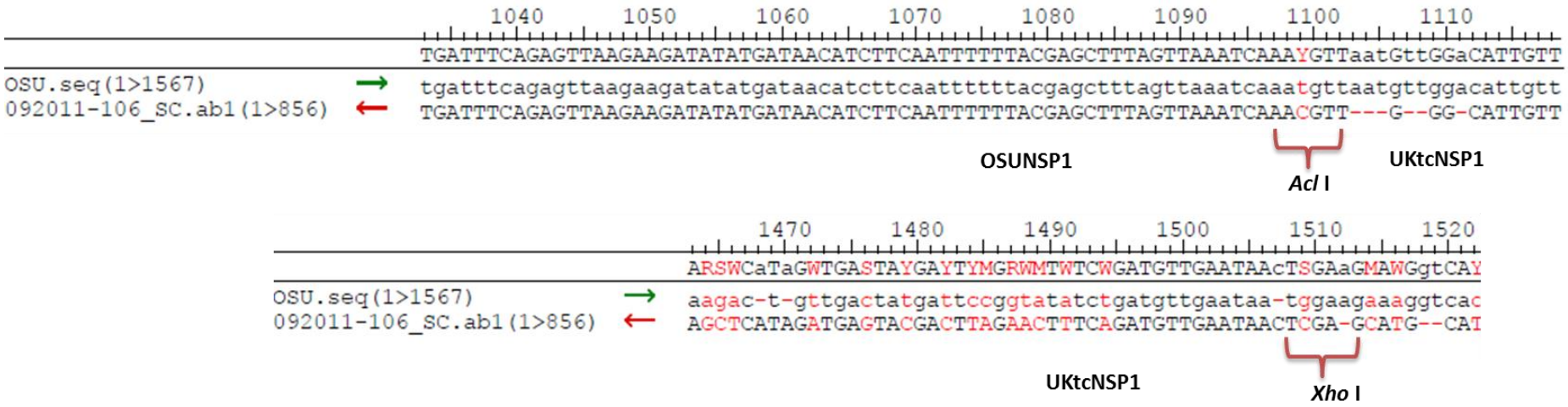
1040 1050 1060 1070 1080 1090 1100 1110
TGATTTCAGAGTTAAGAAGATATATGATAACATCTTCAATTTTTTACGAGCTTTAGTTAAATCAAAYGTTaatGttGGaCATTGTT
OSU.seq(1>1567)
092011-106_SC.ab1(1>856)
tgatttcagagttaagaagatatatgataacatcttcaatttttacgagctttagttaaatcaaatgttaatgttggacattgtt
TGATTTCAGAGTTAAGAAGATATATGATAACATCTTCAATTTTTTACGAGCTTTAGTTAAATCAAACGTT---G--GG-CATTGTT
OSUNSP1
UKtcNSP1
AclI
1470 1480 1490 1500 1510 1520
ARSWCaTaGWTGASTAYGAYTYMGRWMTWTCWGATGTTGAATAAcTSGAaGMAWGgtCAY
OSU.seq(1>1567)
092011-106_SC.ab1(1>856)
aagac-t-gttgactatgattccggtatatctgatgttgaataa-tggaagaaaggtcac
AGCTCATAGATGAGTACGACTTAGAACTTTCAGATGTTGAATAACTCGA-GCATG--CAT
UKtcNSP1
XhoI

Bibliography

Adams, W.R. and Kraft, L. (1963). Epizootic diarrhea of infant mice: indentification of the etiologic agent. *Science* **141**(3578), pp. 359-360.

Afrikanova, I., Miozzo, M.C., Giambiagi, S. and Burrone, O. (1996). Phosphorylation generates different forms of rotavirus NSP5. *J Gen Virol* **77 (Pt 9)**pp. 2059-2065.

Akira, S., Uematsu, S. and Takeuchi, O. (2006). Pathogen recognition and innate immunity. *Cell* **124**(4), pp. 783-801.

Alexopoulou, L., Holt, A.C., Medzhitov, R. and Flavell, R.A. (2001). Recognition of double-stranded RNA and activation of NF-kappaB by Toll-like receptor 3. *Nature* **413**(6857), pp. 732-738.

Andrejeva, J., Childs, K.S., Young, D.F., Carlos, T.S., Stock, N., Goodbourn, S. and Randall, R.E. (2004). The V proteins of paramyxoviruses bind the IFN-inducible RNA helicase, mda-5, and inhibit its activation of the IFN-beta promoter. *Proc Natl Acad Sci U S A* **101**(49), pp. 17264-17269.

Angel, J., Franco, M.A. and Greenberg, H.B. (2007). Rotavirus vaccines: recent developments and future considerations. *Nat Rev Microbiol* **5**(7), pp. 529-539.

Aponte, C., Poncet, D. and Cohen, J. (1996). Recovery and characterization of a replicase complex in rotavirus-infected cells by using a monoclonal antibody against NSP2. *J Virol* **70**(2), pp. 985-991.

Aravind, L., Iyer, L.M. and Koonin, E.V. (2003). Scores of RINGS but no PHDs in ubiquitin signaling. *Cell Cycle* **2**(2), pp. 123-126.

Arnold, M.M. and Patton, J.T. (2009). Rotavirus antagonism of the innate immune response. *Viruses* **1**(3), pp. 1035-1056.

Arnold, M.M. and Patton, J.T. (2011). Diversity of Interferon Antagonist Activities Mediated by NSP1 Proteins of Different Rotavirus Strains. *Journal of Virology* **85**(5), pp. 1970-1979.

Arnoldi, F., Campagna, M., Eichwald, C., Desselberger, U. and Burrone, O.R. (2007). Interaction of rotavirus polymerase VP1 with nonstructural protein NSP5 is stronger than that with NSP2. *J Virol* **81**(5), pp. 2128-2137.

Attoui, H., Jaafar, F.M., Belhouchet, M., de Micco, P., de Lamballerie, X. and Brussaard, C.P. (2006). Micromonas pusilla reovirus: a new member of the family Reoviridae assigned to a novel proposed genus (Mimoreovirus). *J Gen Virol* **87**(Pt 5), pp. 1375-1383.

Au, K.S., Chan, W.K., Burns, J.W. and Estes, M.K. (1989). Receptor activity of rotavirus nonstructural glycoprotein NS28. *J Virol* **63**(11), pp. 4553-4562.

Azevedo, M.S., Yuan, L., Jeong, K.I., Gonzalez, A., Nguyen, T.V., Pouly, S., Gochnauer, M., Zhang, W., Azevedo, A. and Saif, L.J. (2005). Viremia and nasal and rectal shedding of rotavirus in gnotobiotic pigs inoculated with Wa human rotavirus. *J Virol* **79**(9), pp. 5428-5436.

Baeuerle, P.A. and Baltimore, D. (1988). I kappa B: a specific inhibitor of the NF-kappa B transcription factor. *Science* **242**(4878), pp. 540-546.

Bagchi, P., Nandi, S., Chattopadhyay, S., Bhowmick, R., Halder, U.C., Nayak, M.K., Kobayashi, N. and Chawla-Sarkar, M. (2012). Identification of common human host genes involved in pathogenesis of different rotavirus strains: An attempt to recognize probable antiviral targets. *Virus Res*pp.

Ball, J.M., Tian, P., Zeng, C.Q., Morris, A.P. and Estes, M.K. (1996). Age-dependent diarrhea induced by a rotaviral nonstructural glycoprotein. *Science* **272**(5258), pp. 101-104.

Barnes, B., Lubyova, B. and Pitha, P.M. (2002). On the role of IRF in host defense. *J Interferon Cytokine Res* **22**(1), pp. 59-71.

Barnes, B.J., Moore, P.A. and Pitha, P.M. (2001). Virus-specific activation of a novel interferon regulatory factor, IRF-5, results in the induction of distinct interferon alpha genes. *J Biol Chem* **276**(26), pp. 23382-23390.

Barro, M. and Patton, J. (2005). Rotavirus nonstructural protein 1 subverts innate immune response by inducing degradation of IFN regulatory factor 3. *Proc Natl Acad Sci U S A* **102**(11), pp. 4114-4119.

Barro, M. and Patton, J. (2007). Rotavirus NSP1 inhibits expression of type I interferon by antagonizing the function of interferon regulatory factors IRF3, IRF5, and IRF7. *J Virol* **81**(9), pp. 4473-4481.

Beech, S.J., Lethbridge, K.J., Killick, N., McGlincy, N. and Leppard, K.N. (2005). Isoforms of the promyelocytic leukemia protein differ in their effects on ND10 organization. *Exp Cell Res* **307**(1), pp. 109-117.

Berkowitz, B., Huang, D.B., Chen-Park, F.E., Sigler, P.B. and Ghosh, G. (2002). The x-ray crystal structure of the NF-kappa B p50.p65 heterodimer bound to the interferon beta -kappa B site. *J Biol Chem* **277**(27), pp. 24694-24700.

Beutler, B., Eidenschenk, C., Crozat, K., Imler, J.L., Takeuchi, O., Hoffmann, J.A. and Akira, S. (2007). Genetic analysis of resistance to viral infection. *Nat Rev Immunol* **7**(10), pp. 753-766.

Bibeau-Poirier, A., Gravel, S.P., Clément, J.F., Rolland, S., Rodier, G., Coulombe, P., Hiscott, J., Grandvaux, N., Meloche, S. and Servant, M.J. (2006). Involvement of the IkappaB kinase (IKK)-related kinases tank-binding kinase 1/IKKi and cullin-based ubiquitin ligases in IFN regulatory factor-3 degradation. *J Immunol* **177**(8), pp. 5059-5067.

Bican, P., Cohen, J., Charpilienne, A. and Scherrer, R. (1982). Purification and characterization of bovine rotavirus cores. *J Virol* **43**(3), pp. 1113-1117.

Biron, C.A., Nguyen, K.B. and Pien, G.C. (2002). Innate immune responses to LCMV infections: natural killer cells and cytokines. *Curr Top Microbiol Immunol* **263**pp. 7-27.

Bishop, R. (2009). Discovery of rotavirus: Implications for child health. *J Gastroenterol Hepatol* **24 Suppl 3**pp. S81-85.

Bishop, R.F., Davidson, G.P., Holmes, I.H. and Ruck, B.J. (1973). Virus particles in epithelial cells of duodenal mucosa from children with acute non-bacterial gastroenteritis. *Lancet* **2**(7841), pp. 1281-1283.

Bishop, R.F., Davidson, G.P., Holmes, I.H. and Ruck, B.J. (1974). Detection of a new virus by electron microscopy of faecal extracts from children with acute gastroenteritis. *Lancet* **1**(7849), pp. 149-151.

Blutt, S.E., Fenaux, M., Warfield, K.L., Greenberg, H.B. and Conner, M.E. (2006). Active viremia in rotavirus-infected mice. *J Virol* **80**(13), pp. 6702-6705.

Both, G.W., Siegman, L.J., Bellamy, A.R. and Atkinson, P.H. (1983). Coding assignment and nucleotide sequence of simian rotavirus SA11 gene segment 10: location of glycosylation sites suggests that the signal peptide is not cleaved. *J Virol* **48**(2), pp. 335-339.

Boutell, C., Sadis, S. and Everett, R.D. (2002). Herpes simplex virus type 1 immediate-early protein ICP0 and is isolated RING finger domain act as ubiquitin E3 ligases in vitro. *J Virol* **76**(2), pp. 841-850.

Boyle, J.F. and Holmes, K.V. (1986). RNA-binding proteins of bovine rotavirus. *J Virol* **58**(2), pp. 561-568.

Bremont, M., Chabanne-Vautherot, D. and Cohen, J. (1993). Sequence analysis of three non structural proteins of a porcine group C (Cowden strain) rotavirus. *Arch Virol* **130**(1-2), pp. 85-92.

Bremont, M., Charpilienne, A., Chabanne, D. and Cohen, J. (1987). Nucleotide sequence and expression in Escherichia coli of the gene encoding the

nonstructural protein NCVP2 of bovine rotavirus. *Virology* **161**(1), pp. 138-144.

Brikos, C. and O'Neill, L.A. (2008). Signalling of toll-like receptors. *Handb Exp Pharmacol*(183), pp. 21-50.

Broome, R.L., Vo, P.T., Ward, R.L., Clark, H.F. and Greenberg, H.B. (1993). Murine rotavirus genes encoding outer capsid proteins VP4 and VP7 are not major determinants of host range restriction and virulence. *J Virol* **67**(5), pp. 2448-2455.

Brottier, P., Nandi, P., Bremont, M. and Cohen, J. (1992). Bovine rotavirus segment 5 protein expressed in the baculovirus system interacts with zinc and RNA. *J Gen Virol* **73 (Pt 8)**pp. 1931-1938.

Buchman, A.R. and Berg, P. (1988). Comparison of intron-dependent and intron-independent gene expression. *Mol Cell Biol* **8**(10), pp. 4395-4405.

Burke, B. and Desselberger, U. (1996). Rotavirus pathogenicity. *Virology* **218**(2), pp. 299-305.

Callis, J., Fromm, M. and Walbot, V. (1987). Expression of mRNA electroporated into plant and animal cells. *Nucleic Acids Res* **15**(14), pp. 5823-5831.

Campagna, M., Eichwald, C., Vascotto, F. and Burrone, O.R. (2005). RNA interference of rotavirus segment 11 mRNA reveals the essential role of NSP5 in the virus replicative cycle. *J Gen Virol* **86**(Pt 5), pp. 1481-1487.

Chan, W.K., Au, K.S. and Estes, M.K. (1988). Topography of the simian rotavirus nonstructural glycoprotein (NS28) in the endoplasmic reticulum membrane. *Virology* **164**(2), pp. 435-442.

Chemello, M.E., Aristimuño, O.C., Michelangeli, F. and Ruiz, M.C. (2002). Requirement for vacuolar H+ -ATPase activity and Ca2+ gradient during entry of rotavirus into MA104 cells. *J Virol* **76**(24), pp. 13083-13087.

Chen, C.M., Hung, T., Bridger, J.C. and McCrae, M.A. (1985). Chinese adult rotavirus is a group B rotavirus. *Lancet* **2**(8464), pp. 1123-1124.

Chen, L.F., Williams, S.A., Mu, Y., Nakano, H., Duerr, J.M., Buckbinder, L. and Greene, W.C. (2005). NF-kappaB RelA phosphorylation regulates RelA acetylation. *Mol Cell Biol* **25**(18), pp. 7966-7975.

Chwetzoff, S. and Trugnan, G. (2006). Rotavirus assembly: an alternative model that utilizes an atypical trafficking pathway. *Curr Top Microbiol Immunol* **309**pp. 245-261.

Ciarlet, M. and Estes, M.K. (2001). Interactions between rotavirus and gastrointestinal cells. *Curr Opin Microbiol* **4**(4), pp. 435-441.

Cohen, J. and Dobos, P. (1979). Cell free transcription and translation of rotavirus RNA. *Biochem Biophys Res Commun* **88**(3), pp. 791-796.

Contin, R., Arnoldi, F., Campagna, M. and Burrone, O.R. (2010). Rotavirus NSP5 orchestrates recruitment of viroplasmic proteins. *J Gen Virol* **91**(Pt 7), pp. 1782-1793.

Cook, J.L., Walker, T.A., Worthen, G.S. and Radke, J.R. (2002). Role of the E1A Rb-binding domain in repression of the NF-kappa B-dependent defense against tumor necrosis factor-alpha. *Proc Natl Acad Sci U S A* **99**(15), pp. 9966-9971.

Crawford, S.E., Patel, D.G., Cheng, E., Berkova, Z., Hyser, J.M., Ciarlet, M., Finegold, M.J., Conner, M.E. and Estes, M.K. (2006). Rotavirus viremia and extraintestinal viral infection in the neonatal rat model. *J Virol* **80**(10), pp. 4820-4832.

Cuadras, M.A., Arias, C.F. and López, S. (1997). Rotaviruses induce an early membrane permeabilization of MA104 cells and do not require a low intracellular Ca2+ concentration to initiate their replication cycle. *J Virol* **71**(12), pp. 9065-9074.

Deng, X.X., Lü, L., Ou, Y.J., Su, H.J., Li, G., Guo, Z.X., Zhang, R., Zheng, P.R., Chen, Y.G., He, J.G. and Weng, S.P. (2012). Sequence analysis of 12 genome segments of mud crab reovirus (MCRV). *Virology* **422**(2), pp. 185-194.

Der, S.D., Zhou, A., Williams, B.R. and Silverman, R.H. (1998). Identification of genes differentially regulated by interferon alpha, beta, or gamma using oligonucleotide arrays. *Proc Natl Acad Sci U S A* **95**(26), pp. 15623-15628.

Desselberger, U. (1996). Genome rearrangements of rotaviruses. *Adv Virus Res* **46**pp. 69-95.

DiDonato, J.A., Hayakawa, M., Rothwarf, D.M., Zandi, E. and Karin, M. (1997). A cytokine-responsive IkappaB kinase that activates the transcription factor NF-kappaB. *Nature* **388**(6642), pp. 548-554.

Diebold, S.S., Kaisho, T., Hemmi, H., Akira, S. and Reis e Sousa, C. (2004). Innate antiviral responses by means of TLR7-mediated recognition of single-stranded RNA. *Science* **303**(5663), pp. 1529-1531.

Dodd, R.B., Allen, M.D., Brown, S.E., Sanderson, C.M., Duncan, L.M., Lehner, P.J., Bycroft, M. and Read, R.J. (2004). Solution structure of the Kaposi's

sarcoma-associated herpesvirus K3 N-terminal domain reveals a Novel E2-binding C4HC3-type RING domain. *J Biol Chem* **279**(51), pp. 53840-53847.

Du, W. and Maniatis, T. (1992). An ATF/CREB binding site is required for virus induction of the human interferon beta gene [corrected]. *Proc Natl Acad Sci U S A* **89**(6), pp. 2150-2154.

Eisenächer, K. and Krug, A. (2012). Regulation of RLR-mediated innate immune signaling--it is all about keeping the balance. *Eur J Cell Biol* **91**(1), pp. 36-47.

Ericson, B.L., Graham, D.Y., Mason, B.B. and Estes, M.K. (1982). Identification, synthesis, and modifications of simian rotavirus SA11 polypeptides in infected cells. *J Virol* **42**(3), pp. 825-839.

Escalante, C.R., Yie, J., Thanos, D. and Aggarwal, A.K. (1998). Structure of IRF-1 with bound DNA reveals determinants of interferon regulation. *Nature* **391**(6662), pp. 103-106.

Estes, M.K., Crawford, S.E., Penaranda, M.E., Petrie, B.L., Burns, J.W., Chan, W.K., Ericson, B., Smith, G.E. and Summers, M.D. (1987). Synthesis and immunogenicity of the rotavirus major capsid antigen using a baculovirus expression system. *J Virol* **61**(5), pp. 1488-1494.

Estes, M.K., Kang, G., Zeng, C.Q., Crawford, S.E. and Ciarlet, M. (2001). Pathogenesis of rotavirus gastroenteritis. *Novartis Found Symp* **238**pp. 82-96; discussion 96-100.

Estes, M.K. and Kapikian, A.Z. (2007): Rotaviruses. D.M.Knipe: *Fields Virology*, pp. 1917-1974. Philadelphia: Lippincott Williams & Wilkins.

Estes, M.K., Palmer, E.L. and Obijeski, J.F. (1983). Rotaviruses: a review. *Curr Top Microbiol Immunol* **105**pp. 123-184.

Fabbretti, E., Afrikanova, I., Vascotto, F. and Burrone, O.R. (1999). Two non-structural rotavirus proteins, NSP2 and NSP5, form viroplasm-like structures in vivo. *J Gen Virol* **80 (Pt 2)**pp. 333-339.

Feng, N., Sen, A., Nguyen, H., Vo, P., Hoshino, Y., Deal, E.M. and Greenberg, H.B. (2009). Variation in antagonism of the interferon response to rotavirus NSP1 results in differential infectivity in mouse embryonic fibroblasts. *J Virol* **83**(14), pp. 6987-6994.

Fleming, F.E., Graham, K.L., Taniguchi, K., Takada, Y. and Coulson, B.S. (2007). Rotavirus-neutralizing antibodies inhibit virus binding to integrins alpha 2 beta 1 and alpha 4 beta 1. *Arch Virol* **152**(6), pp. 1087-1101.

Flewett, T.H., Bryden, A.S. and Davies, H. (1973). Letter: Virus particles in gastroenteritis. *Lancet* **2**(7844), pp. 1497.

Flewett, T.H., Bryden, A.S. and Davies, H. (1974). Proceedings: Electron microscopy of faeces in acute gastroenteritis. *J Clin Pathol* **27**(6), pp. 512.

Freemont, P.S., Hanson, I.M. and Trowsdale, J. (1991). A novel cysteine-rich sequence motif. *Cell* **64**(3), pp. 483-484.

Fujii, Y., Shimizu, T., Kusumoto, M., Kyogoku, Y., Taniguchi, T. and Hakoshima, T. (1999). Crystal structure of an IRF-DNA complex reveals novel DNA recognition and cooperative binding to a tandem repeat of core sequences. *EMBO J* **18**(18), pp. 5028-5041.

Fukuhara, N., Yoshie, O., Kitaoka, S. and Konno, T. (1988). Role of VP3 in human rotavirus internalization after target cell attachment via VP7. *J Virol* **62**(7), pp. 2209-2218.

Gallegos, C.O. and Patton, J.T. (1989). Characterization of rotavirus replication intermediates: a model for the assembly of single-shelled particles. *Virology* **172**(2), pp. 616-627.

Gardet, A., Breton, M., Trugnan, G. and Chwetzoff, S. (2007). Role for actin in the polarized release of rotavirus. *J Virol* **81**(9), pp. 4892-4894.

Gay, N.J. and Gangloff, M. (2008). Structure of toll-like receptors. *Handb Exp Pharmacol*(183), pp. 181-200.

Geijtenbeek, T.B., den Dunnen, J. and Gringhuis, S.I. (2009a). Pathogen recognition by DC-SIGN shapes adaptive immunity. *Future Microbiol* **4**(7), pp. 879-890.

González, S.A. and Affranchino, J.L. (1995). Assembly of double-layered virus-like particles in mammalian cells by coexpression of human rotavirus VP2 and VP6. *J Gen Virol* **76 (Pt 9)**pp. 2357-2360.

González, S.A. and Burrone, O.R. (1989). Porcine OSU rotavirus segment II sequence shows common features with the viral gene of human origin. *Nucleic Acids Res* **17**(15), pp. 6402.

Gorziglia, M., Larralde, G., Kapikian, A.Z. and Chanock, R.M. (1990). Antigenic relationships among human rotaviruses as determined by outer capsid protein VP4. *Proc Natl Acad Sci U S A* **87**(18), pp. 7155-7159.

Gorziglia, M., Nishikawa, K. and Fukuhara, N. (1989). Evidence of duplication and deletion in super short segment 11 of rabbit rotavirus Alabama strain. *Virology* **170**(2), pp. 587-590.

Graff, J., Ewen, J., Ettayebi, K. and Hardy, M. (2007). Zinc-binding domain of rotavirus NSP1 is required for proteasome-dependent degradation of IRF3 and autoregulatory NSP1 stability. *J Gen Virol* **88**(Pt 2), pp. 613-620.

Graff, J., Mitzel, D., Weisend, C., Flenniken, M. and Hardy, M. (2002). Interferon regulatory factor 3 is a cellular partner of rotavirus NSP1. *J Virol* **76**(18), pp. 9545-9550.

Graff, J.W., Ettayebi, K. and Hardy, M.E. (2009). Rotavirus NSP1 inhibits NFkappaB activation by inducing proteasome-dependent degradation of beta-TrCP: a novel mechanism of IFN antagonism. *PLoS Pathog* **5**(1), pp. e1000280.

Graham, K.L., Fleming, F.E., Halasz, P., Hewish, M.J., Nagesha, H.S., Holmes, I.H., Takada, Y. and Coulson, B.S. (2005). Rotaviruses interact with alpha4beta7 and alpha4beta1 integrins by binding the same integrin domains as natural ligands. *J Gen Virol* **86**(Pt 12), pp. 3397-3408.

Graham, K.L., Halasz, P., Tan, Y., Hewish, M.J., Takada, Y., Mackow, E.R., Robinson, M.K. and Coulson, B.S. (2003). Integrin-using rotaviruses bind alpha2beta1 integrin alpha2 I domain via VP4 DGE sequence and recognize alphaXbeta2 and alphaVbeta3 by using VP7 during cell entry. *J Virol* **77**(18), pp. 9969-9978.

Greenberg, H.B., Valdesuso, J., van Wyke, K., Midthun, K., Walsh, M., McAuliffe, V., Wyatt, R.G., Kalica, A.R., Flores, J. and Hoshino, Y. (1983). Production and preliminary characterization of monoclonal antibodies directed at two surface proteins of rhesus rotavirus. *J Virol* **47**(2), pp. 267-275.

Gu, H. and Roizman, B. (2003). The degradation of promyelocytic leukemia and Sp100 proteins by herpes simplex virus 1 is mediated by the ubiquitin-conjugating enzyme UbcH5a. *Proc Natl Acad Sci U S A* **100**(15), pp. 8963-8968.

Gualtero, D.F., Guzmán, F., Acosta, O. and Guerrero, C.A. (2007). Amino acid domains 280-297 of VP6 and 531-554 of VP4 are implicated in heat shock cognate protein hsc70-mediated rotavirus infection. *Arch Virol* **152**(12), pp. 2183-2196.

Gutiérrez, M., Isa, P., Sánchez-San Martin, C., Pérez-Vargas, J., Espinosa, R., Arias, C.F. and López, S. (2010). Different rotavirus strains enter MA104 cells through different endocytic pathways: the role of clathrin-mediated endocytosis. *J Virol* **84**(18), pp. 9161-9169.

Hamer, D.H. and Leder, P. (1979). Splicing and the formation of stable RNA. *Cell* **18**(4), pp. 1299-1302.

Harb, M., Becker, M.M., Vitour, D., Baron, C.H., Vende, P., Brown, S.C., Bolte, S., Arold, S.T. and Poncet, D. (2008). Nuclear localization of cytoplasmic poly(A)-binding protein upon rotavirus infection involves the interaction of NSP3 with eIF4G and RoXaN. *J Virol* **82**(22), pp. 11283-11293.

Haselhorst, T., Fleming, F.E., Dyason, J.C., Hartnell, R.D., Yu, X., Holloway, G., Santegoets, K., Kiefel, M.J., Blanchard, H., Coulson, B.S. and von Itzstein, M. (2009). Sialic acid dependence in rotavirus host cell invasion. *Nat Chem Biol* **5**(2), pp. 91-93.

Hayden, M.S. and Ghosh, S. (2008). Shared principles in NF-kappaB signaling. *Cell* **132**(3), pp. 344-362.

Heil, F., Hemmi, H., Hochrein, H., Ampenberger, F., Kirschning, C., Akira, S., Lipford, G., Wagner, H. and Bauer, S. (2004). Species-specific recognition of single-stranded RNA via toll-like receptor 7 and 8. *Science* **303**(5663), pp. 1526-1529.

Helmberger-Jones, M. and Patton, J.T. (1986). Characterization of subviral particles in cells infected with simian rotavirus SA11. *Virology* **155**(2), pp. 655-665.

Hemmi, H., Takeuchi, O., Kawai, T., Kaisho, T., Sato, S., Sanjo, H., Matsumoto, M., Hoshino, K., Wagner, H., Takeda, K. and Akira, S. (2000). A Toll-like receptor recognizes bacterial DNA. *Nature* **408**(6813), pp. 740-745.

Hemmi, H., Takeuchi, O., Sato, S., Yamamoto, M., Kaisho, T., Sanjo, H., Kawai, T., Hoshino, K., Takeda, K. and Akira, S. (2004). The roles of two IkappaB kinase-related kinases in lipopolysaccharide and double stranded RNA signaling and viral infection. *J Exp Med* **199**(12), pp. 1641-1650.

Holloway, G., Truong, T.T. and Coulson, B.S. (2009). Rotavirus antagonizes cellular antiviral responses by inhibiting the nuclear accumulation of STAT1, STAT2, and NF-kappaB. *J Virol* **83**(10), pp. 4942-4951.

Honda, K. and Taniguchi, T. (2006a). IRFs: master regulators of signalling by Toll-like receptors and cytosolic pattern-recognition receptors. *Nat Rev Immunol* **6**(9), pp. 644-658.

Honda, K., Yanai, H., Takaoka, A. and Taniguchi, T. (2005). Regulation of the type I IFN induction: a current view. *Int Immunol* **17**(11), pp. 1367-1378.

Hornung, V., Barchet, W., Schlee, M. and Hartmann, G. (2008). RNA recognition via TLR7 and TLR8. *Handb Exp Pharmacol*(183), pp. 71-86.

Hornung, V., Guenthner-Biller, M., Bourquin, C., Ablasser, A., Schlee, M., Uematsu, S., Noronha, A., Manoharan, M., Akira, S., de Fougerolles, A., Endres, S. and Hartmann, G. (2005). Sequence-specific potent induction of IFN-alpha by short interfering RNA in plasmacytoid dendritic cells through TLR7. *Nat Med* **11**(3), pp. 263-270.

Hoshino, Y. and Kapikian, A.Z. (1996). Classification of rotavirus VP4 and VP7 serotypes. *Arch Virol Suppl* **12**pp. 99-111.

Hua, J., Mansell, E.A. and Patton, J.T. (1993). Comparative analysis of the rotavirus NS53 gene: conservation of basic and cysteine-rich regions in the protein and possible stem-loop structures in the RNA. *Virology* **196**(1), pp. 372-378.

Hua, J. and Patton, J. (1994a). The carboxyl-half of the rotavirus nonstructural protein NS53 (NSP1) is not required for virus replication. *Virology* **198**(2), pp. 567-576.

Hua, J., Chen, X. and Patton, J.T. (1994b). Deletion mapping of the rotavirus metalloprotein NS53 (NSP1): the conserved cysteine-rich region is essential for virus-specific RNA binding. *J Virol* **68**(6), pp. 3990-4000.

Huang, M.T. and Gorman, C.M. (1990). Intervening sequences increase efficiency of RNA 3' processing and accumulation of cytoplasmic RNA. *Nucleic Acids Res* **18**(4), pp. 937-947.

Hung, T., Chen, G.M., Wang, C.G., Chou, Z.Y., Chao, T.X., Ye, W.W., Yao, H.L. and Meng, K.H. (1983). Rotavirus-like agent in adult non-bacterial diarrhoea in China. *Lancet* **2**(8358), pp. 1078-1079.

Häcker, H. and Karin, M. (2006). Regulation and function of IKK and IKK-related kinases. *Sci STKE* **2006**(357), pp. re13.

Imai, M., Akatani, K., Ikegami, N. and Furuichi, Y. (1983). Capped and conserved terminal structures in human rotavirus genome double-stranded RNA segments. *J Virol* **47**(1), pp. 125-136.

Izaguirre, A., Barnes, B.J., Amrute, S., Yeow, W.S., Megjugorac, N., Dai, J., Feng, D., Chung, E., Pitha, P.M. and Fitzgerald-Bocarsly, P. (2003). Comparative analysis of IRF and IFN-alpha expression in human plasmacytoid and monocyte-derived dendritic cells. *J Leukoc Biol* **74**(6), pp. 1125-1138.

Jackson, P.K., Eldridge, A.G., Freed, E., Furstenthal, L., Hsu, J.Y., Kaiser, B.K. and Reimann, J.D. (2000). The lore of the RINGs: substrate recognition and catalysis by ubiquitin ligases. *Trends Cell Biol* **10**(10), pp. 429-439.

Janaswami, P.M., Kalvakolanu, D.V., Zhang, Y. and Sen, G.C. (1992). Transcriptional repression of interleukin-6 gene by adenoviral E1A proteins. *J Biol Chem* **267**(34), pp. 24886-24891.

Janeway, C.A. (1989). Approaching the asymptote? Evolution and revolution in immunology. *Cold Spring Harb Symp Quant Biol* **54 Pt 1**pp. 1-13.

Joazeiro, C.A. and Weissman, A.M. (2000). RING finger proteins: mediators of ubiquitin ligase activity. *Cell* **102**(5), pp. 549-552.

Johnson, M.A. and McCrae, M.A. (1989). Molecular biology of rotaviruses. VIII. Quantitative analysis of regulation of gene expression during virus replication. *J Virol* **63**(5), pp. 2048-2055.

Jourdan, N., Maurice, M., Delautier, D., Quero, A.M., Servin, A.L. and Trugnan, G. (1997). Rotavirus is released from the apical surface of cultured human intestinal cells through nonconventional vesicular transport that bypasses the Golgi apparatus. *J Virol* **71**(11), pp. 8268-8278.

Kaljot, K.T., Shaw, R.D., Rubin, D.H. and Greenberg, H.B. (1988). Infectious rotavirus enters cells by direct cell membrane penetration, not by endocytosis. *J Virol* **62**(4), pp. 1136-1144.

Kantharidis, P., Dyall-Smith, M.L. and Holmes, I.H. (1983). Completion of the gene coding assignments of SA11 rotavirus: gene products of segments 7, 8, and 9. *J Virol* **48**(1), pp. 330-334.

Kapikian, A.Z., Wyatt, R.G., Dolin, R., Thornhill, T.S., Kalica, A.R. and Chanock, R.M. (1972). Visualization by immune electron microscopy of a 27-nm particle associated with acute infectious nonbacterial gastroenteritis. *J Virol* **10**(5), pp. 1075-1081.

Kattoura, M.D., Chen, X. and Patton, J.T. (1994). The rotavirus RNA-binding protein NS35 (NSP2) forms 10S multimers and interacts with the viral RNA polymerase. *Virology* **202**(2), pp. 803-813.

Kawai, T. and Akira, S. (2006a). Innate immune recognition of viral infection. *Nat Immunol* **7**(2), pp. 131-137.

Kim, H.J., Park, J.G., Matthijnssens, J., Lee, J.H., Bae, Y.C., Alfajaro, M.M., Park, S.I., Kang, M.I. and Cho, K.O. (2011). Intestinal and extra-intestinal pathogenicity of a bovine reassortant rotavirus in calves and piglets. *Vet Microbiol* **152**(3-4), pp. 291-303.

King, P. and Goodbourn, S. (1994). The beta-interferon promoter responds to priming through multiple independent regulatory elements. *J Biol Chem* **269**(48), pp. 30609-30615.

Kobayashi, N. and Nagashima, S. (2007). [Attention-getting cross infections: Viral enteritis]. *Nihon Naika Gakkai Zasshi* **96**(11), pp. 2476-2483.

Korolev, M.B., Khaustov, V.I. and Shekoian, L.A. (1981). [Morphogenesis of human rotavirus in a cell culture]. *Vopr Virusol*(3), pp. 309-315.

Kouvelos, K., Petric, M. and Middleton, P.J. (1984). Comparison of bovine, simian and human rotavirus structural glycoproteins. *J Gen Virol* **65 (Pt 7)**pp. 1211-1214.

Kray, A.E., Carter, R.S., Pennington, K.N., Gomez, R.J., Sanders, L.E., Llanes, J.M., Khan, W.N., Ballard, D.W. and Wadzinski, B.E. (2005). Positive regulation of IkappaB kinase signaling by protein serine/threonine phosphatase 2A. *J Biol Chem* **280**(43), pp. 35974-35982.

Kroll, M., Margottin, F., Kohl, A., Renard, P., Durand, H., Concordet, J.P., Bachelerie, F., Arenzana-Seisdedos, F. and Benarous, R. (1999). Inducible degradation of IkappaBalpha by the proteasome requires interaction with the F-box protein h-betaTrCP. *J Biol Chem* **274**(12), pp. 7941-7945.

Kumar, A., Charpilienne, A. and Cohen, J. (1989). Nucleotide sequence of the gene encoding for the RNA binding protein (VP2) of RF bovine rotavirus. *Nucleic Acids Res* **17**(5), pp. 2126.

Kumar, K.P., McBride, K.M., Weaver, B.K., Dingwall, C. and Reich, N.C. (2000). Regulated nuclear-cytoplasmic localization of interferon regulatory factor 3, a subunit of double-stranded RNA-activated factor 1. *Mol Cell Biol* **20**(11), pp. 4159-4168.

Labbé, M., Baudoux, P., Charpilienne, A., Poncet, D. and Cohen, J. (1994). Identification of the nucleic acid binding domain of the rotavirus VP2 protein. *J Gen Virol* **75 (Pt 12)**pp. 3423-3430.

Labbé, M., Charpilienne, A., Crawford, S.E., Estes, M.K. and Cohen, J. (1991). Expression of rotavirus VP2 produces empty corelike particles. *J Virol* **65**(6), pp. 2946-2952.

Lane, D.P. and Crawford, L.V. (1979). T antigen is bound to a host protein in SV40-transformed cells. *Nature* **278**(5701), pp. 261-263.

Lawton, J.A., Estes, M.K. and Prasad, B.V. (2001). Identification and characterization of a transcription pause site in rotavirus. *J Virol* **75**(4), pp. 1632-1642.

Lawton, J.A., Zeng, C.Q., Mukherjee, S.K., Cohen, J., Estes, M.K. and Prasad, B.V. (1997). Three-dimensional structural analysis of recombinant rotavirus-like particles with intact and amino-terminal-deleted VP2: implications for the architecture of the VP2 capsid layer. *J Virol* **71**(10), pp. 7353-7360.

Lemaitre, B., Nicolas, E., Michaut, L., Reichhart, J.M. and Hoffmann, J.A. (1996). The dorsoventral regulatory gene cassette spätzle/Toll/cactus controls the potent antifungal response in Drosophila adults. *Cell* **86**(6), pp. 973-983.

Li, Z., Baker, M.L., Jiang, W., Estes, M.K. and Prasad, B.V. (2009). Rotavirus architecture at subnanometer resolution. *J Virol* **83**(4), pp. 1754-1766.

Lilley, C.E., Chaurushiya, M.S., Boutell, C., Landry, S., Suh, J., Panier, S., Everett, R.D., Stewart, G.S., Durocher, D. and Weitzman, M.D. (2010). A viral E3 ligase targets RNF8 and RNF168 to control histone ubiquitination and DNA damage responses. *EMBO J* **29**(5), pp. 943-955.

Lin, R., Heylbroeck, C., Pitha, P. and Hiscott, J. (1998). Virus-dependent phosphorylation of the IRF-3 transcription factor regulates nuclear translocation, transactivation potential, and proteasome-mediated degradation. *Mol Cell Biol* **18**(5), pp. 2986-2996.

Liu, M., Mattion, N.M. and Estes, M.K. (1992). Rotavirus VP3 expressed in insect cells possesses guanylyltransferase activity. *Virology* **188**(1), pp. 77-84.

Liu, M., Offit, P.A. and Estes, M.K. (1988). Identification of the simian rotavirus SA11 genome segment 3 product. *Virology* **163**(1), pp. 26-32.

Lopman, B.A., Payne, D.C., Tate, J.E., Patel, M.M., Cortese, M.M. and Parashar, U.D. (2012). Post-licensure experience with rotavirus vaccination in high and middle income countries; 2006 to 2011. *Curr Opin Virol*pp.

Ludert, J.E., Michelangeli, F., Gil, F., Liprandi, F. and Esparza, J. (1987). Penetration and uncoating of rotaviruses in cultured cells. *Intervirology* **27**(2), pp. 95-101.

Lundgren, O., Peregrin, A.T., Persson, K., Kordasti, S., Uhnoo, I. and Svensson, L. (2000). Role of the enteric nervous system in the fluid and electrolyte secretion of rotavirus diarrhea. *Science* **287**(5452), pp. 491-495.

Luo, Y., Batalao, A., Zhou, H. and Zhu, L. (1997). Mammalian two-hybrid system: a complementary approach to the yeast two-hybrid system. *Biotechniques* **22**(2), pp. 350-352.

López, S. and Arias, C.F. (2006). Early steps in rotavirus cell entry. *Curr Top Microbiol Immunol* **309**pp. 39-66.

López, T., Camacho, M., Zayas, M., Nájera, R., Sánchez, R., Arias, C.F. and López, S. (2005). Silencing the morphogenesis of rotavirus. *J Virol* **79**(1), pp. 184-192.

López, T., Silva-Ayala, D., López, S. and Arias, C.F. (2011). Replication of the rotavirus genome requires an active ubiquitin-proteasome system. *J Virol* **85**(22), pp. 11964-11971.

Malherbe, H.H. and Strickland-Cholmley, M. (1967). Simian virus SA11 and the related O agent. *Arch Gesamte Virusforsch* **22**(1), pp. 235-245.

Mankouri, J., Fragkoudis, R., Richards, K.H., Wetherill, L.F., Harris, M., Kohl, A., Elliott, R.M. and Macdonald, A. (2010). Optineurin negatively regulates the induction of IFNbeta in response to RNA virus infection. *PLoS Pathog* **6**(2), pp. e1000778.

Mansell, E.A. and Patton, J.T. (1990). Rotavirus RNA replication: VP2, but not VP6, is necessary for viral replicase activity. *J Virol* **64**(10), pp. 4988-4996.

Martella, V., Bányai, K., Matthijnssens, J., Buonavoglia, C. and Ciarlet, M. (2010). Zoonotic aspects of rotaviruses. *Vet Microbiol* **140**(3-4), pp. 246-255.

Mason, B.B., Graham, D.Y. and Estes, M.K. (1983). Biochemical mapping of the simian rotavirus SA11 genome. *J Virol* **46**(2), pp. 413-423.

Mattion, N.M., Cohen, J., Aponte, C. and Estes, M.K. (1992). Characterization of an oligomerization domain and RNA-binding properties on rotavirus nonstructural protein NS34. *Virology* **190**(1), pp. 68-83.

Mattion, N.M., Mitchell, D.B., Both, G.W. and Estes, M.K. (1991). Expression of rotavirus proteins encoded by alternative open reading frames of genome segment 11. *Virology* **181**(1), pp. 295-304.

Mattion, N.M., Reilly, P.A., DiMichele, S.J., Crowley, J.C. and Weeks-Levy, C. (1994). Attenuated poliovirus strain as a live vector: expression of regions of rotavirus outer capsid protein VP7 by using recombinant Sabin 3 viruses. *J Virol* **68**(6), pp. 3925-3933.

McCrae, M.A. and Faulkner-Valle, G.P. (1981). Molecular biology of rotaviruses. I. Characterization of basic growth parameters and pattern of macromolecular synthesis. *J Virol* **39**(2), pp. 490-496.

McCrae, M.A. and McCorquodale, J.G. (1983). Molecular biology of rotaviruses. V. Terminal structure of viral RNA species. *Virology* **126**(1), pp. 204-212.

Mebus, C.A., Kono, M., Underdahl, N.R. and Twiehaus, M.J. (1971). Cell culture propagation of neonatal calf diarrhea (scours) virus. *Can Vet J* **12**(3), pp. 69-72.

Mercurio, F., Zhu, H., Murray, B.W., Shevchenko, A., Bennett, B.L., Li, J., Young, D.B., Barbosa, M., Mann, M., Manning, A. and Rao, A. (1997). IKK-1 and IKK-2: cytokine-activated IkappaB kinases essential for NF-kappaB activation. *Science* **278**(5339), pp. 860-866.

Messing, J., Gronenborn, B., Müller-Hill, B. and Hans Hopschneider, P. (1977). Filamentous coliphage M13 as a cloning vehicle: insertion of a HindII fragment of the lac regulatory region in M13 replicative form in vitro. *Proc Natl Acad Sci U S A* **74**(9), pp. 3642-3646.

Meyer, J.C., Bergmann, C.C. and Bellamy, A.R. (1989). Interaction of rotavirus cores with the nonstructural glycoprotein NS28. *Virology* **171**(1), pp. 98-107.

Meylan, E., Curran, J., Hofmann, K., Moradpour, D., Binder, M., Bartenschlager, R. and Tschopp, J. (2005). Cardif is an adaptor protein in the RIG-I antiviral pathway and is targeted by hepatitis C virus. *Nature* **437**(7062), pp. 1167-1172.

Mitchell, D.B. and Both, G.W. (1990). Completion of the genomic sequence of the simian rotavirus SA11: nucleotide sequences of segments 1, 2, and 3. *Virology* **177**(1), pp. 324-331.

Monto, A.S., Koopman, J.S., Longini, I.M. and Isaacson, R.E. (1983). The Tecumseh study. XII. Enteric agents in the community, 1976-1981. *J Infect Dis* **148**(2), pp. 284-291.

Musalem, C. and Espejo, R.T. (1985). Release of progeny virus from cells infected with simian rotavirus SA11. *J Gen Virol* **66 (Pt 12)**pp. 2715-2724.

Nerenberg, B.T., Taylor, J., Bartee, E., Gouveia, K., Barry, M. and Früh, K. (2005). The poxviral RING protein p28 is a ubiquitin ligase that targets ubiquitin to viral replication factories. *J Virol* **79**(1), pp. 597-601.

Offit, P.A., Blavat, G., Greenberg, H.B. and Clark, H.F. (1986). Molecular basis of rotavirus virulence: role of gene segment 4. *J Virol* **57**(1), pp. 46-49.

Palkowitsch, L., Leidner, J., Ghosh, S. and Marienfeld, R.B. (2008). Phosphorylation of serine 68 in the IkappaB kinase (IKK)-binding domain of NEMO interferes with the structure of the IKK complex and tumor necrosis factor-alpha-induced NF-kappaB activity. *J Biol Chem* **283**(1), pp. 76-86.

Pampin, M., Simonin, Y., Blondel, B., Percherancier, Y. and Chelbi-Alix, M.K. (2006). Cross talk between PML and p53 during poliovirus infection: implications for antiviral defense. *J Virol* **80**(17), pp. 8582-8592.

Panne, D., Maniatis, T. and Harrison, S.C. (2004). Crystal structure of ATF-2/c-Jun and IRF-3 bound to the interferon-beta enhancer. *EMBO J* **23**(22), pp. 4384-4393.

Parashar, U.D. and Glass, R.I. (2006). Public health. Progress toward rotavirus vaccines. *Science* **312**(5775), pp. 851-852.

Parashar, U.D., Hummelman, E.G., Bresee, J.S., Miller, M.A. and Glass, R.I. (2003). Global illness and deaths caused by rotavirus disease in children. *Emerg Infect Dis* **9**(5), pp. 565-572.

Patton, J.T. (1986). Synthesis of simian rotavirus SA11 double-stranded RNA in a cell-free system. *Virus Res* **6**(3), pp. 217-233.

Patton, J.T. (1996). Rotavirus VP1 alone specifically binds to the 3' end of viral mRNA, but the interaction is not sufficient to initiate minus-strand synthesis. *J Virol* **70**(11), pp. 7940-7947.

Patton, J.T. and Chen, D. (1999). RNA-binding and capping activities of proteins in rotavirus open cores. *J Virol* **73**(2), pp. 1382-1391.

Patton, J.T., Silvestri, L.S., Tortorici, M.A., Vasquez-Del Carpio, R. and Taraporewala, Z.F. (2006). Rotavirus genome replication and morphogenesis: role of the viroplasm. *Curr Top Microbiol Immunol* **309**pp. 169-187.

Pedley, S., Bridger, J.C., Chasey, D. and McCrae, M.A. (1986). Definition of two new groups of atypical rotaviruses. *J Gen Virol* **67 (Pt 1)**pp. 131-137.

Pennella, M.A., Liu, Y., Woo, J.L., Kim, C.A. and Berk, A.J. (2010). Adenovirus E1B 55-kilodalton protein is a p53-SUMO1 E3 ligase that represses p53 and stimulates its nuclear export through interactions with promyelocytic leukemia nuclear bodies. *J Virol* **84**(23), pp. 12210-12225.

Petrie, B.L., Graham, D.Y., Hanssen, H. and Estes, M.K. (1982). Localization of rotavirus antigens in infected cells by ultrastructural immunocytochemistry. *J Gen Virol* **63**(2), pp. 457-467.

Petrie, B.L., Greenberg, H.B., Graham, D.Y. and Estes, M.K. (1984). Ultrastructural localization of rotavirus antigens using colloidal gold. *Virus Res* **1**(2), pp. 133-152.

Pickart, C.M. (2001). Mechanisms underlying ubiquitination. *Annu Rev Biochem* **70**pp. 503-533.

Pippig, D.A., Hellmuth, J.C., Cui, S., Kirchhofer, A., Lammens, K., Lammens, A., Schmidt, A., Rothenfusser, S. and Hopfner, K.P. (2009). The regulatory domain of the RIG-I family ATPase LGP2 senses double-stranded RNA. *Nucleic Acids Res* **37**(6), pp. 2014-2025.

Piron, M., Vende, P., Cohen, J. and Poncet, D. (1998). Rotavirus RNA-binding protein NSP3 interacts with eIF4GI and evicts the poly(A) binding protein from eIF4F. *EMBO J* **17**(19), pp. 5811-5821.

Pizarro, J.L., Sandino, A.M., Pizarro, J.M., Fernández, J. and Spencer, E. (1991). Characterization of rotavirus guanylyltransferase activity associated with polypeptide VP3. *J Gen Virol* **72 (Pt 2)**pp. 325-332.

Piña-Vázquez, C., De Nova-Ocampo, M., Guzmán-León, S. and Padilla-Noriega, L. (2007). Post-translational regulation of rotavirus protein NSP1 expression in mammalian cells. *Arch Virol* **152**(2), pp. 345-368.

Poncet, D., Aponte, C. and Cohen, J. (1993). Rotavirus protein NSP3 (NS34) is bound to the 3' end consensus sequence of viral mRNAs in infected cells. *J Virol* **67**(6), pp. 3159-3165.

Poncet, D., Lindenbaum, P., L'Haridon, R. and Cohen, J. (1997). In vivo and in vitro phosphorylation of rotavirus NSP5 correlates with its localization in viroplasms. *J Virol* **71**(1), pp. 34-41.

Poruchynsky, M.S., Maass, D.R. and Atkinson, P.H. (1991). Calcium depletion blocks the maturation of rotavirus by altering the oligomerization of virus-encoded proteins in the ER. *J Cell Biol* **114**(4), pp. 651-656.

Prasad, B.V., Burns, J.W., Marietta, E., Estes, M.K. and Chiu, W. (1990). Localization of VP4 neutralization sites in rotavirus by three-dimensional cryo-electron microscopy. *Nature* **343**(6257), pp. 476-479.

Preiss, T. and Hentze, M.W. (1998). Dual function of the messenger RNA cap structure in poly(A)-tail-promoted translation in yeast. *Nature* **392**(6675), pp. 516-520.

Pétrilli, V., Dostert, C., Muruve, D.A. and Tschopp, J. (2007a). The inflammasome: a danger sensing complex triggering innate immunity. *Curr Opin Immunol* **19**(6), pp. 615-622.

Qin, L., Ren, L., Zhou, Z., Lei, X., Chen, L., Xue, Q., Liu, X., Wang, J. and Hung, T. (2011). Rotavirus nonstructural protein 1 antagonizes innate immune response by interacting with retinoic acid inducible gene I. *Virol J* **8**pp. 526.

Qing, J., Liu, C., Choy, L., Wu, R.Y., Pagano, J.S. and Derynck, R. (2004). Transforming growth factor beta/Smad3 signaling regulates IRF-7 function and transcriptional activation of the beta interferon promoter. *Mol Cell Biol* **24**(3), pp. 1411-1425.

Rainsford, E.W. and McCrae, M.A. (2007). Characterization of the NSP6 protein product of rotavirus gene 11. *Virus Res* **130**(1-2), pp. 193-201.

Ramig, R.F. (2004). Pathogenesis of intestinal and systemic rotavirus infection. *J Virol* **78**(19), pp. 10213-10220.

Randall, R.E. and Goodbourn, S. (2008). Interferons and viruses: an interplay between induction, signalling, antiviral responses and virus countermeasures. *J Gen Virol* **89**(Pt 1), pp. 1-47.

Rothenfusser, S., Goutagny, N., DiPerna, G., Gong, M., Monks, B.G., Schoenemeyer, A., Yamamoto, M., Akira, S. and Fitzgerald, K.A. (2005). The RNA helicase Lgp2 inhibits TLR-independent sensing of viral replication by retinoic acid-inducible gene-I. *J Immunol* **175**(8), pp. 5260-5268.

Sabara, M., Gilchrist, J.E., Hudson, G.R. and Babiuk, L.A. (1985). Preliminary characterization of an epitope involved in neutralization and cell attachment that is located on the major bovine rotavirus glycoprotein. *J Virol* **53**(1), pp. 58-66.

Saif, L.J. and Jiang, B. (1994). Nongroup A rotaviruses of humans and animals. *Curr Top Microbiol Immunol* **185**pp. 339-371.

Saito, T., Hirai, R., Loo, Y.M., Owen, D., Johnson, C.L., Sinha, S.C., Akira, S., Fujita, T. and Gale, M. (2007). Regulation of innate antiviral defenses through a shared repressor domain in RIG-I and LGP2. *Proc Natl Acad Sci U S A* **104**(2), pp. 582-587.

Saitoh, T., Tun-Kyi, A., Ryo, A., Yamamoto, M., Finn, G., Fujita, T., Akira, S., Yamamoto, N., Lu, K.P. and Yamaoka, S. (2006). Negative regulation of interferon-regulatory factor 3-dependent innate antiviral response by the prolyl isomerase Pin1. *Nat Immunol* **7**(6), pp. 598-605.

Sandino, A.M., Fernandez, J., Pizarro, J., Vasquez, M. and Spencer, E. (1994). Structure of rotavirus particle: interaction of the inner capsid protein VP6 with the core polypeptide VP3. *Biol Res* **27**(1), pp. 39-48.

Sato, M., Tanaka, N., Hata, N., Oda, E. and Taniguchi, T. (1998). Involvement of the IRF family transcription factor IRF-3 in virus-induced activation of the IFN-beta gene. *FEBS Lett* **425**(1), pp. 112-116.

Sen, A., Feng, N., Ettayebi, K., Hardy, M.E. and Greenberg, H.B. (2009). IRF3 inhibition by rotavirus NSP1 is host cell and virus strain dependent but independent of NSP1 proteasomal degradation. *J Virol* **83**(20), pp. 10322-10335.

Servant, M.J., Grandvaux, N. and Hiscott, J. (2002a). Multiple signaling pathways leading to the activation of interferon regulatory factor 3. *Biochem Pharmacol* **64**(5-6), pp. 985-992.

Servant, M.J., Tenoever, B. and Lin, R. (2002b). Overlapping and distinct mechanisms regulating IRF-3 and IRF-7 function. *J Interferon Cytokine Res* **22**(1), pp. 49-58.

Seth, R.B., Sun, L. and Chen, Z.J. (2006). Antiviral innate immunity pathways. *Cell Res* **16**(2), pp. 141-147.

Shahrabadi, M.S., Babiuk, L.A. and Lee, P.W. (1987). Further analysis of the role of calcium in rotavirus morphogenesis. *Virology* **158**(1), pp. 103-111.

Shahrabadi, M.S. and Lee, P.W. (1986). Bovine rotavirus maturation is a calcium-dependent process. *Virology* **152**(2), pp. 298-307.

Shao, R., Tsai, E.M., Wei, K., von Lindern, R., Chen, Y.H., Makino, K. and Hung, M.C. (2001). E1A inhibition of radiation-induced NF-kappaB activity through suppression of IKK activity and IkappaB degradation, independent of Akt activation. *Cancer Res* **61**(20), pp. 7413-7416.

Sharma, S., tenOever, B.R., Grandvaux, N., Zhou, G.P., Lin, R. and Hiscott, J. (2003). Triggering the interferon antiviral response through an IKK-related pathway. *Science* **300**(5622), pp. 1148-1151.

Silvestri, L.S., Tortorici, M.A., Vasquez-Del Carpio, R. and Patton, J.T. (2005). Rotavirus glycoprotein NSP4 is a modulator of viral transcription in the infected cell. *J Virol* **79**(24), pp. 15165-15174.

Simonsen, L., Viboud, C., Elixhauser, A., Taylor, R.J. and Kapikian, A.Z. (2005). More on RotaShield and intussusception: the role of age at the time of vaccination. *J Infect Dis* **192 Suppl 1**pp. S36-43.

Spencer, E. and Arias, M.L. (1981). In vitro transcription catalyzed by heat-treated human rotavirus. *J Virol* **40**(1), pp. 1-10.

Stacy-Phipps, S. and Patton, J.T. (1987). Synthesis of plus- and minus-strand RNA in rotavirus-infected cells. *J Virol* **61**(11), pp. 3479-3484.

Stetson, D.B. and Medzhitov, R. (2006a). Antiviral defense: interferons and beyond. *J Exp Med* **203**(8), pp. 1837-1841.

Stirzaker, S.C., Whitfeld, P.L., Christie, D.L., Bellamy, A.R. and Both, G.W. (1987). Processing of rotavirus glycoprotein VP7: implications for the retention of the protein in the endoplasmic reticulum. *J Cell Biol* **105**(6 Pt 2), pp. 2897-2903.

Sánchez-San Martín, C., López, T., Arias, C.F. and López, S. (2004). Characterization of rotavirus cell entry. *J Virol* **78**(5), pp. 2310-2318.

Takaoka, A. and Yanai, H. (2005). [Class II cytokine receptors and their ligands]. *Nihon Rinsho* **63 Suppl 4**pp. 193-201.

Takeuchi, O. and Akira, S. (2007). Recognition of viruses by innate immunity. *Immunol Rev* **220**pp. 214-224.

Takeuchi, O. and Akira, S. (2009). Innate immunity to virus infection. *Immunol Rev* **227**(1), pp. 75-86.

Taniguchi, K., Kojima, K. and Urasawa, S. (1996). Nondefective rotavirus mutants with an NSP1 gene which has a deletion of 500 nucleotides, including a cysteine-rich zinc finger motif-encoding region (nucleotides 156 to 248), or which has a nonsense codon at nucleotides 153-155. *J Virol* **70**(6), pp. 4125-4130.

Taniguchi, K. and Komoto, S. (2012). Genetics and reverse genetics of rotavirus. *Curr Opin Virol* **2**(4), pp. 399-407.

Taniguchi, T., Ogasawara, K., Takaoka, A. and Tanaka, N. (2001). IRF family of transcription factors as regulators of host defense. *Annu Rev Immunol* **19**pp. 623-655.

Taniguchi, T. and Takaoka, A. (2002). The interferon-alpha/beta system in antiviral responses: a multimodal machinery of gene regulation by the IRF family of transcription factors. *Curr Opin Immunol* **14**(1), pp. 111-116.

Tanner, N.K. and Linder, P. (2001). DExD/H box RNA helicases: from generic motors to specific dissociation functions. *Mol Cell* **8**(2), pp. 251-262.

Taraporewala, Z., Chen, D. and Patton, J.T. (1999). Multimers formed by the rotavirus nonstructural protein NSP2 bind to RNA and have nucleoside triphosphatase activity. *J Virol* **73**(12), pp. 9934-9943.

Tergaonkar, V. (2006). NFkappaB pathway: a good signaling paradigm and therapeutic target. *Int J Biochem Cell Biol* **38**(10), pp. 1647-1653.

Tian, P., Estes, M.K., Hu, Y., Ball, J.M., Zeng, C.Q. and Schilling, W.P. (1995). The rotavirus nonstructural glycoprotein NSP4 mobilizes Ca2+ from the endoplasmic reticulum. *J Virol* **69**(9), pp. 5763-5772.

Ting, J.P. and Williams, K.L. (2005). The CATERPILLER family: an ancient family of immune/apoptotic proteins. *Clin Immunol* **115**(1), pp. 33-37.

Torres-Vega, M.A., González, R.A., Duarte, M., Poncet, D., López, S. and Arias, C.F. (2000). The C-terminal domain of rotavirus NSP5 is essential for its multimerization, hyperphosphorylation and interaction with NSP6. *J Gen Virol* **81**(Pt 3), pp. 821-830.

Trask, S.D., McDonald, S.M. and Patton, J.T. (2012). Structural insights into the coupling of virion assembly and rotavirus replication. *Nat Rev Microbiol* **10**(3), pp. 165-177.

Trojnar, E., Otto, P., Roth, B., Reetz, J. and Johne, R. (2010). The genome segments of a group D rotavirus possess group A-like conserved termini but encode group-specific proteins. *J Virol* **84**(19), pp. 10254-10265.

Uematsu, S. and Akira, S. (2008). Toll-Like receptors (TLRs) and their ligands. *Handb Exp Pharmacol*(183), pp. 1-20.

Unterholzner, L. and Bowie, A.G. (2008). The interplay between viruses and innate immune signaling: recent insights and therapeutic opportunities. *Biochem Pharmacol* **75**(3), pp. 589-602.

Vasquez-Del Carpio, R., Gonzalez-Nilo, F.D., Riadi, G., Taraporewala, Z.F. and Patton, J.T. (2006). Histidine triad-like motif of the rotavirus NSP2 octamer mediates both RTPase and NTPase activities. *J Mol Biol* **362**(3), pp. 539-554.

Vermeulen, L., De Wilde, G., Van Damme, P., Vanden Berghe, W. and Haegeman, G. (2003). Transcriptional activation of the NF-kappaB p65 subunit by mitogen- and stress-activated protein kinase-1 (MSK1). *EMBO J* **22**(6), pp. 1313-1324.

Vitour, D., Lindenbaum, P., Vende, P., Becker, M.M. and Poncet, D. (2004). RoXaN, a novel cellular protein containing TPR, LD, and zinc finger motifs, forms a ternary complex with eukaryotic initiation factor 4G and rotavirus NSP3. *J Virol* **78**(8), pp. 3851-3862.

Von Bonsdorf, C.H. and Svensson, L. (1988). Human serogroup C rotavirus in Finland. *Scand J Infect Dis* **20**(5), pp. 475-478.

Wakuda, M., Ide, T., Sasaki, J., Komoto, S., Ishii, J., Sanekata, T. and Taniguchi, K. (2011). Porcine rotavirus closely related to novel group of human rotaviruses. *Emerg Infect Dis* **17**(8), pp. 1491-1493.

Weitzman, M.D. and Ornelles, D.A. (2005). Inactivating intracellular antiviral responses during adenovirus infection. *Oncogene* **24**(52), pp. 7686-7696.

Wentz, M.J., Patton, J.T. and Ramig, R.F. (1996). The 3'-terminal consensus sequence of rotavirus mRNA is the minimal promoter of negative-strand RNA synthesis. *J Virol* **70**(11), pp. 7833-7841.

Weycker, D., Sofrygin, O., Kemner, J.E., Pelton, S.I. and Oster, G. (2009). Cost of routine immunization of young children against rotavirus infection with Rotarix versus RotaTeq. *Vaccine* **27**(36), pp. 4930-4937.

Wu, C. and Ghosh, S. (2003). Differential phosphorylation of the signal-responsive domain of I kappa B alpha and I kappa B beta by I kappa B kinases. *J Biol Chem* **278**(34), pp. 31980-31987.

Xu, L., Tian, Y., Tarlow, O., Harbour, D. and McCrae, M.A. (1994). Molecular biology of rotaviruses. IX. Conservation and divergence in genome segment 5. *J Gen Virol* **75 (Pt 12)**pp. 3413-3421.

Yoneyama, M., Kikuchi, M., Matsumoto, K., Imaizumi, T., Miyagishi, M., Taira, K., Foy, E., Loo, Y.M., Gale, M., Akira, S., Yonehara, S., Kato, A. and Fujita, T. (2005). Shared and unique functions of the DExD/H-box helicases RIG-I, MDA5, and LGP2 in antiviral innate immunity. *J Immunol* **175**(5), pp. 2851-2858.

Yoneyama, M., Suhara, W., Fukuhara, Y., Fukuda, M., Nishida, E. and Fujita, T. (1998). Direct triggering of the type I interferon system by virus infection: activation of a transcription factor complex containing IRF-3 and CBP/p300. *EMBO J* **17**(4), pp. 1087-1095.

Yow, M.D., Melnick, J.L., Blattner, R.J., Stephenson, W.B., Robinson, N.M. and Burkhardt, M.A. (1970). The association of viruses and bacteria with infantile diarrhea. *Am J Epidemiol* **92**(1), pp. 33-39.

Zeng, C.Q., Estes, M.K., Charpilienne, A. and Cohen, J. (1998). The N terminus of rotavirus VP2 is necessary for encapsidation of VP1 and VP3. *J Virol* **72**(1), pp. 201-208.

Zeng, C.Q., Wentz, M.J., Cohen, J., Estes, M.K. and Ramig, R.F. (1996). Characterization and replicase activity of double-layered and single-layered rotavirus-like particles expressed from baculovirus recombinants. *J Virol* **70**(5), pp. 2736-2742.

Zárate, S., Romero, P., Espinosa, R., Arias, C.F. and López, S. (2004). VP7 mediates the interaction of rotaviruses with integrin alphavbeta3 through a novel integrin-binding site. *J Virol* **78**(20), pp. 10839-10847.

Zhang, M., Zeng, C.Q., Morris, A.P. and Estes, M.K. (2000). A functional NSP4 enterotoxin peptide secreted from rotavirus-infected cells. *J Virol* **74**(24), pp. 11663-11670.